BIOGEOCHEMICAL CYCLING OF IRON AND CARBON IN HUMID (SUB)TROPICAL FOREST SOILS UNDER FLUCTUATING REDOX CONDITIONS

by

DIEGO BARCELLOS

(Under the Direction of Aaron Thompson)

ABSTRACT

Iron (Fe) is essential to plants, microbes, and animals, is an important element in weathered soils from tropical and subtropical regions due to its reactivity toward carbon (C) and nutrients and its ability to serve as an electron acceptor for anaerobic respiration. Humid (sub)tropical and iron-rich soils naturally experience fluctuations in soil moisture, oxygen content, and hence, redox potential due to elevated but intermittent rainfall and high inputs of labile carbon from decomposed litter. Soils from the Luquillo Critical Zone Observatory (LCZO), Puerto Rico, are well-suited for studying the impact of redox fluctuations on Fe and C biogeochemistry. I conducted two laboratory experiments, exploring coupled Fe-C mechanisms, and one field experiment, using LCZO soils. Both lab experiments were conducted using soil in a slurry, which minimizes spatial variability and involved shifting between anoxic and oxic conditions. In the first lab study, I found that iron reduction rates increased when redox oscillations occurred more frequently. In the second lab experiment, I varied the time under oxic conditions (τ_{oxic}) in both long and short oscillation periods. For the long treatments (τ_{anoxic} at 6 d), I observed that as τ_{oxic} decreased from 72 to 24 to 8 hours, Fe reduction rates increased, CO_2 emissions remained unchanged, and CH_4 emissions decreased; and for the short treatments (τ_{anoxic} at 2 d), Fe^{II} and trace gases emissions decreased throughout the experiment. For the field

experiment, I monitored several biogeochemical variables involved in Fe-C redox processes in triplicate catenas at ridge, slope, and valley positions. I found that soil moisture was a predictor for changes in Fe^{II}, rapidly-reducible Fe oxides (Fe^{III}_{RR}), pH, Eh, and DOC. Valleys were more responsive to environmental changes than the other landscape positions. I also conducted three other lab studies (using LCZO soils) and one field experiment at the Calhoun CZO, in South Carolina (each are reported briefly in the Appendices). In conclusion, under natural and laboratory redox fluctuating systems, iron exerts a strong biogeochemical influence on the carbon dynamics of soils from humid (sub)tropical regions with important climate change and environmental implications.

INDEX WORDS: Soil, iron, carbon, redox oscillations, microbial iron reduction, carbon mineralization, Luquillo Critical Zone Observatory, Puerto Rico

BIOGEOCHEMICAL CYCLING OF IRON AND CARBON IN HUMID (SUB)TROPICAL FOREST SOILS UNDER FLUCTUATING REDOX CONDITIONS

by

DIEGO BARCELLOS

BSE, Universidade Federal de Viçosa, Brazil, 2011

MS, University of Georgia, 2013

A Dissertation Submitted to the Graduate Faculty of The University of Georgia in Partial Fulfillment of the Requirements for the Degree

DOCTOR OF PHILOSOPHY

ATHENS, GEORGIA

2018

BIOGEOCHEMICAL CYCLING OF IRON AND CARBON IN HUMID (SUB)TROPICAL FOREST SOILS UNDER FLUCTUATING REDOX CONDITIONS

by

DIEGO BARCELLOS

Major Professor:	Aaron Thompson
Committee:	Daniel Markewitz
	Christof Meile
	Paul Schroeder
	Mussie Habteselassie

Electronic Version Approved:

Suzanne Barbour
Dean of the Graduate School
The University of Georgia
August 2018

ACKNOWLEDGEMENTS

I want to first praise to God for this accomplishment. To my father, mother, sisters, grandparents, uncles, aunts, cousins, my girlfriend, and everyone that provided me long-term support to obtain this PhD degree in Soil Science. Thanks to all my friends from Athens and beyond, especially Ciro Cordeiro, for support and cheering.

I want to show my greatest gratitude to my advisor, Aaron Thompson. He has been an incredible mentor and constantly provided me training, guidance, and words of wisdom. I am also appreciative for the guidance provided by the committee members, Daniel Markewitz, Christof Meile, Paul Schroeder, and Mussie Habteselassie; and from my master's adviser Larry Morris, who brought me to UGA. Thanks to our collaborators Whendee Silver and Jennifer Pett-Ridge.

Financial support for this research was provided by the National Science Foundation (NSF) through the Critical Zone Observatories program. I want to thank the support from the Graduate School and from the Department of Crop and Soil Sciences of the University of Georgia, especially to Miguel Cabrera. This research would not be possible without the technical assistance of Nehru Mantripragada and Kim Kauffman, and all graduate students and postdoc colleagues at the University of Georgia, Jared Wilmoth, Taylor Cyle, Nadia Noor, Chunmei Chen, Caitlin Hodges, Stephanie Fulton, Rachel Ryland, among others.

TABLE OF CONTENTS

Page

LIST OF TABLES

Page

LIST OF FIGURES

Page

CHAPTER 1

INTRODUCTION AND LITERATURE REVIEW

1.1. INTRODUCTION

This dissertation contains four chapters and five appendices as follows:

Chapter 1: Introduction and Literature Review

Summary of each chapter and appendices as well as a literature review related to iron minerals, redox oscillations in soils, microorganisms involved in iron and carbon biogeochemistry, decomposition/mineralization and stabilization of soil organic carbon.

Chapter 2: Faster Redox Fluctuations Can Lead to Higher Iron Reduction Rates in Humid Forest Soils

The objective of this study was to investigate the impact of redox oscillations on Fe reduction rates by changing the length of the redox cycle (i.e., oscillation period). This study was motivated and aimed at building on the results from Ginn et al. (2014; 2017), Tishchenko et al. (2015), and Wilmoth (2016) all using soils from an upland valley from the Luquillo Critical Zone Observatory (Puerto Rico). In this chapter, we document an increase in iron reduction rates after decreasing the oscillation period (i.e., increasing the number of fluctuations per unit time).

Chapter 3: Length of oxygen exposure during redox oscillations affects rates of iron reduction, anaerobic carbon mineralization, and methane emissions

The objective of this study was to assess Fe reduction rates and correlations with net C mineralization (CO_2 and CH_4 emissions) as a function of the amount of exposure to oxic conditions (τ_{oxic}). Because soils often experience fluctuations between oxic and anoxic conditions (redox fluctuations), the pools of reactive Fe^{III} and Fe^{II} phases are under continuous flux and influence soil carbon cycling. We documented changes in Fe reduction rates and trace gas emissions by varying the oxic interval (τ_{oxic}) and by changing the redox oscillation period from long to short cycles.

Chapter 4: Soil moisture and precipitation explain fluctuations in redox potential, iron reduction, and carbon cycling in a humid forest soil from Puerto Rico

The objective of this study was to quantify daily and weekly variations in iron reduction and C losses by mineralization or release as dissolved organic carbon phases during natural redox fluctuations monitored at different topographic positions (ridge, slope, and valley) in soils from a humid tropical forest. This field study was conducted at the Luquillo Critical Zone Observatory located in El Yunque National Forest, Puerto Rico. We found that soil moisture was the major predictor for Fe-C biogeochemical variables and that the valleys were more susceptible to changes in redox conditions than the slopes or ridges.

Appendices: (A) Supplemental information for Chapter 3; (B) supplemental information for Chapter 4; (C) laboratory redox oscillation experiment tracking iron reduction with amendments of amino acids; (D) an alternative experimental set up using reconstructed mini-aggregates to study iron biogeochemical dynamics in redox oscillating conditions; (E) a study comparing iron reduction rates using initial fresh field-moist versus air-dried soils during redox oscillations; and

(F) a field experiment conducted at the Calhoun CZO (Piedmont of South Carolina, USA) monitoring Fe and C pools and environmental factors (soil moisture and redox potential), through changes in season and topographic positions.

1.2. LITERATURE REVIEW

Iron (Fe) is one of the most abundant and important elements in Earth's critical zone, is an essential plant and animal nutrient, and is correlated with the biogeochemical cycling of soil carbon, nutrients, and contaminants (section 1.2.1). Changes in environmental conditions, such as fluctuations in the partial pressure of molecular oxygen or the content of water in the soil (moisture status) can generate redox fluctuations in soils and create fluctuating oxic and anoxic conditions (section 1.2.2). The major catalysts for valence transformation of iron in soils are microorganisms (section 1.2.3). Iron and carbon biogeochemical cycling are coupled (section 1.2.4), with reactions that favor the decomposition/mineralization of soil organic matter in redox fluctuating environments (section 1.2.5), but iron minerals also serve an important role in the storage and persistence of organic matter in soils (section 1.2.6). Thus, during soil redox oscillations, iron can directly affect the loss or storage of soil carbon with important land management and climate change implications.

1.2.1. Iron Biogeochemistry in the Environment

Iron is the fourth most abundant element in the Earth's crust and the most frequently utilized transition metal in the biosphere, being a fundamental element in the environment and in the life cycles of animals, plants, and microorganisms (Kappler and Straub 2005; Kämpf et al. 2011). Iron biogeochemistry plays an important role in the cycle of carbon and many nutrients, as well as in the remediation of pollutants. There are many forms of Fe species in the

environment, as follows: Fe^{II} in primary minerals, Fe^{III} in secondary minerals, Fe in soluble and exchangeable forms (Fe^{3+} or Fe^{2+}), and Fe bound to organic matter (Colombo et al. 2014; Sposito 2008). Under oxic conditions, solid Fe^{III}-oxyhydroxides phases predominate, whereas in anoxic environments dissolved Fe^{2+} (or Fe^{II}-solids) are favored (Cornell and Schwertman 2003). In soils, iron can occur in different mineral phases: goethite (FeOOH) and hematite (Fe_2O_3) are the most abundant well-crystalline Fe-forms (predominantly under oxic conditions), followed by lepidocrocite, maghemite, and magnetite (Fontes et al. 1992; Schwertmann and Taylor 1989). Low-crystallinity or short-range-ordered (SRO) phases may also co-exist in the soil, such as ferrihydrite, ferroxite, and nano-geothite, which represent a dynamic and reactive pool of Fe^{III} minerals (Cornell and Schwertman 2003). Compared to other Fe^{III} minerals, ferrihydrite has the highest specific surface area (SSA) and dissolution rates (Table 1.1), making this mineral very important for the dynamics of iron reduction and interaction with other soil elements. Dissolution rates depend on temperature, pH, ionic strength, and nature of the chelating agent (Larsen and Postma 2001; Maurice 2009). Moreover, iron speciation can be driven by environmental redox potential (Eh), soil oxygen, moisture, and pH conditions (Brantley et al. 2008).

Table 1.1. Major iron minerals in soils, specific surface area (SSA), and dissolution rates. Adapted from: Bloom and Erich (1987), Herseman et al. (1995), Roden and Zachara (1996), Paige et al. (1997), Larsen and Postma (2001), Cornell and Schwertman (2003), Brantley et al. (2008), and Maurice (2009)

Iron Mineral	**Chemical Formula**	**SSA**	**Dissolution rate**
		$m^2\ g^{-1}$	$mol\ m^{-2}\ h^{-1}$
Goethite	α-FeOOH	8-200	$1.8x10^{-8}$ to $1.5x10^{-9}$
Hematite	α-Fe_2O_3	10-90	10^{-8} to $3x10^{-10}$
Ferrihydrite	$Fe(OH)_3$	200-400	10^{-5} to 10^{-6}
Lepidocrocite	γ-FeOOH	15-260	
Maghemite	γ-Fe_2O_3	8-130	
Magnetite	$Fe^{2+}Fe^{3+}{}_2O_4$	4-100	

1.2.2. Redox Oscillations in natural soils

Soils receiving large amounts of rainfall frequently experience shifts in oxygen (O_2) concentrations, varying from ~21% to ~0% O_2, often termed as oxic and anoxic conditions, respectively (Hansen et al. 2011; Schuur et al. 2001). Fluctuations in soil oxygen concentrations influence the oxidation and reduction of iron, which can in turn influence soil carbon (C) and nutrient dynamics (Henneberry et al. 2012; Weber et al. 2006). Oxygen is the most abundant and thermodynamically favorable element used by microorganisms as a terminal electron acceptor in soils (Lovley and Phillips 1988). When oxygen becomes depleted, iron becomes a major alternative electron acceptor because of it is abundance relative to other terminal electron acceptors such as nitrate and manganese (Lipson et al. 2013). Previous studies have shown that soil redox oscillations can influence Fe reduction and speciation (Ginn et al. 2017; Komlos et al. 2007; Liptzin and Silver 2009; Thompson et al. 2006; Coby et al. 2011). However, the influence of different patterns of redox fluctuations on iron reduction rates are only beginning to be understood (Mejia et al. 2016; Tomaszewski et al. 2016; Vogelsang et al. 2016; Ginn et al. 2017; Chen and Thompson, 2018).

Redox potential can be used to track fluctuations in wet and dry conditions (anoxic and oxic conditions) and is correlated with the potential for iron reduction and oxidation in soils (Fiedler et al. 2007). Eh is an intensity factor, like pH, with high and positive values in oxidizing environments, and low and negative values in reducing environments (Sparks 2003). Eh measurements can be suitable for soils constantly experiencing elevated soil moisture content, while soil atmospheric oxygen measurements are better suited for well-aerated soils. For oxidizing conditions, Eh varies from +300 to +700 mV, for transitioning reducing conditions from -50 to 300 mV, and for highly reducing conditions reaches values around -250 to -300 mV

(Fiedler et al. 2007; Patrick et al. 1996). The facultative anaerobic microorganisms using O_2, NO_3^-, Mn^{4+}, and Fe^{3+} are active between -50 to +300 mV, and the obligatory reducing microbes using SO^{2-}_4 and CO_2 are active below -50 mV (Reddy et al. 2000). Eh values around +300 mV can be considered the boundary between aerobic and anaerobic conditions. The magnitude and rate of changes in Eh depends on intrinsic soil characteristics such as: composition and amount of soil organic carbon, type and content of electron acceptors, temperature, and the time soils are under oxic and anoxic conditions (Sparks 2003).

An oscillating redox cycle can be conceptualized in three main variables: the amplitude of the oscillations, the oscillation period, and the ratio time spent under either oxic (τ_{oxic}) or anoxic (τ_{anoxic}) conditions ($\tau_{oxic}/\tau_{anoxic}$ ratio) (Figure 1.1). The amplitude represents the extent of the redox fluctuation, which under oxic/anoxic conditions is reflected in the maximum O_2 concentration observed over a cycle, and the oscillation period is the time it takes for a full redox cycle to be completed. The $\tau_{oxic}/\tau_{anoxic}$ ratio is the proportion between the time duration of the oxic and the anoxic conditions. We tested some of these different parameters in laboratory incubation experiments, especially the oscillation period, and the time under oxic (τ_{oxic}) and anoxic (τ_{anoxic}) conditions (Chapters 2 and 3, and Appendix A, B, C, and D).

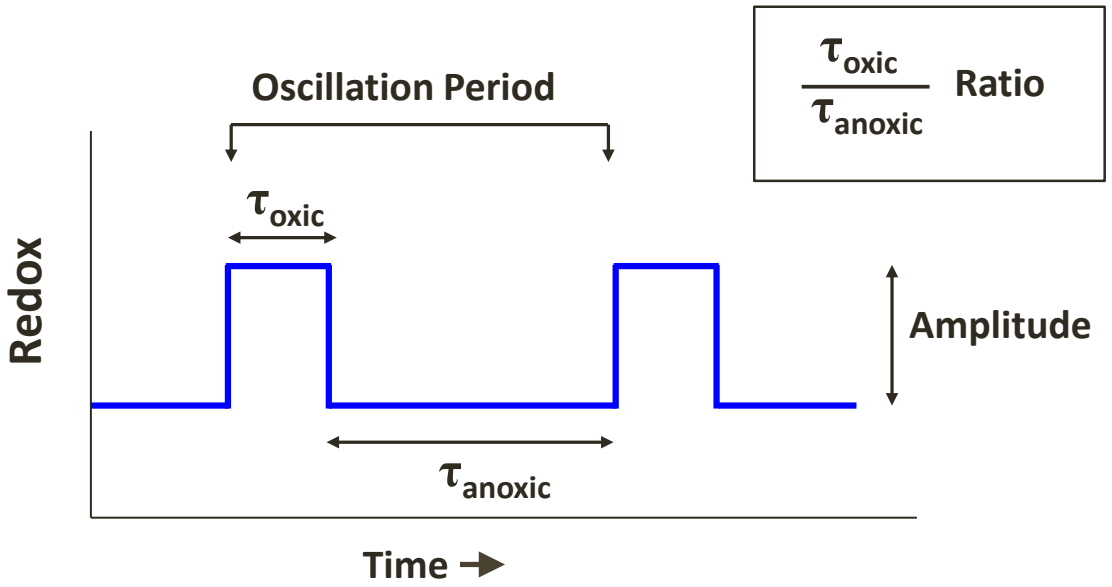

Figure 1.1. Hypothetical redox cycle and its components.

1.2.3. Microbially driven iron oxidation and reduction and abiotic iron oxidation

Microorganisms play an essential role in iron transformations in soils and are capable of catalyzing chemical reactions to reduce or oxidize iron forms and facilitate precipitation and/or dissolution of iron phases (Figure 1.2).

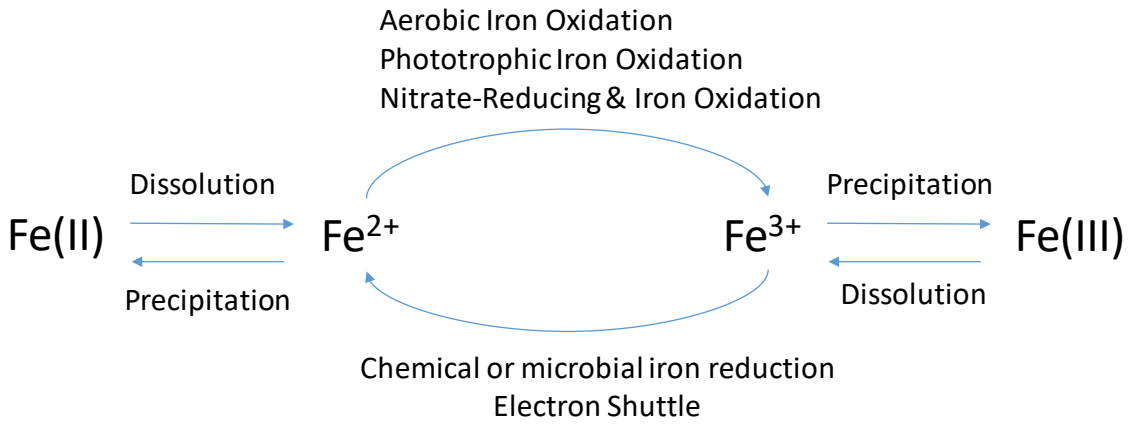

Figure 1.2. Iron cycling and species in the soil and in the environment.

Iron Oxidation

Iron freshly produced forms can be oxidized abiotically, in the presence of oxygen or nitrate, or biotically via iron-oxidizing bacteria, through one of the three following mechanisms: *i. Aerobic Fe^{II} oxidation:* usually favored in circumneutral pH and in well-aerated conditions (Konhauser et al. 2011). Light is a catalyst for the abiotic oxidation of iron. Under acidic conditions, Fe^{II} forms may persist in the environment for long periods of time, in the presence of low oxygen levels. Consequently, some bacteria developed mechanisms to grow under acidic conditions and under low oxygen concentrations (Johnson et al. 2012). The acidophilic bacteria *Acidothiobacillus ferrooxidans* and *Leptospirillum ferrooxidans* are commonly found in acid mine drainage sites (Templeton 2011). Other microorganisms, such as *Gallionella ferruginea* and *Leptothrix ochracea* have developed mechanisms to gain energy for growth from Fe^{II} oxidation and can compete with abiotic oxidation of Fe^{II} by O_2. These bacteria contain stalk structures (slender attachments) that favor the oxidation of Fe^{II} and the precipitation of low-crystallinity Fe^{III} phases, such as ferrihydrite (Emerson 2016)

ii. Anaerobic phototrophic Fe^{II} oxidation: this mechanism has been proposed for the formation of banded iron formations (BIF) in ancient times, when oxygen was absent (Poulton and Canfield 2011; Chan et al. 2016). Recently, several anoxygenic photosynthetic microorganisms has been identified, such as purple sulfur, purple nonsulfur, and green sulfur bacteria (Madigan et al. 2017). These microorganisms need specific conditions to promote Fe^{II} oxidation including being close enough to the water's surface to acquire enough light, as well as a low-O_2 environment, since O_2 may quickly oxidize Fe^{II} abiotically at high concentrations (Kappler and Straub, 2005).

iii. Anaerobic Fe^{II}-oxidizing nitrate-reducing: Some anaerobic microorganisms are capable of oxidizing Fe^{II} coupled to the reduction of nitrate, linking the iron and nitrogen cycles (Lamers et al. 2012). In this case, nitrate is an electron acceptor and Fe^{II} an electron donor. There are several bacteria involved in this process (Lovley et al. 2004), such as: *Aeromonas hydrophila, Anaeromyxobacter dehalogens, Bacillus infernus, Deferribacter Thermophiles, Desulfitobacterium hafniense, Desulfovibrio profundus, Desulfuromusa kysingii, Ferribacterium limneticum, Geobacter humireducens, Pantaea agglomerarans, Shewanella amazonensis, Sulfurospirillum barnesii,* and *Thermus scotoductus.* Depending on the environmental and geochemical conditions, a variety of iron minerals can be formed, such as magnetite, ferrihydrite, goethite, lepidocrocite, etc. (Konhauser et al., 2011).

Iron Reduction

There are three major mechanisms for bacterial dissimilatory iron reduction:

i. Physical contact of microbial cells with iron mineral surfaces favors direct delivery of electrons

Geobacter species are model microorganisms for iron reduction by establishing physical contact between the bacterial cells and the iron mineral surface (Weber et al. 2006). These bacteria can use organic carbon as both an electron donor and acceptor, and to use insoluble Fe^{III} forms as terminal electron acceptors (Eusterhues et al. 2014). The bacteria can bind to the iron surfaces by appendages, outer-membrane cytochromes, electrically conductive pili, flagella, and specialized chemotaxis (Leang et al. 2010). For instance, *Geobacter metallireducens* and *Geobacter sulfurreducens*, which are model iron-reducers, grow flagella and multi-heme cytochromes

together with electrically conductive pili (Shi et al. 2010). Once the bacteria are attached to the mineral surface, electrons from a reduced source (in the cytoplasm) move through the plasma membrane and periplasmic space, out of the cell. Additionally, the electron transfer between cell and mineral surface may occur via conductive pili (i.e. nanowires), which also function as an attachment mechanism (Smith et al. 2013). The formation of these nanowires expands the Geobacter's surface of contact, favoring penetration of the pili into the soil, reaching areas previously unavailable to the cells (Rotaru et al. 2014).

ii. Electron shuttling compounds that mediate the transfer of electrons from the microbial cell to Fe^{III} in the absence of physical contact between cell-iron-surface.

Shewanella species can produce soluble electron-shuttles to transfer electrons from and to Fe^{III} mineral surfaces from significant distances (millimeters) (Breuer et al. 2014; Poggenburg et al., 2016). Solid and dissolved humic substances in the soil organic matter, plant exudates, and antibiotics, have been proposed to serve as electron shuttles for Fe^{III} reduction (Bonneville et al. 2004; Pan et al. 2016). The electron shuttle compounds may be exogenous or endogenous from the microbial cell (Hernandez and Newman 2001). The bacteria oxidize an electron donor coupled to the reduction of a soluble electron shuttle, then the reduced shuttle diffuses and donates electrons to an iron mineral surface, promoting iron reduction. Subsequently, the oxidized electron acceptor restarts the cycle (Lovley et al. 1988).

iii. Iron chelators or complexing ligands increases the solubility of Fe^{III}

Geothrix species are a good example of microorganisms that use chelating moieties to transfer electrons between cells and iron minerals (Nevin and Lovley 2002). The production of

complexing ligands by these bacteria favor the dissolution of solid Fe^{III} minerals, providing soluble Fe^{III} forms and increasing Fe^{III} availability to microbes (Sylvia et al., 2005). An important iron chelator group are siderophores (Powell et al., 1980; Hersman et al. 1995). They are Fe^{III} scavengers and complex dissolved Fe^{III}, impeding these iron forms to precipitate into the solid phase (Kappler and Straub, 2005).

Iron Precipitation and dissolution

The precipitation of mineral phases containing either Fe^{II} or Fe^{III} are common processes in the soil (Figure 1.2). The Fe^{II} is reduced by microorganisms can precipitate biotically or abiotically forming minerals such as the mixed valance magnetite (Schwertmann and Taylor 1989). Fe^{III} can also form polymetric Fe^{III} colloids prior to precipitation as short-range-order (SRO) minerals, such as ferrihydrite (Paul, 2014). According to the reaction conditions, internal rearrangement of iron and oxygen atoms may favor the formation of more crystalline minerals, such as hematite and goethite (Tomaszewski et al. 2016). The SRO-Fe minerals, such as ferrihydrite, function as excellent electron acceptors for iron-reducing-bacteria. These microorganisms can use insoluble forms of extracellular Fe^{III} as terminal electron acceptors coupled to ATP production through the tricarboxylic acid (TCA) cycle (Sylvia et al. 2005). Solution pH is an important factor for iron reduction, as Fe^{III} oxides are mostly insoluble at pH > 4, which is most common in soils, and makes it more difficult for microorganisms to utilize Fe^{III} as a respiratory terminal electron acceptor (Weber et al. 2006).

Feammox: anaerobic ammonium oxidation and iron reduction

A more recent mechanism of nitrogen cycling that involves Fe has been documented, called Feammox, which is the reduction of Fe^{III} coupled to anaerobic ammonium oxidation (NH_4^+) to produce N_2, NO_3^-, or NO_2^- (Clement et al. 2005; Yang et al. 2012). Feammox may occur biotically or abiotically and usually occurs in saturated soils and wetlands (Huang et al., 2016). Some bacteria documented to participate in this process are *Candidatus Brocadia anammoxidans* and *Candidatus Kuenenia stuttgartiensis* (Sawayama 2006).

1.2.4. Coupled iron and carbon biogeochemical cycling and SRO formation

In redox fluctuating environments, Fe^{III} and organic carbon (OC) are often coupled in electron transfer reactions, oxidizing C and reducing Fe^{III} into Fe^{II}, typically catalyzed by microorganisms (Lovley 2000). Since low-crystallinity Fe^{III} minerals (such as ferrihydrite) may also contain adsorbed C, the reductive dissolution of these minerals may cause C to desorb and dissolve into the soil solution, e.g., become dissolved organic carbon (DOC) (Kleber et al., 2015). Fe reduction can also disperse micro-aggregates and mobilize colloidal C stabilized by Fe mineral precipitates (Buettner et al 2014). Reactive forms of Fe^{III} phases are formed during the transitions between anoxic and oxic conditions (seasonal variation of water table, for instance), when the Fe^{II} is oxidized into Fe^{III} oxides, and this process promotes the sequestration of OC during the crystal growth and colloidal aggregation (Pedrot et al., 2011). These iron redox events are also important for the movement of OC within soil profiles. For example, Buettner et al. (2014) found that redox processes were responsible for the mobilization of dissolved (<2.3 nm) and colloidal (2.3 – 430 nm) C from the surface soil to the subsoil, in a basaltic soil from Hawaii. Thus, iron biogeochemical cycling can induce OC decomposition throughout the soil.

The SRO (short-range-ordered) Fe^{III} minerals, formed during the transition from anoxic to oxic conditions, have the potential to control long-term storage of OC by mineral association/co-precipitation (Kögel-Knabner et al., 2008; Kramer et al., 2012). Compared to other soil minerals, iron oxides have the highest specific surface area (SSA) (ranging of 200 to 1200 $m^2\ g^{-1}$ of oxide) (Pronk et al., 2011). Indeed, the SRO-Fe phases have a larger SSA (700–1500 $m^2\ g^{-1}$) than the well-crystalline Fe minerals (10–800 $m^2\ g^{-1}$) (Eusterhues et al., 2005). For example, ferrihydrite ($5Fe_2O_3 \cdot 9H_2O$), a nanocrystalline iron hydroxide, has a surface area of ~300 $m^2\ g^{-1}$ and high reactivity, and is also important in the process of C stabilization through adsorption and co-precipitation (Das et al., 2011). Additionally, ferrihydrite has a ubiquitous occurrence in the environment, and it is formed in the presence of SOM (Schwertmann et al., 2005). Therefore, SRO-Fe minerals have high potential to sequester carbon in soils.

1.2.5. Carbon decomposition/mineralization in redox oscillating environments

Redox fluctuations are common in wetlands, marine sediments, and in humid climates in which soils undergo periodic changes in oxygen and moisture regimes. With exhaustion of oxygen in the environment, carbon degradation under anaerobic conditions is driven by microorganisms using alternative electron acceptors such as the elements nitrogen, iron, manganese, sulfur, and the soil organic matter (that produces methane) (Reddy and DeLaune 2008). Redox oscillations induce oxidation-reduction of iron minerals and the mineralization of soil organic carbon (Marumoto et al., 1982; McNicol and Silver, 2014), which is thermodynamically favorable (Sposito 2008) (Table 1.2).

Regions of high precipitation may impose fluctuations in soils' redox, oxygen and moisture regimes, and create temporary oxic and anoxic conditions. Under these soil conditions,

the first step for organic matter decomposition/mineralization is the production of soluble and more labile compounds (Keiluweit et al. 2016). In this first step, during anoxic conditions, the primary and major mechanism of carbon decomposition is depolymerization reactions, promoted by hydrolytic enzymes and fermentation of low-molecular weight compounds (Hedges and Keil 1995; Megonigal et al. 2003); and under oxic conditions, depolymerization transforms soil organic matter into smaller and more soluble compounds (Sinsabaugh 2010). The second step is the oxidation of low molecular weight compounds (ane emission of CO_2), previously produced during the depolymerization steps.

Additionally, the oxidation of Fe^{II} via O_2 produces reactive oxygen species (ROS), creating another important mechanism responsible for soil carbon degradation (Topudurti et al. 1994). Iron oxidation can promote organic matter decomposition by either oxidation of the organic matter by ROS, or by acidification process that increased carbon substrate availability, in dissolved form, for microbial degradation (Hall and Silver 2013). In redox fluctuating systems, carbon decomposition generally occurs in higher magnitude under aerobic conditions than under anaerobic conditions, mainly because the aerobic metabolic processes are more energetically favorable than the anaerobic metabolism (Ponnamperuma 1972; Burdige 2007). As a result, Fenton reactions (reactions with reactive oxygen species) can degrade and/or solubilize organic carbon during oxic conditions, and carbon degradation may still occur in the subsequent anoxic cycle, but in a smaller magnitude. Consequently, frequent changes in oxic and anoxic conditions in the environment may be responsible for higher decompositions rates of carbon, compared to static oxic or anoxic conditions. The principles of the Fenton reaction have been largely used for the remediation of organic contaminants in the environment (Bossmann et al., 1998; Bogan and Trbovic, 2003; Watts et al., 2004; Villa et al., 2010).

Another environment undergoing constant redox fluctuations and changes in Fe and C biogeochemistry are wetland soils. The wetland soils usually experience longer anoxic intervals, compared to upland soils that experience high rainfall, and may emit higher amounts of trace gases, such as carbon dioxide (CO_2), methane (CH_4), and nitrous oxide (N_2O), through organic matter decomposition (Kirk 2004; Van Bodegom et al. 2005). Wetlands can act as methane producers, when periodically inundated, or can act as methane sink, when dried (Altor and Mitsch 2008). Coastal wetlands produce less methane, because the high salt concentrations inhibit methane production, but sulfate reduction can be much higher (Van Der Nat and Middelburg 2000). Nitrous oxides emissions are lower in wetlands compared to soils. Consequently, organic matter decomposition is more limited by electron acceptor availability than carbon source availability, in the case of wetland soils compared to upland soils. The supply of electron acceptors happens with alternating wet and dry cycles, and about 70% of the organic carbon may be lost as methane (Reddy and DeLaune 2008).

In marine and stream sediments, microbial reactions during redox oscillations are appointed to be responsible for degradation of sedimentary organic matter (Reimers et al. 2013). Aerobic microbes are favored because oxygen functions as both terminal electron acceptor during oxidation of carbon, and as reactant for oxygenase-catalyzed attack on organic compounds (Kristensen et al. 1995). The aerobic decomposition is mostly dependent on the lability, chemical composition, mineral-organo associations, and the age of the organic compound (Sun et al. 2002). Additionally, considering that anaerobic microbes are not capable of hydrolyzing some complex organic compounds and that in most of the organic matter (labile pool especially) has already been decomposed in the oxic zone, the rates of decomposition in anoxic zones are therefore slower compared to oxic zones (Wakeham and Canuel 2006). Aerobic

decomposition involves diverse enzymes and are a more direct metabolic pathway than anaerobic decomposition. Under anoxic conditions, bacteria cannot degrade most polymeric compounds and they need to either use hydrolysis or fermentation and use various inorganic compounds as a terminal electron acceptor in cooperation with many microorganisms (Ahmed et al. 1992). In some cases, aerobic decomposition is 10 times faster than anaerobic decomposition (Kristensen et al. 1995). Bioturbation in marine sediments are highly important for increasing carbon degradation by accelerating the supply of TEA (Aller 1994). Bioturbation promotes changes in redox conditions, especially short-term redox oscillations, which are an important factor for organic matter decomposition in the bioturbated zone (Kristensen et al. 1995).

Some studies have shown that periodic changes in soil redox potential can lead to faster soil organic matter decomposition compared to a more constant redox condition either oxic or anoxic (Aller 1994; Aller 2004). However, other studies have shown that carbon decomposition is higher under oxic conditions compared to fully anoxic or redox fluctuating systems (Hedges et al. 1999; Burdige 2007). Furthermore, Burdige (2007) proposed some mechanisms that may explain the increase in carbon mineralization in redox fluctuation systems compared to fully oxic or anoxic systems, as follows: (i) microbes are stimulated by constant flux of new amounts and different forms of carbon sources; (ii) the periodic introduction of oxygen favors the formation of oxygen-requiring enzymes and the breakdown of certain molecules that would not happen only at anoxic conditions; (iii) organisms may affect carbon mineralization by mixing sediment material (bioturbation); and (iv) increase in reduction and oxidation of Fe and Mn oxides, which may oxidize some refractory compounds such as the aromatics.

Table 1.2. Theoretical stoichiometry of iron minerals coupled to carbon (example for glucose) (Sposito, 2008)

Goethite:
$FeOOH(s) + 3\ H^+ + e^- = Fe^{2+} + 2\ H_2O$ (Log K = 13.34)
$1/24\ C_6H_{12}O_6 + 1/4\ H_2O = ¼\ CO_2 + H^+ + e^-$ (Log K = 0.20)
$FeOOH(s) + 1/24\ C_6H_{12}O_6 + 2\ H^+ = Fe^{2+} + ¼\ CO_2 + 7/4\ H_2O$ (Log K = 13.54)
$\Delta Gr_0 = -RT \ln K = - 8.314 \times 298 \times \ln 10^{13.54} = - 77.243\ kJ\ mol^{-1}$
Hematite:
$½\ Fe_2O_3(s) + 3\ H^+ + e^- = Fe^{2+} + 3/2\ H_2O$ (Log K = 12.96)
$1/24\ C_6H_{12}O_6 + 1/4\ H_2O = ¼\ CO_2 + H^+ + e^-$ (Log K = 0.20)
$½\ Fe_2O_3(s) + 1/24\ C_6H_{12}O_6 + 2\ H^+ = Fe^{2+} + ¼\ CO_2 + 5/4\ H_2O$ (Log K = 13.06)
$\Delta Gr_0 = -RT \ln K = - 8.314 \times 298 \times \ln 10^{13.06} = - 74.505\ kJ\ mol^{-1}$
Ferrihydrite:
$Fe(OH)_3(s) + 3\ H^+ + e^- = Fe^{2+} + 3\ H_2O$ (Log K = 17.14)
$1/24\ C_6H_{12}O_6 + 1/4\ H_2O = ¼\ CO_2 + H^+ + e^-$ (Log K = 0.20)
$½\ Fe_2O_3(s) + 1/24\ C_6H_{12}O_6 + 2\ H^+ = Fe^{2+} + ¼\ CO_2 + 11/4\ H_2O$ (Log K = 17.34)
$\Delta Gr_0 = -RT \ln K = - 8.314 \times 298 \times \ln 10^{17.34} = - 98.921\ kJ\ mol^{-1}$

1.2.5. Soil organic matter preservation/stabilization by Fe oxyhydroxides

Soil organic matter (SOM) is dynamic (residence times on the order of decades) and contains ~1461 Pg of carbon (C) globally, which is larger than the mass of C present in biomass or in the atmosphere (Schlesinger and Bernhardt, 2013; Scharlemann et al., 2014). Consequently, the preservation and storage of C in soils is important for reducing the atmospheric emissions of CO_2 and other greenhouse gases associated with climate change. Furthermore, elucidation of the mechanisms of SOM interaction and dissociation with mineral surfaces is essential for developing strategies to increase carbon sequestration into soils and to avoid larger C losses (Lal, 2004; Lal, 2008; Chassé et al., 2015; Johnson et al., 2015). Many factors have been proposed for controlling C stabilization in soil: (i) the recalcitrance of SOM compounds; (ii) environmental

conditions unfavorable for microbial decomposition (low temperature, low pH, or low oxygen supply); (iii) physical protection by occlusion in soil aggregates; and (iv) stabilization due to sorption by soil minerals (Sollins et al., 1996; Eusterhues et al., 2003). Soil stable C can also be defined by a long mean residence time (MRT), or slow degradation rate; and may persist for 2,000–10,000 years in soil layers below 0.2 m (Schöning et al., 2006).

Mineral-organo associations are one of the major mechanisms for carbon stabilization in soils, and the Fe minerals are one of the most abundant responsible for accumulation of SOM (Lützow et al. 2006; Fontaine 2007; Bruun et al. 2010; Schmidt et al. 2011; Kleber et al. 2015). Recent investigations suggest that reactive Fe- and Al-SRO phases play a major role in the preservation of SOC in highly weathered soils from (sub)tropical regions (Thaymuang et al. 2013; Kleber et al. 2005; Sodano et al. 2016; Rasmussen et al. 2018). Thus, soil iron minerals can shelter and preserving SOM (Kaiser and Guggenberger, 2000) through mechanisms that impede microbial degradation of organic compounds (Lalonde et al., 2012; Baldock and Skjemstad 2000). Oxygen and Fe^{2+} present in solution can react quickly, and the SRO-Fe^{III} minerals formed can sequester the OC. For instance, ferrihydrite—a short range ordered (SRO) Fe oxide—has been noted to provide “sorptive protection” (Eusterhues et al., 2008) of OM from microbial decomposition (Jones and Edwards, 1998). The stabilization of SOM by Fe minerals is mainly influenced by the specific surface area (SSA) and iron speciation, as well as the soil’s particle size distribution (Kaiser and Guggenberger 2003; Mikutta et al. 2006).

The SOM molecules can bind to small micro-aggregates or at the edge of larger particles due to precipitation or coating with minerals; this favors a positive correlation between Fe oxide content and SSA, and between clay content and SSA (Thaymuang et al., 2013). The smaller the mineral particle size and the greater the SSA, the greater the soil’s potential to store SOM.

Eusterhues et al. (2005) found a relationship between SOM resistance to oxidation (extraction with sodium persulfate, $Na_2S_2O_8$), clay content, total-Fe and SRO-Fe content, in Inceptisols and Spodosols from Germany. Similarly, a study conducted in volcanic ash soils in Spain revealed that SOM stocks and resilience are associated with SRO-Fe and -Al minerals, as the non-crystalline minerals protect the SOM by forming stable micro-aggregates that enclose the C for long periods of time and/or by forming mineral coatings that prevent microbial attack (Hernandez et al. 2012). Comparatively, gibbsite (a crystalline Al oxide) can be also a good sorbent for humic substances, natural organic matter and dissolved SOM (Dick et al., 2005). Additionally, in marine sediments, Lalonde et al. (2012) predicted that around 20 % of the total OC (19-45 x 10^{15} g) is associated with iron phases and found that reactions of co-precipitation and/or direct chelation with iron contributes to preservation of OC in marine sediments. Furthermore, redox fluctuations in soils can affect the pool of reactive SRO-Fe inducing the reduction or oxidation of iron species by microorganisms and resulting in mineralization and/or stabilization of soil organic carbon.

1.3. References

Ahmed SI, Williams BL, Johnson, V (1992) Microbial populations isolated from the sediments of an anoxic fjord. An examination of fermentative bacteria involved in organic matter diagenesis in Saanich Inlet, BC, Canada. Marine Microbial Food Webs 6:133-148

Aller RC (1994) Bioturbation and remineralization of sedimentary organic matter: effects of redox oscillation. Chemical Geology 114:331-345

Aller RC (1998) Mobile deltaic and continental shelf muds as suboxic, fluidized bed reactors. Marine Chemistry 61:143-155

Aller RC (2004) Conceptual models of early diagenetic processes: the muddy seafloor as an unsteady, batch reactor. Journal of Marine Research 62:815-835

Altor AE, Mitsch WJ (2008) Methane and carbon dioxide dynamics in wetland mesocosms: effects of hydrology and soils. Ecological Applications 18:1307-1320

Baldock JA, Skjemstad JO (2000) Role of the matrix and minerals in protecting natural organic materials against biological attack. Organic Geochemistry 31:697–710

Bloom PR, Erich MS (1987) Effect of solution composition on the rate and mechanism of gibbsite dissolution in acid solutions. Soil Science Society of America Journal, 51:1131-1136

Bogan BW, Trbovic V (2003) Effect of sequestration on PAH degradability with Fenton's reagent: roles of total organic carbon, humin, and soil porosity. Journal of Hazardous Materials 100:285-300

Bonneville S, Behrends T, Van Cappellen P (2009) Solubility and dissimilatory reduction kinetics of Fe(III) oxyhydroxides: a linear free energy approach. Geochimica et Cosmochimica Acta 73:5273–5282

Bossmann SH, Oliveros E, Göb S, Siegwart S, Dahlen EP, Payawan L, Braun, AM (1998) New evidence against hydroxyl radicals as reactive intermediates in the thermal and photochemically enhanced Fenton reactions. The Journal of Physical Chemistry A, 102:5542-5550.

Brantley SL, Kubicki JD, White AF (Eds.) (2008) Kinetics of water-rock interaction (Vol. 168). New York: Springer. 833p

Breuer M, Rosso KM, Blumberger J, Butt JN (2015) Multi-haem cytochromes in Shewanella oneidensis MR-1: structures, functions and opportunities. Journal of the Royal Society Interface 12:20141117

Bruun TB, Elberling B, Christensen BT (2010) Lability of soil organic carbon in tropical soils with different clay minerals. Soil Biology and Biochemistry 42:888–895

Burdige DJ (2007) Preservation of organic matter in marine sediments: controls, mechanisms, and an imbalance in sediment organic carbon budgets. Chemical reviews 107:467-485

Buettner S, Kramer M, Chadwick OA, Thompson A (2014) Mobilization of colloidal carbon during iron reduction events in basaltic soils. Geoderma 221:139-145

Chan CS, Emerson D, and Luther GW (2016) The role of microaerophilic Fe-oxidizing micro-organisms in producing banded iron formations. Geobiology 14:509-528

Chen C, Thompson A (2018) Ferrous Iron Oxidation under Varying pO_2 Levels: The Effect of Fe (III)/Al (III) Oxide Minerals and Organic Matter. Environmental Science & Technology 52:597-606

Clement JC, Shrestha J, Ehrenfeld JG, Jaffe PR (2005) Ammonium oxidation coupled to dissimilatory reduction of iron under anaerobicconditions in wetland soils. Soil Biology and Biochemistry 37:2323–2328

Coby AJ, Picardal F, Shelobolina E, Xu H, Roden EE. (2011) Repeated anaerobic microbial redox cycling of iron. Applied and Environmental Microbiology 77:6036-6042

Colombo C, Palumbo G, He JZ, Pinton R, Cesco S (2014) Review on iron availability in soil: interaction of Fe minerals, plants, and microbes. Journal of Soils and Sediments 14:538–548

Cornell RM, Schwertmann U (2003) The iron oxides, 2nd edition. Wiley-VCH, Weinheim. 703p.

Das S, Hendry MJ, Essilfie-Dughan J (2011) Effects of adsorbed arsenate on the rate of transformation of 2-line ferrihydrite at pH 10. Environmental Science & Technology 45:5557−5563

Dick DP, Nunes Gonçalves C, Dalmolin RSD, Knicker H, Klamt E, Kögel-Knabner I, Simões ML, and Martin-Neto L (2005) Characteristics of soil organic matter of different Brazilian Ferralsols under native vegetation as a function of soil depth. Geoderma 124:319–333

Echigo T, Aruguete DM, Murayama M, Hochella MF (2012) Influence of size, morphology, surface structure, and aggregation state on reductive dissolution of hematite nanoparticles with ascorbic acid. Geochimica et Cosmochimica Acta 90:149-162

Emerson D (2016) The irony of iron–biogenic iron oxides as an iron source to the Ocean. Frontiers in Microbiology 6:1502

Eusterhues K, Rumpel C, Kleber M, Kogel-Knabner I (2003) Stabilisation of soil organic matter by interactions with minerals as revealed by mineral dissolution and oxidative degradation. Organic Geochemistry 34:1591–1600

Eusterhues K, Rumpel C, Kleber M, Kogel-Knabner I (2005) Organo-mineral associations in sandy acid forest soils: Importance of specific surface area, iron oxides and micropores. European Journal of Soil Science 56:753–763

Eusterhues K, Wagner FE, Häusler W, Hanzlik M, Knicker H, Totsche KU, Kogel-Kabner I, Schwertmann U (2008) Characterization of ferrihydrite-soil organic matter coprecipitates by X-ray diffraction and Mossbauer spectroscopy. Environmental Science & Technology 42:7891-7897

Eusterhues K, Hädrich A, Neidhardt J, Küsel K, Keller TF, Jandt KD, Totsche KU (2014) Reduction of ferrihydrite with adsorbed and coprecipitated organic matter: microbial reduction by Geobacter bremensis vs. abiotic reduction by Na-dithionite. Biogeosciences 11:4953-4966.

Fiedler S, Vepraskas MJ, Richardson JL (2007) Soil redox potential: importance, field measurements, and observations. Advances in Agronomy 94:1-54.

Fontaine S., Barot S, Barré P, Bdioui N, Mary B, Rumpel C (2007) Stability of organic carbon in deep soil layers controlled by fresh carbon supply. Nature 450:277–281.

Fontes, M.R., Weed, S.B. and Bowen, L.H. (1992) Association of microcrystalline goethite and humic acid in some Oxisols from Brazil. Soil Science Society of America Journal 56:982-990.

Ginn BR, Habteselassie MY, Meile C, Thompson A (2014) Effects of sample storage on microbial Fe-reduction in tropical rainforest soils. Soil Biology and Biochemistry 68:44-51

Ginn BR, Meile C, Wilmoth J, Tang Y, Thompson A. (2017) Rapid iron reduction rates are stimulated by high-amplitude redox fluctuations in a tropical forest soil. Environmental Science & Technology 51: 3250-3259

Hall SJ, Silver WL (2013) Iron oxidation stimulates organic matter decomposition in humid tropical forest soils. Global Change Biology 19:2804-2813.

Hall SJ, McDowell WH, Silver WL (2013) When wet gets wetter: decoupling of moisture, redox biogeochemistry, and greenhouse gas fluxes in a humid tropical forest soil. Ecosystems 16: 576-589

Hansen DJ, McGuire JT, Mohanty BP (2011) Enhanced biogeochemical cycling and subsequent reduction of hydraulic conductivity associated with soil-layer interfaces in the vadose zone. Journal of Environmental Quality 40:1941-1954

Hedges JI, Keil RG (1995) Sedimentary organic matter preservation: an assessment and speculative synthesis. Marine Chemistry 49:81-115

Hedges JI, Hu FS, Devol AH, Hartnett HE, Tsamakis E, Keil RG (1999) Sedimentary organic matter preservation; a test for selective degradation under oxic conditions. American Journal of Science 299:529-555

Henneberry YK, Kraus TE, Nico PS, Horwath WR (2012) Structural stability of coprecipitated natural organic matter and ferric iron under reducing conditions. Organic Geochemistry 48:81-89

Hernandez, M. E., & Newman, D. K. (2001) Extracellular electron transfer. Cellular and Molecular Life Sciences CMLS, 58(11), 1562-1571.

Hernandez Z, Almendros G, Carral P, Alvarez A, Knicker H, Perez-Trujillo JP (2012) Influence of non-crystalline minerals in the total amount, resilience and molecular composition of the organic matter in volcanic ash soils (Tenerife Island, Spain). European Journal of Soil Science 63:603-615

Hersman L, Lloyd T, Sposito G (1995) Siderophore-promoted dissolution of hematite. Geochimica et Cosmochimica Acta 59:3327-3330

Huang X, Zhu-Barker X, Horwath WR, Faeflen SJ, Luo H, Xin X, Jiang X (2016) Effect of iron oxide on nitrification in two agricultural soils with different pH. Biogeosciences 13:5609

Johnson DB, Kanao T, Hedrich S (2012) Redox transformations of iron at extremely low pH: fundamental and applied aspects. The microbial ferrous wheel: iron cycling in terrestrial, freshwater, and marine environments. Frontiers in Microbiology 3:96

Johnson K, Purvis G, Lopez-Capel E, Peacock C, Gray N, Wagner T, Greenwell C (2015) Towards a mechanistic understanding of carbon stabilization in manganese oxides. Nature communications 6:7628

Jones DL, Edwards AC (1998) Influence of sorption on the biological utilization of two simple carbon substrates. Soil Biology & Biochemistry 30:1895–1902

Kaiser K, Guggenberger G (2000) The role of DOM sorption to mineral surfaces in the preservation of organic matter in soils. Organic Geochemistry 31:711–725

Kaiser K, Guggenberger G (2003) Mineral surface and soil organic matter. European Journal of Soil Science 54:219–236

Kämpf N, Scheinost AC, Schulze DG. (2011) Oxide minerals in soils. In: Handbook of Soil Sciences: Properties and Processes, Second Edition. CRC Press, pp 1-34

Kappler A, Straub KL (2005) Geomicrobiological cycling of iron. Reviews in Mineralogy and Geochemistry 59:85-108

Keiluweit M, Nico PS, Kleber M, Fendorf S (2016) Are oxygen limitations under recognized regulators of organic carbon turnover in upland soils? Biogeochemistry 127:157-171

Kirk G. (2004) The biogeochemistry of submerged soils. John Wiley & Sons. Chichester, England. 282p

Kleber M, Mikutta R, Torn MS, Jahn R (2005) Poorly crystalline mineral phases protect organic matter in acid subsoil horizons. European Journal of Soil Science 56:717–725

Kleber M, Eusterhues K, Keiluweit M, Mikutta C, Mikutta R, Nico PS (2015) Chapter One: Mineral–Organic Associations: Formation, Properties, and Relevance in Soil Environments. Advances in Agronomy 130:1-140

Kögel-Knabner I, Ekschmitt K, Flessa H, Guggenberger G, Matzner E, Marschner B, von Lützow M (2008) An integrative approach of organic matter stabilization in temperate soils: Linking chemistry, physics, and biology. Journal of Plant Nutrition and Soil Science 171:5–13.

Komlos J, Kukkadapu RK, Zachara JM, Jaffe PR (2007) Biostimulation of iron reduction and subsequent oxidation of sediment containing Fe-silicates and Fe-oxides: Effect of redox cycling on Fe (III) bioreduction. Water Research 41:2996-3004

Konhauser KO, Kappler A, Roden EE (2011) Iron in microbial metabolisms. Elements, 7:89-93

Kramer MG, Sanderman J, Chadwick OA, Chorover J, Vitousek PM (2012) Long-term carbon storage through retention of dissolved aromatic acids by reactive particles in soil. Global Change Biology 18:2594–2605

Kristensen E, Ahmed SI, Devol AH (1995). Aerobic and anaerobic decomposition of organic matter in marine sediment: which is fastest? Limnology and Oceanography 40:430-1437

Lal R (2004) Soil carbon sequestration impacts on global climate change and food security. Science 304:1623–1627

Lal R (2008) Carbon sequestration. Philosophical Transactions of the Royal Society B 363:815-830

Lalonde K, Mucci A, Ouellet A, Gélinas Y (2012) Preservation of organic matter in sediments promoted by iron. Nature 483:198-200

Lamers LP, Van Diggelen JM, Op Den Camp HJ, Visser EJ, Lucassen EC, Vile MA, Roelofs J G (2012). Microbial transformations of nitrogen, sulfur, and iron dictate vegetation composition in wetlands: a review. Frontiers in Microbiology 3:156

Larsen O, Postma D (2001) Kinetics of reductive bulk dissolution of lepidocrocite, ferrihydrite, and goethite. Geochimica et Cosmochimica Acta 65:1367-1379

Leang C, Qian X, Mester T, Lovley DR (2010) Alignment of the c-type cytochrome OmcS along pili of Geobacter sulfurreducens. Applied and Environmental Microbiology 76:4080-4084

Liptzin D, Silver WL (2009) Effects of carbon additions on iron reduction and phosphorus availability in a humid tropical forest soil. Soil Biology and Biochemistry 41:1696-1702

Lipson DA, Raab TK, Goria D, Zlamal J (2013) The contribution of Fe (III) and humic acid reduction to ecosystem respiration in drained thaw lake basins of the Arctic Coastal Plain. Global Biogeochemical Cycles 27:399-409

Lovley DR, Phillips EJ (1988) Novel mode of microbial energy metabolism: organic carbon oxidation coupled to dissimilatory reduction of iron or manganese. Applied and Environmental Microbiology 54:1472-1480

Lovley DR (2000) Fe(III) and Mn(IV) reduction. In: Lovley, D. R. (Ed.), Environmental Microbe-Metal Interactions. ASM Press, Washington, D.C.

Lovley DR, Holmes DE, Nevin KP (2004) Dissimilatory Fe(III) and Mn(IV) reduction. Advances in Microbial Physiology 49:219-286

Lützow MV, Kögel-Knabner I, Ekschmitt K, Matzner E, Guggenberger G, Marschner B, Flessa H (2006) Stabilization of organic matter in temperate soils: mechanisms and their relevance under different soil conditions–a review. European Journal of Soil Science 57:426-445

Maurice PA (2009) Environmental surfaces and interfaces from the nanoscale to the global scale. Wiley. Hoboken, NJ. 464p

Madigan MT, Martinko JM, Parker J (2017) Brock biology of microorganisms (Vol. 13). Pearson. 1152p.

Megonigal JP, Hines ME, Visscher PT (2003). Anaerobic metabolism: linkages to trace gases and aerobic processes. In: Holland HD, Turekian KK (eds) Treatise on geochemistry. Pergamon, Oxford. 317–424

Mejia J, Roden EE, Ginder-Vogel M (2016) Influence of oxygen and nitrate on Fe (hydr)oxide mineral transformation and soil microbial communities during redox cycling. Environmental Science & Technology 50:3580-3588

Mikutta R, Kleber M, Torn M, Jahn R (2006) Stabilization of soil organic matter: Association with minerals or chemical recalcitrance. Biogeochemistry 77:25–56

Nevin KP, Lovley DR (2002) Mechanisms for accessing insoluble Fe (III) oxide during dissimilatory Fe (III) reduction by Geothrix fermentans. Applied and Environmental Microbiology 68:2294-2299

Paige CR, Snodgrass WJ, Nicholson RV, Scharer JM (1997) An arsenate effect on ferrihydrite dissolution kinetics under acidic oxic conditions. Water Research 31:2370-2382.

Pan W, Kan J, Inamdar S, Chen C, Sparks D (2016) Dissimilatory microbial iron reduction release DOC (dissolved organic carbon) from carbon-ferrihydrite association. Soil Biology and Biochemistry 103:232-240

Patrick WH, Gambrell RP, Faulkner SP (1996) Redox measurements of soils. Methods of Soil Analysis, Part 3—Chemical Methods. Madison, WI. pp 1255-1273

Paul EA (2014) Soil microbiology, ecology and biochemistry. Academic press. Elsevier. Burlington, MA. pp 515

Pedrot M, Le Boudec A, Davranche M, Dia A, Henin O (2011) How does organic matter constrain the nature, size and availability of Fe nanoparticles for biological reduction? Journal of Colloid Interface Science 359:75-85

Poggenburg C, Mikutta R, Sander M, Schippers A, Marchanka A, Dohrmann R, Guggenberger G (2016) Microbial reduction of ferrihydrite-organic matter coprecipitates by Shewanella

putrefaciens and Geobacter metallireducens in comparison to mediated electrochemical reduction. Chemical Geology. 447:133-147

Ponnamperuma FN (1972) The chemistry of submerged soils. Advances in Agronomy 24:29-96.

Poulton SW Canfield DE (2011) Ferruginous conditions: A dominant feature of the ocean through Earth's history. Elements 7:107-112

Powell PE, Cline GR, Reid CPP, Szaniszlo PJ (1980) Occurrence of hydroxamate siderophore iron chelators in soils. Nature 287:833

Pronk G. J., K. Helster, and I. Kogel-Knabner. (2011) Iron oxides as major available interface component in loamy arable topsoils. Soil Sci. Soc. Am. J. 75:2158–2168.

Rasmussen C, Heckman K, Wieder WR, Keiluweit M, Lawrence CR, Berhe AA, Blankinship JC, Crow SE, Druhan JL, Pries CE, Marin-Spiotta E, Plante AF, Schädel C, Schimel JP, Sierra CA, Thompson A, Wagai R. (2018) Beyond clay: towards an improved set of variables for predicting soil organic matter content. Biogeochemistry 137:297-306

Reddy KR, Feijtel TC, Patrick Jr WH (1986) Effect of soil redox conditions on microbial oxidation of organic matter. In The role of organic matter in modern agriculture. Springer Netherlands. pp 117-156

Reddy KR, DeLaune RD (2008) Biogeochemistry of wetlands: science and applications. CRC Press, Boca Raton, Florida. pp 774

Reimers CE, Alleau Y, Bauer JE, Delaney J, Girguis PR, Schrader PS, Stecher HA (2013) Redox effects on the microbial degradation of refractory organic matter in marine sediments. Geochimica et Cosmochimica Acta 121:582-598

Roden EE, Zachara JM (1996) Microbial reduction of crystalline iron (III) oxides: Influence of oxide surface area and potential for cell growth. Environmental Science & Technology 30:1618-1628

Rotaru AE, Shrestha PM, Liu F, Markovaite B, Chen S, Nevin KP, Lovley DR (2014) Direct interspecies electron transfer between Geobacter metallireducens and Methanosarcina barkeri. Applied and Environmental Microbiology 80:4599-4605

Sawayama S (2006) Possibility of anoxic ferric ammonium oxidation. Journal of Bioscience and Bioengineering. 101, 70–72

Scharlemann JPW, Tanner EVJ, Hiederer R, Kapos V (2014) Global soil carbon: understanding and managing the largest terrestrial carbon pool. Carbon Manage 5:81−91

Schlesinger WH, Bernhardt ES (2013) Biogeochemistry: an analysis of global change. Third Edition. Elsevier: Boston. pp 672

Schmidt MWI, Torn MS, Abiven S, Dittmar T, Guggenberger G, Janssens IA, Kleber M, Kogel-Knabner I, Lehmann J, Manning DAC, Nannipieri P, Rasse DP, Weiner S, Trumbore SE (2011) Persistence of soil organic matter as an ecosystem property. Nature 478:49-56

Schöning I, Kögel-Knabner I (2006) Chemical composition of young and old carbon pools throughout Cambisol and Luvisol profiles under forests. Soil Biology and Biochemistry 38:2411–2424

Schuur EA, Chadwick OA, Matson PA (2001) Carbon cycling and soil carbon storage in mesic to wet Hawaiian montane forests. Ecology 82:3182-3196.

Schwertmann U, Taylor RM (1989) Iron oxides. Minerals in Soil environments. pp 379-438

Schwertmann U, Wagner F, Knicker H (2005) Ferrihydrite-humic associations: Magnetic hyperfine interactions. Soil Science Society of America Journal 69:1009−1015

Sekar R, DiChristina TJ (2014) Microbially driven Fenton reaction for degradation of the widespread environmental contaminant 1, 4-dioxane. Environmental Science & Technology 48:12858-12867

Shi L, Squier TC, Zachara JM, Fredrickson JK (2007) Respiration of metal (hydr) oxides by Shewanella and Geobacter: a key role for multihaem c-type cytochromes. Molecular Microbiology 65:12-20

Sinsabaugh RL (2010) Phenol oxidase, peroxidase and organic matter dynamics of soil. Soil Biology and Biochemistry 42:391–404

Smith JA, Lovley DR, Tremblay PL (2013) Outer cell surface components essential for Fe (III) oxide reduction by Geobacter metallireducens. Applied and Environmental Microbiology 79:901-907

Sodano M, Said-Pullicino D, Fiori AF, Catoni M, Martin M, Celi L (2016) Sorption of paddy soil-derived dissolved organic matter on hydrous iron oxide–vermiculite mineral phases. Geoderma 261:169-177

Sollins P, Homann P, Caldwell BA (1996) Stabilization and destabilization of soil organic matter: Mechanisms and controls. Geoderma 74:65-105

Sparks DL (2003) Environmental soil chemistry. Academic Press. San Diego, CA. pp 352

Sposito G (2008) The chemistry of soils. Oxford University Press. New York, NY. pp 329

Sun MY, Aller RC, Lee C, Wakeham SG (2002) Effects of oxygen and redox oscillation on degradation of cell-associated lipids in surficial marine sediments. Geochimica et Cosmochimica Acta 66:2003-2012

Sylvia DM, Fuhrmann JJ, Hartel PG, Zuberer DA (Eds.) (2005) Principles and applications of soil microbiology (No. QR111 S674 2005). Upper Saddle River, NJ: Pearson Prentice Hall.

Templeton AS (2011) Geomicrobiology of iron in extreme environments. Elements 7:95-100

Thaymuang W, Kheoruenromne I, Suddhipraharn A, Sparks DL (2013) The role of mineralogy in organic matter stabilization in tropical soils. Soil Science 178:6

Thompson A, Chadwick OA, Rancourt DG, Chorover J (2006) Iron-oxide crystallinity increases during soil redox oscillations. Geochim. Cosmochim. Acta 70:1710–1727

Tishchenko V, Meile C, Scherer MM, Pasakarnis TS, Thompson A (2015) Fe^{2+} catalyzed iron atom exchange and re-crystallization in a tropical soil. Geochimica et Cosmochimica Acta 148:191-202

Tomaszewski EJ, Cronk SS, Gorski CA, Ginder-Vogel M (2016) The role of dissolved Fe (II) concentration in the mineralogical evolution of Fe (hydr) oxides during redox cycling. Chemical Geology 438:163-170

Topudurti K, Keefe M, Wooliever P, Lewis N (1994) Field evaluation of perox-pure™ chemical oxidation technology. Water Science and Technology 30:95-104

Van Bodegom PM, Broekman R, Van Dijk J, Bakker C, Aerts R (2005) Ferrous iron stimulates phenol oxidase activity and organic matter decomposition in waterlogged wetlands. Biogeochemistry 76:69-83

Van Der Nat FJ, Middelburg JJ (2000) Methane emission from tidal freshwater marshes. Biogeochemistry 49:103-121

Villa RD, Trovó AG, Nogueira RFP (2010) Diesel degradation in soil by fenton process. Journal of the Brazilian Chemical Society 21:1089-1095

Vogelsang V, Fiedler S, Jahn R, Kaiser K (2016) In-situ transformation of iron-bearing minerals in marshland-derived paddy subsoil. European Journal of Soil Science 67:676-685

Wakeham SG, Canuel EA (2006) Degradation and preservation of organic matter in marine sediments. In Marine Organic Matter: Biomarkers, Isotopes and DNA. Springer Berlin Heidelberg. pp 295-321

Watts RJ, Stanton PC, Howsawkeng J, Teel AL (2002) Mineralization of a sorbed polycyclic aromatic hydrocarbon in two soils using catalyzed hydrogen peroxide. Water Research 36:4283-4292

Weber KA, Achenbach LA, Coates JD (2006) Microorganisms pumping iron: anaerobic microbial iron oxidation and reduction. Nature Reviews Microbiology 4:752-764

Wilmoth JL (2016) Effects of redox-cycling on iron-mineral transformations and metatranscriptome of iron (III)-reducing bacteria in a humid tropical forest soil. Doctoral Dissertation. University of Georgia

Yang WH, Weber KA, Silver WL (2012). Nitrogen loss from soil through anaerobic ammonium oxidation coupled to iron reduction. Nature Geoscience 5:538-541

CHAPTER 2

FASTER REDOX FLUCTUATIONS CAN LEAD TO HIGHER IRON REDUCTION RATES IN HUMID FOREST SOILS[1]

[1] Barcellos, D., K.T. Cyle, and A. Thompson. Reprinted by permission from Springer Nature, Journal Biogeochemistry. 137, no. 3 (2018): 367-378.

Abstract

Iron (Fe) minerals play an important role in carbon (C) and nutrient dynamics in redox fluctuating soils. We explored how the frequency of redox oscillations influence Fe reduction rates and C content in Puerto Rican soils. We hypothesized that iron reduction rates would be faster during short oscillation periods than in longer oscillation periods. Surface soils from an upland valley in a humid tropical forest were exposed to systematic redox oscillations over 50 days. The oxidation events were triggered by the introduction of air (21% O_2), maintaining the time ratio under oxic or anoxic conditions at 1:6 (τ_{ox}/τ_{anox}). After pre-conditioning the soil to fluctuating redox conditions for one month, we imposed 280- and 70-h (or 11.67- and 2.5-day) redox oscillations, measuring Fe^{II} every few days. We found that by the end of the experiment, Fe reduction rates were higher in the short oscillation period (τ_{ox} = 10 h, τ_{anox} = 60 h) than in the long oscillation period (τ_{ox} = 40 h, τ_{anox} = 240 h). Carbon and nitrogen loss however was similar for both treatments. These results suggest the characteristics of redox fluctuations can alter rates of Fe reduction and potentially influence ecosystem processes that depend on iron behavior.

2.1. Introduction

Soils from tropical humid regions often experience shifts in oxygen concentrations (pO_2) varying from ~21% to ~0% O_2 (oxic and anoxic conditions, respectively), following the introduction of meteoric water into the soil (Hansen et al. 2011; Liptzin et al. 2011; Schuur et al. 2001). These variations in pO_2 can occur within hours to days (Cleveland et al. 2010; Hall et al. 2013; Silver et al. 2001), and are often correlated with rainfall events (Liptzin et al. 2011). Fluctuations in pO_2 influence the oxidation and reduction of iron (Fe) (Weber et al. 2006), which can in turn influence soil carbon (C) and nutrient dynamics (Colombo et al. 2014; Henneberry et al. 2012; Sposito 2008). Fe-C biogeochemical cycles are often coupled in soils through decomposition of C during Fe reduction events and during the immediate oxidation of Fe^{II} (Hall and Silver 2013), and through stabilization of C via sorption to Fe^{III} oxide phases that form during Fe^{II} re-oxidation (Eusterhues et al. 2005; Lovley et al. 2004; Mikutta et al. 2006; Roden and Zachara 1996). Oxygen (O_2) is the most abundant and thermodynamically favorable element used by microorganisms as terminal electron acceptor in soils (Lovley and Phillips 1988). When O_2 becomes depleted in soils, Fe becomes a major alternative electron acceptor because of its abundance relative to other terminal electron acceptors such as nitrate and manganese dioxide (Keiluweit et al. 2016; Lipson et al. 2013).

Short-range-ordered (SRO) iron phases (e.g., ferrihydrite, nano-goethite) dominate the surface reactivity of soil iron toward carbon, nutrients, and pollutants, although well-crystalline Fe minerals (e.g., hematite and goethite) make up the bulk of structural iron in soils (Cornell and Schwertmann 2003b; Kämpf et al. 2011). Highly substituted (by carbon or other ions) SRO-Fe often persist and resist transformations to more crystalline phases (Eusterhues et al. 2008; Frierdich et al. 2015). However, SRO-Fe is susceptible to reductive dissolution converting ferric

iron (Fe^{III}) to ferrous phases (Fe^{II}) when O_2 becomes limiting and microsites in the soils become anoxic (Echigo et al. 2012; Hallberg et al. 2011).

Microorganisms are capable of catalyzing iron reduction by reductive dissolution under anoxic conditions when sufficient labile soil organic carbon is present (Lovley 2000). Microbial iron reduction rates are influenced by the crystallinity of Fe minerals (Bonneville et al. 2004; Roden and Zachara 1996), with lower crystallinity iron minerals (i.e., SRO) favored over more crystalline forms (Jones et al. 2009; Konhauser et al. 2011). In redox fluctuating systems, ferrous iron can be oxidized abiotically, or via the metabolism of iron-oxidizing bacteria, in the presence of oxygen or nitrate (Davison and Seed 1983; Klueglein and Kappler 2013; Straub et al. 1996).

Previous studies have shown that soil redox oscillations can influence the bacterial reduction of iron oxyhydroxides and iron speciation (Ginn et al. 2017; Komlos et al. 2007; Liptzin and Silver 2009; Mejia et al. 2016; Thompson et al. 2006) as well as alter carbon cycling in soils (Coby et al. 2011). However, the influence of different redox fluctuation patterns on iron reduction rates are only beginning to be understood (Tomaszewski et al. 2016; Vogelsang et al. 2016). Most recently, Ginn et al. (2017) showed that redox fluctuations with oscillation periods (e.g., frequencies) of 3.5, 7, and 14 days (oxic:anoxic ratio of 1:6) all stimulated an increase in the Fe reduction rates as the experiment progressed, based on the formation of rapidly reducible Fe(III) phases. The numerical modeling in Ginn et al. (2017) suggested fluctuation frequency also influenced iron reduction rates, with long frequency fluctuations leading to slower instantaneous Fe reduction rates than shorter frequency fluctuations. The Ginn et al. (2017) numerical model ties microbial growth to Fe reduction rate, which is strongly influenced by the presence of rapidly-reducible Fe^{III}. The shorter frequency oscillations result in frequent pulsing of rapidly-reducible Fe^{III} and this generates higher microbial growth in the numerical model and

hence higher instantaneous Fe^{II} reduction rates. However, Ginn et al. (2017) did not sample enough times during the longer frequency cycles to directly confirm this via observation.

Therefore, we sought to test the hypothesis that iron reduction rates will be faster during redox fluctuations with shorter oscillation periods than in those with longer oscillation periods. To test this hypothesis we imposed redox oscillations at two periods (280- and 70-h) on soil slurries prepared in the same way as Ginn et al. (2017), which included beginning with similar air-dried soils from the valley site in the Bisley watershed in the Luquillo Critical Zone Observatory (Puerto Rico). We began the treatments after subjecting all replicates to a pre-conditioning phase of 26 days of redox fluctuations to accommodate the overall rise in Fe availability previously observed (Ginn et al. 2017). During the experiments we tracked HCl-extractable Fe^{II} with sufficient frequencies to establish the Fe^{II} production rate. We also measured carbon and nitrogen throughout the experiment.

2.2. Material and Methods

2.2.1. Field site and soil characterization

A bulk soil sample of ~1 kg from the top 10 cm was collected in the lower valley portion from the Bisley Research Watershed site of the Luquillo Experimental Forest (LEF) in the Luquillo Critical Zone Observatory (LCZO). The top 10 cm of soil is the most biogeochemical active for iron and carbon dynamics in this environment, and it has been extensively studied by several other researchers (Hall et al. 2016; Scatena 1989; Silver et al. 1999). After sample collection, the soil was air dried for 24 h, sieved through a 2 mm screen, homogenized and stored at 22 ^{o}C. Total iron content was determined by ICP-MS following a Li-metaborate fusion (Hossner et al. 1996). Soil texture was determined by a Beckman Coulter LS 13 320 Laser

diffraction Particle Size Analyzer (Muggler et al. 1997; Schulte et al. 2016; Zobeck 2004). The soil collected from Bisley is a Ultisol formed from volcanic parent material (Thomé 1954) and is weakly acidic (pH ~5.5), as described with more details by Peretyazhko and Sposito (2005). The mineral composition of our soil includes quartz, kaolinite, chlorite and goethite determined by x-ray diffraction (Tishchenko et al. 2015).

2.2.2. Redox oscillation experiments

Systematic redox oscillations were imposed on the soil over 49 days in a 1:10 soil:water suspension. Each experimental unit (vessel) consisted of 4.5 g (dry-weight) of soil suspended in a 2 mM KCl and 10 mM MES (2-N-morpholino-ethanesulfonic acid), buffered at pH 5.5 (similar to the native soil pH), with a 45 g final suspension mass. The KCl solution was used as a background electrolyte to retard mineral dissolution and approximate the ionic strength of the native soil solution (Gimsing and Borggaard 2001; Melamed and Boas 1998). The MES increased the C and N by ~10% in the final soil suspension. Buffering the slurries near the native soil pH of 5.5 isolates the effect Fe oxidation/reduction from potentially confounding effect of associated pH shifts (Thompson et al. 2006); initial pH values were similar to those at the end of each treatment (5.5 ± 0.2).

We conceptualize that a typical redox cycle contains three fundamental parameters: amplitude, oscillation period, and the $\tau_{oxic}/\tau_{anoxic}$ ratio (Fig. 1.1). The amplitude represents the magnitude of the redox fluctuation; for instance, a strict oxic/anoxic redox cycle would have an amplitude of 21% O_2. The oscillation period is the time it takes for a full redox cycle to be completed, going under both oxic and anoxic conditions. Finally, the $\tau_{oxic}/\tau_{anoxic}$ ratio is the proportion of time soils are under oxic and anoxic conditions.

All redox oscillation characteristics were held constant except the oscillation period, fixing the oscillation amplitude (set to switch between 0% O_2 during τ_{anoxic} and ~21% O_2 during τ_{oxic}) and the $\tau_{oxic}/\tau_{anoxic}$ ratio (set at 1:6). To impose anoxic conditions, we placed the soil slurries on a shaker at 250 rpm (Eberbach 6130, Ann Arbor, MI) in a 95%:5% (N_2:H_2) glovebox Coy chamber (0% O_2); whereas to impose oxic conditions, we placed the slurries on a similar 250 rpm shaker in the laboratory atmosphere (~21% O_2). Within 1 hour after exposing soil slurries to oxic conditions we verified the dissolved O_2 (DO) value was greater than 7.0 mg L^{-1}, using a Hach (USA) DO meter.

Prior to implementing different redox oscillation periods (short and long), we pre-conditioned the four replicates through two cycles with periods of 168 h redox oscillations (144 h anoxic + 24 h oxic) followed by one 280 h redox oscillation (240 h anoxic + 40 h oxic) (Table 2.1), which was extended to evaluate if any Fe^{II} plateau occurred as was observed after 4 days by Ginn et al. (2017). This pre-conditioning treatment was designed to acclimate the microbes within the prepared air-dried soil to shifts in redox conditions and overcome an initial increase in Fe^{III}-reactivity as observed by Ginn et al (2017) resulting from the formation of rapidly-reducible SRO Fe phases during Fe oxidation/reduction cycles. After three full redox cycles (at 616 h or ~26 d into the experiment), we split the replicates into either (i) a 280 h (11.7 d) oscillation period (240 h anoxic + 40 h oxic) or (ii) a 70 h (2.9 d) oscillation period (60 h anoxic + 10 h oxic) (Table 2.1).

Iron reduction was monitored by measuring Fe^{II} in a 0.5 M HCl-extract of the slurry at intervals ranging from 12 h to 4 days throughout the experiment (sampling a total of 41 times), using wide orifice pipette tips to avoid soil particle size exclusion (Ginn et al. 2014). From each vessel containing 45 g of soil suspension, we withdrew 0.5 mL, then added 1.0 mL of 0.75 M

HCl, i.e., suspending 0.05 g (dry weight equivalent) of the sample in 1.5 mL of 0.5 M HCl. The suspension was then shaken for 2 h on a horizontal shaker, followed by centrifugation at 11,000 rcf (relative centrifugal force) for 10 min. The supernatant was carefully removed and analyzed for Fe^{II} using a modified ferrozine protocol proposed by Thompson et al. (2006), with the buffer solution set at pH 8.2 to accommodate the higher acid content. Ferrous iron concentrations were derived from absorbance measured at 562 nm on a Shimadzu-1700 spectrophotometer. The results were normalized to mmol of Fe^{II} per kg of soil by weighing the dry soil pellets after centrifugation.

Carbon was measured in the supernatant of the 0.5M HCl extracts on a Shimadzu 5050 TOC analyzer. The resulting pellet from the extract was then freeze-dried and analyzed for total carbon and nitrogen via combustion in a CHN Carlo Erba Elemental Analyzer.

2.2.3 Statistical Analysis

Iron reduction rates were compared between each cycle and treatment using a Repeated Measures ANOVA, with the LME function (Dalgaard 2008) of the R software. For carbon and nitrogen content, we used an ANOVA in JMP (SAS Institute) to compare data between treatments. Errors bars are included for replicates, which represent either four replicates (pre-treatment) or duplicates, once the treatments were initiated.

2.3. Results and Discussion

2.3.1. Iron dynamics

Throughout the experiment and in all treatments, the HCl-extractable Fe^{II} concentrations increased during the τ_{anoxic} and sharply decreased during τ_{oxic} (Fig. 2.1). Under anoxic conditions,

Fe^{III} is reduced to Fe^{II}, and under oxic conditions most of the Fe^{II} was re-oxidized and likely re-precipitated as SRO iron minerals. Consistent with prior work on fluctuating redox conditions in these soils when initiated from an air-dried state (Ginn et al. 2017), Fe^{II} concentrations under anoxia increased during the first month of incubation. In our experiment, this increment occurred during the pre-conditioning phase of the experiment—consisting of two 168 h cycles and one 280 h cycle (Table 2.1). Concentrations of Fe^{II} began at 3.5 mmol kg^{-1} soil, reaching 38.9 mmol kg^{-1} soil at the end of the first τ_{anoxic}, and rising to 96.5 mmol kg^{-1} soil by the end of the pre-conditioning phase (Fig. 2.1), which was ~10% of total Fe (1163 mmol kg^{-1}) (Wilmoth 2016).

After the pre-conditioning stage, maximum τ_{anoxic} Fe^{II} concentrations remained similar for the 280-h cycle. However, Fe^{II} concentrations did not exhibit a plateau (decrease to near zero slope), even in the third pre-conditioning cycle when the τ_{anoxic} was increased to 240 h (10 d). In contrast, using similar soils, Ginn et al. (2014, and 2017) found that Fe^{II} concentrations plateaued after 7 d during an initial anoxic period, and observed that after a month of redox fluctuations imposed on P-amended soils, Fe^{II} concentrations plateaued within 4 days of anoxic exposure. As observed previously (Ginn et al. 2017), the baseline Fe^{II} during the τ_{oxic} in each cycle increased over the course of the experiment from an initial concentration of 3.5 mmol kg^{-1} soil to 28.9 mmol kg^{-1} soil at the end of the second pre-conditioning τ_{oxic} and then stabilized at 25 ± 5 mmol kg^{-1} soil for the remainder of the experiment.

2.3.2. Iron reduction rates

Iron reduction rates, calculated in mmol Fe^{II} kg^{-1} soil h^{-1} from the slope of the net Fe^{II} production per unit time during each τ_{anoxic} intervals, varied over the course of the experiment. During the pre-conditioning, iron reduction rates were 0.21 ± 0.12, 0.48 ± 0.18, and 0.31 ± 0.11

mmol kg^{-1} h^{-1} for the first, second, and third cycles, respectively (Fig. 2.2). Rates increased from the first to the second cycle (p=0.042) and then remained similar in the third cycle (p=0.319). After pre-conditioning, we observed nearly constant rates of 0.25 ± 0.14 and 0.26 ± 0.04 mmol kg^{-1} h^{-1} for the longer period treatment (280 h), which comprised τ_{ox} of 40 h and were equal within error to the three pre-conditioning cycles (Fig. 2.2). Thus, maintaining redox oscillation for long period oscillations (280 h) will not likely alter iron reduction rates beyond the initial increase in the pre-conditioning period. This is consistent with the findings for the un-amended treatment of Ginn et al. (2017).

When the short period oscillations (70 h) were initiated, iron reduction rates were at first similar to the pre-conditioning and longer period treatments, but then significantly increased over the course of the experiment from 0.18 to 0.97 mmol kg^{-1} h^{-1} (Fig. 2.1 and 2.2). The last three short-period τ_{anoxic} had rates higher and significantly different than any other rate in the experiment (Fig. 2.2, last three green points). We also noted that the Fe^{II} concentration at the end of the last short period was equal within error to the Fe^{II} concentration in the long period (27 ± 1.6 and 25 ± 1.7 mmol kg^{-1}, respectively).

The rates of iron reduction we observe in these treatments are comparable to prior work from similar soils (Table 2.2). DeAngelis et al. (2010) found iron reduction rates varying from 0.18 to 0.38 mmol kg^{-1} h^{-1} during a redox fluctuation experiment (8 d oscillation period with τ_{anoxic} and τ_{anoxic} both 4 d) using intact soil cores from the Luquillo CZO in Puerto Rico (upper 10 cm, near our sampling location). Likewise, Ginn et al. (2017) found modeled iron reduction rates likely varied from 0.11 to 0.96 mmol kg^{-1} h^{-1} during a 56-d redox fluctuation experiment (period: 3.5 d to 14 d with a constant τ_{oxic}:τ_{anoxic} ratio of 1:6) using slurred soils with and without phosphorus amendments. Rates of iron reduction in the DeAngelis' work are similar to our long

oscillation period rates; while rates in the Ginn's study also suggest iron reduction rates could be higher when redox oscillation period is shorter (Table 2.2). In all three studies there is also some variation and/or increase in the baseline of Fe^{II} concentration during the τ_{oxic}.

Additionally, in a different experiment setup using synthesized iron minerals in solution, Mejia et al. (2016) found that Fe^{II} concentrations in the aqueous phase have the highest amplitude of variation for a redox oscillation (using O_2 as oxidant agent). In the Mejia et al. (2016) study, iron reduction rates increased from the first to the second cycle but decreased in the third and fourth (last) cycles. Iron reduction rates from our long treatment (10 d anoxic + 1.67 d oxic) were comparable to rates of the long cycles of 19 d anoxic + 3 d oxic in the Mejia et al. (2016) study.

2.3.3. Why do iron reduction rates change?

Based on our results, we postulate two reasons for the higher iron reduction rates in the short oscillation period (70 h) treatment compared to the long oscillation period (280 h):
(1) When the length of exposure to oxic conditions (τ_{oxic}) becomes short enough (e.g., 10 hours), the Fe reducers can maintain their capacity (activity) to quickly respond to rapidly-reducible Fe phases. Iron reduction in these soils is likely catalyzed by dissimilatory iron reducing bacteria (DeAngelis et al. 2010; Dubinsky et al. 2010; Hall et al. 2016; Wilmoth 2016). There is some evidence that native microorganisms in these soils are adapted to redox fluctuations with periods less than one week (Pett-Ridge et al. 2006). It is unclear how long an oxic event needs to be to stimulate either a change in the microbial population or a shift in metabolic machinery such that the population is less able to resume Fe reduction immediately when anoxic conditions return. In the case of the short oscillation periods of 70 h (60 h anoxic and 10 h oxic), where the redox

period is likely shorter than the microbial generation time, the microbes are likely using an arrangement of facultative metabolisms and stimulation/suppression of obligate metabolism (DeAngelis et al. 2010).

(2) Iron reducing microorganisms are stimulated by the repeated pulsing of a *de novo* supply of reactive electron acceptor, Fe^{III}. Short-range-order (SRO) Fe^{III} phases are often formed during rapid oxidation events, and these labile forms of iron are rapidly utilized as electron acceptors by iron reducing bacteria. The resultant lability or reactivity of SRO Fe phases is based on the phases' initial crystallinity, but also the amount of exposure to aqueous Fe^{II} (Boland et al. 2014; Handler et al. 2009). Thus, longer redox fluctuation periods, which expose SRO phases to Fe(II) for longer times, should yield less labile SRO phases than correspondingly short redox fluctuation periods. Indeed, there is some evidence from the literature to support this (Couture et al. 2015; Thompson et al. 2006; Yang et al. 2012). For instance, Mejia et al (2016) found ferrihydrite or lepidocrocite were primarily transformed into magnetite, over a 105-day redox oscillation experiment with long periods (19 d anoxic + 3 d oxic). Likewise, ferrihydrite introduced to a redox dynamic soil with mineral bags for 12 months was transformed into crystalline iron phases (hematite, goethite, etc.) (Vogelsang et al. 2016). However, Tomaszewski et al. (2016) found a reactive pool of SRO Fe^{III} persisted—within a mixture of different iron phases—over several redox oscillation cycles with short periods (τ_{anoxic} = 48 h). In addition, if the most reactive Fe^{III} phases are formed during a recent oxidation event (Ginn et al. 2017), more frequent redox fluctuations should provide a higher yield (concentration x time) of labile Fe^{III} electron acceptor over any given length of time. Indeed, this frequent re-generation of reactive Fe^{III}, is what drove higher simulated Fe reduction rates in the Ginn et al. (2017) numerical model.

2.3.4. Carbon and nitrogen dynamics

The initial carbon and nitrogen content of our soil (solid-phase, air-dried) was 46 ± 5 mg C g^{-1} soil and 2.6 ± 0.3 mg N g^{-1} soil, respectively. The addition of the MES buffer solution increased the C and N by ~10% (to a total of 51 ± 6 mg C g^{-1} soil and 2.9 ± 0.3 mg N g^{-1} soil, respectively) at the beginning of the slurry experiment. Both solid-phase and total C (solid plus HCl-extractable and aqueous OC) remained unchanged during the pre-conditioning treatments ($p=0.320$). Total C significantly decreased about 45% from the beginning and the end of both long and short oscillation period treatments, from 56 to 30 mg g^{-1} and from 53 to 29 mg g^{-1}, respectively (Fig. 2.3, Table 2.3). Aqueous and 0.5M HCl-extractable organic carbon (abbreviated extractable-OC) corresponded to between 12 and 33% of the total C and remained nearly constant throughout the experiment across all treatments, with no significant change for either treatment (Table 2.3). Solid phase nitrogen content followed the same trend as carbon: near constant or a minor decrease during the pre-conditioning treatment but decreasing concentrations for both treatments in the latter half of the experiment (Fig. 2.4 and Table 2.3). The solid phase C:N ratios increased over the course of the experiment from 11 to 14, 15 to 21, and 14 to 20, for the pre-conditioning, long, and short oscillation periods treatments, respectively. Losses of total C did not correlate with the differences in Fe reduction rates (R^2 = 0.144), suggesting that the majority of C mineralization was not directly linked to Fe metabolism and was not differentiated between the long and short oscillation period treatments. Indeed, considering a stoichiometry for dissimilatory iron reduction coupled to CO_2 production of 4 moles of Fe^{III} reduced per mol CO_2 produced (Roden and Wetzel 1996), we estimate that respiratory Fe^{III} reduction could explain only 1 ± 0.1 mg C-CO_2 g^{-1} of soil over the whole course

of the experiment, which is substantially lower than the measured loss of ~25 mg g^{-1} for all treatments.

This large loss of soil C and N over a short experimental timeframe (Fig. 2.3 and 2.4) is difficult to explain. We repeated the solid-phase C and N measurements in a different lab but got the same results. We also analyzed the particle size distribution of the dried soil pellets from HCl-extracts at select sampling points to evaluate the potential for selective removal of fine particles during repeated pipetting. However, clay and silt particle size distribution did not change considerably over the course of the experiment—although clay and silt were higher in most of the slurry samples than in the bulk initial/native soil—and there was no correlation between the amount of silt and clay particles and soil carbon content (Table 2.4). Whatever the mechanism, the processes resulting in the bulk of C loss are not as sensitive to differences in the length of τ_{anoxic} and τ_{oxic} as are the processes influencing the rate of Fe reduction (Fig. 2.1 and 2.2).

Fluctuations in soil O_2 concentrations can induce changes in the mineralization rates of soil organic carbon (Marumoto et al. 1982; McNicol and Silver 2014; Reddy et al. 1986). Periodic changes in soil redox potential can lead to faster soil organic matter decomposition compared to more constant redox conditions (Aller 1994; Aller 2004), but more commonly researchers find carbon decomposition is higher under oxic conditions than anoxic or redox fluctuating conditions (Burdige 2007; Hedges and Keil 1995), and in some cases, no difference in CO_2 or CH_4 production is observed between redox states (DeAngelis et al. 2010).

During our experiment, total carbon content and solid phase nitrogen content remained nearly constant during both the τ_{anoxic} and τ_{oxic} of the pre-conditioning (Fig. 2.3 and 2.4, Table 2.3), before decreasing later after the initiation of diverging oscillation period treatments. So, any

explanation of this carbon loss should incorporate this apparent lag in rapid C and N mineralization. We propose two potential mechanisms:

The imposition of the longer τ_{oxic} of 40 h, right before the beginning of the long and short treatments, could have triggered the initial substantial soil carbon loss. Prior to mineralization, organic matter is decomposed through depolymerization reactions (Hedges and Keil 1995; Megonigal et al. 2005), which is catalyzed much faster via oxidative enzymes generated by aerobic microbes than by the hydrolytic enzymes produced in the absence of O_2 (Sinsabaugh 2010). Oxidative enzyme production might have been enhanced during the longer 40 h oxic interval preceding the long and short oscillation treatments and this may have accelerated depolymerization of the organic matter (Keiluweit et al. 2016) compared to the previous two 24 h oxic intervals. Once organic matter has been decomposed to low molecular weight compounds, it would likely be degraded quickly under either aerobic or anaerobic metabolism.

Alternatively, it is well known that oxidation of Fe^{II} via O_2 produces reactive oxygen species (ROS) that can rapidly degrade organic compounds. This mechanism has been documented via artificial additions of Fe^{II} prior to an oxidation event in soils collected from this field site (Hall and Silver 2013) and has been deployed in redox fluctuating bioreactors to rapidly degrade organic pollutants (Sekar and DiChristina 2014). By the second and third τ_{anoxic} of the pre-conditioning period, larger standing pools of Fe^{II} were present and this may have induced higher levels of ROS in the reactors, which could have promoted both mineralization and/or depolymerization of the organic matter.

2.4. Conclusions

The characteristics of redox fluctuations, length of time under oxic or anoxic conditions (τ_{anoxic} and τ_{oxic}), and the rate of transition between anoxic and oxic states (fluctuation amplitude) are important determinants of iron and organic matter cycling in soils. Our main finding—that iron reduction rates increased substantially when short oscillation periods are imposed on a system acclimated to a longer redox oscillation periods—could have important implications for natural and agro-ecosystem iron dynamics if also present in field situations. Rainfall and irrigation patterns that generate short redox fluctuations (Favre et al. 2002; Hall et al. 2013; Liptzin et al. 2011; Silver et al. 1999)—frequent, short, intense water inputs rather than mild, longer input events with long dry periods—will likely lead to more rapid iron reduction rates through their impact on soil moisture. This may be especially important in upland soils with abundant aggregates, which often contain low-O_2 microsites that support iron reduction (Hall et al. 2016; Keiluweit et al. 2016). These aggregates may serve this function even under otherwise bulk oxic conditions and can become hotspots for both carbon loss or accumulation (Porras et al. 2017; Thaymuang et al. 2013; Weber et al. 2006; Yu et al. 2017) depending on the frequency and time length of the redox fluctuations (i.e., oscillation period, $\tau_{oxic,}$ τ_{anoxic}). Higher rates of iron reduction could lead to increases in nutrient availability, e.g., phosphorus (Chacon et al. 2006; Novais and Smyth 1999; Zak et al. 2010), and potentially suppression of methane emissions (Ettwig et al. 2016; Teh et al. 2008) both in natural systems and in irrigated systems, like rice paddies (Kostka et al. 2002; Takai and Kamura 1966; Yao et al. 1999). Placing attention on the dynamics of redox conditions (e.g., length and transition timing) will likely yield important advances in our understanding of carbon and nutrient dynamics in soils, as nearly all soils are exposed to some measure of redox variability.

2.5. References

Aller RC (1994) Bioturbation and remineralization of sedimentary organic matter: effects of redox oscillation. Chemical Geology 114:331-345

Aller RC (2004) Conceptual models of early diagenetic processes: the muddy seafloor as an unsteady, batch reactor. Journal of Marine Research 62:815-835

Boland DD, Collins RN, Miller CJ, Glover CJ, Waite TD (2014) Effect of solution and solid-phase conditions on the Fe (II)-accelerated transformation of ferrihydrite to lepidocrocite and goethite. Environmental science & technology 48:5477-5485

Bonneville S, Van Cappellen P, Behrends T (2004) Microbial reduction of iron (III) oxyhydroxides: effects of mineral solubility and availability. Chemical Geology 212:255-268

Burdige DJ (2007) Preservation of organic matter in marine sediments: controls, mechanisms, and an imbalance in sediment organic carbon budgets? Chemical reviews 107:467-485

Chacon N, Silver WL, Dubinsky EA, Cusack DF (2006) Iron reduction and soil phosphorus solubilization in humid tropical forests soils: the roles of labile carbon pools and an electron shuttle compound. Biogeochemistry 78:67-84

Cleveland CC, Wieder WR, Reed SC, Townsend AR (2010) Experimental drought in a tropical rain forest increases soil carbon dioxide losses to the atmosphere. Ecology 91:2313-2323

Coby AJ, Picardal F, Shelobolina E, Xu H, Roden EE (2011) Repeated anaerobic microbial redox cycling of iron. Applied and environmental microbiology 77:6036-6042

Colombo C, Palumbo G, He J-Z, Pinton R, Cesco S (2014) Review on iron availability in soil: interaction of Fe minerals, plants, and microbes. Journal of soils and sediments 14:538-548

Cornell RM, Schwertmann U (2003) The iron oxides: structure, properties, reactions, occurrences and uses. John Wiley & Sons,

Couture R-M, Charlet L, Markelova E, Madé Bt, Parsons CT (2015) On–off mobilization of contaminants in soils during redox oscillations. Environmental science & technology 49:3015-3023

Dalgaard P (2008) Introductory statistics with R. Springer Science & Business Media,

Davison W, Seed G (1983) The kinetics of the oxidation of ferrous iron in synthetic and natural waters. Geochimica et Cosmochimica Acta 47:67-79

DeAngelis KM, Silver WL, Thompson AW, Firestone MK (2010) Microbial communities acclimate to recurring changes in soil redox potential status. Environmental Microbiology 12:3137-3149

Dubinsky EA, Silver WL, Firestone MK (2010) Tropical forest soil microbial communities couple iron and carbon biogeochemistry. Ecology 91:2604-2612

Echigo T, Aruguete DM, Murayama M, Hochella MF (2012) Influence of size, morphology, surface structure, and aggregation state on reductive dissolution of hematite nanoparticles with ascorbic acid. Geochimica et Cosmochimica Acta 90:149-162

Ettwig KF, Zhu B, Speth D, Keltjens JT, Jetten MS, Kartal B (2016) Archaea catalyze iron-dependent anaerobic oxidation of methane. Proceedings of the National Academy of Sciences 113:12792-12796

Eusterhues K, Rumpel C, Kögel-Knabner I (2005) Organo-mineral associations in sandy acid forest soils: importance of specific surface area, iron oxides and micropores. European Journal of Soil Science 56:753-763

Eusterhues K et al. (2008) Characterization of ferrihydrite-soil organic matter coprecipitates by X-ray diffraction and Mossbauer spectroscopy. Environmental science & technology 42:7891-7897

Favre F, Tessier D, Abdelmoula M, Genin J, Gates W, Boivin P (2002) Iron reduction and changes in cation exchange capacity in intermittently waterlogged soil. European Journal of Soil Science 53:175-183

Frierdich AJ, Helgeson M, Liu C, Wang C, Rosso KM, Scherer MM (2015) Iron atom exchange between hematite and aqueous Fe (II). Environmental science & technology 49:8479-8486

Gimsing AL, Borggaard OK (2001) Effect of KCl and CaCl 2 as background electrolytes on the competitive adsorption of glyphosate and phosphate on goethite. Clays and Clay Minerals 49:270-275

Ginn BR, Habteselassie MY, Meile C, Thompson A (2014) Effects of sample storage on microbial Fe-reduction in tropical rainforest soils. Soil Biology and Biochemistry 68:44-51

Ginn BR, Meile C, Wilmoth J, Tang Y, Thompson A (2017) Rapid iron reduction rates are stimulated by high-amplitude redox fluctuations in a tropical forest soil. Environmental Science & Technology 51:3250-3259

Hall SJ, Liptzin D, Buss HL, DeAngelis K, Silver WL (2016) Drivers and patterns of iron redox cycling from surface to bedrock in a deep tropical forest soil: a new conceptual model. Biogeochemistry 130:177-190

Hall SJ, McDowell WH, Silver WL (2013) When wet gets wetter: decoupling of moisture, redox biogeochemistry, and greenhouse gas fluxes in a humid tropical forest soil. Ecosystems 16:576-589

Hall SJ, Silver WL (2013) Iron oxidation stimulates organic matter decomposition in humid tropical forest soils. Global change biology 19:2804-2813

Hallberg KB, Grail BM, Du Plessis CA, Johnson DB (2011) Reductive dissolution of ferric iron minerals: a new approach for bio-processing nickel laterites. Minerals Engineering 24:620-624

Handler RM, Beard BL, Johnson CM, Scherer MM (2009) Atom exchange between aqueous Fe (II) and goethite: an Fe isotope tracer study. Environmental science & technology 43:1102-1107

Hansen DJ, McGuire JT, Mohanty BP (2011) Enhanced biogeochemical cycling and subsequent reduction of hydraulic conductivity associated with soil-layer interfaces in the vadose zone. Journal of environmental quality 40:1941-1954

Hedges JI, Keil RG (1995) Sedimentary organic matter preservation: an assessment and speculative synthesis. Marine chemistry 49:81-115

Henneberry YK, Kraus TE, Nico PS, Horwath WR (2012) Structural stability of coprecipitated natural organic matter and ferric iron under reducing conditions. Organic geochemistry 48:81-89

Hossner L et al. (1996) Dissolution for total elemental analysis. Methods of soil analysis. Part 3-chemical methods.:49-64

Jones AM, Collins RN, Rose J, Waite TD (2009) The effect of silica and natural organic matter on the Fe (II)-catalysed transformation and reactivity of Fe (III) minerals. Geochimica et Cosmochimica Acta 73:4409-4422

Kämpf N, Scheinost AC, Schulze DG (2011) Oxide minerals in soils. In: Handbook of Soil Sciences: Properties and Processes, Second Edition. CRC Press, pp 1-34

Keiluweit M, Nico PS, Kleber M, Fendorf S (2016) Are oxygen limitations under recognized regulators of organic carbon turnover in upland soils? Biogeochemistry 127:157-171

Klueglein N, Kappler A (2013) Abiotic oxidation of Fe (II) by reactive nitrogen species in cultures of the nitrate-reducing Fe (II) oxidizer Acidovorax sp. BoFeN1–questioning the existence of enzymatic Fe (II) oxidation. Geobiology 11:180-190

Komlos J, Kukkadapu RK, Zachara JM, Jaffe PR (2007) Biostimulation of iron reduction and subsequent oxidation of sediment containing Fe-silicates and Fe-oxides: Effect of redox cycling on Fe (III) bioreduction. Water research 41:2996-3004

Konhauser KO, Kappler A, Roden EE (2011) Iron in microbial metabolisms. Elements 7:89-93

Kostka JE, Dalton DD, Skelton H, Dollhopf S, Stucki JW (2002) Growth of iron (III)-reducing bacteria on clay minerals as the sole electron acceptor and comparison of growth yields on a variety of oxidized iron forms. Applied and Environmental Microbiology 68:6256-6262

Lipson DA, Raab TK, Goria D, Zlamal J (2013) The contribution of Fe (III) and humic acid reduction to ecosystem respiration in drained thaw lake basins of the Arctic Coastal Plain. Global Biogeochemical Cycles 27:399-409

Liptzin D, Silver WL (2009) Effects of carbon additions on iron reduction and phosphorus availability in a humid tropical forest soil. Soil Biology and Biochemistry 41:1696-1702

Liptzin D, Silver WL, Detto M (2011) Temporal Dynamics in Soil Oxygen and Greenhouse Gases in Two Humid Tropical Forests. Ecosystems 14:171-182 doi:10.1007/s10021-010-9402-x

Lovley DR (2000) Fe (III) and Mn (IV) reduction. In: Environmental microbe-metal interactions. American Society of Microbiology, pp 3-30

Lovley DR, Holmes DE, Nevin KP (2004) Dissimilatory fe (iii) and mn (iv) reduction. Advances in microbial physiology 49:219-286

Lovley DR, Phillips EJ (1988) Novel mode of microbial energy metabolism: organic carbon oxidation coupled to dissimilatory reduction of iron or manganese. Applied and environmental microbiology 54:1472-1480

Marumoto T, Anderson J, Domsch K (1982) Mineralization of nutrients from soil microbial biomass. Soil Biology and Biochemistry 14:469-475

McNicol G, Silver WL (2014) Separate effects of flooding and anaerobiosis on soil greenhouse gas emissions and redox sensitive biogeochemistry. Journal of Geophysical Research: Biogeosciences 119:557-566

Megonigal J, Mines M, Visscher P (2005) Linkages to Trace Gases and Aerobic Processes. Biogeochemistry 8:350-362

Mejia J, Roden EE, Ginder-Vogel M (2016) Influence of oxygen and nitrate on Fe (hydr) oxide mineral transformation and soil microbial communities during redox cycling. Environmental science & technology 50:3580-3588

Melamed R, Boas RV (1998) Phosphate-background electrolyte interaction affecting the transport of mercury through a Brazilian Oxisol. Science of the total environment 213:151-156

Mikutta R, Kleber M, Torn MS, Jahn R (2006) Stabilization of soil organic matter: association with minerals or chemical recalcitrance? Biogeochemistry 77:25-56

Muggler C, Pape T, Buurman P (1997) Laser grain-size determination in soil genetic studies 2. Clay content, clay formation, and aggregation in some brazilian oxisols. Soil Science 162:219-228

Novais R, Smyth T (1999) Phosphorus in soil and plant in tropical conditions. Federal University of Viçosa, Viçosa, MG, Brazil 399

Peretyazhko T, Sposito G (2005) Iron (III) reduction and phosphorous solubilization in humid tropical forest soils. Geochimica et Cosmochimica Acta 69:3643-3652

Pett-Ridge J, Silver WL, Firestone MK (2006) Redox fluctuations frame microbial community impacts on N-cycling rates in a humid tropical forest soil. Biogeochemistry 81:95-110

Porras RC, Pries CEH, McFarlane KJ, Hanson PJ, Torn MS (2017) Association with pedogenic iron and aluminum: effects on soil organic carbon storage and stability in four temperate forest soils. Biogeochemistry:1-13

Reddy K, Feijtel T, Patrick Jr W (1986) Effect of soil redox conditions on microbial oxidation of organic matter. In: The role of organic matter in modern agriculture. Springer, pp 117-156

Roden EE, Wetzel RG (1996) Organic carbon oxidation and suppression of methane production by microbial Fe (III) oxide reduction in vegetated and unvegetated freshwater wetland sediments. Limnology and Oceanography 41:1733-1748

Roden EE, Zachara JM (1996) Microbial reduction of crystalline iron (III) oxides: Influence of oxide surface area and potential for cell growth. Environmental Science & Technology 30:1618-1628

Scatena FN (1989) An introduction to the physiography and history of the Bisley Experimental Watersheds in the Luquillo Mountains of Puerto Rico. Gen. Tech. Rep. SO-72. New Orleans, LA: US Dept of Agriculture, Forest Service, Southern Forest Experiment Station. 22 p. 72

Schulte P et al. (2016) Influence of HCl pretreatment and organo-mineral complexes on laser diffraction measurement of loess–paleosol-sequences. Catena 137:392-405

Schuur EA, Chadwick OA, Matson PA (2001) Carbon cycling and soil carbon storage in mesic to wet Hawaiian montane forests. Ecology 82:3182-3196

Sekar R, DiChristina TJ (2014) Microbially driven Fenton reaction for degradation of the widespread environmental contaminant 1, 4-dioxane. Environmental science & technology 48:12858-12867

Silver WL, Herman DJ, Firestone MK (2001) Dissimilatory nitrate reduction to ammonium in upland tropical forest soils. Ecology 82:2410-2416

Silver WL, Lugo A, Keller M (1999) Soil oxygen availability and biogeochemistry along rainfall and topographic gradients in upland wet tropical forest soils. Biogeochemistry 44:301-328

Sinsabaugh RL (2010) Phenol oxidase, peroxidase and organic matter dynamics of soil. Soil Biology and Biochemistry 42:391-404

Sposito G (2008) The chemistry of soils. Oxford university press,

Straub KL, Benz M, Schink B, Widdel F (1996) Anaerobic, nitrate-dependent microbial oxidation of ferrous iron. Applied and Environmental Microbiology 62:1458-1460

Takai Y, Kamura T (1966) The mechanism of reduction in waterlogged paddy soil. Folia Microbiologica 11:304-313

Teh YA, Dubinsky EA, Silver WL, Carlson CM (2008) Suppression of methanogenesis by dissimilatory Fe (III)-reducing bacteria in tropical rain forest soils: Implications for ecosystem methane flux. Global Change Biology 14:413-422

Thaymuang W, Kheoruenromne I, Suddhipraharn A, Sparks DL (2013) The role of mineralogy in organic matter stabilization in tropical soils. Soil Science 178:308-315

Thomé RCM (1954) A Survey of the Geology of Puerto Rico. University of Puerto Rico, Agricultural Experiment Station,

Thompson A, Chadwick OA, Rancourt DG, Chorover J (2006) Iron-oxide crystallinity increases during soil redox oscillations. Geochimica et Cosmochimica Acta 70:1710-1727

Tishchenko V, Meile C, Scherer MM, Pasakarnis TS, Thompson A (2015) Fe 2+ catalyzed iron atom exchange and re-crystallization in a tropical soil. Geochimica et Cosmochimica Acta 148:191-202

Tomaszewski EJ, Cronk SS, Gorski CA, Ginder-Vogel M (2016) The role of dissolved Fe (II) concentration in the mineralogical evolution of Fe (hydr) oxides during redox cycling. Chemical Geology 438:163-170

Vogelsang V, Fiedler S, Jahn R, Kaiser K (2016) In-situ transformation of iron-bearing minerals in marshland-derived paddy subsoil. European Journal of Soil Science 67:676-685

Weber KA, Achenbach LA, Coates JD (2006) Microorganisms pumping iron: anaerobic microbial iron oxidation and reduction. Nature Reviews Microbiology 4:752-764

Wilmoth JL (2016) Effects of redox-cycling on iron-mineral transformations and metatranscriptome of iron (III)-reducing bacteria in a humid tropical forest soil. Doctoral Dissertation. University of Georgia

Yang J, Kukkadapu RK, Dong H, Shelobolina ES, Zhang J, Kim J (2012) Effects of redox cycling of iron in nontronite on reduction of technetium. Chemical Geology 291:206-216

Yao H, Conrad R, Wassmann R, Neue H (1999) Effect of soil characteristics on sequential reduction and methane production in sixteen rice paddy soils from China, the Philippines, and Italy. Biogeochemistry 47:269-295

Yu G et al. (2017) Mineral Availability as a Key Regulator of Soil Carbon Storage. Environmental Science & Technology 51:4960-4969

Zak D, Wagner C, Payer B, Augustin J, Gelbrecht J (2010) Phosphorus mobilization in rewetted fens: the effect of altered peat properties and implications for their restoration. Ecological Applications 20:1336-1349

Zobeck TM (2004) Rapid soil particle size analyses using laser diffraction. Applied Engineering in Agriculture 20:633

TABLES AND FIGURES

Table 2.1. Treatment descriptions with period, τ_{anoxic} or τ_{ox} durations in hours (and days), and $\tau_{oxic}/\tau_{anoxic}$ ratios

Treatments	Cycles	Period	Oxic condition (τ_{oxic})	Anoxic condition (τ_{anoxic})	$\tau_{oxic}/\tau_{anoxic}$ ratio
		---------- *hours (days)* ----------			
Pre-conditioning	1st cycle	168 (6.0)	24 (1.0)	144 (6.0)	1:6
	2nd cycle	168 (6.0)	24 (1.0)	144 (6.0)	1:6
	3rd cycle	280 (11.67)	40 (1.67)	240 (10.0)	1:6
Long period (280 h period)	1st cycle	280 (11.67)	40 (1.67)	240 (10.0)	1:6
	2nd cycle	280 (11.67)	40 (1.67)	240 (10.0)	1:6
Short period (70 h period)	1st to 6th cycles	70 (2.92)	10 (0.42)	60 (2.5)	1:6

Table 2.2. Comparison of iron reduction rates in different redox fluctuation studies. All soils are from the valley portion of Bisley Watershed, Luquillo CZO, Puerto Rico

Work/Paper	Total Fe ($mmol\ kg^{-1}$)	SRO-Fe[a] ($mmol\ kg^{-1}$)	C content ($mg\ g^{-1}$)	Fe reduction rate ($mmol\ kg^{-1}\ h^{-1}$)	Days (fluctuating conditions)	
					Anoxic	Oxic
Ginn et. al 2017 & Tishchenko et al. 2015	1122.8	144	25.5	0.07 - 0.36	12	2
				0.11 - 0.96	6	1
				0.14 - 0.87	3	0.5
DeAngelis et al. 2010 [b]	NA	158	NA	0.18 - 0.38	4	4
This study (chapter 2)	1162.5[c]	148	46.7	0.25 - 0.26	11.67	1.67
				0.18 - 0.97	2.92	0.42

[a]Citrate Ascorbate Extraction

[b]Total Fe and C content not provided in DeAngelis et al. 2010

[c]Value from Wilmoth 2016

Table 2.3. Total Carbon (C in solid phase + extractable-OC[a]) and Nitrogen during redox oscillations treatments (Mean of duplicates ± standard deviation). Lowercase letters indicate significant differences within each treatment (pre-conditioning, 280 h, and 70 h) for each of the pools of C and N measured, using ANOVA and Tukey's HSD test at the 95% probability level. Soils from Bisley watershed, Puerto Rico, sampled in 2014

Hours of Experiment	C solid phase		extractable-OC[a]		Total C[b]		N solid phase		Redox Condition
	---------- *(mg g^{-1})* ----------								
Pre-Conditioning									
12	47.8 ± 1.7	a	7.3 ± 0.1	ab	55.2 ± 1.9	a	4.2 ± 0.6	a	Anoxic
156	42.8 ± 0.8	a	6.8 ± 0.1	a	49.6 ± 0.9	a	3.2 ± 0.1	a	Oxic
312	47.4 ± 1.6	a	7.8 ± 0.1	b	55.2 ± 1.7	a	3.0 ± 0.1	a	Anoxic
336	48.9 ± 5.4	a	7.9 ± 0.3	b	56.8 ± 5.7	a	2.9 ± 0.2	a	Oxic
516	49.1 ± 4.5	a	7.8 ± 0.1	b	56.8 ± 4.6	a	3.4 ± 0.0	a	Anoxic
280 h period (10 d anoxic: 40 h oxic)									
616	48.1 ± 1.2	a	8.2 ± 0.8	b	56.3 ± 2.0	a	3.4 ± 0.1	a	Oxic
706	36.8 ± 0.2	ab	8.2 ± 0.3	b	45.0 ± 0.5	ab	1.9 ± 0.0	b	Anoxic
778	29.4 ± 1.6	ab	6.5 ± 0.2	b	35.9 ± 1.8	b	1.6 ± 0.3	b	Anoxic
856	27.8 ± 9.7	b	6.5 ± 0.2	b	34.3 ± 9.9	b	1.5 ± 0.3	b	Anoxic
876	36.6 ± 6.6	ab	8.0 ± 0.8	b	44.6 ± 7.4	ab	1.9 ± 0.3	b	Oxic
952	27.2 ± 6.5	b	7.1 ± 0.2	b	34.4 ± 6.7	b	1.4 ± 0.2	b	Anoxic
1019	20.0 ± 0.1	b	6.5 ± 0.5	b	26.5 ± 0.5	b	1.3 ± 0.1	b	Anoxic
1115	24.4 ± 5.5	b	7.0 ± 0.7	b	31.3 ± 6.2	b	1.5 ± 0.1	b	Anoxic
1136	23.0 ± 3.6	b	7.1 ± 0.1	b	30.1 ± 3.8	b	1.5 ± 0.1	b	Anoxic
70 h period (60 h anoxic: 10 h oxic)									
616	46.6 ± 2.8	a	6.6 ± 0.7	b	53.2 ± 3.6	a	2.3 ± 0.1	ab	Oxic
676	38.5 ± 0.1	ab	8.4 ± 1.4	b	46.9 ± 1.4	ab	2.3 ± 0.2	ab	Anoxic
686	42.7 ± 4.0	a	7.5 ± 0.4	b	50.3 ± 4.4	ab	2.9 ± 0.1	a	Oxic
756	46.5 ± 1.3	a	7.4 ± 0.1	b	53.9 ± 1.4	a	2.3 ± 0.3	ab	Oxic
816	46.7 ± 2.1	a	7.2 ± 0.5	b	53.9 ± 2.7	a	2.7 ± 0.1	a	Anoxic
826	38.6 ± 6.3	ab	7.3 ± 1.3	b	45.9 ± 7.6	abc	2.2 ± 0.4	ab	Oxic
886	46.9 ± 1.0	a	7.6 ± 0.3	b	54.6 ± 1.3	a	2.5 ± 0.2	ab	Anoxic
896	37.1 ± 8.0	ab	7.4 ± 1.0	b	44.4 ± 9.0	abc	2.0 ± 0.1	b	Oxic
956	25.8 ± 3.7	bc	8.2 ± 0.9	b	34.0 ± 4.7	bc	1.5 ± 0.1	bc	Anoxic
966	32.4 ± 4.1	abc	8.2 ± 0.1	b	40.6 ± 4.1	abc	1.9 ± 0.1	bc	Oxic
1036	19.3 ± 2.1	c	9.5 ± 2.1	b	28.7 ± 4.2	c	1.2 ± 0.1	c	Oxic

[a]Extractable-OC = Aqueous and 0.5 M HCl-extractable organic carbon

[b]Total C = C solid phase + extractable-OC

Table 2.4. Particle size distribution (in percent) for different sampling points for initial soil, and pre-conditioning, 280 h, and 70 h treatments, according to the USDA particle size classes

Hours of Experiment	Redox Condit.	Treatment	C (mg g^{-1})	Fe(II) (mmol kg^{-1} of soil)	Clay	Silt	Total Sand	Very Fine Sand	Fine Sand	Medium Sand	Course sand	Very Coarse Sand	Clay + Silt
Initial[a]	-	-	-	-	3.1	32.1	64.9	14.2	27.8	14.2	8.0	0.5	35.2
12	Anoxic	Pre-cond.	47.8	5.4	3.4	23.5	73.1	9.6	23.2	18.3	20.1	1.9	26.9
312	Anoxic	Pre-cond.	47.4	79.2	5.3	32.9	61.9	13.3	26.5	15.5	6.6	0.0	38.2
336	Oxic	Pre-cond.	48.9	28.9	9.6	51.5	39.0	13.8	17.8	4.4	2.9	0.1	61.1
516	Anoxic	Pre-cond.	49.1	81.2	7.7	41.9	50.4	12.0	19.8	9.2	7.7	1.7	49.6
706	Anoxic	280 h	36.8	45.3	6.7	42.6	50.8	18.3	26.0	4.7	1.8	0.0	49.3
952	Anoxic	280 h	27.2	42.4	8.7	47.5	43.9	15.5	19.1	6.7	2.6	0.0	56.2
1019	Anoxic	280 h	20.0	59.9	5.3	30.0	64.6	14.8	26.9	13.5	9.2	0.2	35.3
956	Anoxic	70 h	25.8	67.8	9.0	50.9	40.1	19.3	20.0	0.8	0.0	0.0	59.9
1036	Oxic	70 h	19.3	27.9	5.7	30.3	64.0	17.2	31.4	10.5	4.9	0.0	36.0

[a]Initial soil sample (no chemicals added, or treatment imposed) from Bisley watershed, Puerto Rico, sampled in 2014

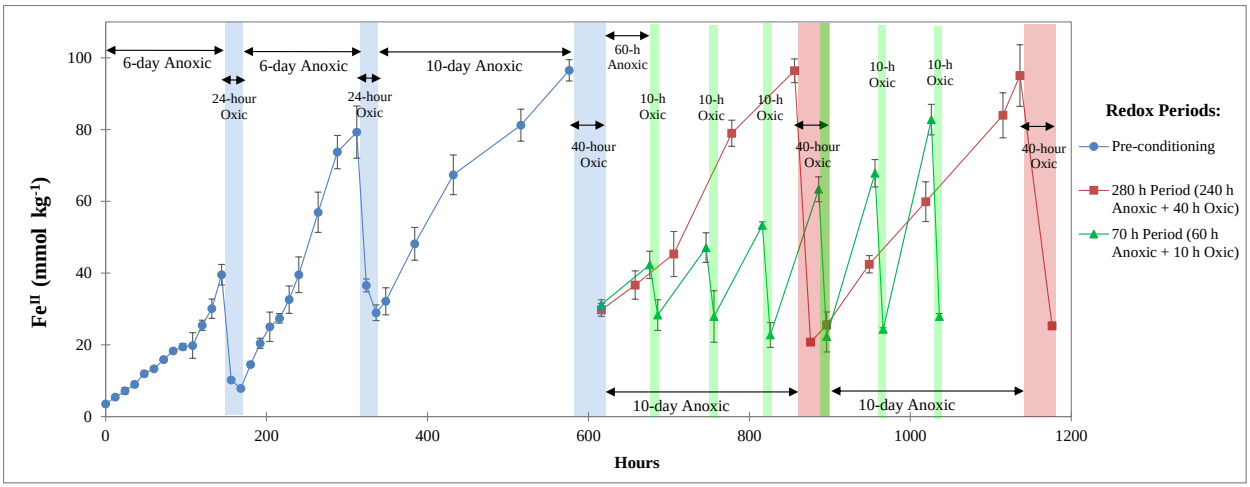

Fig. 2.1. Fe^{II} concentrations under different redox oscillation periods. The pre-treatment in Blue was split into 280 h (Red) and 70 h (Green) period treatments. The time under oxic vs. anoxic conditions, τ_{oxic}/ τ_{anoxic}, was maintained at 1:6 throughout the experiment. The error bars indicate a ± 1 standard deviation. Soils from Bisley watershed, Puerto Rico, sampled in 2014.

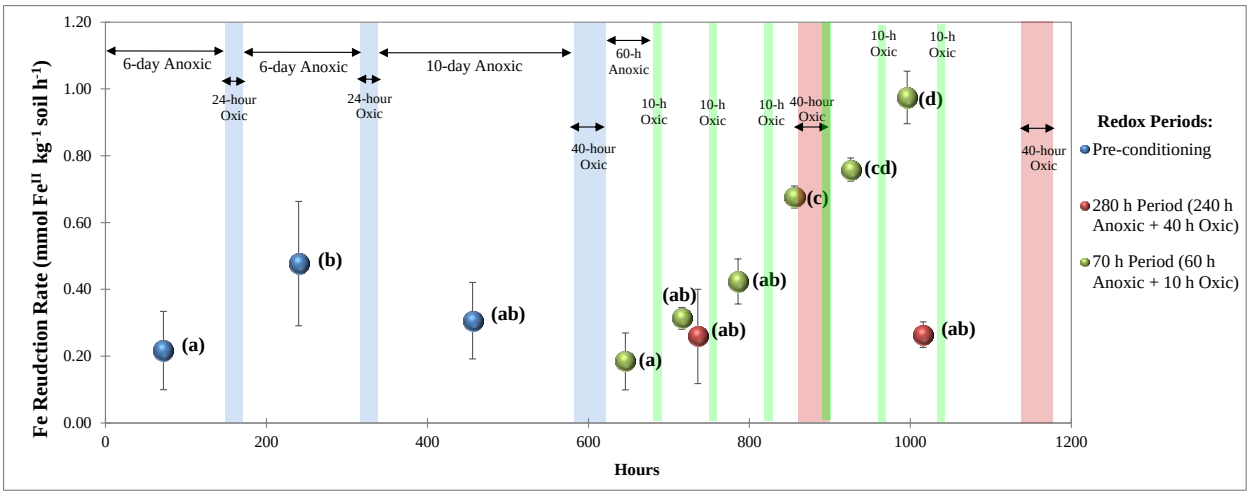

Fig. 2.2. Iron reduction rates (mmol of Fe^{II} kg^{-1} of soil h^{-1}) for the pre-treatment (Blue), 280 h period (Red) and 70 h period (Green) treatments. Lowercase letters in parentheses (a, b, c, d) indicate significant differences among iron reduction rates by ANOVA and Tukey's HSD test at the 5% probability level. The data-points correspond to the average of iron reduction rates (slope) and were plotted at the middle of each cycle. The error bars indicate a ± 1 standard deviation. Soils from Bisley watershed, Puerto Rico, sampled in 2014

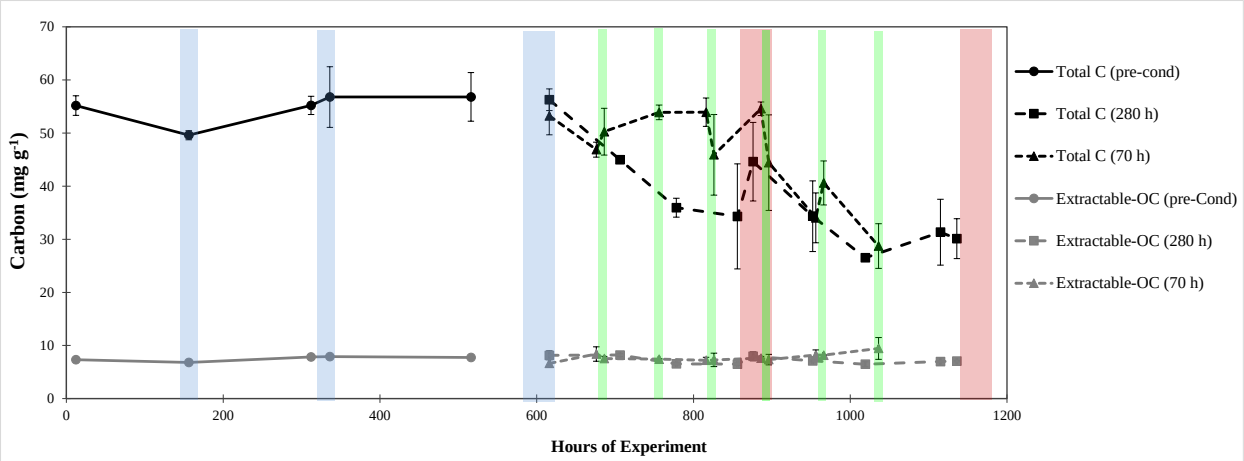

Fig. 2.3. Total Carbon (C solid phase + extractable-OC) and extractable-OC-only during the pre-conditioning (Blue), 280 h period (Red) and 70 h period (Green) treatments. The error bars indicate a ± 1 standard deviation. Soils from Bisley watershed, Puerto Rico, sampled in 2014

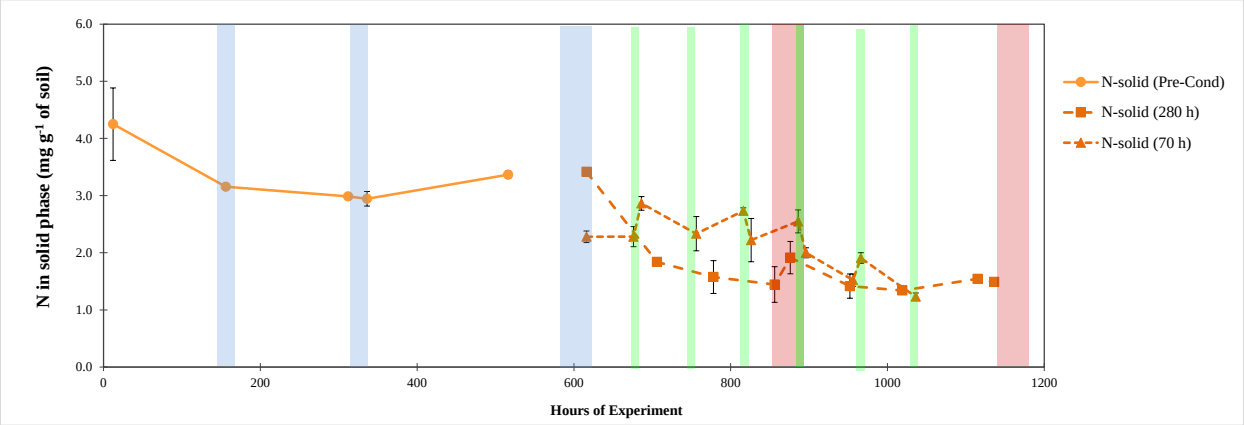

Fig. 2.4. Nitrogen (solid phase only, after extraction) during the pre-conditioning (Blue), 280 h period (Red) and 70 h period (Green) treatments. The error bars indicate a ± 1 standard deviation. Soils from Bisley watershed, Puerto Rico, sampled in 2014

CHAPTER 3

LENGTH OF OXYGEN EXPOSURE DURING REDOX OSCILLATIONS AFFECTS RATES OF IRON REDUCTION, ANAEROBIC CARBON MINERALIZATION, AND METHANE EMISSIONS[2]

[2] Barcellos, D., A. Campbell, J. Pett-Ridge, and A. Thompson. To be submitted to the Journal Environmental Science & Technology

Abstract

Redox fluctuations can alter the pools of reducible Fe^{III} and mineralizable C, and shift the activity and composition of the microbial community that drive these biogeochemical cycles. We hypothesized that in redox fluctuating soils, the rates of Fe reduction and C mineralization during anoxic conditions (τ_{anoxic}) will respond to the length of time the system was exposed to the previous oxic conditions (τ_{oxic}). To test this hypothesis, we exposed a soil from the upper 15 cm of the Luquillo Critical Zone Observatory (CZO), Puerto Rico, to five redox fluctuation scenarios. A Long τ_{anoxic} of 6 d with τ_{oxic} of 8, 24, and 72 h (L-8, L-24, and L-72), or a Short τ_{anoxic} of 2 d with τ_{oxic} of 8 or 24 h (S-8 and S-24). For the long oscillation periods, we found that a decrease from 72 to 24 to 8 h in the preceding τ_{oxic} impacted the subsequent τ_{anoxic} as follows: Fe reduction rates increased, CH_4 emissions decreased, and CO_2 fluxes did not change. For the short oscillation treatments (S-8 and S-24), under τ_{anoxic}, rates of Fe reduction, CO_2 and CH_4 emissions all decreased throughout the experiment. Our results demonstrate that in redox dynamic environments, the length of time a soil is exposed to oxygen can impact the rates of iron reduction and methanogenesis in the subsequent anoxic intervals. Predictions of anaerobic processes (e.g., CH_4 production) must take this environmental memory effect of oxygen exposure into account when estimating the influence of anaerobic processes on greenhouse gas emissions.

3.1. Introduction

Iron minerals rapidly change valence (Fe^{III} to Fe^{II} and vice-versa) in response to variations in soil moisture, oxygen (O_2), and carbon (C) availability, with Fe^{III} reduction—and in some cases the Fe^{II} oxidation—largely catalyzed by microbial communities (Bouskill et al. 2016; Cornell and Schwertmann 2003b; Silver et al. 1999). Rapid Fe^{II} oxidation associated with redox fluctuations favors the formation of microbial-reducible Fe^{III} oxides (abbreviated as Fe^{III}_{RR}) (Ginn et al. 2017), which have a high sorption capacity and a high specific surface area, and comprise phases with short range crystal order (SRO) (Bonneville et al. 2004; Chen and Thompson 2018; Coward et al. 2017). These Fe^{III}_{RR} phases are the most reactive subset of the SRO-Fe minerals (often called amorphous or poorly-crystalline) that collectively are important for controlling the release or storage of soil organic carbon (Kaiser and Guggenberger 2003; Rasmussen et al. 2018; Yu et al. 2017; Zhao et al. 2017), nutrients such as phosphorus, calcium, and magnesium (de Mesquita Filho and Torrent 1993; Hall and Huang 2017), and pollutants (Bauer and Blodau 2006; Borch et al. 2009; White and Peterson 1998).

High rainfall and soil moisture can lead to a decrease in soil O_2 concentrations and create anoxic microsites that are ideal habitats for iron reducing bacteria (DeAngelis et al. 2013; Fredrickson et al. 1998; Keiluweit et al. 2016). Iron is often the most abundant electron acceptor in highly weathered soils, and iron reducing bacteria can account for up to 6 % of total microbial cell density in soils from humid tropical regions, achieving abundance as high as 1.2×10^9 cells g^{-1} soil (Dubinsky et al. 2010). Due to this high abundance of iron reducers in soils, current ecosystem models may underestimate C mineralization that results in both carbon dioxide (CO_2) and methane (CH_4) emissions from microbial Fe respiration. Furthermore, by not considering the protected C pools within mineral-organic associations that may be released during frequent redox

fluctuation events, C mineralization may be underestimated (by >50% in some cases) (Huang and Hall 2017a).

Iron-rich and fine-textured soils under highly productive tropical forests can act as sources or sinks of soil organic C, leading to C decomposition or sequestration, respectively, and emitting or consuming greenhouse gases, such as CO_2 and CH_4 (Liptzin et al. 2011; O'Connell et al. 2018). In redox-fluctuating systems, soil microbes can produce CO_2 via heterotrophic respiration during anoxic conditions (Weber et al. 2006). In a laboratory incubation using soils from a montane forest of Puerto Rico, iron reduction was attributed to 4-44% of organic carbon oxidation (34 to 263 g CO_2-C m^{-2} $year^{-1}$) considering that 1 mol of C oxidizes for every 4 mols of Fe^{III} reduced (Dubinsky et al. 2010; Liptzin and Silver 2009; Roden and Wetzel 1996). Additionally, redox fluctuations can induce production of CH_4 by anaerobic microbial respiration and fermentation (Pett-Ridge et al. 2006), or microbial-iron-reducers may suppress CH_4 evolution by competing for acetate and hydrogen with methanogenic archaea (Teh et al. 2008). Methanotrophs can also be involved in the reduction of Fe oxyhydroxides with the oxidation of methane under anaerobic conditions (Bar-Or et al. 2017; Ettwig et al. 2016). Since humid tropical forests have one of the highest rates of carbon decomposition (Cusack et al. 2009), it is essential to understand the dynamics of iron biogeochemistry during natural soil redox fluctuations to predict how changing environmental conditions at multiple time scales (daily, annually, decadally) may effect soil organic matter (SOM) content and CO_2 and CH_4 emissions (Bailey et al. 2017; Carvalhais et al. 2014).

The characteristics of how a redox fluctuation occurs can directly influence iron reduction, carbon dynamics, and microbial processes in soils. We conceptualized that a controlled redox oscillation cycle has three fundamental parameters (Barcellos et al. 2018): amplitude (variation

in the amount of O_2 in the system), oscillation period (time lengths for a full cycle to go under oxic and anoxic conditions), and the time under either oxic (τ_{oxic}) or anoxic conditions (τ_{anoxic}) (Fig. 1.1). Ginn et al. (2017) has shown that different redox oscillations (τ_{oxic}:τ_{anoxic} fixed at 1:6) can induce an increase in iron reduction rates over the course of an experiment through the production of rapidly reducible Fe^{III} phases (Fe^{III}_{RR}). Subsequently Barcellos et al. (2018) illustrated that more frequent, shorter oscillation periods led to faster Fe reduction rates than less frequent, longer oscillation periods (amplitude fixed at 0 or 21% O_2 and τ_{oxic}:τ_{anoxic} fixed at 1:6). However, it is not clear if it was the length of oxic exposure (τ_{oxic}) or the frequency of newly produced Fe^{III}_{RR} that was responsible for the higher Fe reduction rates in the Barcellos et al. (2018) study. Thus, in the present study we tested the effects of different oxic time lengths (τ_{oxic}) directly in both long (less frequent) and short (more frequent) redox oscillation periods.

We hypothesized that during sequential redox oscillation cycles, soils exposed to short oxic intervals (τ_{oxic}) would exhibit an increase in Fe reduction rates during anoxic intervals (τ_{anoxic}) and would be correlated with greenhouse gas emissions. We monitored Fe^{II} concentrations in solid and aqueous soil phases and measured CO_2 and CH_4 efflux.

3.2. Material and Methods

3.2.1. Site and sample characterization

Five composited soil samples were collected from the valley position of the Bisley Research Watershed in the Luquillo Experimental Forest, Puerto Rico (Luquillo Critical Zone Observatory, LCZO). Fresh samples collected from 0-10 cm depth were placed in plastic bags, stored in a cooler, and immediately shipped to the University of Georgia where soils were received within 24 h of sampling. The field-moist samples were then carefully homogenized and

sieved (2-mm) under anoxic conditions in a 95%:5% (N_2:H_2) glovebox (Ginn et al. 2014) (Fig. A.1). The initial gravimetric moisture content of the fresh soil was 0.77 g g^{-1}. Soils from the Bisley watershed are predominantly Ultisols (Typic Haplohumults) formed from volcanic parent material, weakly acidic, mineralogically composed of quartz, kaolinite, chlorite, and goethite (Peretyazhko and Sposito 2005). These sites have been extensively studied previously (Ginn et al. 2014; Hall and Silver 2015; Scatena 1989; Silver et al. 1999; Tishchenko et al. 2015). Total Fe and Al content were determined by ICP-MS following a Li-metaborate fusion (Hossner et al. 1996). Standard approximations of short-range-ordered (SRO) Fe and Al phases were obtained by citrate/ascorbate extraction at the concentration of 0.2 M sodium citrate/0.05 M ascorbic acid (Reyes and Torrent 1997) and were also analyzed by ICP-MS. Soil texture was measured by a Beckman Coulter LS 13 320 Laser diffraction Particle Size Analyzer (Schulte et al. 2016).

3.2.2. Redox oscillations and iron reduction

We subjected soil suspensions (1:10 soil:water ratio) to five different redox oscillation treatments for up to 47 days. We set up the experiment in a manner similar to that of our previous work (Barcellos et al. 2018), but we incubated fresh, field-moist soils instead of using air-dried soils as was done previously. We conducted the experiment with fresh soils to best capture the ambient microbial community dynamics. The soil slurries were buffered to maintain the natural soil pH (5.5) by using MES (2-N-morpholino-ethanesulfonic acid) with KCl as a background electrolyte. Each reactor contained 4.5 g (dry-weight equivalent) of soil in a 2 mM KCl + 10 mM MES buffered solution at pH 5.5 ± 0.2, with a 45 g final suspension mass. Soil slurries were placed in a 95%:5% (N_2:H_2) glovebox Coy chamber (0% O_2) for the anoxic condition, and in laboratory room air (~21% O_2) for the oxic condition. All reactors were

constantly mixed on an orbital shaker (250 rpm). Ferrous iron (Fe^{II}) was measured by 0.5 M HCl extraction as described previously (Barcellos et al. 2018; Ginn et al. 2014; Thompson et al. 2006). Concentrations of Fe^{II} after ferrozine colorimetric analysis were obtained from 562 nm intensities using 96-well microplates (Huang and Hall 2017b) in a Tecan infinite m200 pro plate reader.

In separate slurries, dissolved O_2 (DO) was monitored through a single cycle in the reactors using a Hach (USA) DO meter. Within 1 h after exposing anoxic soil slurries to oxic conditions, DO increased to > 7.0 mg L^{-1}. Likewise, for soil slurries that were previously exposed to oxic conditions over 24 hours, we observed that DO decreased from 9.90 to 0.24 mg L^{-1} within 2 h and reached 0.06 mg L^{-1} after 24 h of anoxia exposure (Table A.1).

To test our hypothesis regarding the effects of τ_{oxic} on iron reduction, we varied the oscillation period ($\tau_{oxic,}$ and τ_{anoxic}) and fixed the amplitude parameter at 0% (anoxic) or ~21% (oxic) of O_2 concentrations. We started our experiment by pre-conditioning all reactors to three sequential oscillation periods of 6-d anoxic and 1-d oxic—similar to Wilmoth (2016), Ginn et al. (2017), and Barcellos et al. (2018)—aiming to acclimate the microbial communities into the same shifts in redox conditions after the stress imposed by soil sampling and experimental preparation, and mimicking common in situ conditions, e.g. Silver et al. (1999) and Liptzin et al. (2011). In our recent field study in Puerto Rico (see Chapter 4), we also observed changes within 6 days, as follows: decrease in the soil redox potential (Eh) from 256 to -344 mV, decrease in O_2 content from 9.2 to 2.3%, and increase in volumetric water content (θ_v) from 0.45 to 0.50 m^3 m^{-3}, after an intensive precipitation event, indicating shifts from oxic to anoxic conditions. These conditions of low O_2 and Eh, and high θ_v, may persist in the environment for 6 or more days, and

subsequent drying events may re-expose the soil to oxic conditions, demonstrating the cycling of redox fluctuations in natural soils.

After the pre-conditioning period (at 480 h into the experiment), we split the vessels into five triplicated treatments: L-72 with 144 h anoxic + 72 h oxic, L-24 with 144 h anoxic + 24 h oxic, L-8 with 144 h anoxic + 8 h oxic, S-24 with 48 h anoxic + 24 h oxic, and 48 h anoxic + 8 h oxic (Table 3.1). As a result, we compare the effect of the time iron-reducing-bacteria would be exposed to oxygen (τ_{oxic}) from 72, 24, and 8 h coupled with either a long (L) or short (S) anoxic period (τ_{anoxic}) of 144 h (6 d) or 48 h (2 d), respectively (Table 3.1). The L and S treatments underwent 3 and 7 consecutive redox cycles, respectively. The treatment L-24 continued the standard 6-d anoxic and 1-d oxic that was imposed to all treatments during the pre-conditioning cycles. In addition, control treatments of either constant anoxic or oxic conditions were included.

3.2.3. Trace gas and carbon analyses

Instantaneous fluxes of CO_2 (in mmol kg^{-1} of soil h^{-1}) and CH_4 (in μmol kg^{-1} of soil h^{-1}) were measured typically at the beginning, middle, and end of each redox cycle. Each gas flux measurement involved capping the triplicate reactors with rubber septa and sampling the headspace gas at 0, 10, and 30 minutes with gastight syringes and storing the collected gas in pre-evacuated 3 mL glass vials (Exetainer, Labco Inc., UK). Samples were analyzed in a gas chromatograph (Shimadzu Corporation GC-14A, Kyoto, Japan) using a flame ionization detector (FID) and electron capture detector (ECD). Nitrogen (280 kPa) was used as the carrier gas and the flow in the column was 24.3 mL min^{-1}. Measurements of CO_2 and CH_4 were expressed both as instantaneous fluxes (in mmol kg^{-1} of soil h^{-1} and μmol kg^{-1} of soil h^{-1}, respectively) and as

cumulative fluxes (in mmol kg^{-1} of soil and μmol kg^{-1} of soil, respectively), which was calculated by multiplying the instantaneous flux by all hours prior to the measurement.

Samples for total carbon and nitrogen were analyzed via combustion in a CHN Carlo Erba Elemental Analyzer. The native soil (no treatment added) had 37.4 mg g^{-1} of total C and 2.2 mg g^{-1} of total N (solid phase). The MES buffer added another 7.5 mg of C comprising 14% of carbon in each reactor, which made for 44.9 mg g^{-1} of total C at the start of the experiment.

3.2.4. Statistical analyses

To compare the effect of the different redox oscillation treatments on Fe^{II}, CO_2, and CH_4 fluxes, we conducted an ANOVA analysis using Kenward-Roger approximation and parametric bootstrap function for linear mixed models, using the lmer function from the lme4 and lmer Test packages in R (Bates et al. 2014; Halekoh and Højsgaard 2014). For the effects of the redox oscillation treatment, we observed significant changes within the cycles for S-24 and S-8 for the parameters Fe^{II}, CO_2, and CH_4, and we re-analyzed the data splitting the first three cycles from the last three cycles for both S-24 and S-8. To make these comparisons across all treatments for either CO_2 or CH_4 independently during τ_{anoxic}, we calculated the average flux rates of CO_2 and CH_4, dividing the cumulative fluxes (from end-start of each τ_{anoxic}) by 6 d for the Long treatments and by 2 d for the Short treatments.

An overall correlation among Fe^{II}, CO_2, and CH_4, including both oxic and anoxic conditions, and all treatments were computed with the function cor in R. We further computed linear models for comparisons among Fe^{II}, CO_2 and CH_4 under oxic or anoxic conditions separately, and then we conducted linear regressions individually for each of the five treatments

comparing two of these variables at a time under anoxic conditions only, all using lm function from the lme4 package in R (Bates et al. 2014).

3.3. Results

3.3.1. Ferrous Iron Dynamics and Iron Reduction Rates

Ferrous iron (Fe^{II}) dynamics differed between treatments. Consistent with prior work on redox oscillating systems, Fe^{II} concentrations increased during anoxic conditions and abruptly decreased upon exposure to oxic conditions (Barcellos et al. 2018; Chen and Thompson 2018; Ginn et al. 2017; Tishchenko et al. 2015; Wilmoth 2016). The native soil (prior to incubation) contained 943 ± 4 and 439 ± 7 mmol kg^{-1} soil of total Fe and SRO-Fe, and 2491 ± 14 and 53 ± 2 mmol kg^{-1} soil of total Al and SRO-Al (Table A.2). During the pre-conditioning period (Fig. 3.1), concentrations of Fe^{II} began at 3.9 mmol kg^{-1} soil and reached 29.3 mmol kg^{-1} soil at the end of the first τ_{anoxic} for a calculated iron reduction rate of 0.16 mmol kg^{-1} h^{-1}. These Fe^{II} concentration dynamics were repeated without an increase in the peak of Fe^{II} concentration for the rest of pre-conditioning cycles and were also repeated for the L-24 treatment, which maintained the standard oscillation behavior of the pre-conditioning cycles (i.e., 6 d anoxic and 1 d oxic) (Fig. 3.1c). Across all treatments, the maximum Fe^{II} concentration was 49.6 mmol kg^{-1} soil during the first τ_{anoxic} of the L-8 treatment. The Fe^{II} concentrations in the oxic controls (non-fluctuating) remained at 3.8 ± 0.5 mmol kg^{-1} throughout the experiment, and in most cycles of the other treatments, Fe^{II} concentrations in the τ_{oxic} reached this lower baseline. Fe^{II} concentrations in the anoxic controls (non-fluctuating) increased continuously, with Fe^{II} concentrations peaking at 185 ± 16 mmol kg^{-1} at the end of the experiment (a value approximately half the SRO-Fe content, 439 ± 7 mmol kg^{-1}).

Iron reduction rates during the pre-conditioning and L-24 treatments (both contain the same τ_{oxic} and τ_{anoxic}) were statistically similar (0.16 mmol kg^{-1} h^{-1}), the Fe reduction rate decreased slightly during the L-72 treatment (0.12 mmol kg^{-1} h^{-1}) but was not significantly different than the rates during the pre-conditioning period (Fig. 3.2). However, the Fe reduction rate was statistically higher for the L-8 treatment (0.26 mmol kg^{-1} h^{-1}) than the pre-conditioning, L-72, and L-24 treatments. For the long treatments (pre-cond, L-72, L-24, and L-8), Fe reduction rates within each treatment's three cycles were not statistically different from one another (Table A.3). Thus, our major finding for this study regarding Fe dynamics is that the shorter the τ_{oxic}, the higher the iron reduction rate, when comparing rates among Long treatments (τ_{anoxic} = 6 d, and τ_{oxic} between 8 and 72 h).

In the short treatments, Fe reduction rates increased relative to the pre-conditioning cycles in the first three cycles of both short treatments S-24 and S-8 (0.35 and 0.23 mmol kg^{-1} h^{-1}, respectively), which were also statistically similar to the L-8 treatment (Fig. 3.2). Therefore, a shorter τ_{oxic} resulted in higher Fe reduction rates in both the long treatment L-8 and the first three cycles of the short treatment S-8. However, for both short treatments S-24 and S-8, the Fe reduction rates decreased by ~ 50% during the last 3 oscillation cycles, to 0.14 and 0.12 mmol kg^{-1} h^{-1}, respectively (Fig. 3.2).

3.3.2. CO_2 and CH_4 Emissions

Overall, instantaneous CO_2 fluxes decreased over the course of the experiment, from the pre-conditioning to the subsequent treatments, ranging from 0.03 – 0.12 mmol CO_2 kg^{-1} soil h^{-1} (Fig. 3.3a and A.2). These values are within the range obtained by incubation studies using similar soils from the Luquillo CZO: 0.02 – 0.11 mmol CO_2 kg^{-1} soil h^{-1} (DeAngelis et al. 2010;

Dubinsky et al. 2010). The temporal trend of CO_2 flux was similar during the pre-conditioning cycles with CO_2 flux decreasing over the course of each τ_{anoxic}, followed by a slightly higher CO_2 flux in the subsequent τ_{oxic} (Fig. 3.3). In contrast, instantaneous CH_4 fluxes exhibited a general increasing trend throughout each τ_{anoxic}, followed by lower values in the subsequent τ_{oxic} (Fig. 3.4a and A.3). This trend during τ_{anoxic} was more pronounced in the Long oscillation periods, with peak values of 0.36, 0.59, 0.68, and 0.32 μmol CH_4 kg^{-1} soil h^{-1} for pre-conditioning, L-72, L-24, and L-8, respectively. After the pre-conditioning cycles, we began to detect some CH_4 consumption (i.e., negative CH_4 fluxes) during τ_{oxic} of some of the long and short treatments (Fig. 3.4).

Fluxes of CO_2 and CH_4 exhibited some differences among treatments. To make comparisons across all treatments for each gas, we calculated average flux rates (per hour) of CO_2 and CH_4 over the start-end of τ_{anoxic} for each cycle (6 d for the Long and 2 d for the Short treatments) and additionally, we separated the 3 initial cycles from the 3 last cycles for the S-24 and S-8 treatments as we did for the Fe reduction rates. The averaged CO_2 flux rates were significantly higher during the pre-conditioning period than for all long treatments (L-72, L-24, L-8), and they were similar to the first cycles of S-24 and S-8, but higher than the last cycles of S-24 and S-8 (Fig. 3.5a). The averaged CH_4 flux rates decreased significantly from L-72 to L-24 to L8, with the pre-conditioning not statistically different from L-24 (Fig. 3.5b). The averaged CH_4 flux rates for the L-8 treatment were like the first and last cycles of S-8 and to the last cycles of S-24. For the short oscillation treatments, averaged CH_4 flux rates in the S-24 treatment decreased over time and those rates in the S-8 treatment remained equal within error over the course of the experiment. Furthermore, there were statistical differences between each cycle for each treatment for both trace gases fluxes (Tables A.4 and A.5). Thus, comparing the three long treatments,

averaged CH_4 flux rates decreased from L-72 to L-24 to L-8 (i.e., the shorter the τ_{oxic}, the lower CH_4 emissions) (Fig. 3.5a), but averaged CO_2 flux rates was the same among these three treatments (Fig. 3.5b).

3.3.3. Correlations among Fe^{II}, CO_2, and CH_4 measurements

Overall statistical correlations of the entire dataset among the variables Fe^{II}, CO_2, and CH_4, under both oxic and anoxic conditions, showed moderate to strong statistically significant correlations between Fe^{II} vs CO_2 ($p<0.001$ and $R^2 = 0.76$), Fe^{II} vs CH_4 ($p<0.001$ and $R^2 = 0.46$), and CO_2 vs CH_4 ($p<0.001$ and $R^2 = 0.70$) (Fig. A.4). Linear models for Fe^{II} concentrations were correlated positively with cumulative CO_2 and negatively with CH_4 under anoxic conditions, and to cumulative CO_2 (negatively) under oxic conditions but were not significantly correlated with CH_4 under oxic conditions.

Thus, under anoxic conditions, Fe^{II} increased by 2.2 units for every unit increase in CO_2 flux and decreased by 0.13 unit for every unit increase of CH_4 flux. For all treatments, during anoxic conditions, for every 2.2 moles of Fe^{II} produced, 1 mole of CO_2 is emitted; and for every 0.13 mole of Fe^{II} produced, 1 mmol of CH_4 is consumed. Moreover, in our linear models, cumulative CO_2 was positively correlated with cumulative CH_4 under anoxic conditions, so that CH_4 increased by 2.36 mmol for every mole increase in CO_2.

Running linear regressions separately for each treatment under anoxic conditions and only between two of the variables at a time, we found differences among treatments for Fe^{II}:CO_2, Fe^{II}:CH_4, and CO_2:CH_4 (Fig. 3.6, 3.7, and A.5). There was a significant regression between Fe^{II} concentrations and cumulative CO_2 (Fig. 3.6a), and we observed a slope transition (all significant slopes) between L-72, the pre-conditioning, L-24, and L-8 of 1.76, 1.84, 2.50, and 3.10,

respectively (Fig. 3.6b and Table 3.2). For the short treatments, S-24 had a significant Fe^{II}:CO_2 slope of 3.51 (like L-8), but the S-8 Fe^{II}:CO_2 slope (1.12) was not significant. For the Fe^{II} and CH_4 regression, we also observed a transition in slope from L-72 (0.29, significant), L-24 (0.85, significant), and L-8 (1.32, non-significant), meaning that with a decrease in the τ_{oxic} we found that more CH_4 was produced for less Fe^{II} (L-72), and less CH_4 was produced for more Fe^{II} (L-8) (Fig. 3.7 and Table 3.2). For the short redox oscillations, the Fe^{II}:CH_4 slope was significant for S-24 (0.69) and non-significant for S-8 (0.13) (Fig. 3.7c). When τ_{oxic} is higher (L-72), more CH_4 is produced for every unit of CO_2, when compared to the other long treatments (pre-conditioning, L-24, and L-8) (Fig. A.5b), with significant slopes ranging from 1.5 to 5.0 (Table 3.2). For the short treatments, the CO_2:CH_4 slope was non-significant for both S-24 (2.75) and S-8 (-0.26) (Fig. A.5c).

3.4. Discussion

3.4.1. Iron reduction rates are influenced by the length of prior oxygen exposure (τ_{oxic})

Our results suggest that during continuous redox oscillations, the length of time a soil is exposed to oxygen (τ_{oxic}) impacts the rate of Fe reduction in the subsequent anoxic interval (τ_{anoxic}). We observed an increase in Fe reduction rate when τ_{oxic} decreased from 72 to 24 to 8 h, for the long treatments (L-72, L-24, and L-8, respectively with τ_{anoxic} = 6 d), consistent with the hypothesis of this study. Soils from humid tropical regions naturally experience fluctuations between oxic and anoxic conditions in response to rainfall and periodic inundation (Baldwin and Mitchell 2000; Liptzin et al. 2011). During these redox fluctuations the microbial community (Pett-Ridge and Firestone 2005) and the pool of rapidly reducible Fe^{III} phases (Fe^{III}_{RR}) likely respond dynamically (Ginn et al. 2017; Hall and Silver 2015). Changes in the microbial

community and/or shifts in the availability of reducible Fe phases could explain the observed increase in Fe reduction rates with decreasing oxygen exposure time. Below, we examine evidence supporting each mechanism and discuss the likelihood of these mechanisms based on the literature.

The abundance and activity of microbes that can use Fe^{III} as an electron acceptor depends not only on the availability of Fe^{III} or the availability of suitable electron donors (e.g., reduced C or H_2), but also on the presence of alternative electron donors that could be used by competing microbes or competing electron transfer enzymes within Fe reducers, and it also depends on the presence of inhibitory substances to the microorganisms (Ding et al. 2016; Konhauser et al. 2011). During oxic conditions, competition for a reduced C electron donor by aerobic organisms—which use the more thermodynamically favorable O_2 electron acceptor—can prevent growth and metabolism of the Fe reducers. In addition, O_2 can be potentially toxic for many anaerobic organisms, and its presence triggers them to generate protective enzymes or form cysts (Gambrell et al. 1991; Tiedje et al. 1984). Presumably, very short pulses of O_2 (i.e., < 0.5 h) in otherwise anoxic conditions would not be sufficient for aerobic organisms to out-compete Fe-reducers for reduced-C electron donors, whereas very long exposure to O_2 (i.e., 1 week) would likely cause a large-scale transformation of the microbial community. However, where that temporal threshold is for a given microbial community is unknown and has not been studied. If the threshold for Fe-reducer to maintain activity is between 8 h and 24 h for our system, this could explain the higher Fe reduction rates in the treatments with short τ_{oxic}. Low O_2 concentrations may suppress facultative anaerobic iron reducers (such as *Shewanella* sp.) (Straub and Schink 2004) that can survive over the oxygenated interim and resume activity in the subsequent deoxygenated interim. *Geobacter* sp. that was considered strictly anaerobic iron

reducer can tolerate O_2 exposure over 24 h (Lin et al. 2004). Thus, the "oxygen-dependent microbial cycling of Fe" (Kappler and Straub 2005) likely relies on the length of oxic exposure between anoxic intervals. In our experiment, the τ_{oxic} length likely led to a differentiation in the soil microbial composition in both long and short oscillation period treatments, affecting the observed rates of Fe reduction, with higher rates of Fe reduction when τ_{oxic} decreases to 8 hr.

Conversely, the formation of rapidly reducible Fe^{III} phases during oxic conditions may explain faster reduction of Fe phases in the next anoxic event. An increase in Fe reduction rates with decreasing τ_{oxic} (72, 24, and 8 h) could reflect differences in the formation and crystallization of Fe^{III} phases driven by Ostwald ripening mechanisms (Aeppli et al. 2017; Hu et al. 2012; Schwertmann and Cornell 2008). Although pO_2, as well as Fe^{II} oxidation rates, are known to impact the formation and crystallinity of incipient Fe^{III}-minerals with high pO_2 yielding Fe^{III}-oxyhydroxides of lower crystallinity than low pO_2 (Wilmoth 2016; Chen et al. 2018), all our treatments were exposed to similar pO_2 (~21% O_2). This similarity of pO_2 in the beginning of τ_{oxic} for all treatments suggests the initial Fe^{III} nucleation events were similar between treatments. However, the length of O_2 exposure (8 h to 72 h) could generate different amounts of crystal ripening. In controlled laboratory experiments at 98 °C for 6 h under vigorous stirring, Schwaminger et al. (2017) found Fe nanoparticles increased in size from 20 nm to 200 nm between 0.17 h and 6 h after synthesis, observing at first the formation of ferrihydrite, which then aggregated and transitioned to hematite. Even at room temperature, the size of Fe nanoparticles have been observed to increase from 2 to 6 nm within 150 h under acidic conditions with aluminum minerals present (Hu et al. 2013). Once formed, ferrihydrite can be transformed to hematite through dissolution and re-crystallization, or by aggregation of

nanoparticles and phase transformation (Ray et al. 2013). Thus, the length of aging for Fe^{III} under oxic conditions may influence the crystallinity of the Fe minerals.

There may potentially be an optimum τ_{oxic} during redox oscillations that leads to the highest rates of iron reduction, although it may be at even shorter timescales than explored in this study. One interpretation of our results is that the renewed flush of Fe^{III} phases, formed during τ_{oxic} and available in the subsequent τ_{anoxic}, was able to maintain the higher Fe reduction rates for L-8 compared to L-24 and L-72 (see Fig. 3.2). In the L-8 treatment (τ_{oxic} = 8 h), smaller nanoparticles, mixed Fe-phases, and more low-crystallinity Fe^{III}-minerals (such as ferrihydrite) would lead to a larger and more accessible flush of Fe^{III} in the subsequent τ_{anoxic} event within the L-8 redox cycles. While in treatment L-72, the longer τ_{oxic} of 72 h could facilitate the formation of more crystalline Fe minerals, which would be more difficult to reduce in the subsequent τ_{anoxic} event, as evidenced the lower Fe reduction rates in L-72 (compared to L-8).

In short redox oscillation periods (such as the S-24 and S-8 treatments), the more frequent redox cycling can lead to higher Fe reduction rates, as observed and explained in Barcellos et al. (2018). When comparing treatments with the same τ_{oxic}, but different τ_{anoxic} (L-24 and the first three cycles of S-24) the higher rate of Fe reduction in S-24 compared to L-24 can be explained by the greater periodicity of the redox cycles and the repeated re-supply of Fe^{III}_{RR} (Ginn et al. 2017; Barcellos et al. 2018), rather than the oxic time length. Coupled to the higher Fe reduction rates, we observed higher averaged CO_2 flux during τ_{anoxic} in S-24 (first three cycles) compared to L-24 with the same τ_{oxic}. Also comparing the long and short treatments, the long treatments were able to maintain statistically similar rates of Fe reduction over the consecutive 3 cycles, as the τ_{anoxic} was longer (6 d versus 2 d for the short treatments) and favored the reduction of larger amounts of Fe^{III} phases.

3.4.2. Fe reduction rates and trace gas fluxes decrease as short oscillation periods progressed

The short oscillation period treatments did exhibit an increase in Fe reduction rates during the first 3 cycles of both S-24 and S-8 treatments compared to three previous cycles of pre-conditioning (1 d oxic and 6 d anoxic). However, over the full experiment, Fe reduction rates as well as CO_2 and CH_4 emissions decreased as the short period treatments (S-24 and S-8) progressed. For all treatments, we observed higher CO_2 flux for the pre-conditioning period and a decrease in CO_2 flux for all following treatments (Fig. 3.3 and 3.5a). The production of Fe^{II}, CO_2, and CH_4, are largely driven by microbial activity in our redox oscillation experiments. We interpret this decrease in biogeochemical reaction rates to be due to both depletion of labile C throughout the experiment and also due to shifts in microbial communities since we used fresh soils for the lab incubations. Comparatively, during a 32-d redox oscillation experiment using fresh intact soil cores from the Luquillo CZO, DeAngelis et al. (2010) also observed higher CO_2 production and Fe reduction rates early in the experiment (16 d) compared to later in the experiment (32 d), decreasing from 0.095 to 0.065 mmol kg^{-1} h^{-1} for CO_2, and from 0.38 to 0.18 mmol kg^{-1} h^{-1} for the Fe reduction rates (Table A.6). This experiment alternated redox conditions over consecutive 4 d anoxic and 4 d oxic. Other studies have also demonstrated a decline in microbial activity over alternating soil redox conditions for Fe, N, and P cycling and C degradation, including changes in microbial composition (Chacon et al. 2006; Pett-Ridge et al. 2006). Additionally, the rapid shifts in the redox condition that we imposed in the short treatments (τ_{anoxic} fixed at 2 d, and τ_{oxic} either at 24 or 8 h) may stress the soil microorganisms at

time scales below their threshold physiological capacity for adaptation (DeAngelis et al. 2010; Schmidt et al. 2007).

Thus, either using soil slurry experiments (our study) or intact soil cores (DeAngelis et al. 2010), microbes were able to mineralize more soil organic matter early in the redox oscillation experiment. Under field conditions, new inputs of soil organic matter will restore the depleted soil carbon pool. Consequently, in a redox fluctuating environment, the initial events of high soil moisture and precipitation may create microsites of low O_2 and anoxic conditions that will favor rapid decomposition of organic matter following fresh C inputs, and over time microbial activity could become slower for the later redox cycles.

3.4.3. Coupled Fe^{II} production and CO_2 emissions during redox oscillations

We aimed to measure how much C mineralization as CO_2 emissions was correlated with Fe reduction over different redox oscillation treatments by varying τ_{oxic} and τ_{anoxic}. In humid tropical environments, large amounts of highly reactive SRO-Fe phases, abundant iron-reducing bacteria, a warm and wet climate, fluctuating low soil O_2 content, high NPP, and plentiful labile organic C, all favor the coupled reaction of Fe reduction with C oxidation (Brokaw et al. 2012; McGroddy and Silver 2000; Schuur et al. 2001; Schwartz et al. 2007). In redox fluctuating systems, Fe^{III} can serve as a terminal electron acceptor for soil microbes, affecting the soil carbon cycle, and producing CO_2 via heterotrophic respiration during anoxic periods (Konhauser et al. 2011; Subke et al. 2006). In our study, we observed an increase in the slopes of regression lines of Fe^{II}:CO_2 from L-72 to L-8, i.e. from larger to smaller τ_{oxic} (Fig. 3.6 a, b and c). By plotting a 4:1 Fe^{II}:CO_2 line, which represents stoichiometric conversion of glucose to CO_2 via Fe^{III} reduction (Sposito 2008), one can observe our data is more concentrated below the line for

the pre-conditioning, L-72, and L-24, and above the line for L-8, exhibiting a Fe^{II}:CO_2 slope transition from L-72 to L-24 to L-8 of 1.76, 2.50, and 3.10, respectively (Fig. 3.6b and Table 3.2). The short treatments S-24 and S-8 varied from above and below the 4:1 line, and both tend to be more concentrated above the 4:1 line, with significant S-24 slope of 3.51 and non-significant S-8 slope of 1.12 (Fig. 3.6c and Table 3.2). Higher Fe^{II}:CO_2 slope values that are closer to 4:1 (like L-8) represent that most of the CO_2 produced is due to Fe reduction, while lower Fe^{II}:CO_2 slope values (like L-72) indicate that other biogeochemical processes apart from Fe reduction are producing CO_2 under anoxic conditions. Roden and Wetzel (1996) found that incubations of wetland soils produced excess Fe^{II} relative to the 4:1 Fe^{II}:CO_2 stoichiometry; and Chen et al. (2018) found Fe^{II} and CO_2 production in a 5:1 ratio under anoxic conditions, in a redox oscillating experiment using similar soils from the Luquillo CZO.

In terms of percentage, the mineralized soil organic carbon (CO_2 emissions) attributed to Fe reduction increased from 43 to 70 to 97 % for L-72, L-24, and L-8, respectively; and from 56 to 73 % for S-24 and S-8 (Table 3.3). Thus, for both long and short treatments the CO_2 due to Fe reduction increased when τ_{oxic} decreased. Comparable studies found that Fe reduction was responsible for up to 65% of the C oxidized in anaerobic wetland sediments (Roden and Wetzel 1996). Across a range of soil redox potential (Eh) conditions and across different topographic positions of the Luquillo CZO forest, Dubinsky et al. (2010) estimated that the CO_2 production from Fe^{III} reduction varied from 4 to 44 %, and concluded that wetter soils produce more CO_2 due to Fe reduction. Liptzin and Silver (2009) found that 13 to 40 % of the added carbon during soil incubations was likely respired via Fe reduction. In an Oxisol from the State of São Paulo (Brazil), CO_2 measured under field conditions had a positive correlation with the well-crystalline iron oxides hematite, goethite, and dithionite-citrate-bicarbonate extractable-Fe (Bahia et al.

2015; Duiker et al. 2003). Therefore, Fe reduction can be attributed as one of the major forms of microbial respiration in humid tropical environments.

3.4.4. Higher Fe reduction vs. lower CH_4 emissions during anoxic conditions in redox fluctuating upland soils

Similar to the trends in Fe reduction rates, we found time under oxic conditions (τ_{oxic}) consistently impacted CH_4 emissions in the subsequent anoxic cycles (τ_{anoxic}) and was inversely correlated with Fe reduction rates, as stated in our hypothesis. For the long oscillation period treatments, we observed that as the preceding τ_{oxic} decreased from 72 to 8 h, the Fe^{II} production rate increased and the CH_4 emission decreased during τ_{anoxic}. These trends are also evident in the shift of the Fe^{II}:CH_4 slope from 0.29 to 1.32 for the L-72 to L-8 treatments (Fig. 3.7b).

In systems undergoing rapid Fe reduction, such as wetlands (Roden and Wetzel 1996; Sivan et al. 2016) and humid tropical upland soils (Teh et al 2008), methane production can be suppressed by stimulating Fe reduction, either by adding acetate or freshly precipitated Fe^{III} (i.e., Fe^{III}_{RR}). Methanogenic microorganisms use acetate, H_2, CO_2, formate, or methylated compounds as substrates for metabolic functions (Le Mer and Roger 2001). Competition for these substrates (especially acetate) between iron-reducers and methanogens microorganisms is one of the main controls for CH_4 emissions in anoxic and highly humid environments (Serrano-Silva et al. 2014; Teh et al. 2005), although this process is not well understood in upland soils. The oxidation of methane under oxic conditions has been frequently documented, but the anaerobic oxidation of methane (AOM) coupled to Fe reduction by archaea and bacteria have been only recently identified in natural systems (Egger et al. 2017; Knittel and Boetius 2009; Valenzuela et al. 2017). In an anoxic slurry incubation using lake sediments, Bar-Or et al. (2017) found that AOM

was correlated with Fe reduction: the amendment of Fe minerals (goethite and synthetic amorphous iron oxides) decreased the emission of CH_4 compared to natural lake sediment treatments. This Fe-CH_4 coupling effect resulted in a decrease in CH_4 emissions by 50% in freshwater systems containing low amounts of sulfate (Bar-Or et al. 2017). Additionally, Ettwig et al. (2016) found a strong negative linear correlation between Fe^{II} and CH_4 within 30 h of incubating freshwater sediments, under anoxic conditions.

Our observations of shifts in methane production as a function of τ_{oxic} (e.g., Fig. 3.7b) could simply reflect the impact of the τ_{oxic} on Fe reduction rates, which impacted methanogenesis indirectly. However, it may also be that the length of the previous τ_{oxic} in redox fluctuating soils favors the predominance of one microbial group over another in the subsequent τ_{anoxic} event; i.e., certain groups of microorganisms may be able to maintain activity during periods of aeration better than others and resume metabolic activity faster in the subsequent τ_{anoxic} period. So, it may be that methanogens are able to survive longer oxic periods better than Fe reducing microorganisms, and this may contribute to the higher methane production rates in the L-72 treatment compared with the L-8 treatments (Fig. 3.7b).

Iron-reducers can outcompete the methanogens in the presence of freshly precipitated Fe^{III} forms and abundant acetate substrate, for instance, Teh et al. (2008) conducted anaerobic incubations over 10 days using freshly-sampled soils and evaluated Fe reduction and CH_4 emissions, using soils from the same location (valley of the Bisley watershed, Luquillo LCZO). They found that by adding acetate + freshly-formed Fe^{III} oxides to the soils, the Fe-reduction was favored over methanogenesis with a Fe^{II}:CH_4 production ratio of 1.45 (mmol kg^{-1} of Fe^{II} : µmol kg^{-1} of CH_4), which is similar to what we observed in our L-8 treatment. The flush of reducible Fe^{III} phases freshly formed during the short τ_{oxic} of 8 h was likely used by Fe-reducers to conduct

dissimilatory Fe reduction and this may have suppressed methanogens. Furthermore, in wetland soils, where the wetter conditions likely approximate our L-8 treatment (less aeration time) than the other treatments, Fe reduction suppressed CH_4 production, with iron-reducers outcompeting methanogens (Roden and Wetzel 1996; Sivan et al. 2016). Thus, we observed lower CH_4 emissions and higher Fe reduction rates in the treatment L-8 (smaller τ_{oxic}), compared to the treatment L-24 (larger τ_{oxic}), concluding that the length of preceding τ_{oxic} have a strong influence on Fe and CH_4 biogeochemistry during anoxic conditions in redox oscillating soils.

At a similar upland valley soil from the Luquillo CZO, O'Connell et al. (2018) found that the valley topographic position emitted more CH_4 compared to slope and ridge positions when soils were transitioning from drought to wetter conditions. Over the drought period, valley soils were under fully oxic conditions, and over the post-drought/wetter event, these soils were able to generate anoxic microsites for Fe reduction. In tropical forests, CH_4 oxidation is predominant during a drier period, compared to a wetter period, due to higher O_2 content and faster CH_4 diffusion within the soil (Kiese et al. 2003). Findings from O'Connell et al. (2018) are similar to our study—higher CH_4 emissions in the treatment L-72 (longer τ_{oxic} of 72 h)—as soils at field conditions were transitioning from a longer oxic event (like a drying period) into the anoxic conditions (like a post-drought and wetter period).

Our study reports this unique inverse trend between Fe^{II} concentrations and cumulative CH_4 during anoxic conditions (Fig. A.6) in upland soils as a function of the preceding time exposed to oxygen (τ_{oxic}) undergoing redox fluctuations. Soils containing highly reactive Fe pools (Fe^{III}_{RR}) can be important inhibitors of methane emissions during the process of Fe reduction (with Fe^{II} leaching through the soil profile and reaching streams, for example), and decreasing effects of greenhouse gas emissions from tropical humid forests.

3.5. Conclusions and Environmental Implications

We found that the amount of time redox-dynamic soils are exposed to oxygen can affect the subsequent anoxic processes, including iron reduction rates, anaerobic carbon mineralization, and methane emissions. For longer oscillation periods, which have anoxic periods of 6 d, as oxygen exposure decreases from 72 to 24 to 8 hours, the subsequent anaerobic periods have higher Fe reduction rates and lower CH_4 emissions, but CO_2 fluxes did not vary (Fig. 3.8). For shorter oscillation periods, which have anoxic periods of 2 d, similar trends occurred, but only in the initial cycles after which anoxic rates of Fe reduction, CO_2 and CH_4 emissions all decreased suggesting that short oscillations did not allow sufficient time for anoxic processes to persist (Fig. 3.8).

Iron reduction is an important ecosystem process in upland soils and our findings illustrate that the duration of oxygen exposure is an important determinate of Fe reduction rates. Short periods of oxygen exposure are likely to drive rapid Fe reduction, whereas longer oxic exposure might hinder iron reduction.

Although this study focused on upland valley soils, similar timescales of oxic and anoxic exposure are likely in wetlands, sediments, and other natural systems with fluctuating redox zones. Our findings suggest that redox dynamic systems with long periods of oxic exposure may exhibit higher methane emissions than those with short periods of oxygen exposure. This could be important to land managers who regulate water table fluctuations or to climate modelers who might have *a priori* expectations that anoxic methane production would be suppressed by longer oxic exposure. Most broadly, our work highlights the need to consider oxygen exposure times in

predicting biogeochemical rates from anaerobic processes, which are critical for understanding global grand challenges involving soil carbon losses and preservation and greenhouse gas emissions.

3.6. References

Aeppli M, Voegelin A, Gorski CA, Hofstetter TB, Sander M (2017) Mediated electrochemical reduction of iron (oxyhydr-) oxides under defined thermodynamic boundary conditions. Environmental Science & Technology 52:560-570

Bahia ASRS et al. (2015) Field-scale spatial correlation between contents of iron oxides and CO_2 emission in an Oxisol cultivated with sugarcane. Scientia Agricola 72:157-166

Bailey VL et al. (2017) Soil carbon cycling proxies: Understanding their critical role in predicting climate change feedbacks. Global Change Biology 24:895-905

Baldwin DS, Mitchell AM (2000) The effects of drying and re-flooding on the sediment and soil nutrient dynamics of lowland river–floodplain systems: a synthesis. Regulated Rivers: Research & Management: An International Journal Devoted to River Research and Management 16:457-467

Bar-Or I et al. (2017) Iron-Coupled Anaerobic Oxidation of Methane Performed by a Mixed Bacterial-Archaeal Community Based on Poorly Reactive Minerals. Environmental Science & Technology 51:12293-12301

Barcellos D, Cyle KT, Thompson A (2018) Faster redox fluctuations can lead to higher iron reduction rates in humid forest soils. Biogeochemistry 137:367-378

Bates D, Mächler M, Bolker B, Walker S (2014) Fitting linear mixed-effects models using lme4. 1406.5823

Bauer M, Blodau C (2006) Mobilization of arsenic by dissolved organic matter from iron oxides, soils and sediments. Science of the Total Environment 354:179-190

Bonneville S, Van Cappellen P, Behrends T (2004) Microbial reduction of iron(III) oxyhydroxides: effects of mineral solubility and availability. Chemical Geology 212:255-268

Borch T, Kretzschmar R, Kappler A, Cappellen PV, Ginder-Vogel M, Voegelin A, Campbell K (2009) Biogeochemical redox processes and their impact on contaminant dynamics. Environmental Science & Technology 44:15-23

Bouskill NJ et al. (2016) Belowground response to drought in a tropical forest soil. I. Changes in microbial functional potential and metabolism. Frontiers in Microbiology 7:525

Brokaw N, Crowl T, Lugo A, McDowell W, Scatena F, Waide R, Willig M (2012) A Caribbean Forest Tapestry. Oxford University Press. New York. pp 3-443

Bruun TB, Elberling B, Christensen BT (2010) Lability of soil organic carbon in tropical soils with different clay minerals. Soil Biology and Biochemistry 42:888-895

Carvalhais N et al. (2014) Global covariation of carbon turnover times with climate in terrestrial ecosystems. Nature 514:213-217

Chacon N, Silver WL, Dubinsky EA, Cusack DF (2006) Iron reduction and soil phosphorus solubilization in humid tropical forests soils: the roles of labile carbon pools and an electron shuttle compound. Biogeochemistry 78:67-84

Chen C, Thompson A (2018) Ferrous Iron Oxidation under Varying pO_2 Levels: The Effect of Fe (III)/Al (III) Oxide Minerals and Organic Matter. Environmental Science & Technology 52:597-606

Chen C, Meile C, Wilmoth JL, Barcellos D, Thompson A (2018) Influence of pO2 on Iron Redox Cycling and Anaerobic Organic Carbon Mineralization in a Humid Tropical Forest Soil. Environmental Science & Technology 52:7709-7719

Cornell RM, Schwertmann U (2003) The iron oxides: structure, properties, reactions, occurrences and uses. Wiley-VCH. Weinheim, Germany. pp 1-667

Costa Ad, Bigham J (2009) Óxidos de ferro. In: Melo V, Alleoni L (eds) Química e mineralogia do solo, vol I. Sociedade Brasileira de Ciência do Solo, Viçosa, MG, Brasil, pp 505-573

Coward EK, Thompson AT, Plante AF (2017) Iron-mediated mineralogical control of organic matter accumulation in tropical soils. Geoderma 306:206-216

Cusack DF, Chou WW, Yang WH, Harmon ME, Silver WL (2009) Controls on long-term root and leaf litter decomposition in neotropical forests. Global Change Biology 15:1339-1355

de Mesquita Filho M, Torrent J (1993) Phosphate sorption as related to mineralogy of a hydrosequence of soils from the Cerrado region (Brazil). Geoderma 58:107-123

DeAngelis KM, Chivian D, Fortney JL, Arkin AP, Simmons B, Hazen TC, Silver WL (2013) Changes in microbial dynamics during long-term decomposition in tropical forests. Soil Biology and Biochemistry 66:60-68

DeAngelis KM, Silver WL, Thompson AW, Firestone MK (2010) Microbial communities acclimate to recurring changes in soil redox potential status. Environmental Microbiology 12:3137-3149

Del Grosso S et al. (2000) General CH_4 oxidation model and comparisons of CH_4 oxidation in natural and managed systems. Global Biogeochemical Cycles 14:999-1019

Ding W, Stewart DI, Humphreys PN, Rout SP, Burke IT (2016) Role of an organic carbon-rich soil and Fe(III) reduction in reducing the toxicity and environmental mobility of chromium(VI) at a COPR disposal site. Science of the Total Environment 541:1191-1199

Dubinsky EA, Silver WL, Firestone MK (2010) Tropical forest soil microbial communities couple iron and carbon biogeochemistry. Ecology 91:2604-2612

Duiker SW, Rhoton FE, Torrent J, Smeck NE, Lal R (2003) Iron (hydr) oxide crystallinity effects on soil aggregation. Soil Science Society of America Journal 67:606-611

Egger M et al. (2017) Iron oxide reduction in methane-rich deep Baltic Sea sediments. Geochimica et Cosmochimica Acta 207:256-276

Ettwig KF, Zhu B, Speth D, Keltjens JT, Jetten MS, Kartal B (2016) Archaea catalyze iron-dependent anaerobic oxidation of methane. Proceedings of the National Academy of Sciences 113:12792-12796

Falkowski PG, Fenchel T, Delong EF (2008) The microbial engines that drive Earth's biogeochemical cycles. science 320:1034-1039

Gaffney JW, White KN, Boult S (2008) Oxidation State and Size of Fe Controlled by Organic Matter in Natural Waters. Environmental Science & Technology 42:3575-3581

Gambrell RP, DeLaune RD, Patrick Jr WH (1991) Redox processes in soils following oxygen depletion. Plant Life Under Oxygen Deprivation. SPB Academic Publishing BV, The Hague, The Netherlands:101-117

Ginn BR, Habteselassie MY, Meile C, Thompson A (2014) Effects of sample storage on microbial Fe-reduction in tropical rainforest soils. Soil Biology and Biochemistry 68:44-51

Ginn BR, Meile C, Wilmoth J, Tang Y, Thompson A (2017) Rapid iron reduction rates are stimulated by high-amplitude redox fluctuations in a tropical forest soil. Environmental Science & Technology 51:3250-3259

Halekoh U, Højsgaard S (2014) A kenward-roger approximation and parametric bootstrap methods for tests in linear mixed models–the R package pbkrtest. Journal of Statistical Software 59:1-30

Hall SJ, Huang W (2017) Iron reduction: a mechanism for dynamic cycling of occluded cations in tropical forest soils? Biogeochemistry 136:91-102

Hall SJ, Silver WL (2013) Iron oxidation stimulates organic matter decomposition in humid tropical forest soils. Global change biology 19:2804-2813

Hall SJ, Silver WL (2015) Reducing conditions, reactive metals, and their interactions can explain spatial patterns of surface soil carbon in a humid tropical forest. Biogeochemistry 125:149-165

Hossner L et al. (1996) Dissolution for total elemental analysis. Methods of soil analysis. Part 3-chemical methods. pp 49-64

Hu Y, Lee B, Bell C, Jun Y-S (2012) Environmentally abundant anions influence the nucleation, growth, ostwald ripening, and aggregation of hydrous Fe(III) oxides. Langmuir 28:7737-7746

Hu Y, Li Q, Lee B, Jun Y-S (2013) Aluminum affects heterogeneous Fe(III) (Hydr)oxide nucleation, growth, and ostwald ripening. Environmental science & technology 48:299-306

Huang W, Hall SJ (2017a) Elevated moisture stimulates carbon loss from mineral soils by releasing protected organic matter. Nature communications 8:1774

Huang W, Hall SJ (2017b) Optimized high-throughput methods for quantifying iron biogeochemical dynamics in soil. Geoderma 306:67-72

Kaiser K, Guggenberger G (2003) Mineral surfaces and soil organic matter. European Journal of Soil Science 54:219-236

Kämpf N, Scheinost AC, Schulze DG (2011) Oxide minerals in soils. In: Huang P, Li Y, Sumner M (eds) Handbook of Soil Sciences: Properties and Processes, Second Edition. CRC Press, Boca Raton, Fl, pp 1-34

Kappler A, Straub KL (2005) Geomicrobiological cycling of iron. Reviews in Mineralogy and Geochemistry 59:85-108

Keiluweit M, Nico PS, Kleber M, Fendorf S (2016) Are oxygen limitations under recognized regulators of organic carbon turnover in upland soils? Biogeochemistry 127:157-171

Kiese R, Hewett B, Graham A, Butterbach-Bahl K (2003) Seasonal variability of N_2O emissions and CH_4 uptake by tropical rainforest soils of Queensland, Australia. Global Biogeochemical Cycles 17:12(1-13)

Kleber M, Eusterhues K, Keiluweit M, Mikutta C, Mikutta R, Nico PS (2015) Mineral–organic associations: formation, properties, and relevance in soil environments. In: Advances in agronomy, vol 130. Elsevier, pp 1-140

Knittel K, Boetius A (2009) Anaerobic oxidation of methane: progress with an unknown process. Annual review of microbiology 63:311-334

Konhauser KO, Kappler A, Roden EE (2011) Iron in microbial metabolisms. Elements 7:89-93

Le Mer J, Roger P (2001) Production, oxidation, emission and consumption of methane by soils: A review. European Journal of Soil Biology 37:25-50

Lin WC, Coppi MV, Lovley DR (2004) Geobacter sulfurreducens can grow with oxygen as a terminal electron acceptor. Applied and Environmental Microbiology 70:2525-2528

Liptzin D, Silver WL (2009) Effects of carbon additions on iron reduction and phosphorus availability in a humid tropical forest soil. Soil Biology and Biochemistry 41:1696-1702

Liptzin D, Silver WL, Detto M (2011) Temporal Dynamics in Soil Oxygen and Greenhouse Gases in Two Humid Tropical Forests. Ecosystems 14:171-182 doi:10.1007/s10021-010-9402-x

Lovley DR (1991) Dissimilatory Fe(III) and Mn(IV) reduction. Microbiological reviews 55:259-287

Lovley DR (2017) Happy together: microbial communities that hook up to swap electrons. The ISME journal 11:327

Majzlan J, Navrotsky A, Schwertmann U (2004) Thermodynamics of iron oxides: Part III. Enthalpies of formation and stability of ferrihydrite, schwertmannite, and ε-Fe_2O_3. Geochimica et cosmochimica acta 68:1049-1059

McGroddy M, Silver WL (2000) Variations in belowground carbon storage and soil CO2 flux rates along a wet tropical climate gradient. Biotropica 32:614-624

O'Connell CS, Ruan L, Silver WL (2018) Drought drives rapid shifts in tropical rainforest soil biogeochemistry and greenhouse gas emissions. Nature communications 9:1348

Peretyazhko T, Sposito G (2005) Iron (III) reduction and phosphorous solubilization in humid tropical forest soils. Geochimica et Cosmochimica Acta 69:3643-3652

Pett-Ridge J, Firestone M (2005) Redox fluctuation structures microbial communities in a wet tropical soil. Applied and environmental microbiology 71:6998-7007

Pett-Ridge J, Silver WL, Firestone MK (2006) Redox fluctuations frame microbial community impacts on N-cycling rates in a humid tropical forest soil. Biogeochemistry 81:95-110

Rasmussen C et al. (2018) Beyond clay: towards an improved set of variables for predicting soil organic matter content. Biogeochemistry 137:297-306

Ray JR, Wan W, Gilbert B, Jun Y-S (2013) Effects of formation conditions on the physicochemical properties, aggregation, and phase transformation of iron oxide nanoparticles. Langmuir 29:1069-1076

Reyes I, Torrent J (1997) Citrate-ascorbate as a highly selective extractant for poorly crystalline iron oxides. Soil Science Society of America Journal 61:1647-1654

Roden EE (2006) Geochemical and microbiological controls on dissimilatory iron reduction. Comptes Rendus Geoscience 338:456-467

Roden EE, Wetzel RG (1996) Organic carbon oxidation and suppression of methane production by microbial Fe (III) oxide reduction in vegetated and unvegetated freshwater wetland sediments. Limnology and Oceanography 41:1733-1748

Scatena FN (1989) An introduction to the physiography and history of the Bisley Experimental Watersheds in the Luquillo Mountains of Puerto Rico. Gen. Tech. Rep. SO-72. New Orleans, LA: US Dept of Agriculture, Forest Service, Southern Forest Experiment Station. 22 p. 72

Schmidt S et al. (2007) Biogeochemical consequences of rapid microbial turnover and seasonal succession in soil. Ecology 88:1379-1385

Schulte P et al. (2016) Influence of HCl pretreatment and organo-mineral complexes on laser diffraction measurement of loess–paleosol-sequences. Catena 137:392-405

Schuur EA, Chadwick OA, Matson PA (2001) Carbon cycling and soil carbon storage in mesic to wet Hawaiian montane forests. Ecology 82:3182-3196

Schwaminger SP, Surya R, Filser S, Wimmer A, Weigl F, Fraga-García P, Berensmeier S (2017) Formation of iron oxide nanoparticles for the photooxidation of water: Alteration of finite size effects from ferrihydrite to hematite. Scientific Reports 7:12609

Schwartz E, Adair KL, Schuur EA (2007) Bacterial community structure correlates with decomposition parameters along a Hawaiian precipitation gradient. Soil Biology and Biochemistry 39:2164-2167

Schwertmann U, Cornell RM (2008) Iron oxides in the laboratory: preparation and characterization. John Wiley & Sons,

Segarra K, Schubotz F, Samarkin V, Yoshinaga M, Hinrichs K, Joye S (2015) High rates of anaerobic methane oxidation in freshwater wetlands reduce potential atmospheric methane emissions. Nature communications 6:7477

Segers R, Leffelaar P (1996) On explaining methane fluxes from weather, soil and vegetation data via the underlying processes. In: Laiho R, Laine J, Vasander H (eds) Northern Peatlands in Global Climate Change. Academy of Finland, Helsinki, Finland, pp 226-241

Serrano-Silva N, Sarria-Guzman Y, Dendooven L, Luna-Guido M (2014) Methanogenesis and Methanotrophy in Soil: A Review. Pedosphere 24:291-307

Silver WL, Lugo A, Keller M (1999) Soil oxygen availability and biogeochemistry along rainfall and topographic gradients in upland wet tropical forest soils. Biogeochemistry 44:301-328

Sivan O, Adler M, Pearson A, Gelman F, Bar-Or I, John SG, Eckert W (2011) Geochemical evidence for iron-mediated anaerobic oxidation of methane. Limnology and Oceanography 56:1536-1544

Sivan O, Shusta S, Valentine D (2016) Methanogens rapidly transition from methane production to iron reduction. Geobiology 14:190-203

Spohn M (2016) Element cycling as driven by stoichiometric homeostasis of soil microorganisms. Basic and Applied Ecology 17:471-478

Sposito G (2008) The chemistry of soils. Second edn. Oxford university press, New York. pp 3-329

Straub KL, Schink B (2004) Ferrihydrite reduction by Geobacter species is stimulated by secondary bacteria. Archives of Microbiology 182:175-181

Subke JA, Inglima I, Francesca Cotrufo M (2006) Trends and methodological impacts in soil CO2 efflux partitioning: a metaanalytical review. Global Change Biology 12:921-943

Tang KW, McGinnis DF, Ionescu D, Grossart H-P (2016) Methane Production in Oxic Lake Waters Potentially Increases Aquatic Methane Flux to Air. Environmental Science & Technology Letters 3:227-233

Teh YA, Dubinsky EA, Silver WL, Carlson CM (2008) Suppression of methanogenesis by dissimilatory Fe (III)-reducing bacteria in tropical rain forest soils: Implications for ecosystem methane flux. Global Change Biology 14:413-422

Teh YA, Silver WL, Conrad ME (2005) Oxygen effects on methane production and oxidation in humid tropical forest soils. Global Change Biology 11:1283-1297

Thompson A, Chadwick OA, Rancourt DG, Chorover J (2006) Iron-oxide crystallinity increases during soil redox oscillations. Geochimica et Cosmochimica Acta 70:1710-1727

Tiedje J, Sexstone A, Parkin T, Revsbech N (1984) Anaerobic processes in soil. Plant and Soil 76:197-212

Tishchenko V, Meile C, Scherer MM, Pasakarnis TS, Thompson A (2015) Fe 2+ catalyzed iron atom exchange and re-crystallization in a tropical soil. Geochimica et Cosmochimica Acta 148:191-202

Valenzuela EI et al. (2017) Anaerobic methane oxidation driven by microbial reduction of natural organic matter in a tropical wetland. Applied and Environmental Microbiology 83:e00645-00617

Van Cappellen P, Viollier E, Roychoudhury A, Clark L, Ingall E, Lowe K, Dichristina T (1998) Biogeochemical cycles of manganese and iron at the oxic− anoxic transition of a stratified marine basin (Orca Basin, Gulf of Mexico). Environmental science & technology 32:2931-2939

Weber KA, Achenbach LA, Coates JD (2006) Microorganisms pumping iron: anaerobic microbial iron oxidation and reduction. Nature Reviews Microbiology 4:752-764

Wegener G, Krukenberg V, Riedel D, Tegetmeyer HE, Boetius A (2015) Intercellular wiring enables electron transfer between methanotrophic archaea and bacteria. Nature 526:587

Weiss JV, Emerson D, Megonigal JP (2004) Geochemical control of microbial Fe (III) reduction potential in wetlands: comparison of the rhizosphere to non-rhizosphere soil. FEMS Microbiology Ecology 48:89-100

White AF, Peterson ML (1998) The reduction of aqueous metal species on the surfaces of Fe (II)-containing oxides: The role of surface passivation. In. ACS Publications

Wilmoth JL (2016) Effects of redox-cycling on iron-mineral transformations and metatranscriptome of iron (III)-reducing bacteria in a humid tropical forest soil. Doctoral Dissertation. University of Georgia

Yu G et al. (2017) Mineral Availability as a Key Regulator of Soil Carbon Storage. Environmental Science & Technology 51:4960-4969

Zachara JM, Fredrickson JK, Li S-M, Kennedy DW, Smith SC, Gassman PL (1998) Bacterial reduction of crystalline Fe (super 3+) oxides in single phase suspensions and subsurface materials. American Mineralogist 83:1426-1443

Zhao Q et al. (2017) Coupled dynamics of iron and iron-bound organic carbon in forest soils during anaerobic reduction. Chemical Geology 464:118-126

TABLES AND FIGURES

Table 3.1. Treatments for different oscillation periods and τ_{ox} or τ_{anoxic} durations in hours (and days)

Treatment	**τ_{oxic}**	**τ_{anoxic}**	**$\tau_{oxic}/\tau_{anoxic}$ ratio**	**Num. of Cycles**
Pre-conditioning (15 vessels)	24 h	144 h (6 d)	1:6	3

Started different treatments ↓ *At 480 h of experiment*

Treatments	**τ_{oxic}**	**τ_{anoxic}**	**$\tau_{oxic}/\tau_{anoxic}$ ratio**	**Reps**	**Num. of Cycles**
L-72h	72 h (3 d)	144 h (6 d)	1:2	3	3
L-24h	24 h	144 h (6 d)	1:6	3	3
L-8h	8 h	144 h (6 d)	1:18	3	3
S-24h	24 h	48 h	1:2	3	7
S-8h	8 h	48 h	1:6	3	7

+ Anoxic Control (3 reps)
+ Oxic Control (3 reps)

Table 3.2. Slopes and R^2 for regression analysis between Fe^{II}, CO_2, and CH_4

Treatment	Fe^{II} concentration vs Cumulative CO_2		Fe^{II} concentration vs Cumulative CH_4		Cumulative CO_2 vs Cumulative CH_4	
	Slope	R^2	Slope	R^2	Slope	R^2
All treatments	1.94*	0.51	0.33*	0.18	2.36*	0.47
Pre-conditioning	1.84*	0.85	0.88*	0.77	1.60*	0.65
L-72	1.76*	0.82	0.29*	0.62	5.01*	0.89
L-24	2.50*	0.84	0.85*	0.65	1.84*	0.56
L-8	3.10*	0.69	1.32	0.28	1.82*	0.44
S-24	3.51*	0.56	0.69*	0.72	2.75	0.26
S-8	1.12	0.25	0.13	0.12	-0.26	0.06

*significantly different from zero at 5%

Table 3.3. Percentage of CO_2 production due to respiratory iron-reducing bacteria, calculated from Fe reduction rates and CO_2 fluxes using the 1:4 stoichiometry (1 mol of CO_2 oxidized for every 4 mols of Fe^{II} reduced). Soils from Bisley watershed, Puerto Rico, sampled in 2015.

Treatment	Fe reduction rates		CO_2 flux		CO_2 from Fe^{II} production	
	mmol kg^{-1} h^{-1}	(± St Dev)	mmol kg^{-1} h^{-1}	(± St Dev)	%	(± St Dev)
Pre-conditioning	0.152	(0.049)	0.087	(0.025)	50.4	(8.8)
L-72	0.110	(0.045)	0.069	(0.018)	43.5	(8.2)
L-24	0.167	(0.102)	0.062	(0.017)	70.0	(12.8)
L-8	0.255	(0.072)	0.066	(0.020)	96.6	(14.5)
S-24	0.140	(0.129)	0.062	(0.021)	56.2	(16.8)
S-8	0.149	(0.041)	0.062	(0.026)	73.5	(13.4)

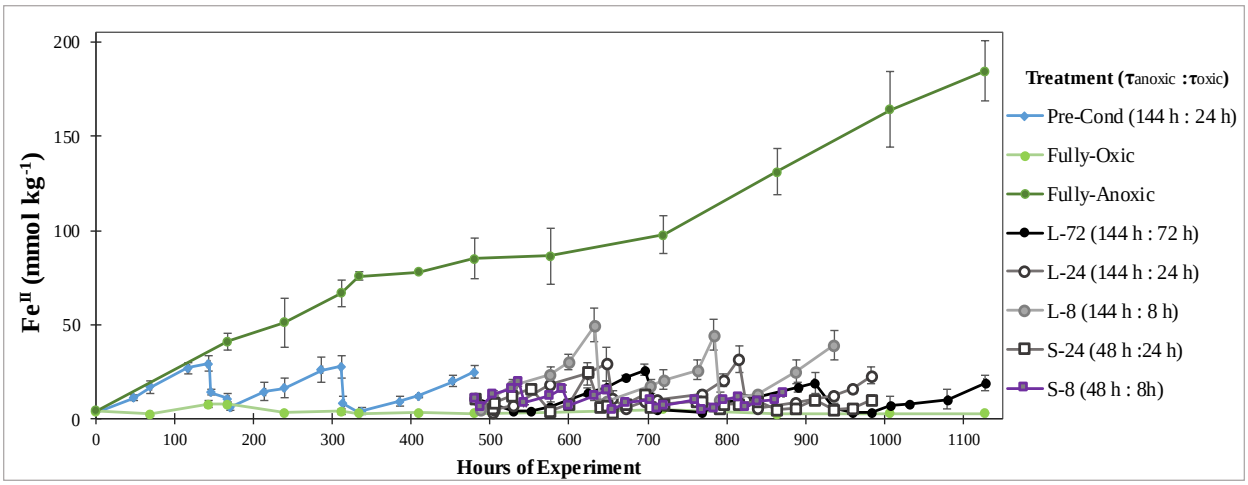
Fe^{II} (mmol kg^{-1})
Hours of Experiment
Treatment (τanoxic : τoxic)
Pre-Cond (144 h : 24 h)
Fully-Oxic
Fully-Anoxic
L-72 (144 h : 72 h)
L-24 (144 h : 24 h)
L-8 (144 h : 8 h)
S-24 (48 h :24 h)
S-8 (48 h : 8h)

(a)

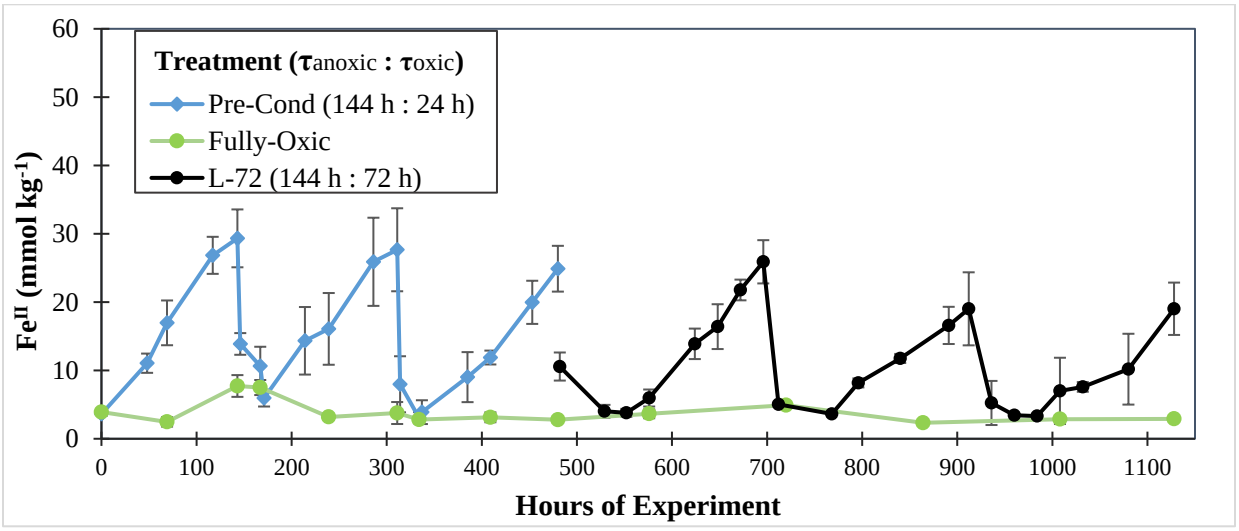
Fe^{II} (mmol kg^{-1})
Hours of Experiment
Treatment (τanoxic : τoxic)
Pre-Cond (144 h : 24 h)
Fully-Oxic
L-72 (144 h : 72 h)

(b)

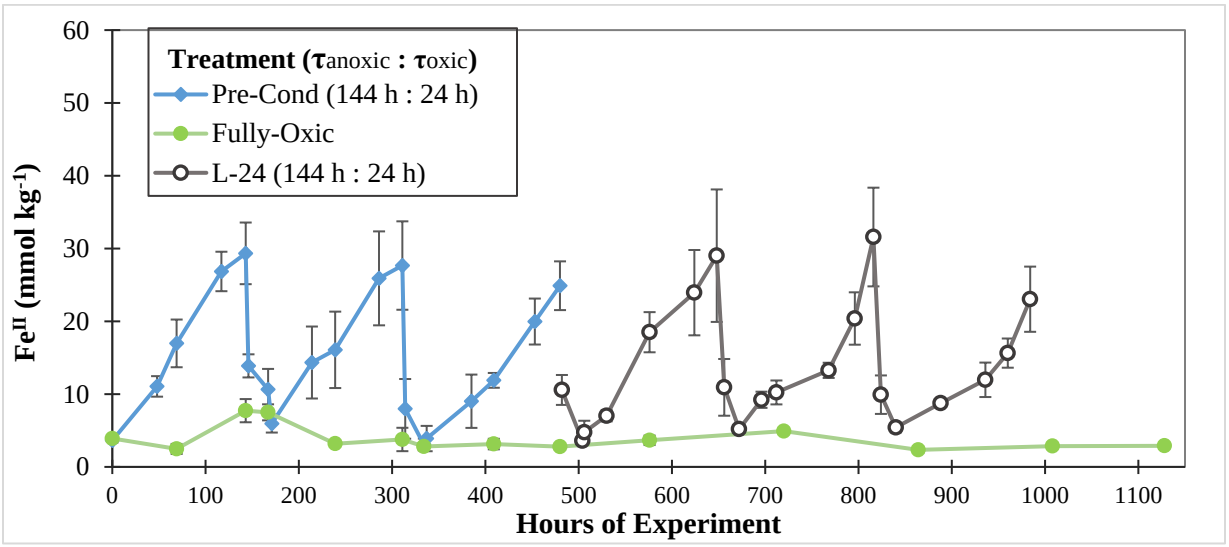
Fe^{II} (mmol kg^{-1})
Hours of Experiment
Treatment (τanoxic : τoxic)
Pre-Cond (144 h : 24 h)
Fully-Oxic
L-24 (144 h : 24 h)

(c)

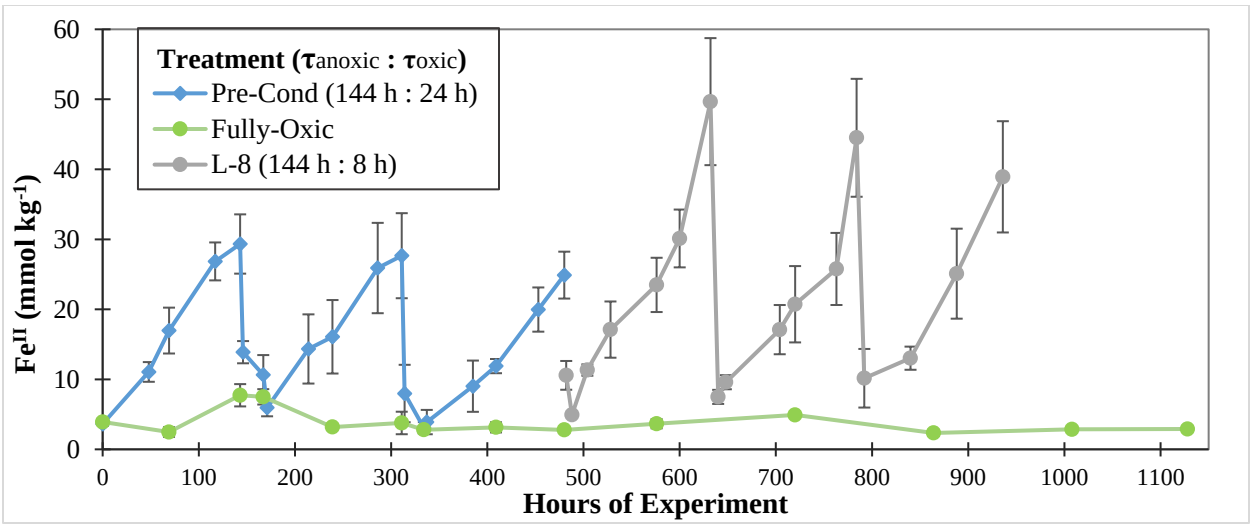

(d)

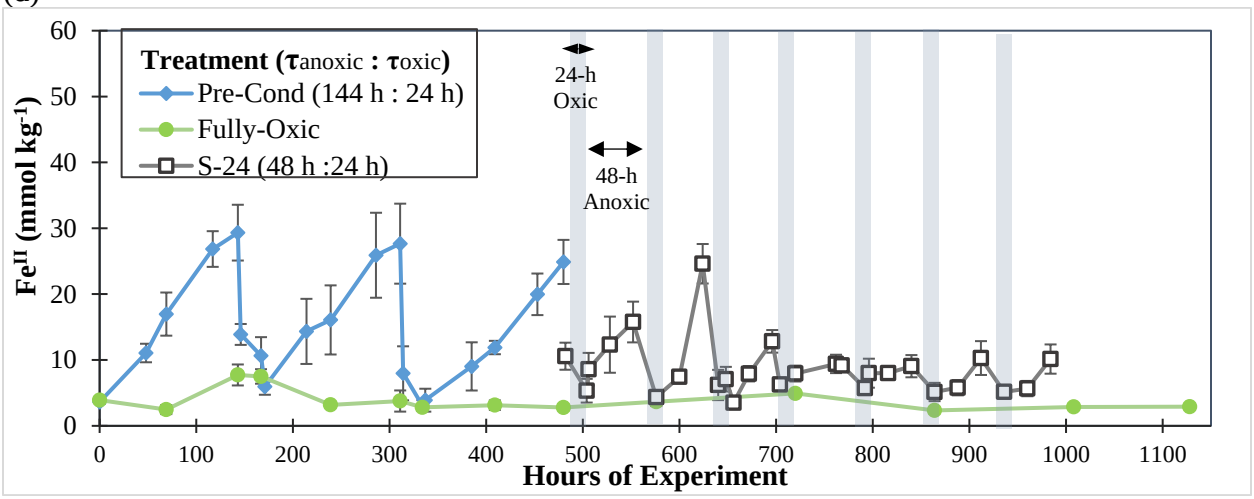

(e)

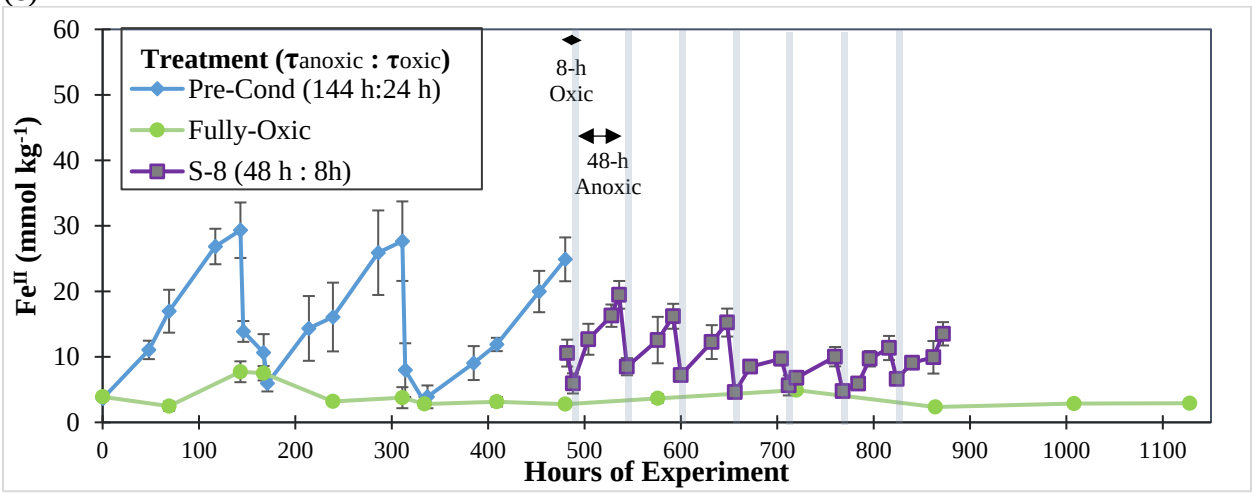

(f)

Fig 3.1. Fe^{II} dynamics all treatments together (a) and over the different treatments separately (a) to (f). Soils from Bisley watershed, Puerto Rico, sampled in 2015.

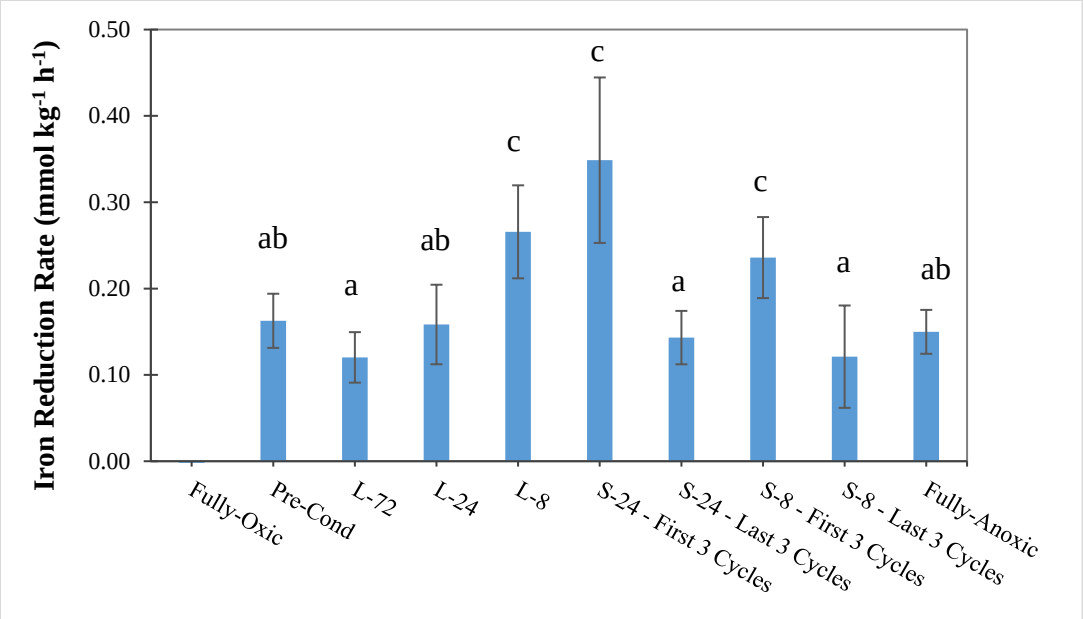

Fig 3.2. Averaged Fe reduction rates for all treatments. The short treatments S-24 and S-8 were split into the 3 initial cycles and the 3 last cycles, due to observed changes in Fe^{II} over these treatments. The long treatments were not split. Lowercase letters in parentheses (a, b, c, d) indicate significant differences at the 5% probability level. The error bars indicate a ± 1 standard deviation. Soils from Bisley watershed, Puerto Rico, sampled in 2015.

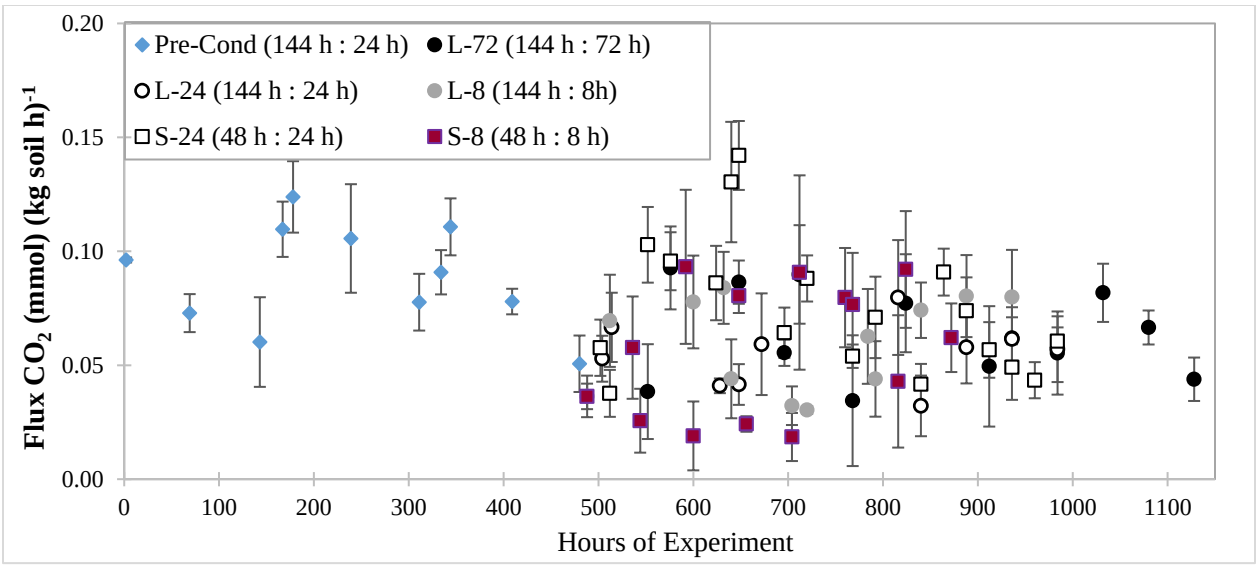
Pre-Cond (144 h : 24 h)
L-72 (144 h : 72 h)
L-24 (144 h : 24 h)
L-8 (144 h : 8h)
S-24 (48 h : 24 h)
S-8 (48 h : 8 h)
Flux CO2 (mmol) (kg soil h)-1
Hours of Experiment

(a)

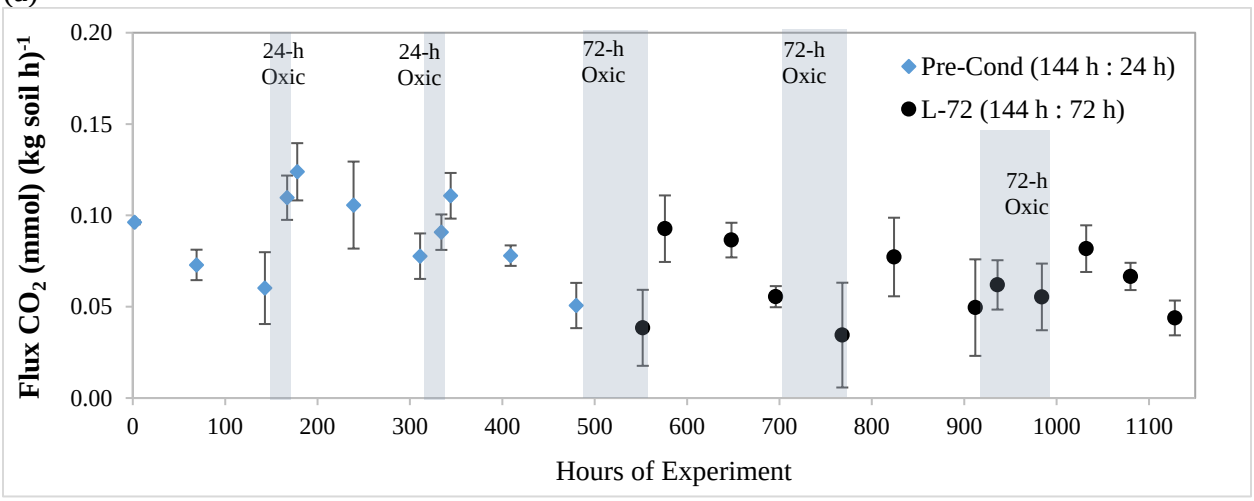
24-h Oxic
24-h Oxic
72-h Oxic
72-h Oxic
72-h Oxic
Pre-Cond (144 h : 24 h)
L-72 (144 h : 72 h)
Flux CO2 (mmol) (kg soil h)-1
Hours of Experiment

(b)

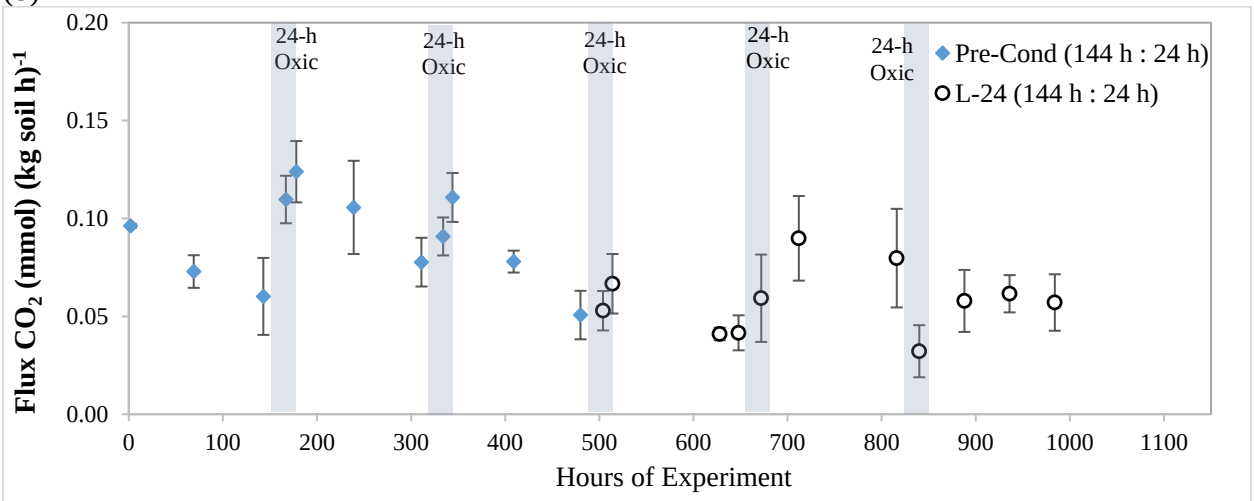
24-h Oxic
24-h Oxic
24-h Oxic
24-h Oxic
24-h Oxic
Pre-Cond (144 h : 24 h)
L-24 (144 h : 24 h)
Flux CO2 (mmol) (kg soil h)-1
Hours of Experiment

(c)

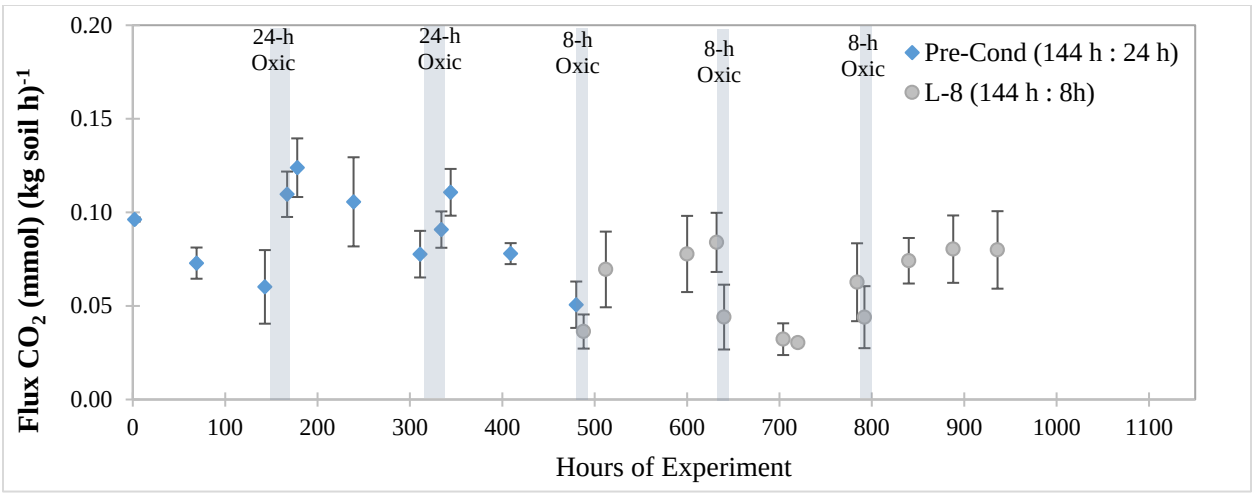

(d)

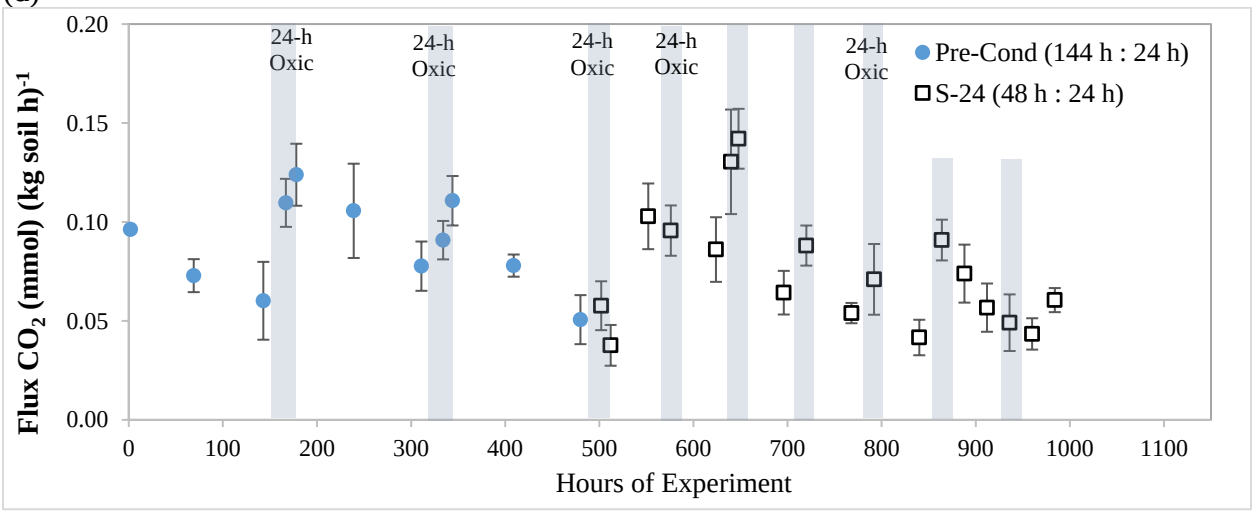

(e)

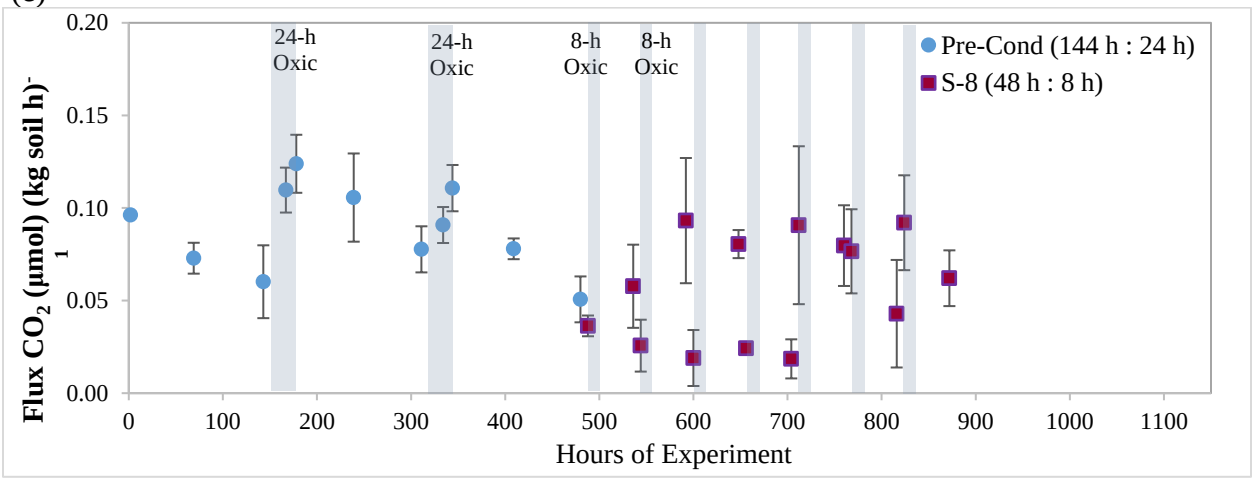

(f)

Fig 3.3 Instantaneous CO_2 flux for all treatments together (a) and over the different treatments (b) to (f). Soils from Bisley watershed, Puerto Rico, sampled in 2015.

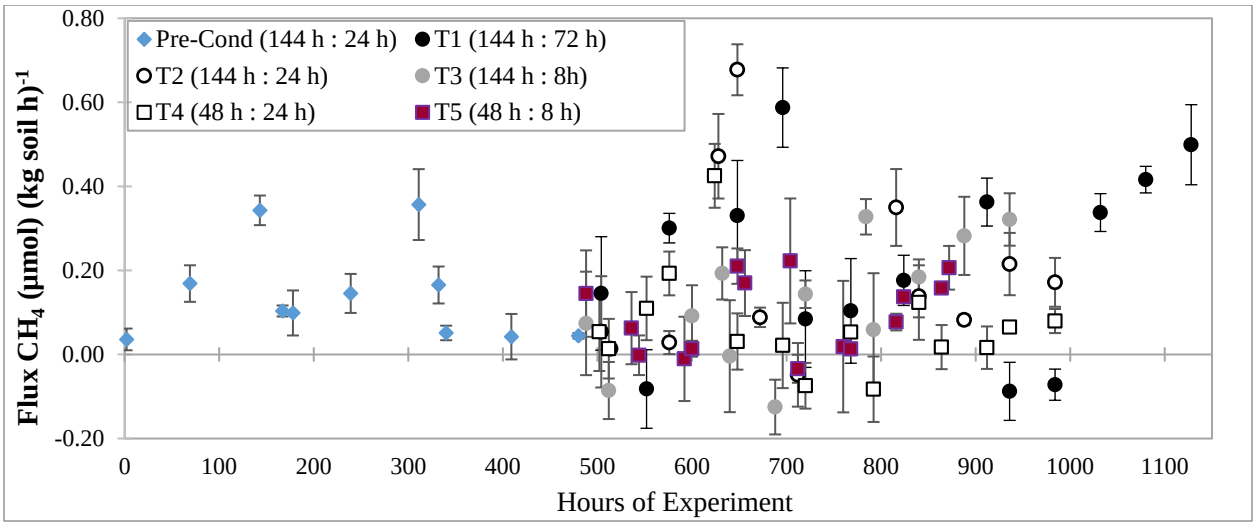
Pre-Cond (144 h : 24 h)
T1 (144 h : 72 h)
T2 (144 h : 24 h)
T3 (144 h : 8h)
T4 (48 h : 24 h)
T5 (48 h : 8 h)
Flux CH_4 (µmol) (kg soil h)$^{-1}$
Hours of Experiment

(a)

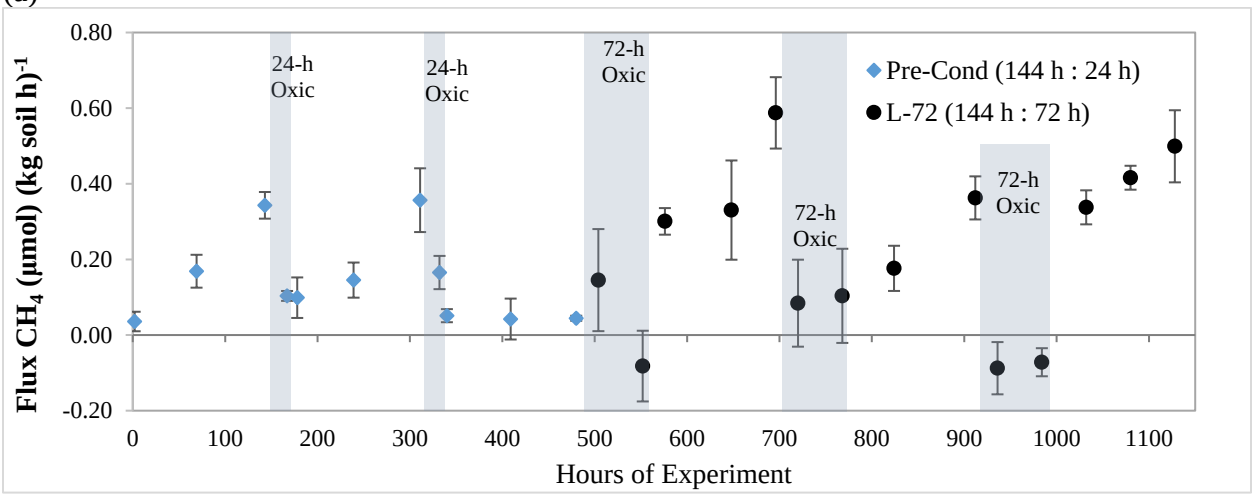
24-h Oxic
24-h Oxic
72-h Oxic
72-h Oxic
72-h Oxic
Pre-Cond (144 h : 24 h)
L-72 (144 h : 72 h)
Flux CH_4 (µmol) (kg soil h)$^{-1}$
Hours of Experiment

(b)

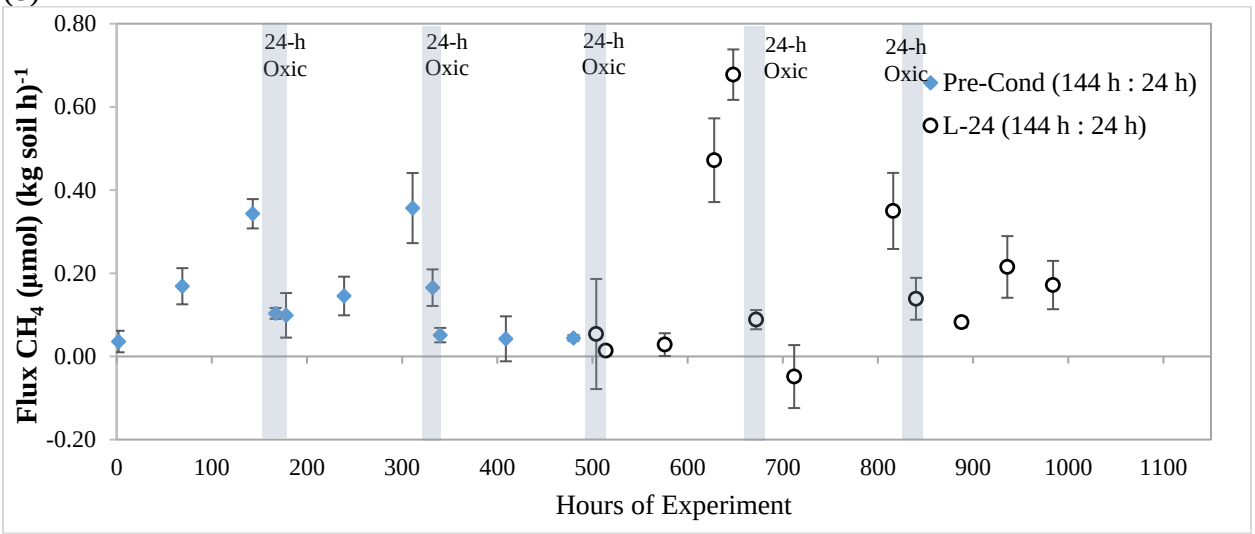
24-h Oxic
24-h Oxic
24-h Oxic
24-h Oxic
24-h Oxic
Pre-Cond (144 h : 24 h)
L-24 (144 h : 24 h)
Flux CH_4 (µmol) (kg soil h)$^{-1}$
Hours of Experiment

(c)

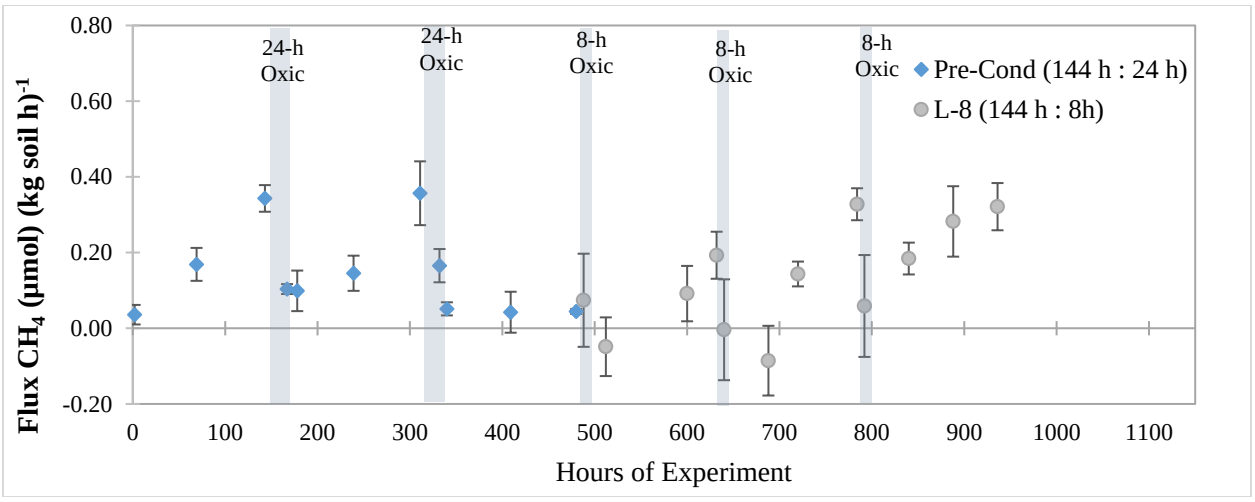

(d)

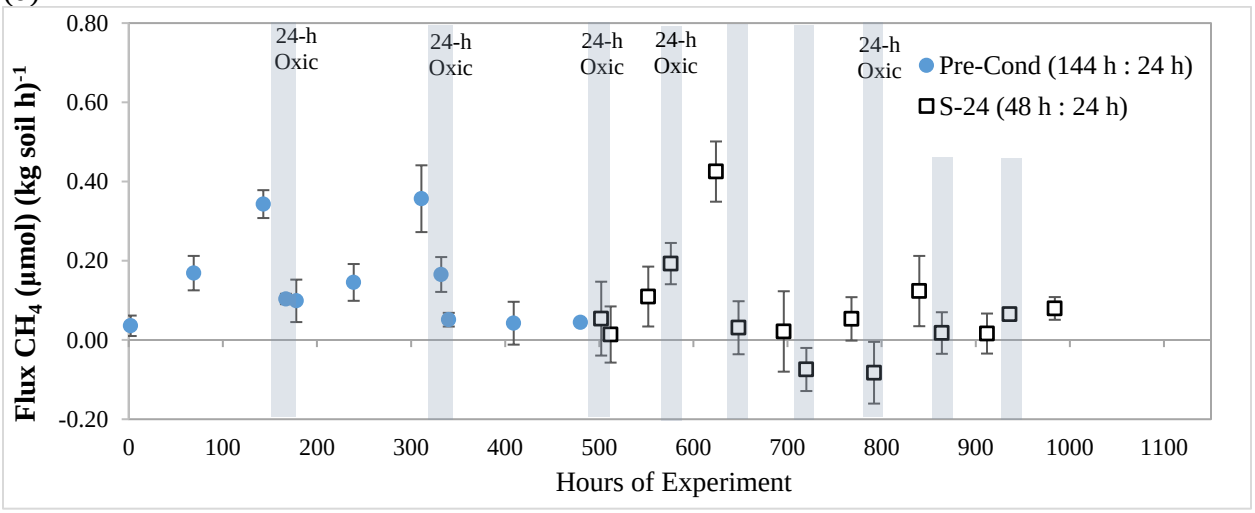

(e)

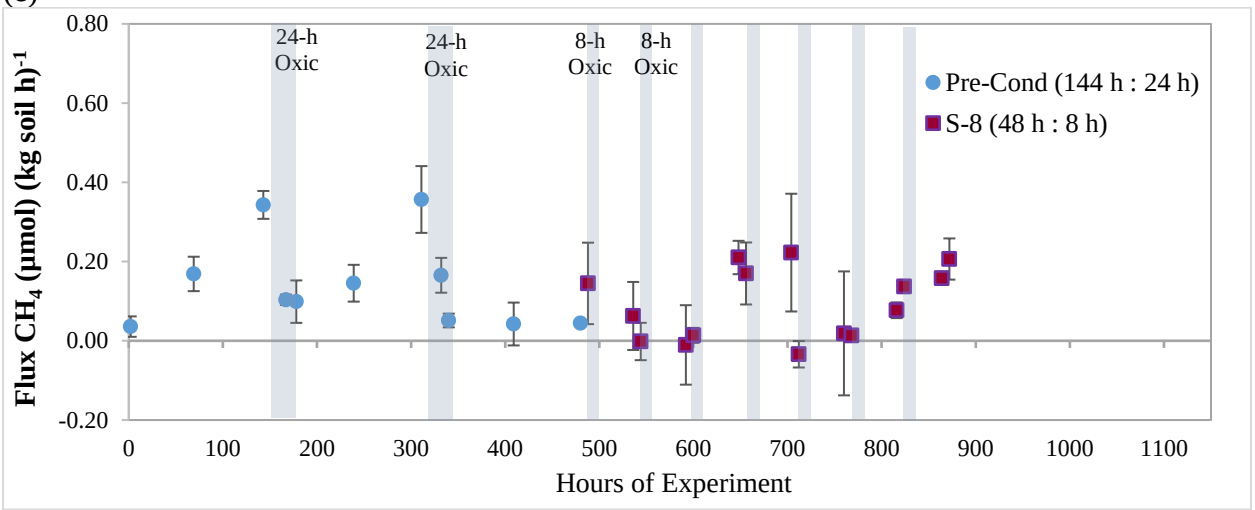

(f)

Fig 3.4. Instantaneous CH_4 flux for all treatments together (a) and over the different treatments (b) to (f). Soils from Bisley watershed, Puerto Rico, sampled in 2015.

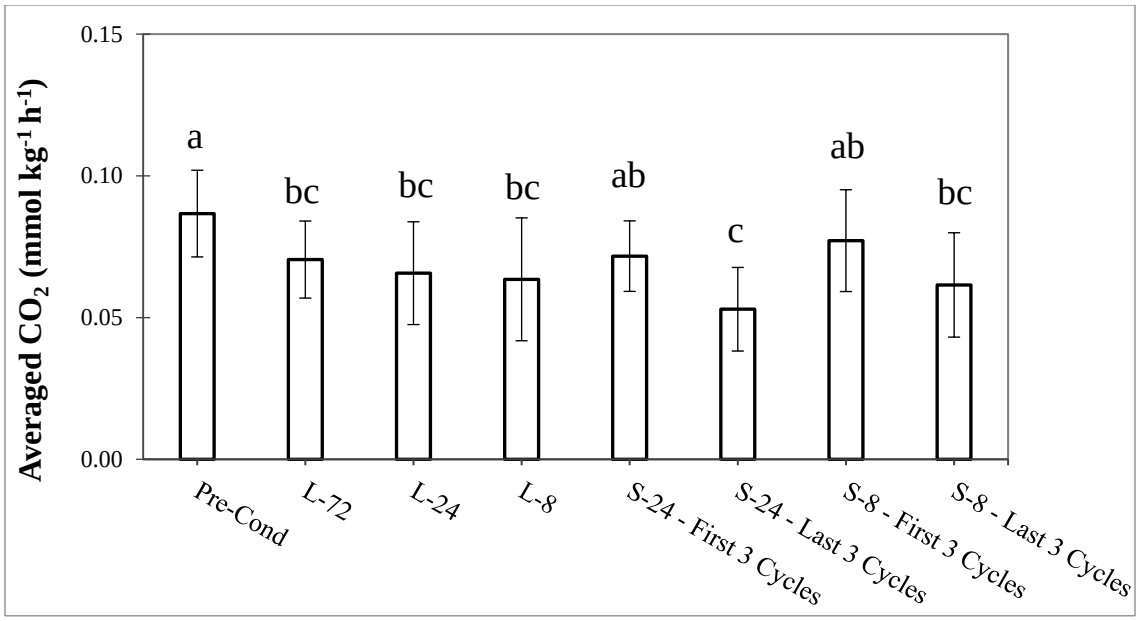

(a)

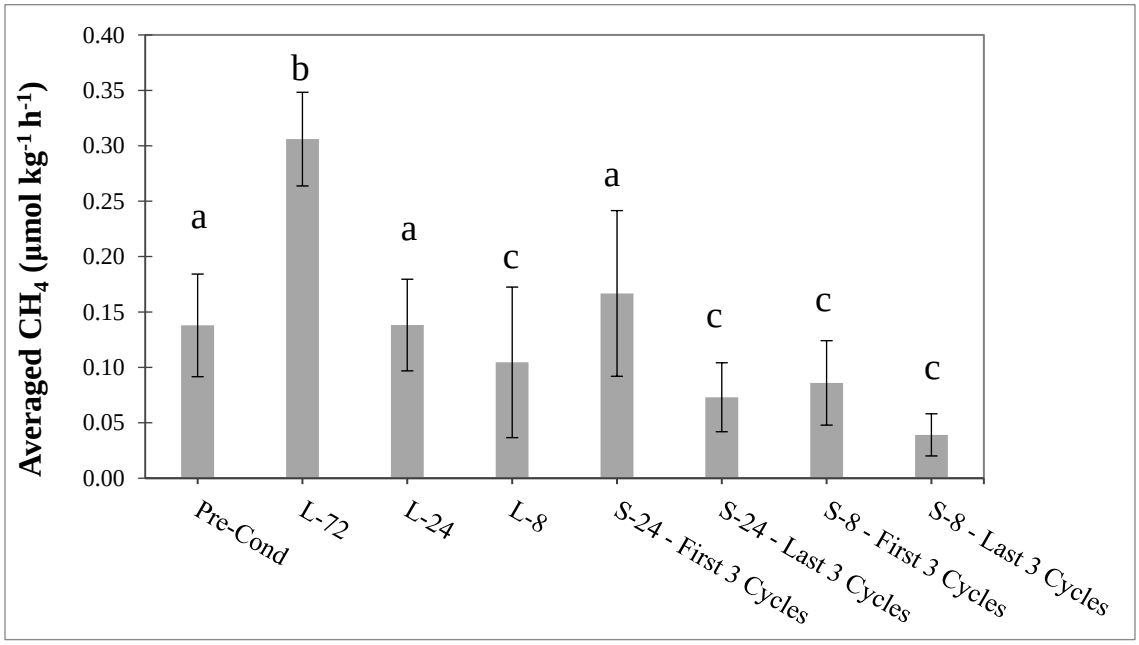

(b)

Fig 3.5. Averaged fluxes of CO_2 (a) and CH_4 (b) during τ_{anoxic}: values of cumulative CO_2 or cumulative CH_4 divided by the length of the anoxic cycle (6 d for Long treatments, and 2 d for Short treatments). Lowercase letters in parentheses (a, b, c, d) indicate significant differences at the 5% probability level. The error bars indicate a ± 1 standard deviation. Soils from Bisley watershed, Puerto Rico, sampled in 2015.

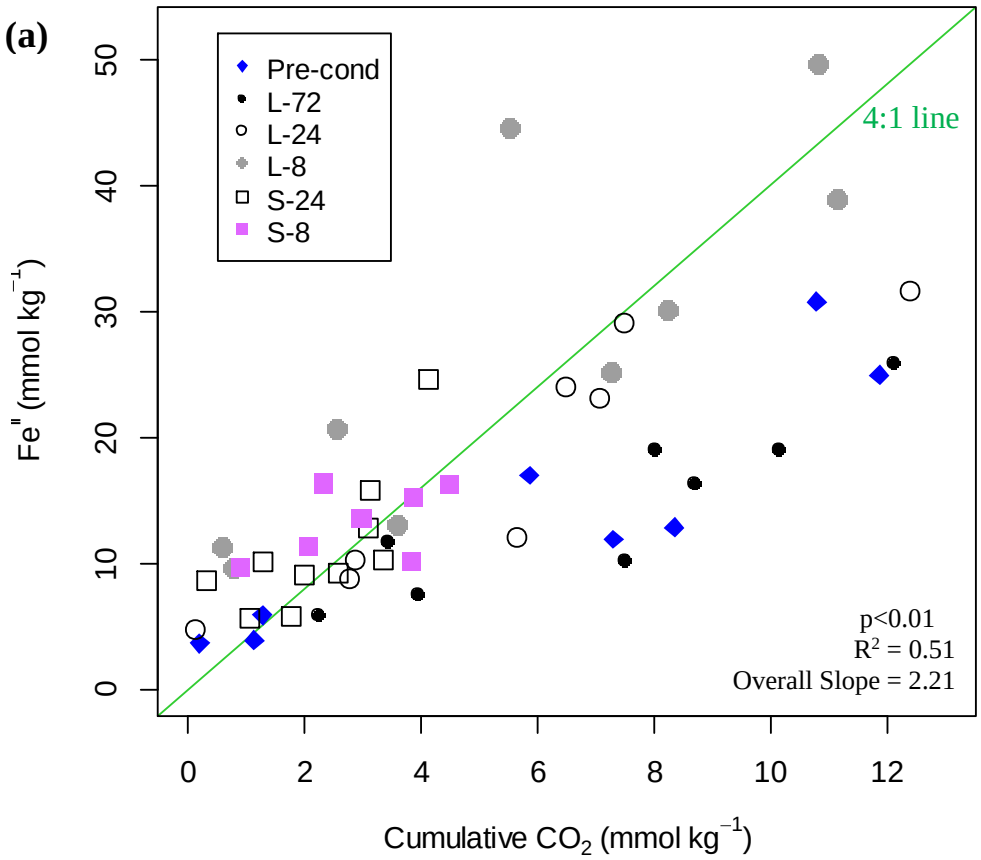
(a)
Pre-cond
L-72
L-24
L-8
S-24
S-8
4:1 line
p<0.01
R2 = 0.51
Overall Slope = 2.21
Fe" (mmol kg-1)
Cumulative CO2 (mmol kg-1)
0
10
20
30
40
50
0
2
4
6
8
10
12

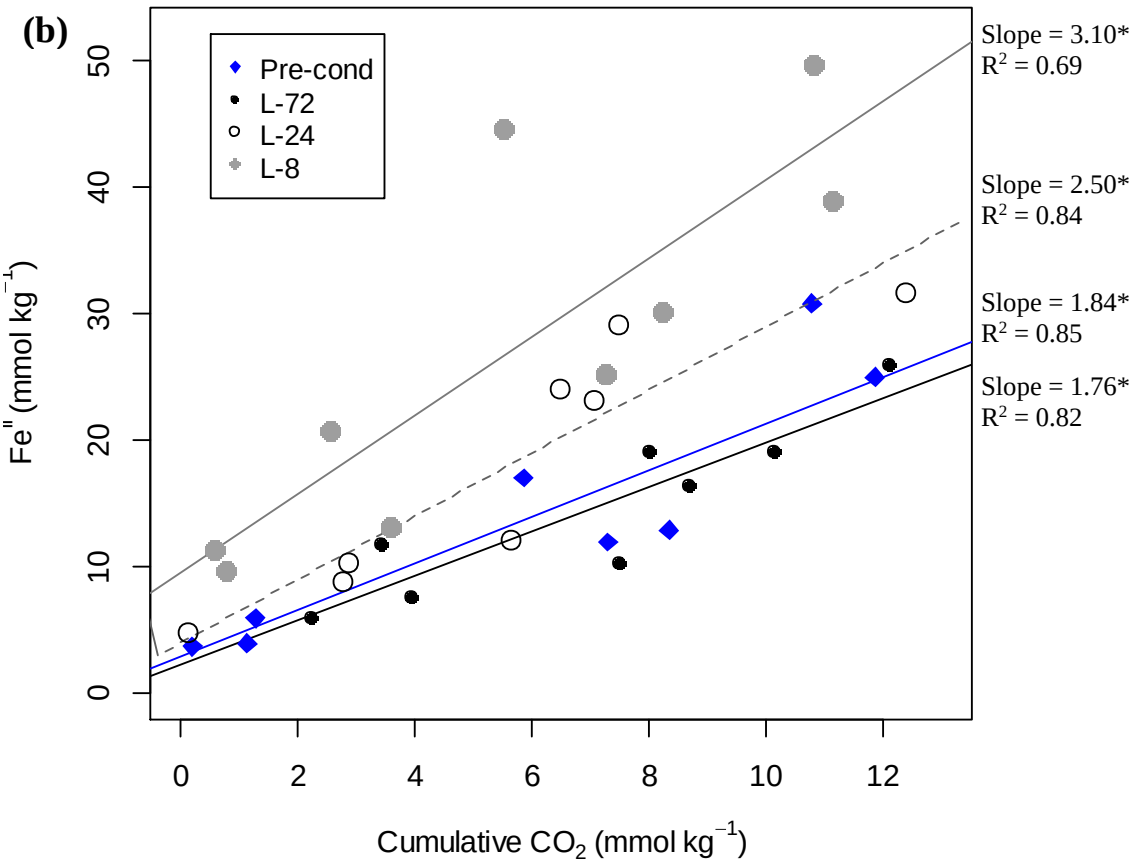
(b)
Pre-cond
L-72
L-24
L-8
Slope = 3.10*
R2 = 0.69
Slope = 2.50*
R2 = 0.84
Slope = 1.84*
R2 = 0.85
Slope = 1.76*
R2 = 0.82
Fe" (mmol kg−1)
Cumulative CO2 (mmol kg−1)
0
10
20
30
40
50
0
2
4
6
8
10
12

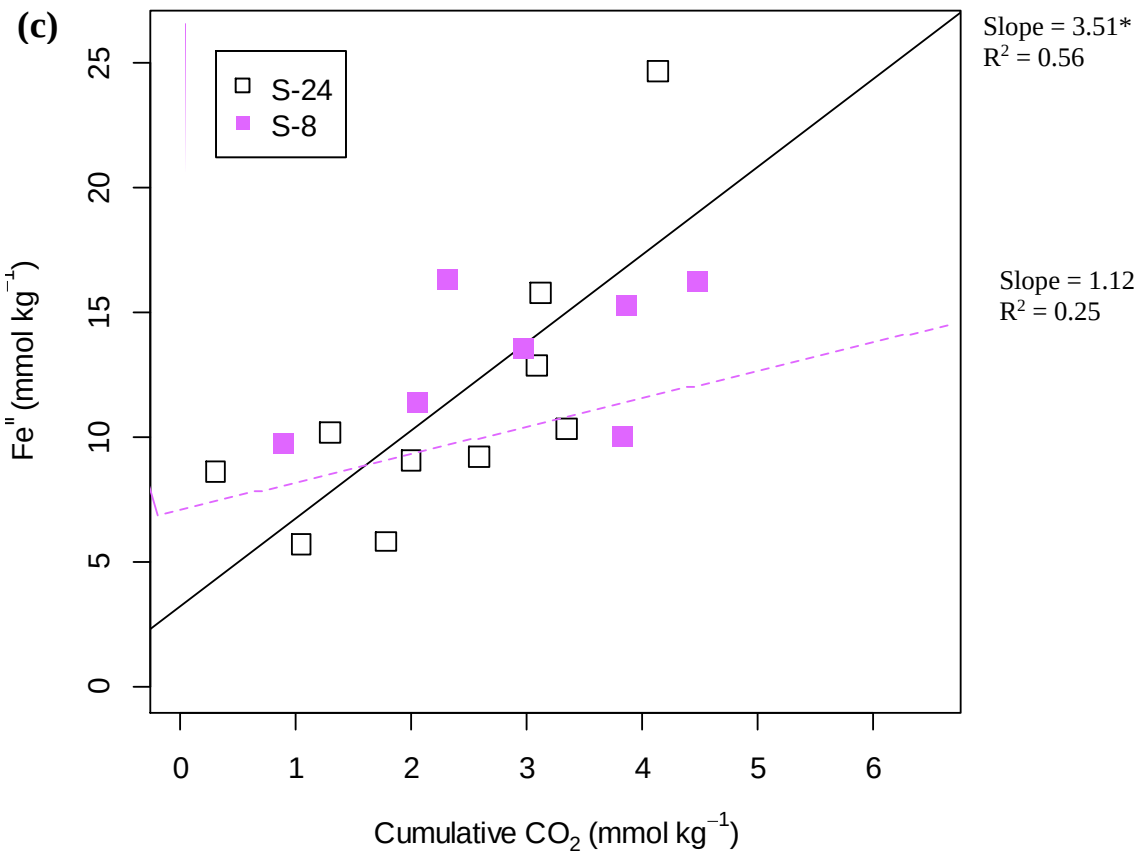

Fig 3.6 Linear regressions for Fe^{II} concentrations vs Cumulative CO_2 under anoxic conditions only: (a) for all 5 treatments with, (b) details for the Long treatments only with regression lines, (c) and Short treatments only. Asterisks represents slopes that are significant at 5% probably for the linear models. Green Line comparing the 4:1 stoichiometric correlation of 4 mols of Fe^{II} reduced for every 1 mol of CO_2 oxidized (Roden and Wetzel 1996). Soils from Bisley watershed, Puerto Rico, sampled in 2015.

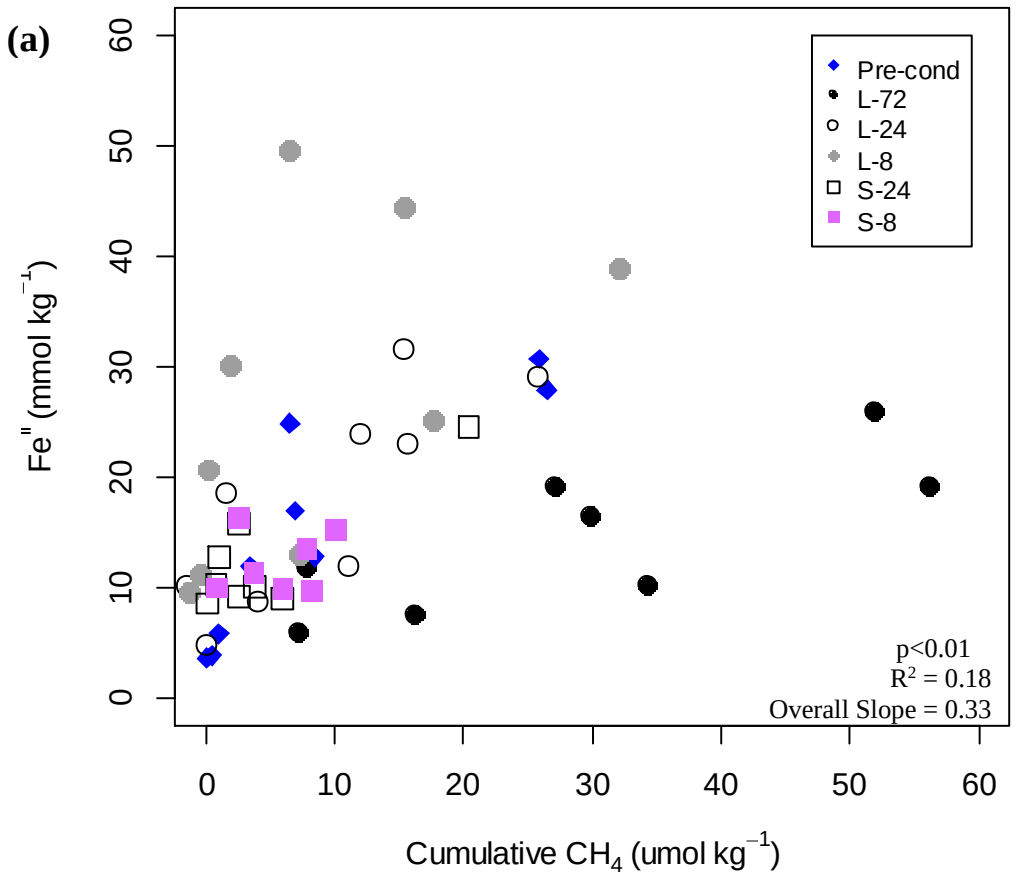
(a)
Pre-cond
L-72
L-24
L-8
S-24
S-8
p<0.01
R2 = 0.18
Overall Slope = 0.33
Fe" (mmol kg-1)
Cumulative CH4 (umol kg-1)
0
10
20
30
40
50
60

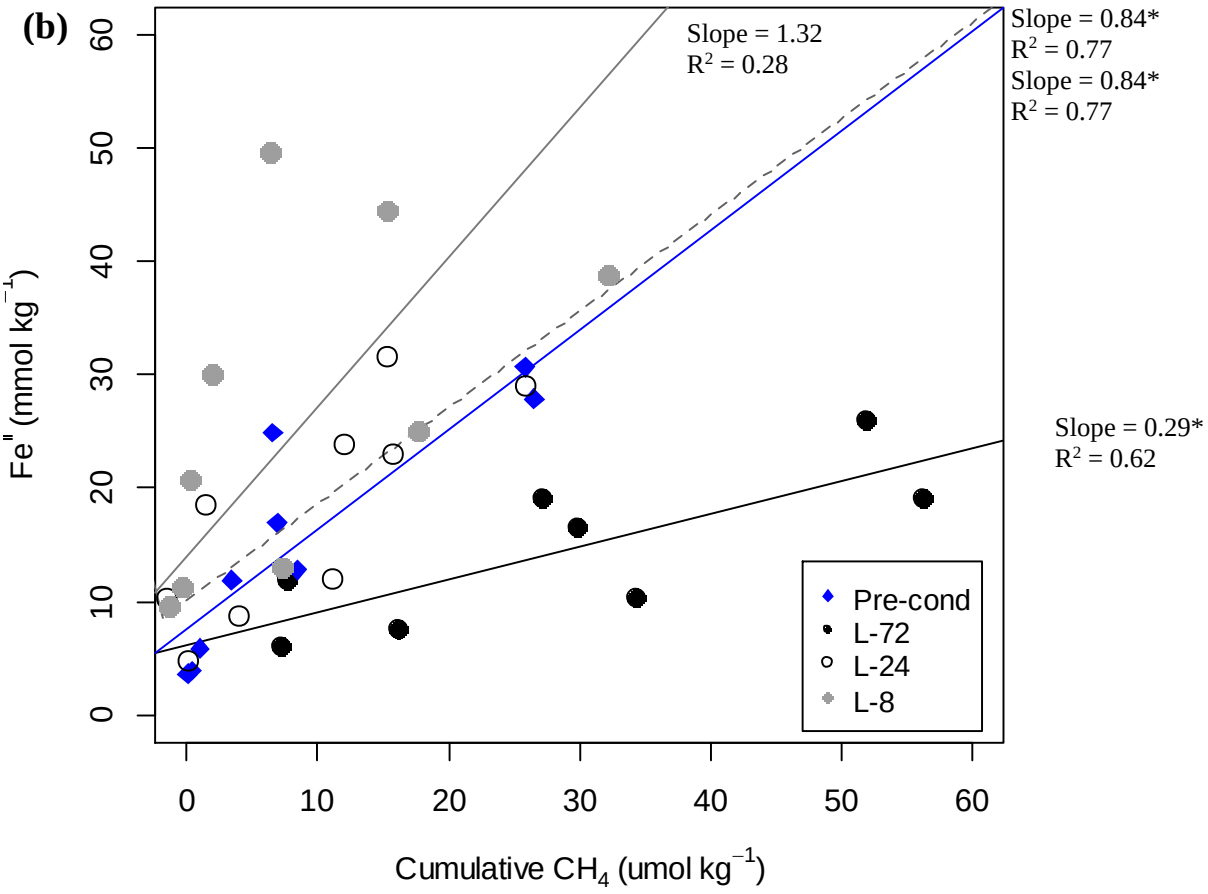
(b)
Slope = 1.32
R2 = 0.28
Slope = 0.84*
R2 = 0.77
Slope = 0.84*
R2 = 0.77
Slope = 0.29*
R2 = 0.62
Pre-cond
L-72
L-24
L-8
Fe" (mmol kg-1)
Cumulative CH4 (umol kg-1)
0
10
20
30
40
50
60

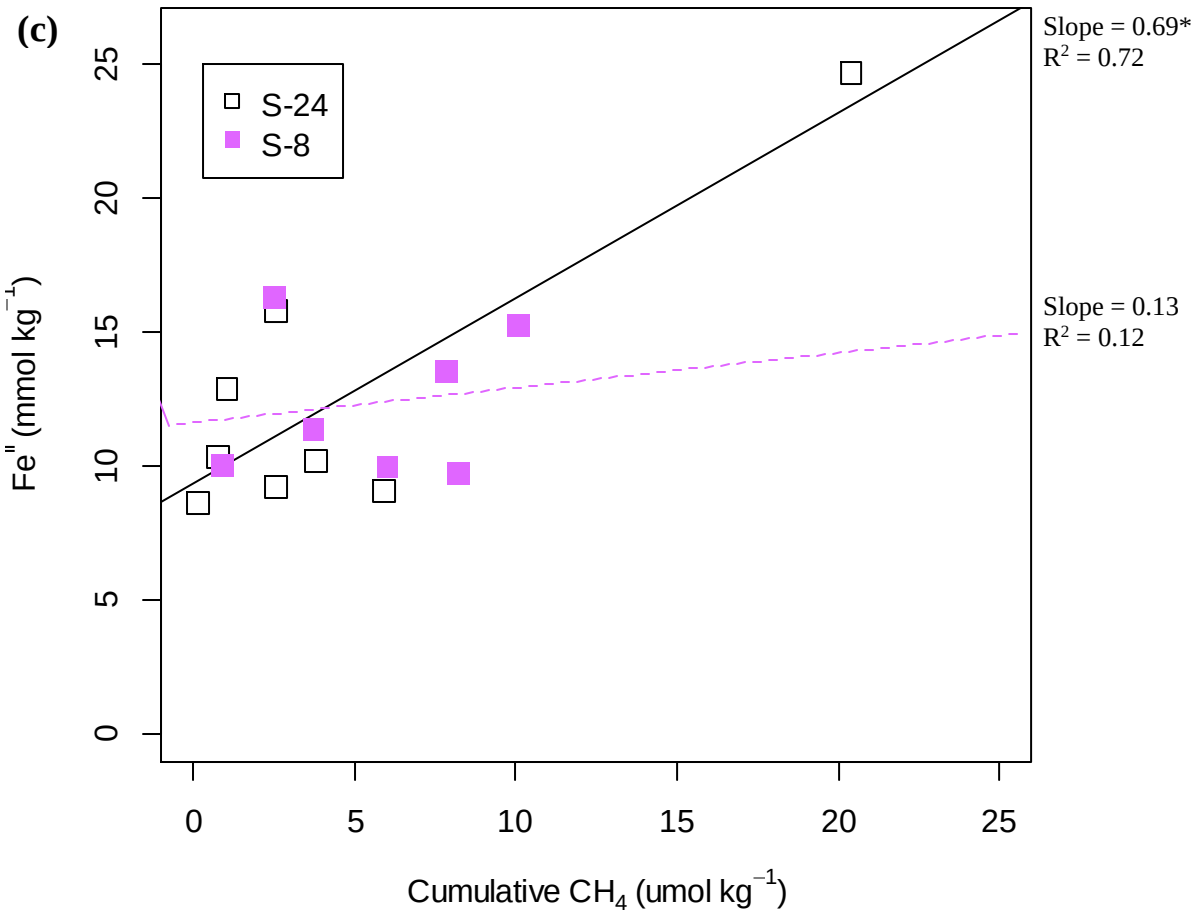

Fig 3.7. Linear regressions for Fe^{II} concentrations vs Cumulative CH_4 under anoxic conditions only: (a) for all 5 treatments, (b) details for the Long treatments only, (c) and Short treatments only. Asterisks represents slopes that are significant at 5% probably for the linear models. Soils from Bisley watershed, Puerto Rico, sampled in 2015.

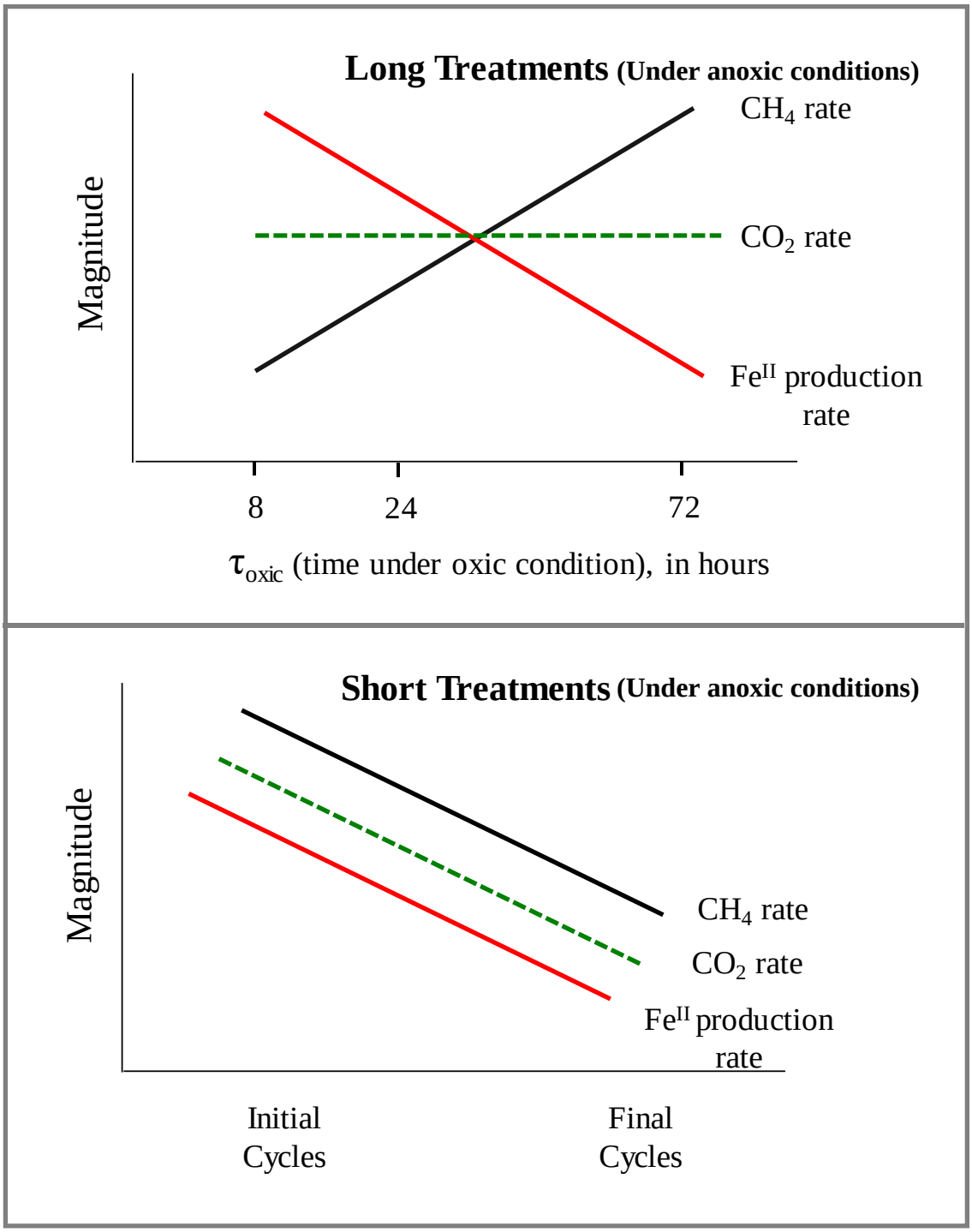

Fig 3.8. Alterations in Fe^{II}, CO_2, and CH_4 during anoxic conditions, with changes in τ_{oxic} for the long treatments (upper figure), and over the course of the experiment for the short treatments (lower figure).

CHAPTER 4

SOIL MOISTURE AND PRECIPITATION EXPLAIN FLUCTUATIONS IN REDOX POTENTIAL, IRON REDUCTION, AND CARBON CYCLING IN A HUMID FOREST SOIL FROM PUERTO RICO[3]

[3] Barcellos, D., C.S. O'Connell, W. Silver, C. Meile, and A. Thompson. To be submitted to the Journal Catena

Abstract

Soils from tropical rainforests undergo spatial and temporal variations in moisture and oxygen content in response to rainfall events. These environmental variations can induce changes in redox potential, iron (Fe) reduction rates, and carbon (C) decomposition and/or accumulation. We hypothesized that during an increase in rainfall and soil moisture (i) Fe reduction rates, organic C mineralization, and DOC release (hot moments) would increase, and that (ii) the lowest landscape position (valley) would have higher rates Fe and C cycling. To test these hypotheses, we measured soil Fe and C biogeochemical parameters across three catenas at valley, slope, and ridge topographic positions approximately every 2 days for a 2-month-period in a montane forest in Puerto Rico (USA). Measurements included soil extractions of Fe^{II}, rapidly-reducible Fe oxides (Fe^{III}_{RR}), DOC, and pH. Sensors monitored redox potential (Eh), soil moisture and O_2, and fluxes of CO_2 and CH_4. Over a 12-day period without rain, we observed a decline in soil moisture, Fe^{II}, Fe^{III}_{RR}, DOC, and an increase in Eh and O_2 values; conversely, during a 10-day intense rain event (290 mm) we observed the opposite trends. Using mixed-effects models, we found that precipitation was a predictor for the environmental factors (soil moisture, Eh, and O_2), which in turn drove Fe reduction-oxidation, C dissolution and mineralization processes. We also found the turnover times for Fe^{II} production and consumption were centered around 4 days. Our results demonstrated that periods of high precipitation, soil moisture, and low O_2 (hot moments) influenced biogeochemical processes such as Fe reduction and C-cycling within day-to-week timescales, and these effects are more pronounced in certain topographic positions, such as valleys (hot spots).

4.1. Introduction

Rainfall infiltrates into the soil, changing soil moisture and oxygen content, and modifying substantially the soil biogeochemical processes that govern carbon (C) and iron (Fe) cycling. These processes have important implications for land management and climate change (Broedel et al. 2017; FAO 2015; Hall et al. 2016; Kleber et al. 2015). In humid tropical regions, rainfall can be very high with annual averages ranging from 3 – 10 meters across the neo-tropics (e.g., the Caribbean and Amazon forests) (Álvarez-Dávila et al. 2017; Brokaw et al. 2012b; Saleska et al. 2003). High precipitation accelerates soil genesis by rapidly removing reaction products and maintaining a moist environment for microbial activity, which ultimately results in the accumulation of iron and aluminum oxides at the expense of other minerals in the most heavily weathered soils (Muggler et al. 1999; Rezende et al. 2002). Patterns of precipitation directly influence soil moisture content (Cleveland 2006), which governs carbon and nutrient biogeochemical cycling and mineral-organic associations and, together with pH, largely determine the net primary productivity (NPP) of ecosystems (Kleber et al. 2015).

Variations in soil moisture can lead to changes in oxygen (O_2) concentrations across the landscape (Silver et al. 1999), influencing elements sensitive to reduction/oxidation (i.e., redox) reactions, such as nitrogen, manganese, iron, sulfur, and carbon (Martin 2005; Peters and Conrad 1996). Iron oxyhydroxides are particularly important in soils from humid tropical regions, as Fe often becomes the most utilized terminal electron acceptor when O_2 is depleted, and the reductive dissolution of Fe minerals can release sorbed nutrients and C (Hall and Huang 2017; Lovley 2000; Mikutta et al. 2006). With enough labile C and active microorganisms, fluctuating soil moisture and oxygen can generate pockets of anoxic conditions even in finely textured well-drained upland soils, which creates “slope wetlands” (Lugo et al. 1990). Changes in soil redox

status can stimulate Fe cycling by repeatedly forming low-crystallinity or short-range-order (SRO) Fe^{III} phases, some of which are rapidly-reducible by microorganisms (abbreviated as Fe^{III}_{RR}) during anaerobic conditions (Ginn et al. 2017). Other portions of the SRO Fe^{III} phases, along with more crystalline Fe^{III} phases, such as hematite or well-crystalline goethite, supply electron accepting capacity over longer timescales (Cornell and Schwertmann 2003b; Weber et al. 2006). Thus, assessing the pools of reduced (Fe^{II}) and rapidly-reducible (Fe^{III}_{RR}) iron phases are important to predict key soil biogeochemical processes.

Soils experiencing spatial and temporal variation in soil moisture and O_2 content may lead to different rates of Fe reduction, dissolution of solid-phase C (release as DOC bound to Fe phases), and may result in C mineralization via microbial respiration (CO_2 and CH_4 emissions) (Carmo et al. 2006; Gottschalk et al. 2012; Lovley et al. 2004; Neff and Asner 2001). High DOC concentrations are often found to be correlated with dissolved ferrous iron (Fe^{II}) concentrations (Blodau et al. 2008; Knorr 2013). In addition, Fenton reactions produce OH radicals, oxidize Fe^{II}-rich solutions, and can drive additional CO_2 loss (Hall and Silver 2013). The oxidation of Fe^{II} can also facilitate the formation of Fe^{III} phases that can co-precipitate with DOC or serve as sorbents for DOC (Chen and Thompson 2018). Iron minerals are highly important for the stabilization and preservation of soil organic carbon in humid tropical ecosystems (Silva et al. 2015; Silva Neto et al. 2008; Souza et al. 2018; Thaymuang et al. 2013). These mineral-organic associations may account for 80-90% of the total C stocks in mineral soils with low particulate organic matter (Hall and Silver 2015).

Much of our understanding of Fe-C biogeochemical processes derives from careful laboratory incubation studies while detailed field measurements of short-term (days – weeks) shifts in Fe and C dynamics are lacking. The rapid fluctuations in soil moisture and O_2 content

(O'Connell et al. 2018) can create hot-moments of anoxic soil microsites that facilitate Fe reduction and C decomposition (Liptzin et al. 2011). However, repeated soil sampling necessary to identify this phenomenon in the field is rarely conducted. Spatially, topographic position (i.e. ridges, slopes, and valleys) often generates distinct hydrological and geomorphological characteristics that respond differently to water drainage or accumulation (Hook and Burke 2000), which leads to distinct hot-spots throughout the landscape. For instance, soils from the Luquillo Experimental Forest (in Puerto Rico) exhibited a large variability in Fe^{II} concentrations over different landscape positions and along an elevation gradient, and varied from 22 to 212 mmol of Fe^{II} per kg of dry soil (Hall and Silver 2015). Thus, redox processes likely proliferate in hot spots and at specific hot moments across the landscape where and when biogeochemical reaction rates are more rapid (Bernhardt et al. 2017; McClain et al. 2003).

We aimed to capture hot moments (of hours to days) of Fe reduction associated with C decomposition and redox processes across different landscape positions (ridge, slopes, valleys) that can be potential hot spots. We also assessed the turnover times for Fe redox cycling in these humid tropical forest soils. We hypothesized that (1) rainfall events will alter soil moisture and oxygen within hours to days increasing Fe reduction rates, organic C mineralization, and DOC release, with rapid changes in redox potential (constituting hot moments), (2) these hot moments will occur more rapidly and persist longer in valley topographic positions (hot spots) and will lead to greater rates of Fe redox transformations associated with C cycling. To test these hypotheses, we collected soil samples over a two-month period from three topographic positions (valley, slope, and ridge) every two to three days from three replicated catenas in a montane forest in Puerto Rico (USA). Measurements included bulk soil extractions of Fe^{II}, DOC, pH, gravimetric water content, and soil incubations to measure Fe reduction potential and the

availability of rapidly reducible Fe^{III} oxides. In addition, we monitored soil redox potential (Eh), soil O_2, volumetric water content, and CO_2 and CH_4 fluxes. Relationships between these measurements were then analyzed using multivariate statistical techniques with repeated measures (sampling days and topographic position of each catena).

4.2. Material and Methods

4.2.1. Site Description, Experimental Design, and Soil Sampling Procedure

We sampled soils from three topographic positions (ridge, slope, and valley) across three replicated catenas (Fig. B.1 and B.2) from May to June of 2016 near the El Verde Field Station (University of Puerto Rico, Río Piedras). The studied sites are in the Espíritu Santo watershed, part of the Luquillo Critical Zone Observatory (LCZO) and Luquillo Experimental Forest, in the northeast of Puerto Rico. The parent material is predominantly volcanoclastic rocks derived from Cretaceous andesitic magma (Hodge 1920; Seiders 1971). Mean annual precipitation is ~3500 mm y^{-1} varying from 2600 to 5800 mm y^{-1}, with low seasonality and extreme events as high as 100 mm d^{-1} (Heartsill-Scalley et al. 2007). The dominant tree species in this part of the Luquillo montane forest is the Tabonuco (*Dacryodes excelsa*).

The catenas form steep and convex-concave hillslopes draining to ephemeral streams and are characterized by heterogeneous soil distribution and microsites across ridges, slopes, and valleys (Scatena 1989). Catena-1 is relatively small, about 5 m of vertical rise, with steep slope, a gentle ridge, and valley usually characterized by high soil moisture (GPS coordinates in Table B.1). Catena-2 is in another hillslope, about 80 m apart from Catena-1, with ~20 m of vertical rise, containing a spine ridge, a steep and long slope, and a valley that is occasionally flooded with water. Catena-3 is downstream of Catena-1, in the same hillslope, with a similar gentle

ridge and steep slope, but a valley not as saturated as Catena-1, with a vertical rise of ~10 m. Catena-1 was previously studied by O'Connell et al. (2018) and Catena-3 was studied by Almaraz (2017). The hillslope hydrology is characterized by valleys constantly receiving water and sediments from upper slope and ridge positions by runoff or lateral movement of water within the soil. Typically, the soils in the Tabonuco forest are Ultisols (Typic Haplohumults) in stable ridges, Oxisols (Inceptic and Aquic Hapludox) in the slopes, and predominately Inceptisols (Typic Eutrudepts) in the valleys (Hall and Silver, 2015; Soil Survey Staff, 2002).

We studied a total of 9 sites, with 3 located on ridges, slopes, and in valleys, respectively. For each sampling site we allocated three replicate plots of 1.5 m x 1.5 m for soil sampling (Fig. B.1). Composite soil samples were randomly taken within plots in triplicate for chemical characterization. We sampled soils from the top 15 cm, using a 1-cm diameter soil probe and each soil sample was taken at least 20 cm apart from previous sampling spots (Fig. B.1). Soil samples were placed in polypropylene bags within a cooler and analysis was started within 20 min of sampling at the El Verde Field Station. Samples were taken every 2 to 3 d except when lack of power in the field station prevented sample processing. We collected soil samples a total of 17 times during the experimental time span of 44 d.

4.2.2. Soil biogeochemical characterization and extractions (measurements within days)

We conducted a series of triplicate biogeochemical bulk characterizations (within 20 min of sampling) including: ferrous iron (Fe^{II}), water-extractable dissolved organic carbon (DOC), pH, gravimetric water content (θ_G), an assessment of rapidly-reducible Fe oxides (abbreviated as Fe^{III}_{RR}), and a general soil characterization (including total Fe, C pools, and soil texture).

Ferrous iron (Fe^{II}) was determined by extraction with 0.5 M HCl at 1:10 soil:solution ratio, by shaking for 2 h (horizontal shaker), and centrifuging for 10 min at 11,000 RCF (Ginn et al. 2014). The supernatant was taken and Fe^{II} analyzed by the colorimetric Ferrozine method, according to Barcellos et al. (2018) and Thompson et al. (2006) with the 562 and 500 nm intensities measured in 96-well microplates (Huang and Hall 2017b) using a portable Tecan Infinite F50 plate reader.

Water-extractable dissolved organic carbon (DOC) was obtained by extraction at 1:5 soil:DI-water ratio and shaking for 1 h in a horizontal shaker at room temperature (Boyer and Groffman 1996; Ghani et al. 2003; Haynes and Francis 1993). The suspension was centrifuged for 15 min at 4,600 RCF and the supernatant was filtrated with 0.70 μm glass fiber filters (Guigue et al. 2014). Filtered supernatants were immediately frozen to -20 ^{o}C and then shipped to the University of Georgia at the end of the field session and analyzed on a Shimadzu 5050 TOC analyzer.

Soil pH was measured in 1:1 soil:DI-water ratio using an Orion Ross sure-flow pH electrode. Gravimetric water content (θ_G) was determined by oven-drying soils for >24 h and reported as dry-weight basis. Composite samples selected from random days of sampling (over 10 samples) were pooled and analyzed in triplicate for the following: total elemental analysis by lithium borate fusion prior to acid dissolution followed by ICP-MS analysis, short-range-order (SRO) Fe by 0.2 M sodium citrate/0.05 M ascorbic acid extraction followed by ICP-MS analysis, total carbon and nitrogen measured in a CHN Carlo Erba Elemental Analyzer, and soil texture determined by a Beckman Coulter LS 13 320 Laser diffraction Particle Size Analyzer.
We additionally archived soil samples from each sampling time-point and site and stored ~15 g soil (frozen at -20 ^{o}C) for future analysis.

The rainfall data-set was acquired from the rainfall gauge collected daily at the El Verde Field Station, available on the website of the Luquillo Long-Term Ecological Research Program. Collection procedures are described in McDowell and Estrada-Pinto (1988).

4.2.2.1. Rapidly-reducible Fe oxides (Fe^{III}_{RR}) microbial bioreduction assay

We assayed the amount of rapidly-reducible ferric iron (Fe^{III}_{RR}) using an incubation method adapted from Ginn et al. (2017) to work at the field station using the field-moist fresh soils. Microbial bioreduction assays have been used in other studies to assess the soil's potential for iron reduction (Bonneville et al. 2009; Bonneville et al. 2004; Eusterhues et al. 2014; Ginn et al. 2017). We conducted two different assays: one that involved adding a *Shewanella oneidensis* MR-1 culture along with a growth medium (Ginn et al. 2017) to the soil (abbreviated as Shewa-Fe^{III}_{RR}), and in the other the native soil was incubated with growth media only (abbreviated as Media-Fe^{III}_{RR}). This assessed the availability of the soil Fe^{III} phases for Fe reduction by the indigenous microbial communities when appropriate nutrients and carbon were provided, while the addition of the Fe-reducer *Shewanella* sp. aimed at overcoming microbial limitations.

For the Shewa-Fe^{III}_{RR} treatment, *Shewanella oneidensis* MR-1 was grown to the late exponential and early stationary phase in a selective media containing 0.5 g L^{-1} KH_2PO_4, 1.0 g L^{-1} $NaSO_4$, 2.0 g L^{-1} NH_4Cl, 1.0 g L^{-1} yeast extract, 0.5 mM $CaCl_2$, 0.1 mM $MgSO_4$, 10 mM Na-lactate, and 50 mM Fe-citrate (adapted from Ginn et al., 2017). Cell densities were obtained by optical density measurements at a wavelength of 660 nm that had been previously calibrated by direct count of cells using epifluorescence microscopy to reach population density over 10^8 CFU mL^{-1} (Bonneville et al. 2009). After *S. oneidensis* growth, we conducted a washing procedure twice, by first centrifuging the cells at 3,000 RCF for 30 minutes, discarding the supernatant, and

adding a new fresh selective media with the same composition as above but without yeast extract or Fe-citrate, and then re-doing the centrifugation procedure and disposing the supernatant (Ginn et al. 2017). In sequence, we added the fresh collected soil with the washed bacterial culture suspended in new fresh selective media (same composition, without yeast extract or Fe-citrate), at a ratio of 1:10 soil:media, in a gas tight tube. In parallel, for the Media-Fe^{III}_{RR} treatment, we added the fresh soil to the fresh selective media above (without yeast extract or Fe-citrate) and with no *S. oneidensis*, and placed in similar gas tight tubes, at a ratio of 1:10 soil:media. For both Shewa-Fe^{III}_{RR} and Media-Fe^{III}_{RR}, we flushed the tube headspace with inert N_2 gas to create anoxic conditions and placed it on an end-over-end shaker for 7 d in the dark. After 7 d of incubation, we pipetted 0.5 mL of either Shewa-Fe^{III}_{RR} or Media-Fe^{III}_{RR} suspension treatments, centrifuged at 11,000 RCF for 30 min, removed the supernatant, revolved and extracted the pellet with 0.5 M HCl for 2 h to obtain Fe^{II} concentrations using the ferrozine protocol described above. Results were expressed in mmol Fe kg^{-1} d^{-1} (iron reduction rates), on a dry soil mass basis by the difference in Fe^{II} concentrations between day 0 and 7 of the incubation.

4.2.3. Soil sensors and data collection (measurements within hours)

For each site within each of the 3 catenas, we deployed 4 platinum electrodes (Paleo Terra Inc., Amsterdam, Netherlands) adjacent to the plots (Fig. B.1) measuring the redox potential (Eh) every min and storing the data every hour via CR23X Campbell dataloggers. Measurements of Eh recorded the voltage difference between the reference electrode and a redox electrode (Pt sensor). The Pt sensor was placed for Eh readings at 7.5 cm depth from the soil surface.

At catena-1 only, volumetric water content (θ_V), soil oxygen content (O_2), and fluxes of CO_2 and CH_4 were measured near the ridge, slope, and valley sampling plots (O'Connell et al. 2018). Time-domain reflectometry (TDR) probes were used to track volumetric water content and galvanic Apogee oxygen sensors encapsulated in plastic chambers were used to track soil oxygen concentrations (Liptzin et al. 2011). For each site in catena-1, we deployed 5 TDR and 5 O_2 sensors installed in the top 15 cm of the soil, and data was stored every hour in CR1000 Campbell dataloggers. Emissions of CO_2 and CH_4 were measured using automated flux chambers deployed in each location (3 for valley, 3 for slope, and 3 for ridge). Gases were collected within the chambers over 10 min of sampling, 3 min of flushing between measurements, and automatically transported to a Cavity Ring-Down Spectroscopy (CRDS) gas analyzer (Picarro, Santa Clara, CA, USA) within the site (O'Connell et al. 2018). Gas samples were collected daily at a maximum of 12 samplings per day per chamber with CO_2 expressed in $\mu mol\ m^{-2}\ s^{-1}$ and CH_4 in $nmol\ m^{-2}\ s^{-1}$.

4.2.4. Statistical analyses

We computed models using the daily average for the environmental factors (Eh, O_2, and θ_V, measured by sensors) and the daily average precipitation to predict the drivers for Eh, O_2, and θ_V (see initial parameters in Table B.4), using the lmer function from the lme4 package in R (Bates et al. 2014). We further computed the turnover times for Fe production and consumption (concentration/rate) for all sites and for each individual site, reporting the highest occurrence, the mean, and the median of Fe^{II} turnover time ($T\text{-}Fe^{II}$).

We analyzed the relationship between the biogeochemical measurements using a linear mixed model fit by restricted maximum likelihood (REML), within the sampling days and within

the different topographic positions (and sites) of the catenas using the lmer function from the lme4 package in R (Bates et al. 2014). Outcome variables run in separate models included parameters from soil samples taken every 2+ days: Fe^{II}, Fe^{III}_{RR} (Media or Shewa), DOC, pH, and θ_G. We additionally ran models just for catena-1 using the sensors (Eh, O_2, θ_V) and CO_2 and CH_4 fluxes emitted from soils along with other variables. We used a data-set with 17 days of observation spread across 44 days.

Precipitation, Eh, O_2, and θ_V were collected continuously and may have a timing effect (of hours/days) in the biogeochemical variables. Thus, we calculated multiple versions of each of these variables for potential use as independent variable in the models, using Akaike Information Criterion (AIC), and we chose the optimum model (lowest AIC). For precipitation, we compared the averages of 1, 2, 3, 4, 5, and 10 days prior to soil sample collection and choose the one with the lowest AIC. For the Eh, O_2, and θ_V sensors, we compared the AIC at the hour in which the soil sample was taken, and for the average of these sensor readings in the last 2, 3, 6, 12, 24, 36, and 48 hours before the soil sampling. For example, for a soil sample taken at 14:00 on 05/14/2016 (day 10), we averaged the Eh measurement at 14:00 (Eh_1), then from 13:00 to 14:00 (Eh_2), 12:00 to 14:00 (Eh_3), and so on until 48 hours prior to the measurement. We used the models with lowest AIC for the best combination of these sensor variables (Eh, O_2, and θ_V) to be used in the models for the dependent variable.

We reported both AIC and R^2 of the models calculated by r.squaredGLMM from the R package MuMIn for generalized linear mixed effects models (GLMMs) (Johnson 2014; Nakagawa and Schielzeth 2013) in order to compare the models.

4.3. Results

4.3.1. Soil Characteristics across Sites

Soil characteristics varied along the replicated topographic positions. Valley-1 had the highest SRO-Fe among all samples (Table 4.1), followed by valley-2, and the other locations. However, valley-1 contained the lowest total-Fe compared to all other locations. Even with the lowest total-Fe, valley-1 had the highest amount of reactive iron (SRO-Fe) and ferrous iron (Fe^{II}), compared to all other locations (Table 4.1). Total-C was higher in ridges (5.9% for ridge-2, for example) and for valley-1 and -2 (4.6 and 4.0 %, respectively), compared to other sites. Soils had a loam texture for most of the sites or sandy loam and silt loam for a few sites (Table 4.1). Detailed results for all elements analyzed are available in Table B.2.

We assessed the similarity of the sites based on a principal component analysis (PCA) of the following measurements: Total-Fe, SRO-Fe, Total-C, and texture (sand, silt, and clay) (Fig. B.3). We observed that ridges (R1, R2, R3) are grouped together, which could reflect a strong influence by Total-C and sand content. Likewise, the slopes S1 and S2 could be grouping based on fine texture (clay and silt), and S3 is possibly influenced by Total-Fe. However, valleys V1, V2, and V3 varied greatly over the different biplot quadrants (Fig. B.3): V1 is possibly driven by SRO-Fe and Total-C, V2 by SRO-Fe, and V3 by clay content. Thus, each of the studied valleys have different characteristics, which may be reflected in the variation in Eh and other biogeochemical variables within valleys.

4.3.2. Precipitation and Environmental Factors involved in Redox Processes

Over the course of the sampling period (May and June 2016), we were able to distinguish four periods of precipitation that influenced the other variables studied (Fig. 4.1): (1) intermittent rainfall periods of 5-10 mm every few days (from 05/03 to 05/21/2016, phase-1), (2) a short

absence of rain/dry period (from 05/21 to 05/26/2016, phase-2), (3) an intense rainfall event of 290 mm for 10 days with a one-day event of 114 mm (from 05/27 to 06/05/2016, phase-3), and (4) a longer dry period of 12 days (from 06/06 to 06/17/2016, phase-4) with only one day of rain (26 mm). These patterns of precipitation directly affected variables that were measured hourly by the sensors (Eh, O_2, and θ_V) in most of the locations and catenas (Fig. 4.2 and 4.3). For example, in Slope-1 (of Catena-1), θ_V fluctuated closely with precipitation and decreased from 0.45 to 0.35 $m^3\ m^{-3}$ for the short dry period (phase-2), followed by an increase up to 0.47 $m^3\ m^{-3}$ in the intense rainfall event (phase-3), and decreased again to 0.36 $m^3\ m^{-3}$ in the long days without rain (phase-4). The valley-1 had a lower magnitude of variation, as water appeared to remain longer in this landscape position (i.e., a poorly drained soil), from 0.45 to 0.50 $m^3\ m^{-3}$. Soil O_2 did not fluctuate much for ridge-1 and slope-1 except for a slight change from 17.5 to 15.5 % O_2 during phase-3. The valley-1 was more responsive to absences of precipitation than ridge-1 and slope-1, with O_2 increasing in valley-1 from 2.5 to 9.2% and 1.9 to 11.8% for the drying phases-2 and -4, respectively (Fig. 4.2).

Changes in redox potential had higher amplitude (magnitude) in the valley topographic positions compared to ridges and slopes. In valley-2 (catena-2) the four phases of precipitation (intermittent rain, no-rain, intensive rain, and no-rain again) were directly correlated with the Eh variation as follows (Fig. 4.3): (i) Eh behaved similar to a redox oscillation (Eh went up and down within days) varying from ~200 to ~500 mV within 1 to 2 days (phase-1); (ii) Eh increased from 325 to 550 mV (phase-2); (iii) Eh decreased greatly from 550 to ~0 mV (phase-3); and (iv) Eh increased back to 550 mV within the long drier days (phase-4). Evidently, Eh fluctuated from oxic to anoxic conditions in valley-2 according to precipitation events and soil moisture content. A notable redox fluctuation pattern also occurred in valley-3, with Eh reaching very negative

values (from 260 to -360 mV) during the extreme rainfall event and returning to positive values (200 mV) for the long drier days. However, Eh in valley-1 (catena-1) remained mostly negative (-500 to -270 mV) due to poor water drainage (Fig. 4.3). Eh values in the slopes and ridges across all 3 catenas remained at values characteristic of oxic conditions (varying from 420 to 580 mV).

Using mixed-effects models with stepwise backwards elimination, daily average precipitation was a significant predictor for the daily averages of Eh, O_2, and θ_V (negatively, negatively, and positively) (Table 4.2). We computed cross correlations for the averaged daily measurements for the sensors and we found no time lags between Eh, O_2, and θ_V.

4.3.3. Dynamic Biogeochemical Soil Measurements

Soil extractions for iron and carbon pools also varied over time in response to precipitation and soil moisture. The HCl-extractable Fe^{II} varied across ridges to slopes to valleys for all 3 catenas (Fig. 4.4). Valley-1 had much higher Fe^{II} concentrations compared to all other locations in all catenas. During the 290-mm intense precipitation (phase-3), most of the ridges and slopes increased Fe^{II} content from 3 to 9 mmol kg^{-1}, and valley-1 from 50 to 126 mmol kg^{-1}. Ridge-2 and slope-2, particularly, had larger variation in Fe^{II} concentration during this phase-3. During the subsequent 12-d drying event (phase-4), Fe^{II} content decreased in most of the sites, for example, from 8 to 1 mmol kg^{-1} in slope-2 and from 4 to 1 in ridge-1 and in ridge-2. Shewa-Fe^{III}_{RR} and Media-Fe^{III}_{RR} were also correlated with high or low rainfall events and soil moisture contents varying overall from 1 to 50 mmol kg^{-1} soil day^{-1} (Fig. 4.5). Shewa-Fe^{III}_{RR} was correlated with Media-Fe^{III}_{RR} ($R^2 = 0.82$), and both behaved like the alterations in Fe^{II} concentrations over the course of the experiment as these Fe^{III}_{RR} measurements assessed the pool

of Fe that can be potentially reduced. Rates for potential Fe reduction were higher for Shewa-Fe^{III}_{RR} compared to Media-Fe^{III}_{RR} in most of the locations and sampling times, with some exceptions. The observed values of Shewa-Fe^{III}_{RR} were similar to Media-Fe^{III}_{RR} values in some instances, which demonstrates that these well-weathered and perudic soils can be nutrient and carbon deficient for microbial metabolism since our selective media that were used for the incubation experiments provided innumerous nutrients and carbon.

DOC did not fluctuate as much as other variables, such as Eh and θ_V. Across most of the locations, DOC remained near constant in the intense rainfall phase and decreased during the following 12 drier days. For example, DOC declined from 264 to 95 mg kg^{-1} in valley-3 and from 132 to 114 mg kg^{-1} in slope-2 during this final drying event (Fig. 4.6). Values for pH also did not clearly fluctuate along precipitation and soil moisture patterns (Fig. B.4). The overall pH, averaged over the 17 sampling-days, was higher in the valleys, with values decreasing from 6.1 to 5.1 to 4.9 for valley-1, slope-1, and ridge-1, respectively. This increase in pH from ridge to slope to valley in catena-1 is correlated with the greater amount of Fe^{II}, SRO-Fe, and total-C in valley-1. Acidic waterlogged soils commonly exhibit increase in pH due to proton consumption during reduction of nitrate, manganese, and iron (Ponnamperuma 1972).

Gravimetric water content (θ_G) was somewhat responsive to changes in precipitation (Fig. B.5). For example, in valley-2 gravimetric water content varied from 0.62 to 0.84 g g^{-1} for the intense precipitation and dried down to 0.52 g g^{-1} over the next 12 days; although the volumetric water content (measured hourly by sensors) captured in more detail the fluctuations in soil moisture. Fluxes of CO_2 were lower in valley-1 compared to slope-1 and ridge-1, with average values of 0.6, 1.6, and 1.3 μmol m^{-2} s^{-1} for each of these locations (Fig. 4.7). Valley-1

was a source of CH_4, while slope-1 and rigde-1 were sinks of CH_4, with average values for the time of the experiment of 3.0, -5.6, and -0.4 nmol m^{-2} s^{-1} (Fig. 4.7).

4.3.5. Turnover Timescales for Fe Redox and Statistical Models to Predict Soil Biogeochemical Parameters

Across all nine sites within the three catenas, the most common calculated turnover time for Fe^{II} (T-Fe^{II}) production was 4 days and for Fe^{II} consumption was 3 to 4 days (Fig. 4.8). The T-Fe^{II} production and consumption for each individual site was also mostly distributed within 3 to 4 days with a few cases of higher range of turnover times (Table B.3).

We determined the optimal mixed-effects models for the biogeochemical variables Fe^{II}, Media-Fe^{III}_{RR}, Shewa-Fe^{III}_{RR}, DOC, CO_2, and CH_4 (Table 4.3) using stepwise backwards elimination, which removes all non-significant variables one by one, and keeps only the significant variable in the final elimination step (see initial parameters in Table B.4). We chose the model with the lowest AIC (best model) by comparing the average of the measurements taken for Eh, O_2 and θ_V from 1, 2, 3, 6, 12, 24, 36, and 48 hours preceding the time and date when the soil samples were taken, for the biogeochemical models. For instance, in the DOC model the lowest AIC was the model with O_2 averaged over the preceding 48 h from the measurement (O_2_48) (Table B.5). For precipitation, we used the 2-day averaged precipitation, which had the lowest AIC (Precipitation_2day), compared to the averages of 1, 3, 4, 5, and 10 days prior to soil sampling. The 2-day averaged precipitation was also found to be the time lag between precipitation and the studied environmental factors and biogeochemical variables.

In predicting Fe^{II} dynamics, Media-Fe^{III}_{RR} and pH were positively correlated for all catenas (all 9 sites), and O_2 was negatively correlated for the sites in Catena 1 (Table 4.3). We

used Media-Fe^{III}_{RR} (and not Shewa-Fe^{III}_{RR}) for the Fe^{II} models because Media-Fe^{III}_{RR} had the lowest AIC compared to Shewa-Fe^{III}_{RR} or both Media-Fe^{III}_{RR} and Shewa-Fe^{III}_{RR} together in the model. Gravimetric water content (θ_G) and Fe^{II} were positively correlated in both Media-Fe^{III}_{RR} and Shewa-Fe^{III}_{RR} models, Eh was negatively correlated to Media-Fe^{III}_{RR}, and pH was positively correlated to Shewa-Fe^{III}_{RR} for all catenas (Table 4.3). DOC was positively correlated to θ_G and Fe^{II}. The CO_2 flux was negatively correlated to θ_V (Table 4.3). For flux CH_4 models, we observed the regression results were significantly impacted by 5 outlier values, and by removing these outliers we observed a positive correlation of flux CH_4 and pH (Fig. B.6).

4.4. Discussion

4.4.1. Turnover Times and Drivers of Fe Redox Processes

We aimed to find the timescales for Fe^{II} turnover and to determine what controls Fe^{II} biogeochemical cycling. Our field timeseries measurements revealed that Fe^{II} turnover times (T-Fe^{II}) for consumption and production were centered around 4 days across ridges, slopes, and valleys, in these humid tropical forest soils. This results compare favorably to our controlled laboratory experiment (Chapter 3), where the mean for the turnover for Fe^{II} production varied from 3 to 5 days, and from 0.5 to 5 days for Fe^{II} consumption, which are fast turnover times as expected for a soil slurry incubation. To our knowledge, there are no reports of Fe^{II} turnover times for soils under natural conditions. Coastal marine systems can also exhibit high rates of Fe reduction (Wang and Van Cappellen 1996). Consequently, one can possibly compare rates of Fe biogeochemical cycling across these two environments. Multicomponent early diagenetic models have been used to study Fe cycling and other redox-driven elements such as C, N, S, and Mn in marine systems (Boudreau 1996; Berg et al. 2003). For example, Wang and Van Cappellen

(1996) reported rates of dissimilatory Fe reduction and Fe^{II} concentrations for coastal marine sediments. From these values, we estimated the turnover time for Fe^{II} pool was between 91 and 120 days. Thus, the T-Fe^{II} according to these models are at least an order of magnitude longer than our results for the Luquillo CZO soils, showing these humid tropical soils can exhibit incredibly rapid rates of Fe^{II} turnover.

Our mixed-effect models suggest that Fe reduction and oxidation, measured by HCl-extracted Fe^{II} concentrations, is driven by O_2, pH, and the pool of rapidly reducible Fe^{III} oxides (Fe^{III}_{RR}). We interpret this correlation as follows: at certain soil pH and O_2 content, Fe^{II} concentrations are responsive to the pool of Fe^{III} oxides that are readily available to be reduced, either by amendment with non-native bacteria (*Shewanella* sp.) or by the activity of indigenous microorganisms (Shewa-Fe^{III}_{RR} and Media-Fe^{III}_{RR}, respectively). Although soil moisture was not a predictor in the final Fe^{II} model, θ_G was a predictor for the rapidly reducible Fe^{III} oxides (Media-Fe^{III}_{RR}, in this case), which strongly impact the availability of Fe^{II} in soils. These findings corroborate our first hypothesis in that precipitation is driving O_2 and soil moisture is driving the Fe^{III}_{RR} pool, so that both O_2 and Fe^{III}_{RR} control Fe^{II} and thus precipitation and soil moisture are indirectly influencing Fe reduction and oxidation. Our modeling results are in accordance with previous investigations, demonstrating that dissimilatory Fe reduction, for example, is controlled by environmental factors such as soil O_2 and water content, and the inherent soil Fe-mineral composition (Hall et al. 2016; Silver et al. 1999; Weber et al. 2006).

Regarding our second hypothesis of the valleys exhibiting different Fe-C behavior than other topographic positions, we observed that valley-1 contained much higher Fe^{II} concentrations (50 to 126 mmol kg^{-1}) and Fe^{III}_{RR} rates (18-49 mmol kg^{-1} d^{-1}) compared to the other two valleys and all other ridges and slopes. For other biogeochemical variables, such as DOC, the values did

not vary among the topographic positions. In our models for biogeochemical variables we did not detect statistical differences among ridges, slopes, and valleys, which does not support our second hypothesis. Thus, biogeochemical processes can be site specific, as we observed the three valleys had distinct dynamics (of Eh, for example), and these processes can also be similar across different topographic positions in humid tropical ecosystems.

4.4.2. Soil moisture and Precipitation Influence Fe-C Redox Cycling

Soil moisture was a predictor for the Media-Fe^{III}_{RR}, Shewa-Fe^{III}_{RR}, DOC, and CO_2 models. Soil moisture influenced the Fe^{III}_{RR} pool, and consequently influenced Fe^{II} concentrations. Precipitation was a predictor for the environmental factors Eh, O_2, and θ_V, which are important parameters that influence Fe-C reduction and oxidation. We first hypothesized that precipitation would be a strong predictor for most of the soil biogeochemical variables. But, unlike soil moisture, precipitation was not present in the models for Fe^{II}, Media-Fe^{III}_{RR}, Shewa-Fe^{III}_{RR}, DOC, CO_2, and CH_4. These results suggest that rainfall does not have an immediate impact on Fe and C biogeochemistry, but rather the accumulation of water in the soil (soil moisture) does have a rapid impact on these parameters. The influence of precipitation in the Eh, O_2, and θ_V variables is clearly illustrated in Figures 4.2 and 4.3. Prior work has shown that precipitation was inversely correlated with soil O_2 concentrations across the Luquillo CZO landscape (Silver et al. 1999). By evaluating the relationship between precipitation and O_2, Liptzin et al. (2011) found that dry periods of at least 4 days were able to aerate soils, while a small rainfall event (< 1 mm) were able to create low O_2 concentrations.

High precipitation regimes and elevated soil moisture content had a strong relationship with the potential for iron reduction as measured by uniformly oxidized steel rods (i.e., Indicator

of Reduction in Soils—IRIS) deployed across a topographic gradient in volcanic soils from Hawaii (Hodges et al. 2018), and also in upland iron-rich and weathered soils from the USA Southeastern piedmont (Hodges 2017). In these studies, Fe reduction was likely stimulated by exogenous carbon inputs (such as DOC). Therefore, temporal and spatial variation in redox conditions may create a hot moment for Fe reduction in soils within certain hot spots of the landscape (Hall et al. 2013; McClain et al. 2003).

We also observed a decline in precipitation and soil moisture in the last 12 days of the field campaign, which correlated with an observed decrease in Fe^{II}, Fe^{III}_{RR}, DOC, and an increase in Eh and O_2 values, in most of the sites. The decrease in both Fe^{II} and DOC concentrations could be due to the potential disappearance of anoxic microsites within the soils as the soil dried and O_2 content increased (Hall et al. 2013). Thus, decreasing soil moisture conditions appeared to directly impact the dynamics of Fe and C with important ecosystem implications for the availability of nutrients to plants and microorganisms.

4.4.3. The Dynamic Pool of Rapidly-Reducible Fe Oxides (Fe^{III}_{RR})

We conducted soil incubations to assess the abundance of reactive Fe available for bacteria (Media-Fe^{III}_{RR} and Shewa-Fe^{III}_{RR}) as a bioreduction alternative to the selective chemical extractions such as citrate-ascorbate, oxalate, and hydroxylamine (e.g., Coward et al. 2017; Ginn et al. 2017; Hall and Silver 2015). In our models, we found that both Media-Fe^{III}_{RR} and Shewa-Fe^{III}_{RR} had a positive correlation with θ_G and Fe^{II}, Media-Fe^{III}_{RR} was negatively correlated with Eh, and Shewa-Fe^{III}_{RR} was positively correlated with pH.

Comparing Fe^{III}_{RR} and SRO-Fe pools, the average for the 17 sampling-days for Shewa-Fe^{III}_{RR} and Media-Fe^{III}_{RR} accounted for 17-66 % and 12-64 % of the SRO-Fe pool, respectively,

and reached a maximum value of ~100% of the SRO-Fe pool in some instances (Table 4.4). There is an overall increase in the Fe^{III}_{RR}/SRO-Fe ratio from ridges to slopes to valleys (Table 4.4). Thus, valleys are likely more prone to frequent shifts in redox fluctuations and contain higher pools of reactive iron phases than the other topographic positions.

We propose that the reducible Fe pool is a more dynamic and fluctuating pool than typically understood, and it depends on multiple environmental predictors for each time analyzed (such as the Fe^{III}_{RR} measurements in our study), compared to SRO-Fe pools obtained by selective extractions such as citrate-ascorbate. For example, in two distinct days of sampling for valley-1, the Fe^{III}_{RR} pool varied from 140 to 336 mmol kg^{-1}, reaching values as high as the SRO-Fe pool (Fig. B.7). Furthermore, Ginn et al. (2017) observed that the SRO-Fe abundance is a poor predictor of Fe reduction rates as shifts in Fe mineral composition was not detected by selective extractions (citrate-ascorbate), Mössbauer spectroscopy, or X-ray adsorption spectroscopy. But, shifts in Fe valence state over multiple redox oscillations was detected by incubations using the same Shewa-Fe^{III}_{RR} procedure. As a result, the Fe^{III}_{RR} pool is dynamic and variable as a function of soils type, environmental conditions, and distinct topographic positions.

4.4.4. Variations in Eh and Redox Fluctuations

To comprehensively understand redox processes across different landscape positions, complementary variables such as Eh, soil O_2, and bulk soil extractions for Fe^{II} (as an indicator of reducing conditions), can be used to assess the redox status of the environment. Eh measurements are suitable for soils constantly experiencing elevated soil moisture content (such as the valleys 1, 2, and 3). We observed a more pronounced variation in soil Eh in valley-2 and -3 than in valley-1, which followed similar trends in precipitation, soil moisture and O_2 (valley-1

was constantly anoxic, with highly negative Eh values). Eh values (normalized to pH 7, Eh_7) serve as a proxy for four major redox conditions in soils: Eh_7 values over +400 mV indicate oxidizing conditions (aerated soils), Eh_7 values between +100 to +400 mV indicate moderately reducing conditions, Eh_7 values between -100 to +100 mV indicate reducing conditions, and Eh_7 values below -100 mV indicate highly reducing (anoxic) conditions (Fiedler et al. 2007; Husson 2013; Patrick et al. 1996). Eh_7 values around +300 mV can be considered the boundary between aerobic and anaerobic conditions (Sparks 2003). Given the relatively constant negative Eh values in Valley-1, we investigated Eh models using only valley-2 and valley-3, which had greater variance in Eh in response to precipitation. In these analyses, we found a significant negative correlation ($p<0.05$) between Fe^{II} and Eh. Thus, in wetter valley positions, the variations in redox potential can be directly correlated with Fe reduction.

Different redox conditions (demonstrating different Eh, O_2, and θ_V values) are also correlated with the distribution of plant species and nutrient bioavailability to plants (Josselyn et al. 1990; Mendelssohn et al. 1981; Peretyazhko and Sposito 2005). In the Luquillo CZO Forest, vegetation can be a good indicator of redox conditions across topographic positions. The predominant species tabonuco (*Dacryodes excelsa*) prefers well-aerated soils from ridges and slopes, while sierra palm (*Prestoea montana*) and dragon blood tree (*Pterocarpus officinalis*) grows in the valleys where soils are saturated and have an accumulation of organic matter, and the montillo trees (*Sloanea berteroana*) can be found in slope positions (Lugo et al. 2012). Thus, plants can alter soil conditions that would impact Fe and nutrient cycling within the rhizosphere under different redox conditions (Dubinsky et al. 2010; Fimmen et al. 2008; Weiss et al. 2004).

In our recent laboratory experiments incubating soil slurries from a similar valley topographic position (Bisley watershed) from Puerto Rico, we explored changes in the redox

oscillations parameters, such as the magnitude (or amplitude) of O_2, frequency/periodicity, and time length under oxic and anoxic conditions. In these incubations, we found that these parameters strongly influence Fe and C dynamics with clear patterns of iron reduction during anoxia and iron oxidation during oxic conditions (Barcellos et al. 2018; Chen et al. 2018; Ginn et al. 2017; Wilmoth 2016). Indeed, the number of hours and days for the natural redox fluctuations in the valleys 2 and 3 (such as the notable changes in Eh), and the soil sampling periodicity we have done in the field, are comparable to the imposed 2.5, 6, and 10 days of anoxic conditions in the laboratory experiment conducted in Chapter 2.

4.4.5. Coupled Fe-C Dynamics and C Mineralization

In soils that undergo redox fluctuations, C can be either accumulated (stabilized) or lost by dissolution, leached, or mineralized by soil microorganisms (Kögel-Knabner 2017; Six et al. 2002). In this study, DOC was positively correlated to Fe^{II} and θ_G, so that the release of DOC is likely correlated to the desorption of organic matter from reactive Fe^{III} phases that underwent reductive dissolution. Consequently, DOC concentrations depend on the resident iron reduction processes (as Fe^{II} is a predictive variable in the model for DOC) and on the soil moisture conditions. These results and models corroborate with prior work reporting that variations in DOC are correlated with changes in dissolved ferrous iron (Fe^{II}) (Blodau et al. 2008; Grybos et al. 2009; Knorr 2013). During anoxic incubations of wetland soils, Grybos et al. (2009) observed that with the increase of DOC release there was an increase in pH as well as in Fe^{II} and Mn^{II} concentrations, and a decline in Eh values. During periods of high precipitation and soil moisture, Fe reduction takes place within anoxic microsites and the associated Fe^{III}-oxide C phases can be transformed into colloidal and soluble forms (Buettner et al. 2014). These soluble

forms can be depolymerized and/or mineralized to CO_2 and CH_4 emissions by microbial activity (Keiluweit et al. 2016), which were driven by soil moisture (CO_2 flux) and soil pH (CH_4 flux) in our study.

In addition to the Fe reduction coupled to the C mineralization/decomposition, Fe minerals are important for carbon stabilization, forming mineral-organic associations (MOAs) (Kleber et al. 2015). These MOAs can be induced by elevated soil moisture, high plant and microbial exudates, an abundance of highly reactive soil minerals (such as SRO-Fe) and a lower soil pH. The Luquillo CZO soils studied here contain all these factors in abundance (Brokaw et al. 2012), and thus are likely to favor the formation of strong MOAs. Adsorption or co-precipitation together with physical protection and aggregation induced by low crystallinity Fe minerals are the most important mechanisms for storage and preservation of soil organic carbon against microbial decomposition in these humid tropical ecosystems (Schaefer et al. 2004; Souza et al. 2018; Xiao et al. 2015). However, after multiple redox fluctuation cycles, with prolonged anoxic conditions within soil microsites containing elevated soil moisture, some portions of this well-preserved carbon pool that is associated to Fe minerals can be accessible to dissimilatory Fe reduction bacteria and consequent C mineralization (CO_2 and CH_4 emissions) and release C in soluble and colloidal forms (DOC) (Buettner et al. 2014; Pan et al. 2016; Wagai and Mayer 2007). Although the detailed mechanistic understanding needs further investigation, our current ecosystem models likely underestimate C mineralization (by >50% in some cases) due to both CO_2 and CH_4 emissions, by not accounting the protected C forms that can be released during redox fluctuation events in humid environments (Huang and Hall 2017a).

4.5. Conclusions and Environmental Implications

We found that variation in precipitation, soil moisture, and oxygen content impacted the pools of Fe and C extracted from soils across different landscape positions and influenced fluctuations in soil redox potential. The pool of reactive and rapidly reducible Fe oxides (Fe^{III}_{RR}) is dynamic and depends on fluctuating environmental conditions. We also found that the more frequent turnover time for Fe^{II} production and consumption was 4 days, across the studied topographic positions in the Luquillo CZO. In conclusion, intensive days of precipitation and prolonged dried days were able to create distinct hot moments for biogeochemical redox processes, and valleys were subtler to soil environmental changes (hot spots).

Robust relationships between soil moisture and the variables Media-Fe^{III}_{RR}, Shewa-Fe^{III}_{RR}, DOC, and CO_2, demonstrates the strong influence of soil water content in these biogeochemical processes. Both Media-Fe^{III}_{RR} and Shewa-Fe^{III}_{RR} were correlated to Fe^{II} concentrations in the studied soils. Thus, large amounts of precipitation or the occurrence of drier periods could likely further constrain these biogeochemical processes. For instance, hurricane events that are common in the Caribbean bring massive amounts of precipitation and lead to large amounts of plant litter accumulating on the top of water-logged soils. In warm environments, such as in the Luquillo CZO forests, litter decomposition is rapid, breaking down organic matter into lower molecular weight carbon compounds, such as colloidal DOC. Redox processes also affect the biogeochemistry of plant limiting nutrients (such as phosphorus) in ecosystems located in highly weathered soils.

We demonstrated that precipitation and the environmental factors soil moisture and oxygen content are interconnected and important predictors for iron reduction, dissolved organic carbon release, carbon mineralization, and fluctuations in soil redox potential, with important

ecosystem implications over variant topographic positions in highly weathered iron-rich soils from humid tropical regions.

4.6. References

Almaraz M (2017) Nitrogen Availability and Loss from Unmanaged and Managed Ecosystems. Doctoral Dissertation. Brown University

Álvarez-Dávila E et al. (2017) Forest biomass density across large climate gradients in northern South America is related to water availability but not with temperature. PloS One 12:e0171072

Baldwin DS, Mitchell A (2000) The effects of drying and re-flooding on the sediment and soil nutrient dynamics of lowland river–floodplain systems: a synthesis. River research and applications 16:457-467

Barcellos D, Cyle KT, Thompson A (2018) Faster redox fluctuations can lead to higher iron reduction rates in humid forest soils. Biogeochemistry 137:367-378 doi:10.1007/s10533-018-0427-0

Bates D, Mächler M, Bolker B, Walker S (2014) Fitting linear mixed-effects models using lme4.

Berg P, Rysgaard S, Thamdrup, B (2003) Dynamic modeling of early diagenesis and nutrient cycling. A case study in an artic marine sediment. American Journal of Science 303:905-955

Bernhardt ES, Blaszczak JR, Ficken CD, Fork ML, Kaiser KE, Seybold EC (2017) Control points in ecosystems: moving beyond the hot spot hot moment concept. Ecosystems 20:665-682

Blodau C, Fulda B, Bauer M, Knorr K-H (2008) Arsenic speciation and turnover in intact organic soil mesocosms during experimental drought and rewetting. Geochimica et Cosmochimica Acta 72:3991-4007

Bonneville S, Behrends T, Van Cappellen P (2009) Solubility and dissimilatory reduction kinetics of iron (III) oxyhydroxides: a linear free energy relationship. Geochimica et Cosmochimica Acta 73:5273-5282

Bonneville S, Van Cappellen P, Behrends T (2004) Microbial reduction of iron (III) oxyhydroxides: effects of mineral solubility and availability. Chemical Geology 212:255-268

Boudreau B P (1996) A method-of-lines code for carbon and nutrient diagenesis in aquatic sediments. Computers & Geosciences 22:479-496

Bouma TJ, Bryla, DR (2000) On the assessment of root and soil respiration for soils of different textures: interactions with soil moisture contents and soil CO_2 concentrations. Plant and Soil 227:215-221

Boyer J, Groffman P (1996) Bioavailability of water extractable organic carbon fractions in forest and agricultural soil profiles. Soil Biology and Biochemistry 28:783-790

Broedel E, Tomasella J, Cândido LA, Randow C (2017) Deep soil water dynamics in an undisturbed primary forest in central Amazonia: Differences between normal years and the 2005 drought. Hydrological Processes 31:1749-1759

Brokaw N, Crowl TA, Lugo A, McDowell WH, Scatena F, Waide RB, Willig MR (2012) A Caribbean forest tapestry: the multidimensional nature of disturbance and response. Oxford University Press, New York. pp 3-443

Buettner SW, Kramer MG, Chadwick OA, Thompson A (2014) Mobilization of colloidal carbon during iron reduction in basaltic soils. Geoderma 221:139-145

Carmo JBd, Keller M, Dias JD, Camargo PBd, Crill P (2006) A source of methane from upland forests in the Brazilian Amazon. Geophysical Research Letters 33

Chen C, Thompson A (2018) Ferrous Iron Oxidation under Varying pO_2 Levels: The Effect of Fe (III)/Al (III) Oxide Minerals and Organic Matter. Environmental Science & Technology 52:597-606

Chen C, Meile C, Wilmoth JL, Barcellos D, Thompson A (2018) Influence of pO_2 on Iron Redox Cycling and Anaerobic Organic Carbon Mineralization in a Humid Tropical Forest Soil. Environmental Science & Technology 52:7709-7719

Christensen TH, Bjerg PL, Banwart SA, Jakobsen R, Heron G, Albrechtsen H-J (2000) Characterization of redox conditions in groundwater contaminant plumes. Journal of Contaminant Hydrology 45:165-241

Cleveland C (2006) Nitrogen and phosphorus additions cause substantial losses of soil carbon from a lowland tropical rain forest. Proc Natl Acad Sci USA 103:10316-10321

Cornell RM, Schwertmann U (2003) The iron oxides: structure, properties, reactions, occurrences and uses. John Wiley & Sons

Coward EK, Thompson AT, Plante AF (2017) Iron-mediated mineralogical control of organic matter accumulation in tropical soils. Geoderma 306:206-216

Davidson EA, Belk E, Boone RD (1998) Soil water content and temperature as independent or confounded factors controlling soil respiration in a temperate mixed hardwood forest. Global Change Biology 4:217-227

Dubinsky EA, Silver WL, Firestone MK (2010) Tropical forest soil microbial communities couple iron and carbon biogeochemistry. Ecology 91:2604-2612

Dziak JJ, Coffman DL, Lanza ST, Li R (2017) Sensitivity and specificity of information criteria. PeerJ PrePrints

Eusterhues K, Hädrich A, Neidhardt J, Küsel K, Keller T, Jandt K, Totsche K (2014) Reduction of ferrihydrite with adsorbed and coprecipitated organic matter: microbial reduction by Geobacter bremensis vs. abiotic reduction by Na-dithionite. Biogeosciences 11:4953

FAO (2015) Status of the World's Soil Resources (SWSR)–Main Report. Food and Agriculture Organization of the United Nations and Intergovernmental Technical Panel on Soils, Rome, Italy. pp 650

Fiedler S, Vepraskas MJ, Richardson J (2007) Soil redox potential: importance, field measurements, and observations. Advances in Agronomy 94:1-54

Fimmen RL, Vasudevan D, Williams MA, West LT (2008) Rhizogenic Fe–C redox cycling: a hypothetical biogeochemical mechanism that drives crustal weathering in upland soils. Biogeochemistry 87:127-141

Fontes M, Weed S (1996) Phosphate adsorption by clays from Brazilian Oxisols: relationships with specific surface area and mineralogy. Geoderma 72:37-51

Fredrickson JK, Zachara JM, Kennedy DW, Dong H, Onstott TC, Hinman NW, Li S-m (1998) Biogenic iron mineralization accompanying the dissimilatory reduction of hydrous ferric oxide by a groundwater bacterium. Geochimica et Cosmochimica Acta 62:3239-3257

Ghani A, Dexter M, Perrott K (2003) Hot-water extractable carbon in soils: a sensitive measurement for determining impacts of fertilisation, grazing and cultivation. Soil Biology and Biochemistry 35:1231-1243

Ginn BR, Habteselassie MY, Meile C, Thompson A (2014) Effects of sample storage on microbial Fe-reduction in tropical rainforest soils. Soil Biology and Biochemistry 68:44-51

Ginn BR, Meile C, Wilmoth J, Tang Y, Thompson A (2017) Rapid iron reduction rates are stimulated by high-amplitude redox fluctuations in a tropical forest soil. Environmental Science & Technology 51:3250-3259

Gottschalk P et al. (2012) How will organic carbon stocks in mineral soils evolve under future climate? Global projections using RothC for a range of climate change scenarios. Biogeosciences 9:3151

Grenthe I, Stumm W, Laaksuharju M, Nilsson A, Wikberg P (1992) Redox potentials and redox reactions in deep groundwater systems. Chemical Geology 98:131-150

Grybos M, Davranche M, Gruau G, Petitjean P, Pédrot M (2009) Increasing pH drives organic matter solubilization from wetland soils under reducing conditions. Geoderma 154:13-19

Guigue J et al. (2014) A comparison of extraction procedures for water-extractable organic matter in soils. European Journal of Soil Science 65:520-530

Hall SJ, Huang W (2017) Iron reduction: a mechanism for dynamic cycling of occluded cations in tropical forest soils? Biogeochemistry 136:91-102

Hall SJ, Liptzin D, Buss HL, DeAngelis K, Silver WL (2016) Drivers and patterns of iron redox cycling from surface to bedrock in a deep tropical forest soil: a new conceptual model. Biogeochemistry 130:177-190

Hall SJ, McDowell WH, Silver WL (2013) When wet gets wetter: decoupling of moisture, redox biogeochemistry, and greenhouse gas fluxes in a humid tropical forest soil. Ecosystems 16:576-589

Hall SJ, Silver WL (2013) Iron oxidation stimulates organic matter decomposition in humid tropical forest soils. Global Change Biology 19:2804-2813

Hall SJ, Silver WL (2015) Reducing conditions, reactive metals, and their interactions can explain spatial patterns of surface soil carbon in a humid tropical forest. Biogeochemistry 125:149-165

Hanson P, Edwards N, Garten CT, Andrews J (2000) Separating root and soil microbial contributions to soil respiration: a review of methods and observations. Biogeochemistry 48:115-146

Haynes R, Francis G (1993) Changes in microbial biomass C, soil carbohydrate composition and aggregate stability induced by growth of selected crop and forage species under field conditions. European Journal of Soil Science 44:665-675

Heartsill-Scalley T, Scatena FN, Estrada C, McDowell W, Lugo AE (2007) Disturbance and long-term patterns of rainfall and throughfall nutrient fluxes in a subtropical wet forest in Puerto Rico. Journal of Hydrology 333:472-485

Hodge ET (1920) Geology of the Coamo-Guayama district vol 28. vol 4. New York Academy of Sciences

Hodges C, King E, Pett-Ridge J, Thompson A (2018) Potential for Iron Reduction Increases with Rainfall in Montane Basaltic Soils of Hawaii. Soil Science Society of America Journal 82:176-185

Hodges CA (2017) Drivers and Variability of Iron Reduction in Upland Soils. Master Thesis. University of Georgia. pp 1-175

Hook PB, Burke IC (2000) Biogeochemistry in a shortgrass landscape: control by topography, soil texture, and microclimate. Ecology 81:2686-2703

Hou A, Chen G, Wang Z, Van Cleemput O, Patrick W (2000) Methane and nitrous oxide emissions from a rice field in relation to soil redox and microbiological processes. Soil Science Society of America Journal 64:2180-2186

Huang W, Hall SJ (2017a) Elevated moisture stimulates carbon loss from mineral soils by releasing protected organic matter. Nature Communications 8:1774

Huang W, Hall SJ (2017b) Optimized high-throughput methods for quantifying iron biogeochemical dynamics in soil. Geoderma 306:67-72

Husson O (2013) Redox potential (Eh) and pH as drivers of soil/plant/microorganism systems: a transdisciplinary overview pointing to integrative opportunities for agronomy. Plant and Soil 362:389-417

Johnson PC (2014) Extension of Nakagawa & Schielzeth's R2GLMM to random slopes models. Methods in Ecology and Evolution 5:944-946

Josselyn MN, Faulkner SP, Patrick WH (1990) Relationships between seasonally wet soils and occurrence of wetland plants in California. Wetlands 10:7-26

Keiluweit M, Nico PS, Kleber M, Fendorf S (2016) Are oxygen limitations under recognized regulators of organic carbon turnover in upland soils? Biogeochemistry 127:157-171

Kimbrough DE, Kouame Y, Moheban P, Springthorpe S (2006) The effect of electrolysis and oxidation–reduction potential on microbial survival, growth, and disinfection. International Journal of Environment and Pollution 27:211-221

Kleber M, Eusterhues K, Keiluweit M, Mikutta C, Mikutta R, Nico PS (2015) Mineral–organic associations: formation, properties, and relevance in soil environments. In: Advances in agronomy, vol 130. Elsevier, pp 1-140

Knorr K-H (2013) DOC-dynamics in a small headwater catchment as driven by redox fluctuations and hydrological flow paths-are DOC exports mediated by iron reduction/oxidation cycles? Biogeosciences 10:891

Kögel-Knabner I (2017) The macromolecular organic composition of plant and microbial residues as inputs to soil organic matter: fourteen years on. Soil Biology and Biochemistry 105:A3-A8

Liptzin D, Silver WL, Detto M (2011) Temporal Dynamics in Soil Oxygen and Greenhouse Gases in Two Humid Tropical Forests. Ecosystems 14:171-182 doi:10.1007/s10021-010-9402-x

Lovley DR (2000) Fe (III) and Mn (IV) reduction. In: Environmental microbe-metal interactions. American Society of Microbiology, pp 3-30

Lovley DR, Holmes DE, Nevin KP (2004) Dissimilatory fe (iii) and mn (iv) reduction. Advances in Microbial Physiology 49:219-286

Lugo AE, Brown S, Brinson MM (1990) Concepts in wetland ecology. Ecosystems of the World 15:53-85

Lugo AE et al. (2012) Ecological paradigms for the tropics: old questions and continuing challenges. In: Brokaw N, Crowl TA, Lugo A, McDowell WH, Scatena F, Waide RB, Willig MR (eds) A Caribbean forest tapestry: the multidimensional nature of disturbance and response. Oxford University Press, New York. pp 3-41

Manabe S, Wetherald RT (1986) Reduction in summer soil wetness induced by an increase in atmospheric carbon dioxide. Science 232:626-628

Martin ST (2005) Precipitation and dissolution of iron and manganese oxides. Environmental Catalysis:61-81

McClain ME et al. (2003) Biogeochemical hot spots and hot moments at the interface of terrestrial and aquatic ecosystems. Ecosystems 6:301-312

McDowell W, Estrada-Pinto A (1988) Rainfall at the El Verde Field Station, 1964–1986. University of Puerto Rico CEER T-228

Mendelssohn IA, McKee K, Patrick W (1981) Oxygen deficiency in Spartina alterniflora roots: metabolic adaptation to anoxia. Science 214:439-441

Mikutta R, Kleber M, Torn MS, Jahn R (2006) Stabilization of soil organic matter: association with minerals or chemical recalcitrance? Biogeochemistry 77:25-56

Muggler CC, van Griethuysen C, Buurman P, Pape T (1999) Aggregation, organic matter, and iron oxide morphology in oxisols from Minas Gerais, Brazil. Soil Science 164:759-770

Nakagawa S, Schielzeth H (2013) A general and simple method for obtaining R2 from generalized linear mixed-effects models. Methods in Ecology and Evolution 4:133-142

Neff JC, Asner GP (2001) Dissolved organic carbon in terrestrial ecosystems: synthesis and a model. Ecosystems 4:29-48

O'Connell CS, Ruan L, Silver WL (2018) Drought drives rapid shifts in tropical rainforest soil biogeochemistry and greenhouse gas emissions. Nature Communications 9:1348

Pan W, Kan J, Inamdar S, Chen C, Sparks D (2016) Dissimilatory microbial iron reduction release DOC (dissolved organic carbon) from carbon-ferrihydrite association. Soil Biology and Biochemistry 103:232-240

Ponnamperuma FN (1972) The chemistry of submerged soils. Advances in Agronomy 24:29-96

Patrick W, Gambrell R, Faulkner S (1996) Redox measurements of soils. Methods of Soil Analysis Part 3—Chemical Methods. pp 1255-1273

Peretyazhko T, Sposito G (2005) Iron (III) reduction and phosphorous solubilization in humid tropical forest soils. Geochimica et Cosmochimica Acta 69:3643-3652

Peters V, Conrad R (1996) Sequential reduction processes and initiation of CH4 production upon flooding of oxic upland soils. Soil Biology and Biochemistry 28:371-382

Prem M, Hansen HCB, Wenzel W, Heiberg L, Sørensen H, Borggaard OK (2015) High spatial and fast changes of iron redox state and phosphorus solubility in a seasonally flooded temperate wetland soil. Wetlands 35:237-246

Reddy K, D'Angelo E, Harris W (2000) Biogeochemistry of Wetlands. . In: Sumner M (ed) Handbook of Soil Science. CRC Press, Boca Raton, FL, pp G89–G119

Rezende M, Curi N, Rezende S, Corrêa G (2002) Pedologia: base para distinção de ambientes. NEPUT–Núcleo de Estudos de Planejamento e Uso da Terra. Viçosa, Minas Gerais. 4ª Ed. pp 1-338

Ruser R, Flessa H, Russow R, Schmidt G, Buegger F, Munch JC (2006) Emission of N_2O, N_2 and CO_2 from soil fertilized with nitrate: effect of compaction, soil moisture and rewetting. Soil Biology and Biochemistry 38:263-274

Saleska SR et al. (2003) Carbon in Amazon forests: unexpected seasonal fluxes and disturbance-induced losses. Science 302:1554-1557

Scatena FN (1989) An introduction to the physiography and history of the Bisley Experimental Watersheds in the Luquillo Mountains of Puerto Rico. Gen. Tech. Rep. SO-72. New Orleans, LA: US Dept of Agriculture, Forest Service, Southern Forest Experiment Station. 22. pp 72

Schaefer C, Gilkes R, Fernandes R (2004) EDS/SEM study on microaggregates of Brazilian Latosols, in relation to P adsorption and clay fraction attributes. Geoderma 123:69-81

Seiders VM (1971) Cretaceous and lower Tertiary stratigraphy of the Gurabo and El Yunque quadrangles, Puerto Rico.

Silva LC, Doane TA, Corrêa RS, Valverde V, Pereira EI, Horwath WR (2015) Iron-mediated stabilization of soil carbon amplifies the benefits of ecological restoration in degraded lands. Ecological Applications 25:1226-1234

Silva Neto LF, Vasconcellos Inda A, Bayer C, Pinheiro Dick D, Tiago Tonin A (2008) Óxidos de ferro em latossolos tropicais e subtropicais brasileiros em plantio direto. Revista Brasileira de Ciência do Solo 32:1873-1881

Silver WL, Lugo A, Keller M (1999) Soil oxygen availability and biogeochemistry along rainfall and topographic gradients in upland wet tropical forest soils. Biogeochemistry 44:301-328

Six J, Conant R, Paul EA, Paustian K (2002) Stabilization mechanisms of soil organic matter: implications for C-saturation of soils. Plant and Soil 241:155-176

Snakin VV, Prisyazhnaya A, Kovács-Láng E (2001) Soil liquid phase composition. Elsevier. Amsterdam, Netherlands. pp 5-315

Souza IF, Almeida LF, Jesus GL, Pett-Ridge J, Nico PS, Kleber M, Silva IR (2018) Carbon Sink Strength of Subsurface Horizons in Brazilian Oxisols. Soil Science Society of America Journal 82:76-86

Sparks DL (2003) Environmental soil chemistry. Academic Press. San Diego, California. pp 1-351

Thaymuang W, Kheoruenromne I, Suddhipraharn A, Sparks DL (2013) The role of mineralogy in organic matter stabilization in tropical soils. Soil Science 178:308-315

Thompson A, Chadwick OA, Rancourt DG, Chorover J (2006) Iron-oxide crystallinity increases during soil redox oscillations. Geochimica et Cosmochimica Acta 70:1710-1727

Wagai R, Mayer LM (2007) Sorptive stabilization of organic matter in soils by hydrous iron oxides. Geochimica et Cosmochimica Acta 71:25-35

Wang Z, Delaune R, Patrick W, Masscheleyn P (1993) Soil redox and pH effects on methane production in a flooded rice soil. Soil Science Society of America Journal 57:382-385

Wang Y, Van Cappellen P (1996) A multicomponent reactive transport model of early diagenesis: Application to redox cycling in coastal marine sediments. Geochimica et Cosmochimica Acta 60:2993-3014.

Weber KA, Achenbach LA, Coates JD (2006) Microorganisms pumping iron: anaerobic microbial iron oxidation and reduction. Nature Reviews Microbiology 4:752-764

Weiss JV, Emerson D, Megonigal JP (2004) Geochemical control of microbial Fe (III) reduction potential in wetlands: comparison of the rhizosphere to non-rhizosphere soil. FEMS Microbiology Ecology 48:89-100

Xiao J et al. (2015) In situ visualisation and characterisation of the capacity of highly reactive minerals to preserve soil organic matter (SOM) in colloids at submicron scale. Chemosphere 138:225-232

Xu M, Qi Y (2001) Soil-surface CO2 efflux and its spatial and temporal variations in a young ponderosa pine plantation in northern California. Global Change Biology 7:667-677

TABLES AND FIGURES

Table 4.1. Summary of soil characterization for each Catena and topographic position. Soils from Luquillo CZO, Puerto Rico, sampled in 2016

Site	SRO-Fe[a] mmol kg^{-1}	Total-Fe mmol kg^{-1}	Carbon (%)	Clay (%)	Sand (%)	Silt (%)	pH[b]
Valley-1	336	1162	4.6	7	45	48	6.1
Valley-2	305	1353	4.0	8	36	56	5.3
Valley-3	195	1409	3.1	10	33	56	5.3
Slope-1	178	1403	3.4	10	27	63	5.1
Slope-2	213	1503	3.1	12	28	60	4.8
Slope-3	131	1434	3.4	8	45	47	5.1
Ridge-1	190	1428	4.5	6	43	51	4.9
Ridge-2	227	1334	5.9	5	52	43	4.8
Ridge-3	206	1340	4.6	5	60	36	5.0

[a]Citrate Ascorbate Extraction.

[b]pH average for all 17 days of soil collection.

Table 4.2. Summary of mixed-effect linear models for the environmental factors obtained by stepwise backwards elimination. All variables are daily averages

Variable	Catenas	AIC[a] (R^2c)[b]	Num. of observ.[c]	Model (significant predictors in bold at p<0.05)
Eh	All	3850.41 (0.944)	324	Eh = - 0.7187***Precipitation**
O_2	1	866.20 (0.992)	240	O_2 = - 0.0129 ***Precipitation**
θ_V	1	-880.34 (0.853)	213	$\theta_V = 4.894e^{-04}$***Precipitation**

[b] AIC = Akaike Information Criterion

[c] R^2c: conditional R squared

[d] Maximum number of observations is 415 for all catenas and 243 for Catena 1 only

Units: Eh = dV, θ_V = m^3 m^{-3}, O_2 = %, and Precipitation = mm.

Table 4.3. Summary of mixed-effect linear models for the Biogeochemical variables obtained by stepwise backwards elimination

Variable	Catenas	AIC[a] (R^2c)[b]	Num. of observ.[c]	Model (significant predictors in bold at p<0.05)
Fe^{II}	All	990.725 (0.727)	110	Fe^{II} = 2.130***Media-Fe^{III}_{RR}** + 20.286***pH**
	Catena 1	377.89 (0.789)	39	Fe^{II} = 2.4758***Media-Fe^{III}_{RR}** - 4.3644***O_2_48**
Media-Fe^{III}_{RR}	All	413.32 (0.835)	73	Media-Fe^{III}_{RR} ~ 0.1073***Fe^{II}** + 20.295***θ_G** - 0.845***Eh_6**
Shewa-Fe^{III}_{RR}	All	654.06 (0.810)	110	Shewa-Fe^{III}_{RR} ~ 0.1202***Fe^{II}** + 21.221***θ_G** + 3.861***pH**
DOC	All	718.68 (0.441)	132	DOC = 0.1909***Fe^{II}** + 12.47***θ_G**
Flux CO_2	Catena 1	117.2 (0.429)	45	Flux CO_2 = - 10.995 ***θ_V**
Flux CH_4	Catena 1	126.01 (0.545)	43	Flux CH_4 = 2.782***pH**

[b] AIC = Akaike Information Criterion

[c] R^2c: conditional R squared

[d] Maximum number of observations is 153 for all catenas and 51 for Catena 1 only

Units: Fe^{II} = mmol kg^{-1}, Media-Fe^{III}_{RR} and Shewa-Fe^{III}_{RR} = mmol kg^{-1} d^{-1}, DOC = mg kg^{-1}; pH = unitless; θ_G = g g^{-1}; Eh = dV, θ_V = m^3 m^{-3}, O_2 = %, Flux CO_2 = μmol m^{-2} s^{-1}, and Flux CH_4 = nmol m^{-2} s^{-1}.

Table 4.4. Comparison of reactive iron pool (SRO-Fe) extracted by Citrate-Ascorbate and the Fe reduced within 7 days by incubations with Shewa-Fe^{III}_{RR} and Media-Fe^{III}_{RR}: (A) for the actual values in mmol kg^{-1} for the 7 day-incubation, and (B) for the percent correlation of the Fe^{III}_{RR} pool and the SRO-Fe pool. Soils from Luquillo CZO, Puerto Rico, sampled in 2016

Table 4.4 (A)

Site	SRO-Fe	Shewa-Fe^{III}_{RR}				Media-Fe^{III}_{RR}			
		Min	Mean	(SD)	Max	Min	Mean	(SD)	Max
		mmol kg^{-1}							
Valley-1	336	140	221	(19)	344	128	214	(17)	342
Valley-2	305	8	80	(13)	139	6	73	(12)	120
Valley-3	195	8	63	(11)	113	3	60	(11)	104
Slope-1	178	3	53	(12)	144	3	33	(6)	68
Slope-2	213	5	52	(9)	89	6	34	(8)	76
Slope-3	131	3	35	(8)	81	5	20	(5)	62
Ridge-1	190	4	49	(7)	87	5	33	(7)	88
Ridge-2	227	8	49	(7)	95	12	34	(4)	51
Ridge-3	206	5	36	(6)	91	4	24	(4)	49

Table 4.4 (B)

Site	SRO-Fe	Shewa-Fe^{III}_{RR}				Media-Fe^{III}_{RR}			
		Min	Mean	(SD)	Max	Min	Mean	(SD)	Max
	mmol kg^{-1}	% (Fe^{III}_{RR} / SRO-Fe)							
Valley-1	336	42	66	(6)	102	38	64	(5)	101
Valley-2	305	3	26	(4)	46	2	24	(4)	39
Valley-3	195	4	32	(6)	58	1	31	(5)	53
Slope-1	178	2	30	(7)	81	1	18	(3)	38
Slope-2	213	2	24	(4)	42	3	16	(4)	36
Slope-3	131	3	27	(6)	62	4	16	(4)	47
Ridge-1	190	2	26	(4)	46	3	17	(4)	46
Ridge-2	227	3	21	(3)	42	5	15	(2)	22
Ridge-3	206	2	17	(3)	44	2	12	(2)	24

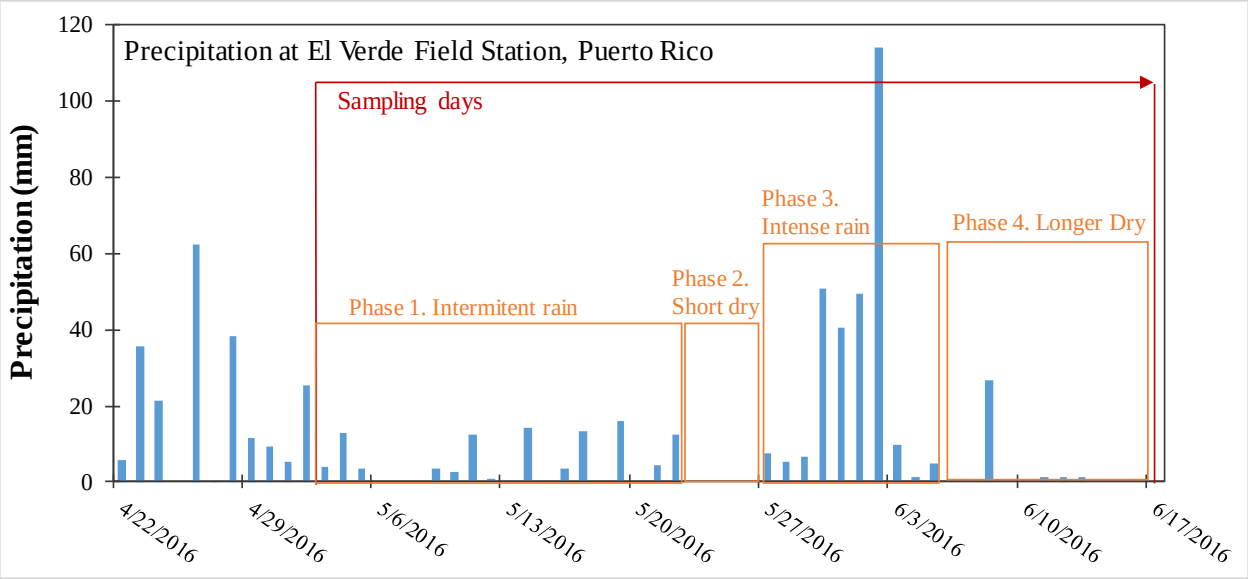

Fig 4.1. Precipitation at the El Verde Field Station, Puerto Rico, with records before and during the sampling campaign.

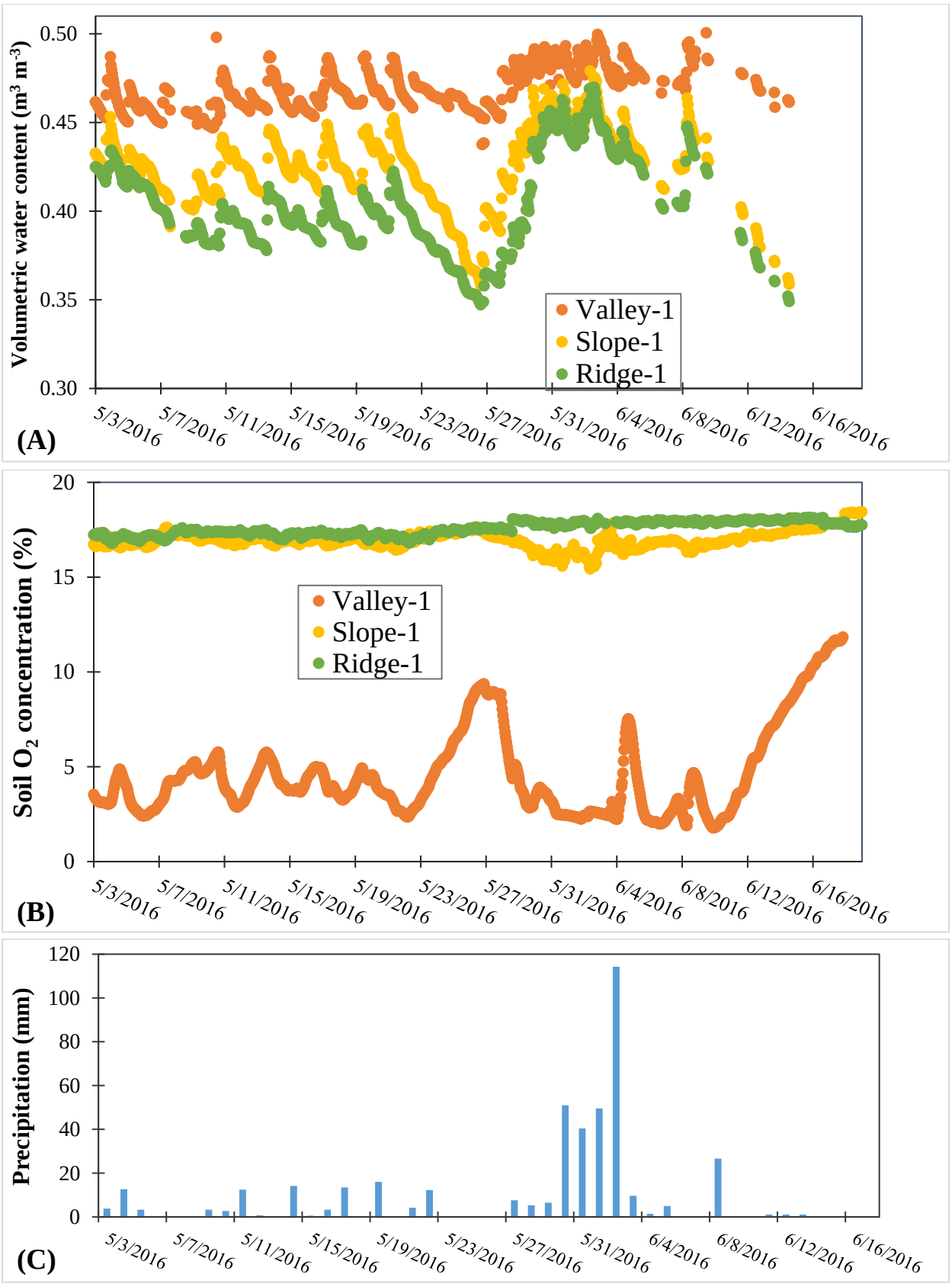

Fig 4.2 Soil volumetric water content (A), oxygen (B), and precipitation (C) at Luquillo CZO, PR.

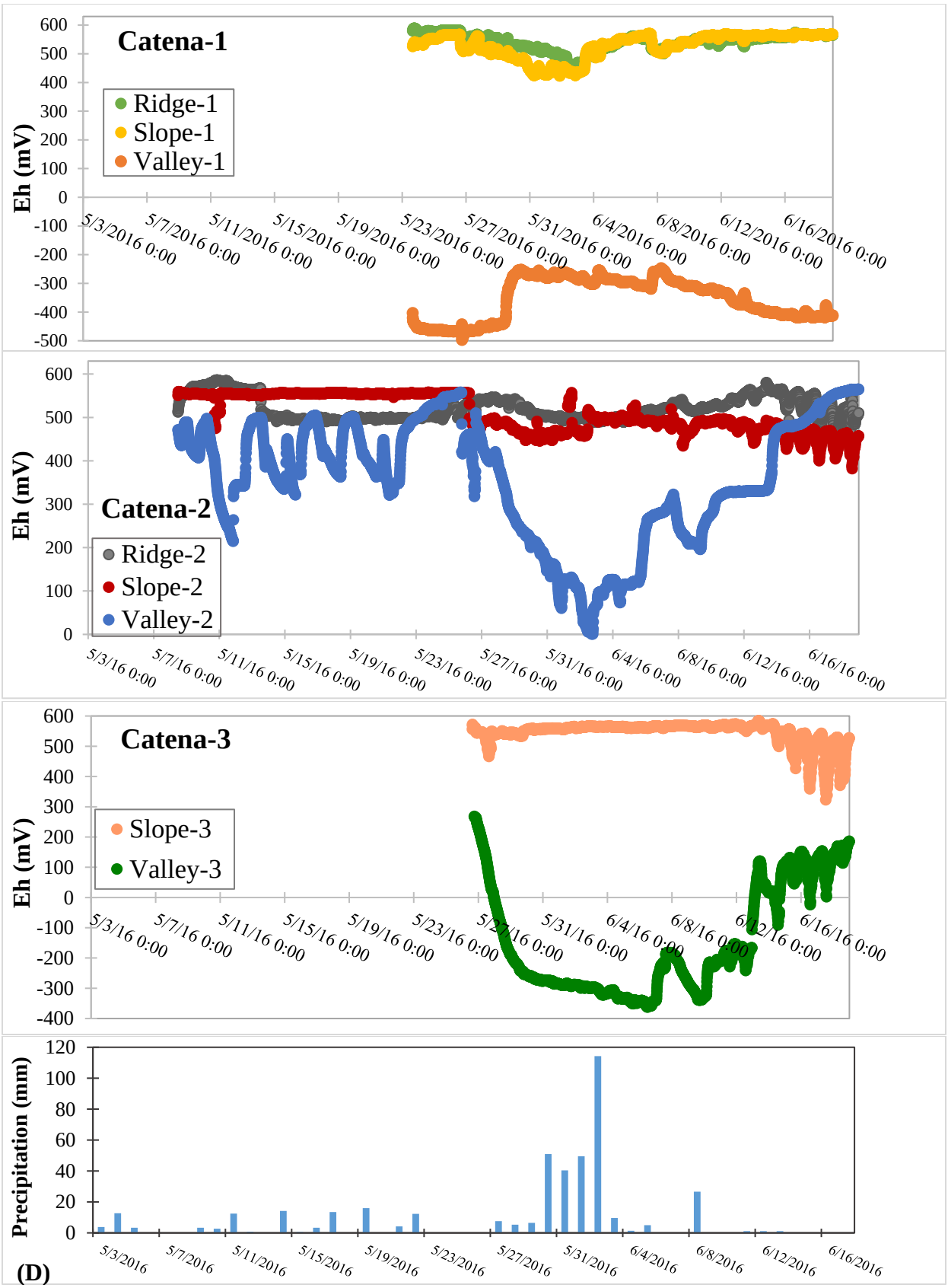

Fig 4.3. Redox Potential (Eh) using Platinum electrodes for each location within 3 catenas, Luquillo CZO.

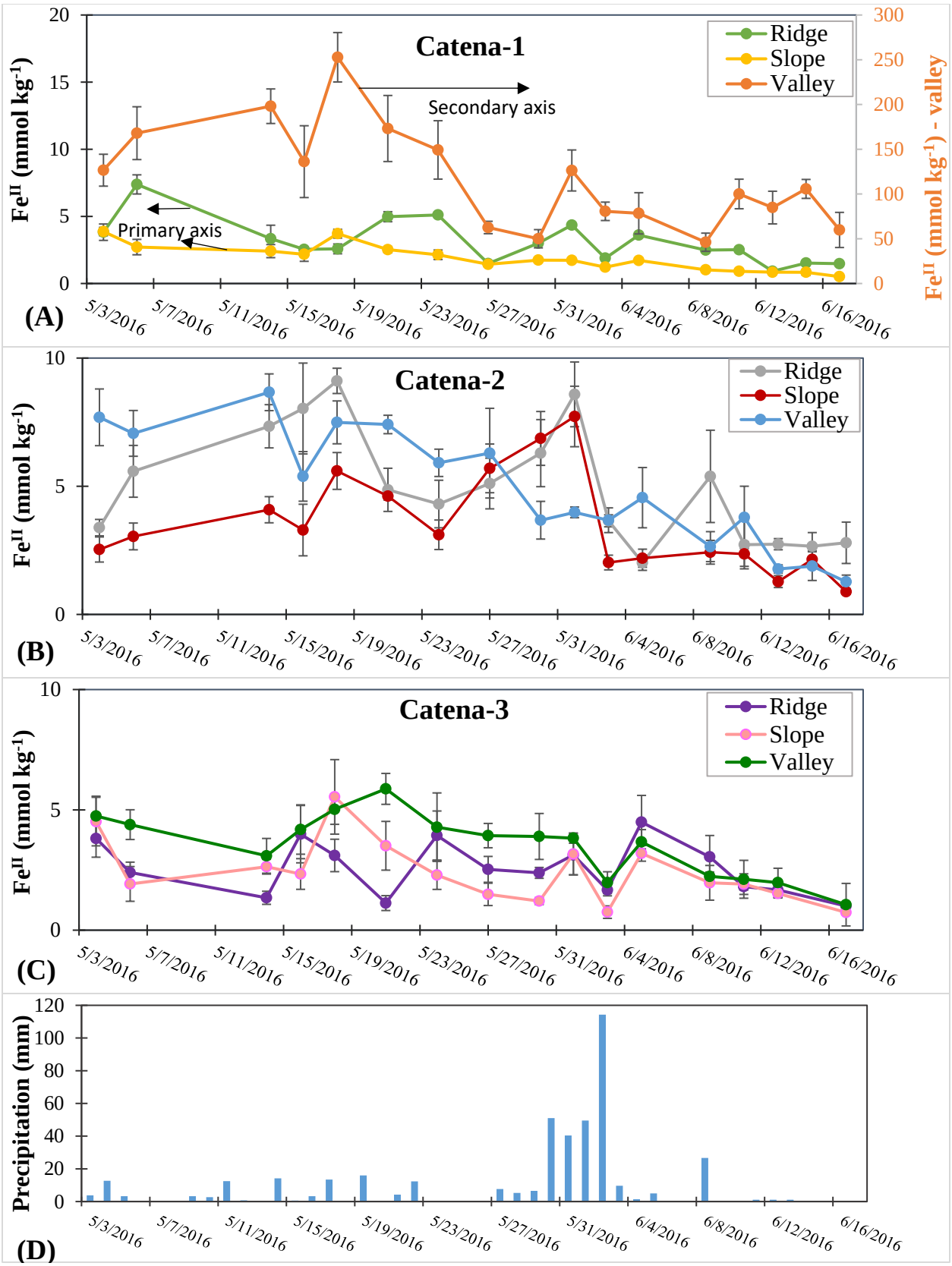

Fig 4.4. Fe^{II} at Ridge, Slope, and Valley for all 3 catenas (A, B, and C), and precipitation (D), Luquillo CZO.

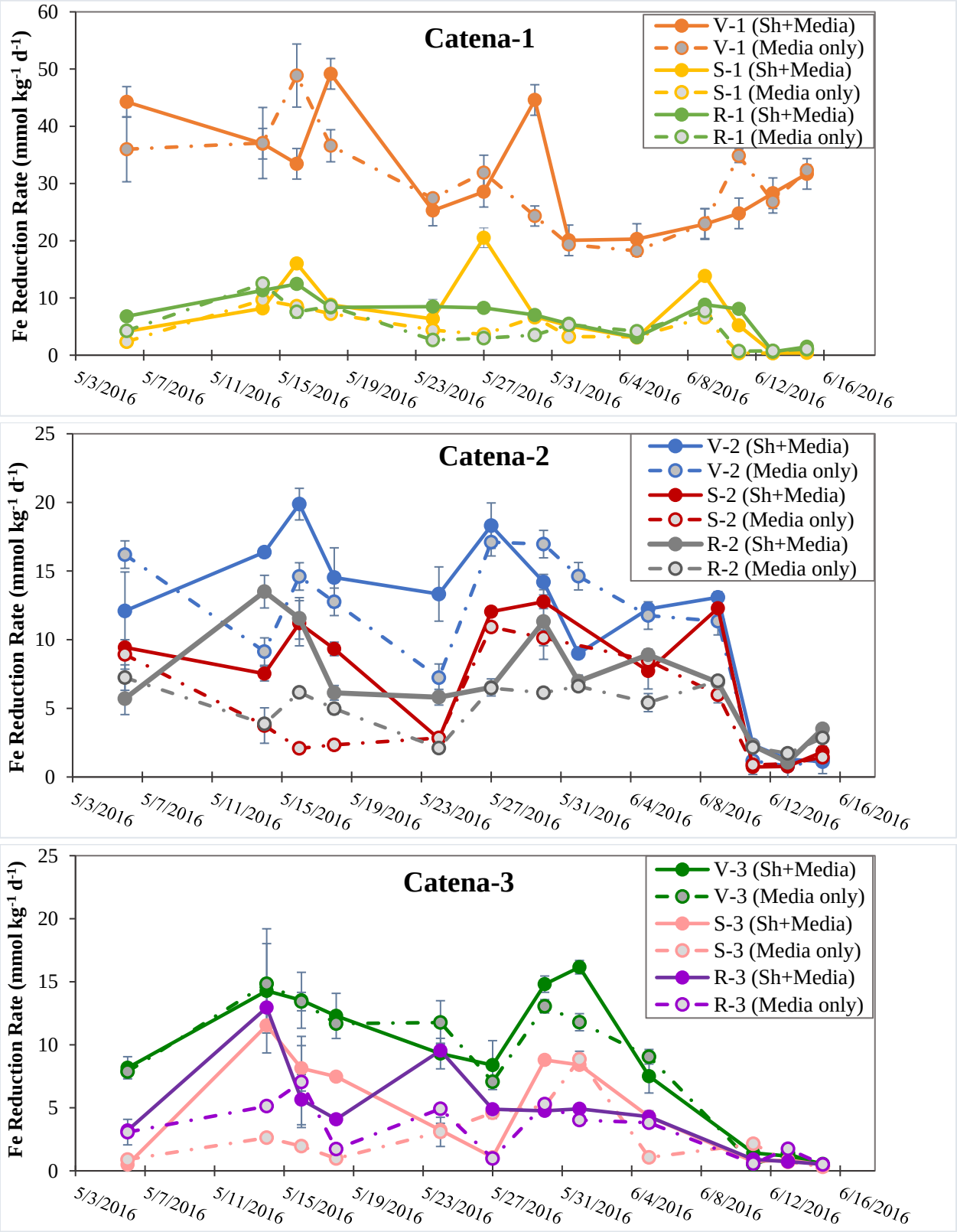

Fig 4.5. Soil Fe reduction rates (7 days) by Shewanella+media (Shewa-Fe^{III}_{RR}) or media only (Media-Fe^{III}_{RR}) incubations. Soils from Luquillo CZO, PR.

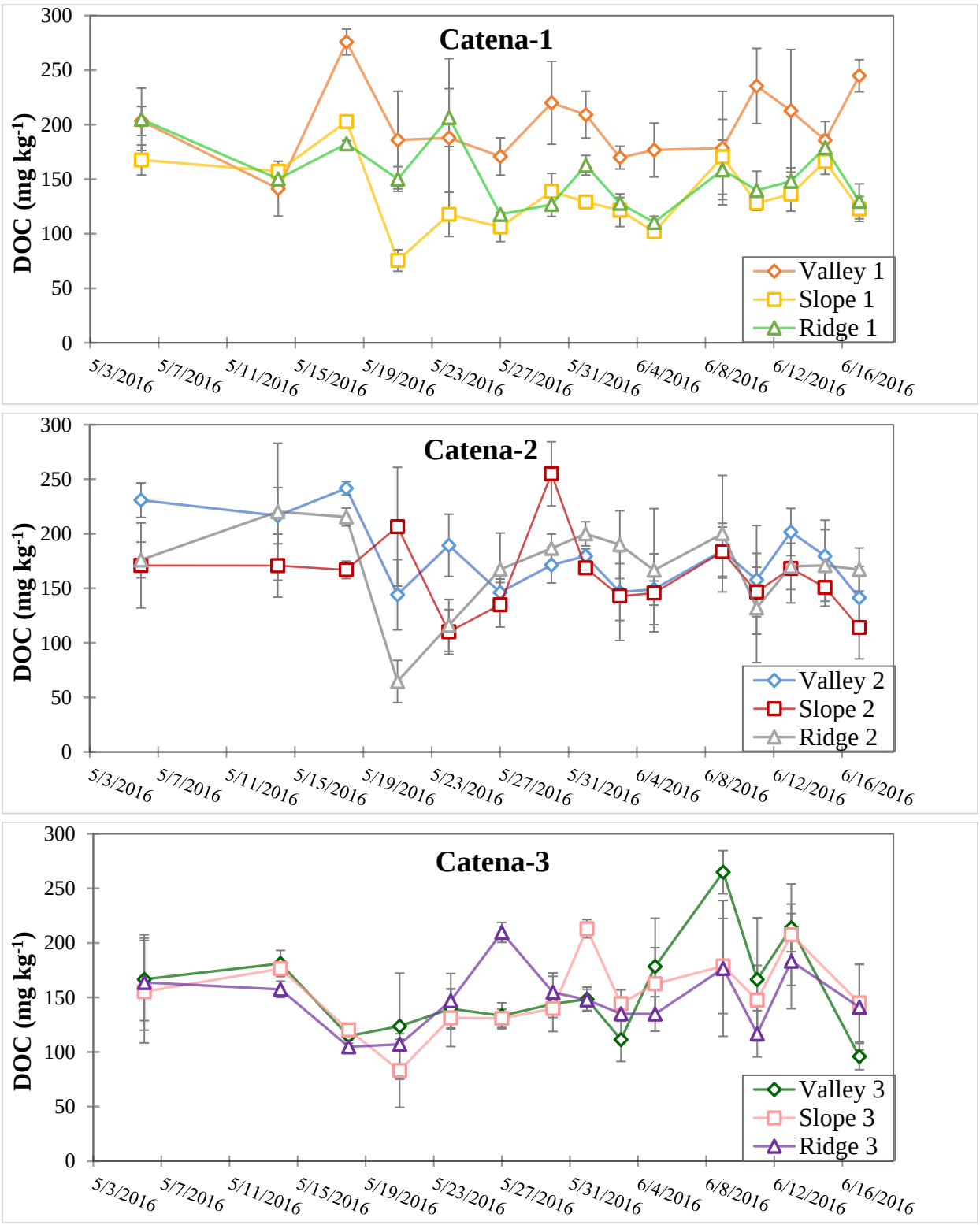

Fig 4.6. Dissolved Organic Carbon (DOC), 1:5 soil:water extraction. Soils from Luquillo CZO, PR.

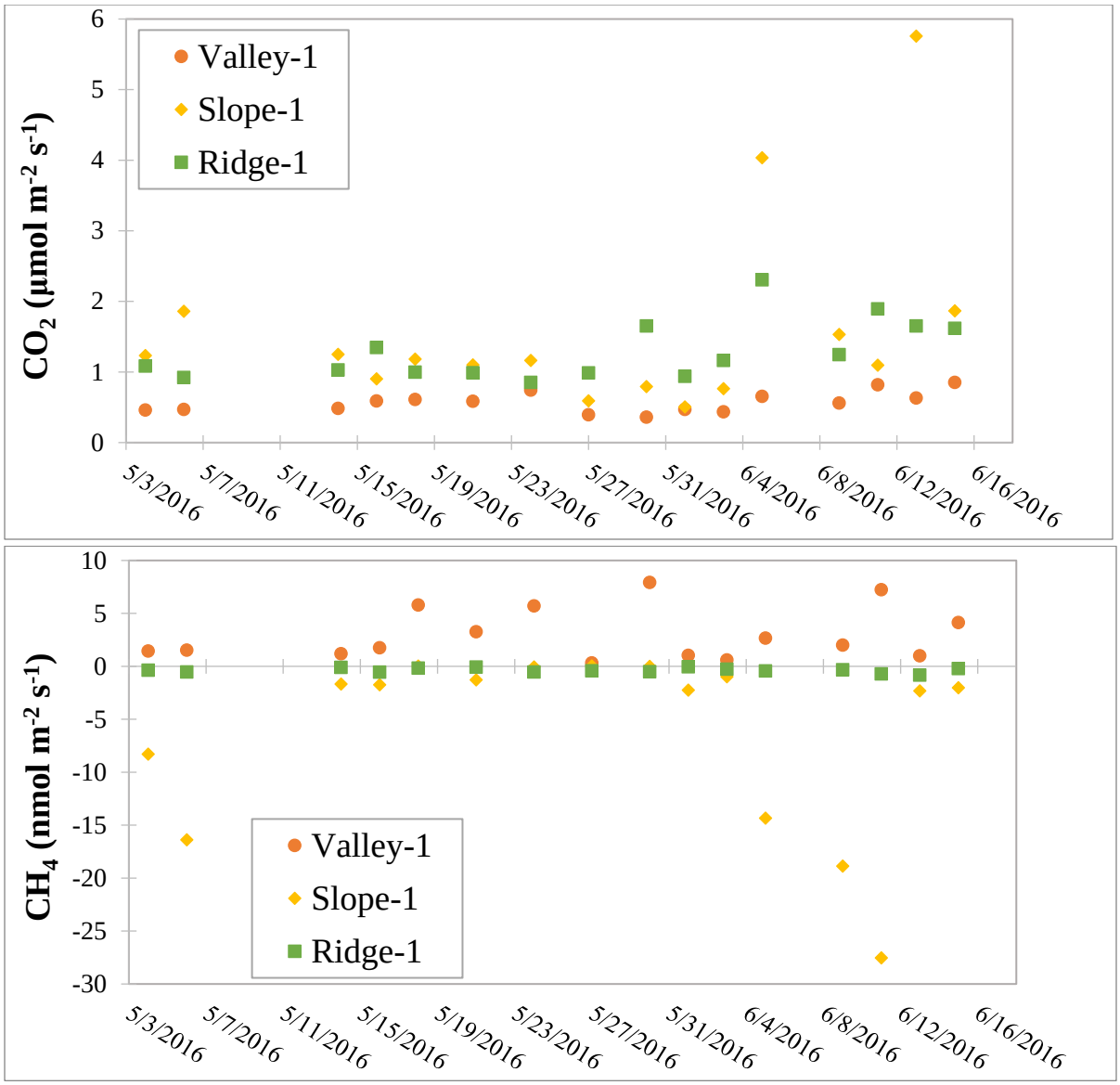

Fig 4.7. Soil CO_2 and CH_4 emissions. Soils from Luquillo CZO, PR.

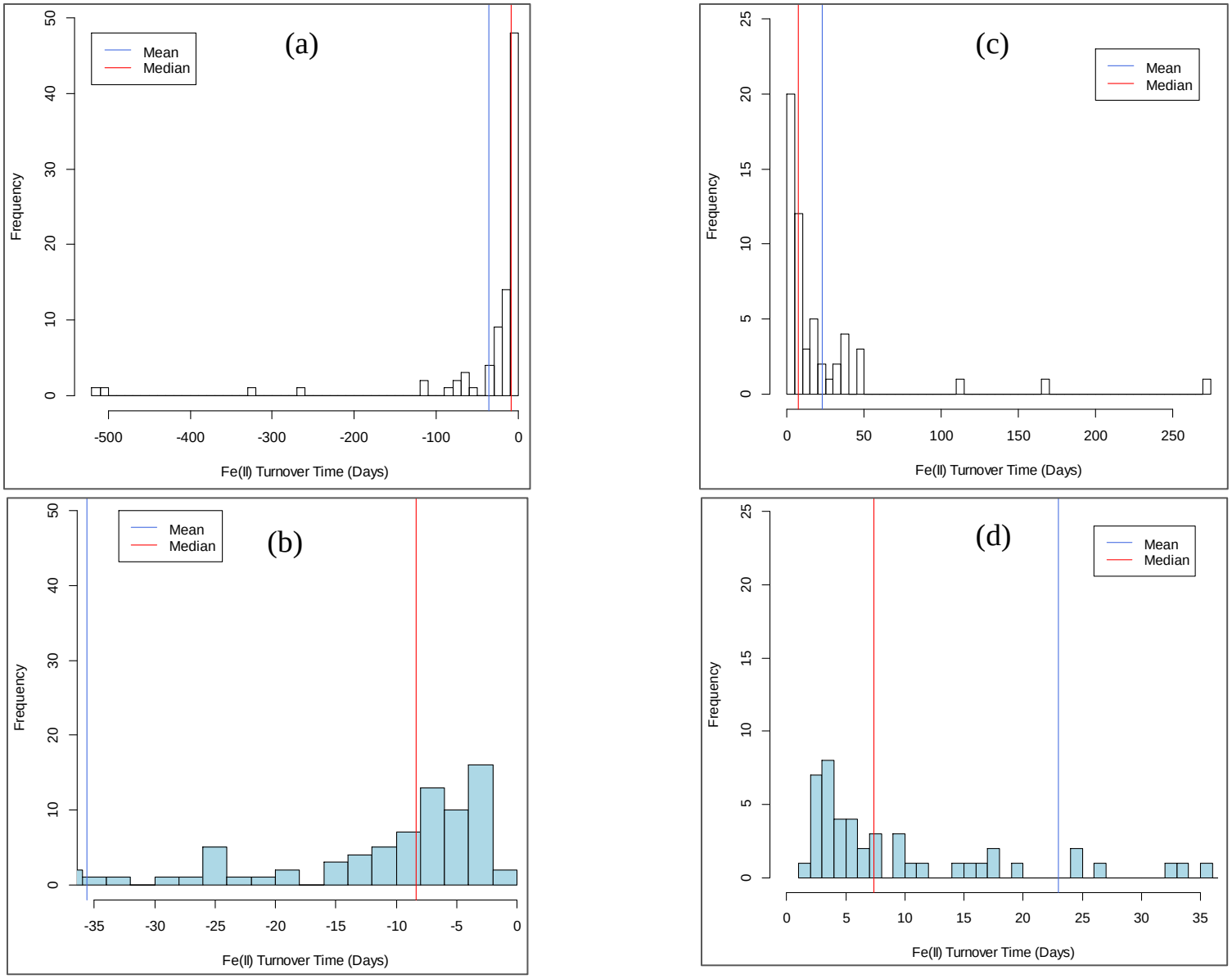

Fig 4.8. Turnover times for Fe^{II} consumption (a and b) and Fe^{II} production (c and d) for all catenas. Figures (b) and (d) were zoomed near zero.

CHAPTER 5

CONCLUSIONS

I demonstrated using controlled laboratory and monitored field experiments that redox fluctuations impact the biogeochemistry of iron and carbon in soils from a Critical Zone Observatory (CZO). In humid, (sub)tropical, and well-weathered environments containing iron-rich and fine textured soils, Fe is a key biogeochemical element involved in the cycling of carbon, nutrients, and in the metabolism of microorganisms and plants. To study these processes, I conducted two redox oscillating laboratory studies and one field experiment from a tropical rainforest in Puerto Rico (Luquillo CZO). In the Appendices I presented complementary laboratory studies as well as one field study from a subtropical forest in the Piedmont of South Carolina (Calhoun CZO).

In the first laboratory redox oscillation experiment, I found that Fe reduction rates increased when more frequent (i.e. short oscillation periods) were imposed. I suggested these changes occurred because of more frequent flushes of short-range-order (SRO) Fe^{III} phases and/or a higher iron-reducing-bacteria activity in the short oscillation periods. I further observed a decrease in total carbon concentration and suggested this was due to mineralization, depolymerization, and Fenton reactions.

In the second redox oscillation study, I evaluated how the time exposure to oxygen (τ_{oxic}) influenced Fe reduction and C mineralization by comparing treatments with long oscillation periods (τ_{anoxic} of 6 d) and short oscillation periods (τ_{anoxic} of 2 d). In the Long oscillation

treatments, as τ_{oxic} decreased from 72 to 24 to 8 h, we observed an increase in Fe reduction rates, non-significant variation in CO_2 emissions, but a decline in CH_4 emissions. In the treatments with short oscillation periods (τ_{anoxic} of 2 d, and τ_{oxic} at either 24 or 8 h) we found a decline in Fe reduction, and in both CO_2 and CH_4 emissions under anoxic conditions as the redox oscillations progressed.

Extending our understanding from laboratory manipulations to in-situ biogeochemical processes, I conducted a field experiment in the Luquillo CZO monitoring redox sensitive Fe and C pools at different topographic positions (ridges, slopes, and valleys) over two months. I found that changes in soil moisture and precipitation patterns impacted soil Fe and C pools in the distinct topographies and influenced changes in soil oxygen content and redox potential (Eh). The variables obtained from soil extractions (Fe^{II}, Fe^{III}_{RR}, DOC, and pH) were responsive in most of the cases to changes in soil moisture. Indeed, the valleys were more responsive to the changes in environmental factors (soil moisture, O_2, and Eh) compared to the ridges and slopes.

The amount of time soils are exposed to oxic and anoxic conditions (redox fluctuations) can also be essential for agriculture and irrigation management in iron-rich soils from the tropics. Important research questions can motivate future investigations, such as: What is the impact of different irrigation regimes applied in these iron-rich soils on soil phosphorus availability to plants, for instance? What is the correlation of irrigation cycles with optimum nutrient uptake and availability to plants and microorganisms? What is the impact of irrigation on the net mineralization and preservation of organic matter? Based on the results from this dissertation and aligned with previous investigations, one can ask: Would be better to apply irrigation water to the crops with short and frequent cycles of irrigation or within long and spaced-out cycles of irrigation?; or Would these distinct irrigation regimes distinctly affect the availability and

adsorption of phosphorus fertilizers in these crop systems as P is often sorbed to iron oxyhydroxides? Similar questions and land management applications can be posed for inundated irrigation systems (such as rice paddies) presenting important applications for food security, land management, and impacts on climate change.

In total, these sets of experimental results have several ecosystem, environmental, and agricultural implications. Shifts in Fe oxidation state (Fe^{III} to Fe^{II} and vice-versa) can directly affect soil carbon budgets in iron-rich soils by either decreasing (desorption or mineralization) or increasing (adsorption or stabilization) soil carbon stocks. Redox fluctuations in marine sediments and wetland systems have been extensively investigated but are only beginning to be fully understood in upland soils. Therefore, this dissertation expanded our knowledge of terrestrial Fe and C biogeochemistry and demonstrated that the characteristics of redox fluctuations—such as the time length under oxic or anoxic conditions (τ_{anoxic} and τ_{oxic})—are important determinants of iron cycling and organic matter loss or accumulation in upland soils and may influence ecosystem processes in humid (sub)tropical regions.

APPENDIX A

SUPPLEMENTAL INFORMATION FOR CHAPTER 3

TABLES AND FIGURES

Table A.1. Dissolved oxygen (DO) concentrations exposed to anoxic conditions, from soil slurries previously exposed to oxic conditions. Zero time is still under oxic condition, measurement taken right before placing inside the anoxic chamber. Soils from Bisley watershed, Puerto Rico, sampled in 2015

Time exposed to anoxic conditions *Hours*	**Dissolved Oxygen (DO)** $\mu g\ L^{-1}$
0	9800 ± 100
0.05	2967 ± 208
0.1	1068 ± 46
2	241 ± 13
5	119 ± 9

Table A.2. Total elemental analysis for initial native soil sample (no treatments or chemicals added). Soils from Bisley watershed, Puerto Rico, sampled in 2015

Fe	Al	Si	Ca	Mg	Na	K	Ti	Mn	P
---------- mmol kg^{-1} --------			---------- % ----------						
943	2501	13636	1.54	0.65	1.00	0.43	0.39	0.14	0.035

Table A.3. Statistical significance for Fe^{II} among cycles within treatments only (not comparing among treatments) at 95% confidence interval

Treatment	Cycles						
	1	**2**	**3**	**4**	**5**	**6**	**7**
Pre-conditioning	a	a	a				
L-72h	a	a	a				
L-24h	a	a	a				
L-8h	a	a	a				
S-24h	a	b	a	a	a	a	a
S-8h	ab	b	b	a	a	ab	a

Table A.4. Statistical significance for CO_2 among cycles within treatments only (not comparing among treatments) at 95% confidence interval

Treatment	Cycles						
	1	**2**	**3**	**4**	**5**	**6**	**7**
Pre-conditioning	a	b	a				
L-72h	a	ab	b				
L-24h	a	b	a				
L-8h	a	b	a				
S-24h	abc	b	abc	abc	c	abc	c
S-8h	abc	a	a	b	a	bc	a

Table A.5. Statistical significance for CH_4 among cycles within treatments only (not comparing among treatments) at 95% confidence interval

Treatment	Cycles						
	1	**2**	**3**	**4**	**5**	**6**	**7**
Pre-conditioning	a	a	b				
L-72h	a	b	a				
L-24h	a	b	c				
L-8h	a	a	b				
S-24h	acd	b	acd	acd	ac	ad	acd
S-8h	a	a	b	b	a	a	b

Table A.6. Comparison of iron reduction rates in different redox fluctuation studies. All soils are from the valley portion of Bisley Watershed, Luquillo CZO, Puerto Rico

Work/Paper	Total Fe ($mmol\ kg^{-1}$)	SRO-Fe[a] ($mmol\ kg^{-1}$)	C content ($mg\ g^{-1}$)	Fe reduction rate ($mmol\ kg^{-1}\ h^{-1}$)	Days (fluctuating conditions)	
					Anoxic	Oxic
Ginn et. al. 2017 & Tishchenko et al. 2015	1122.8	144	25.5	0.07 - 0.36	12	2
				0.11 - 0.96	6	1
				0.14 - 0.87	3	0.5
DeAngelis et al. 2010 [b]	NA	158	NA	0.18 - 0.38	4	4
Barcellos et. al. 2018 (Chapter 2)	1162.5	148	46.7	0.21 - 0.47	6	1
				0.25 - 0.26	11.67	1.67
				0.18 - 0.97	2.92	0.42
This study (Chapter 3)	943.1	439	37.4	0.10 - 0.15	6	3
				0.13 - 0.18	6	1
				0.20 - 0.30	6	1/3
				0.05 - 0.40	2	1
				0.09 - 0.25	2	1/3

[a]Citrate Ascorbate Extraction
[b]Total Fe and C content not provided in DeAngelis et al. (2010)

Fig A.1. Soil sample sieved at 2 mm inside the 95%:5% (N_2:H_2) glovebox Coy chamber (0% O_2). Soils from Bisley watershed, Puerto Rico, sampled in 2015.

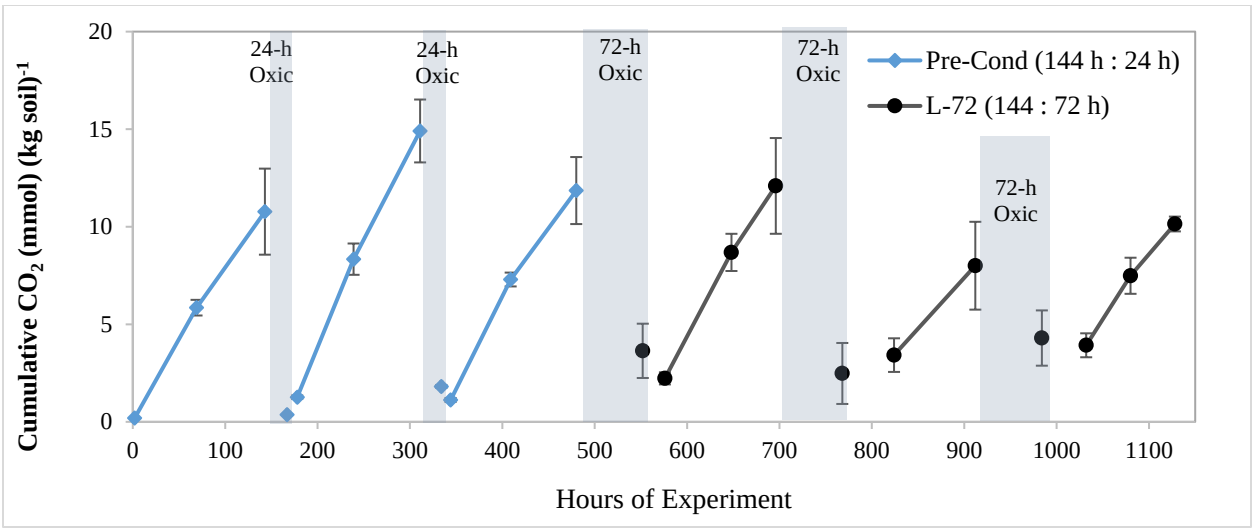

(a)

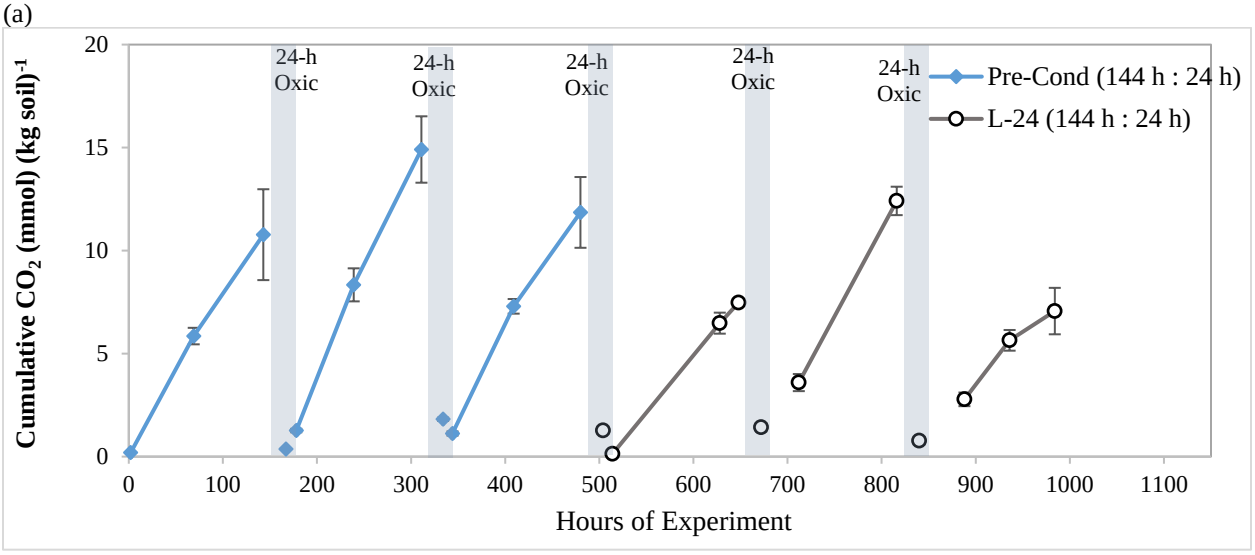

(b)

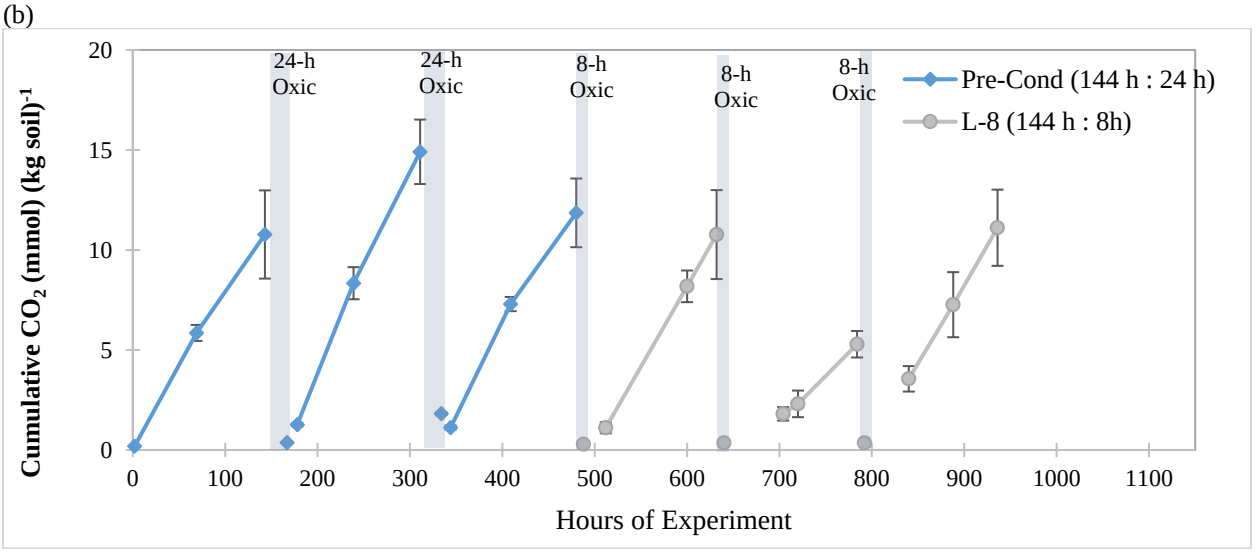

(c)

Fig A.2. Cumulative CO_2 flux within anoxic conditions only for all treatments (a) to (c). Soils from Bisley watershed, Puerto Rico, sampled in 2015.

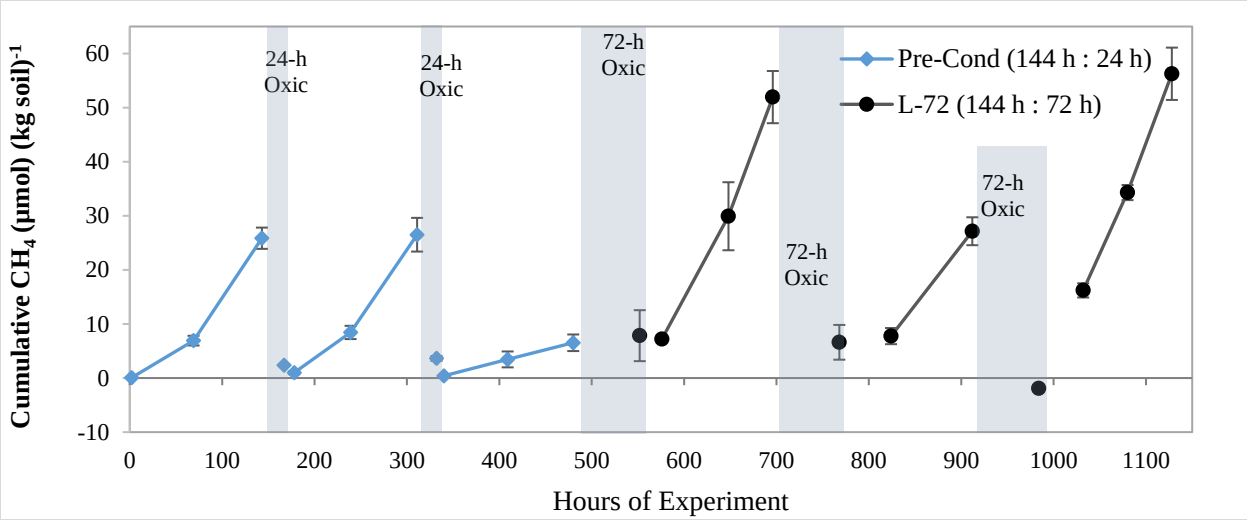

(a)

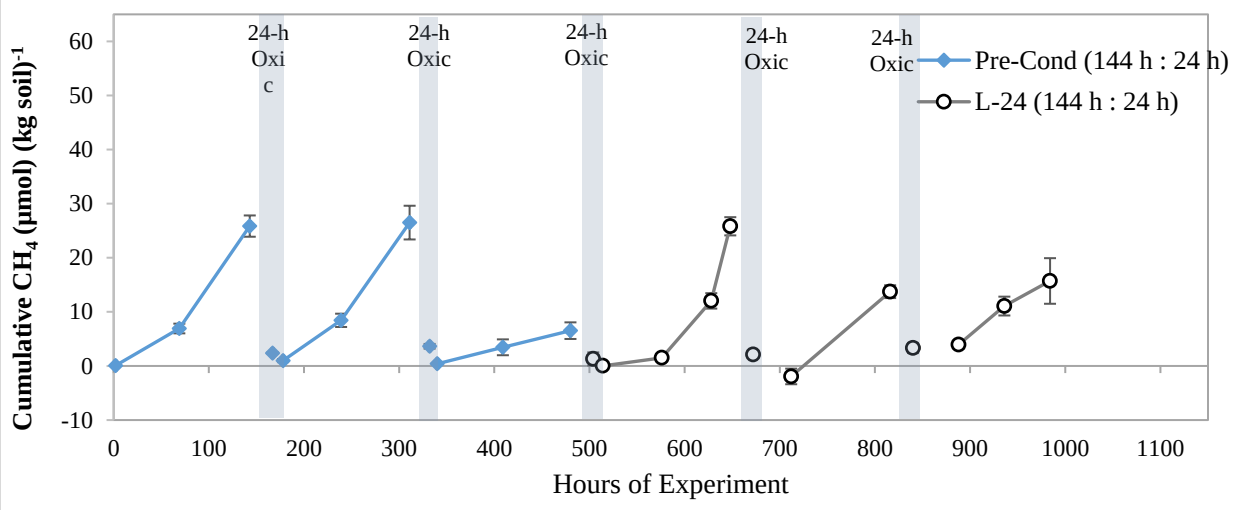

(b)

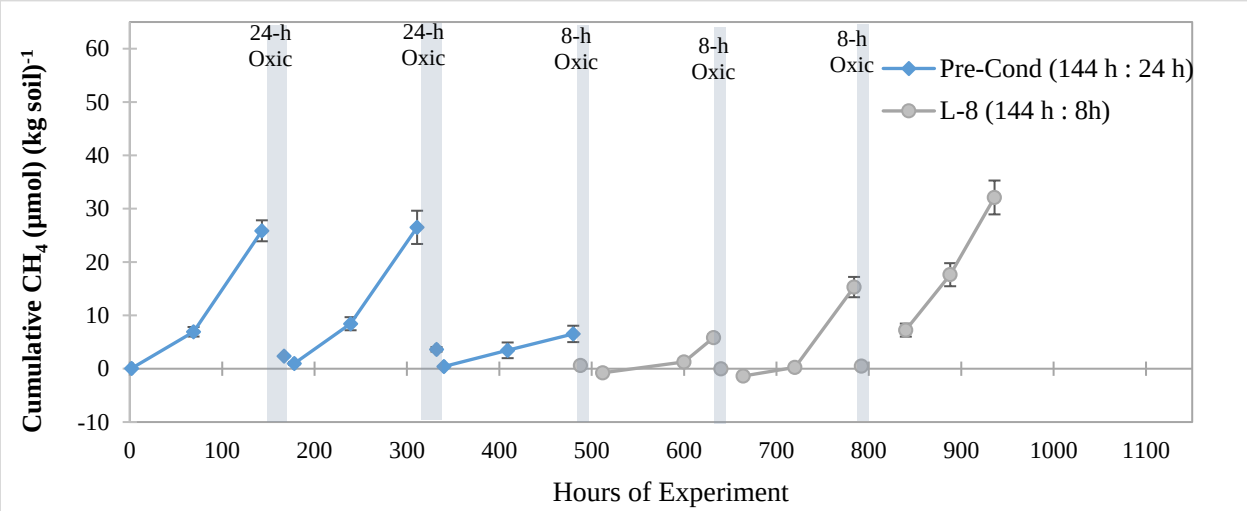

(c)

Fig A.3. Cumulative CH_4 flux within anoxic conditions only for all treatments (a) to (c). Soils from Bisley watershed, Puerto Rico, sampled in 2015.

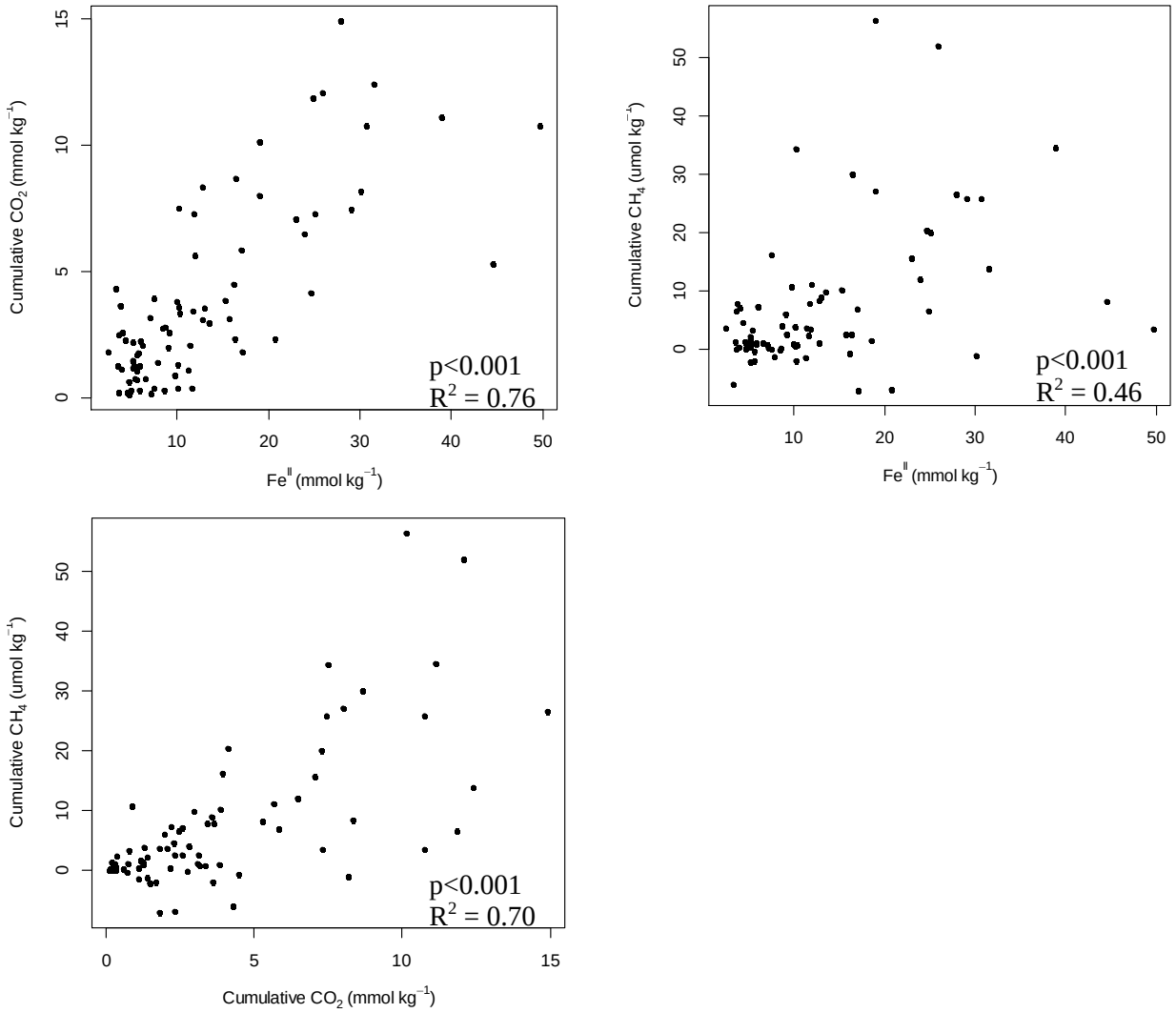

Fig A.4. Overall regression of all treatments, including both anoxic and oxic conditions, for among Fe^{II} concentrations and cumulative CO_2 and CH_4 effluxes. Soils from Bisley watershed, Puerto Rico, sampled in 2015.

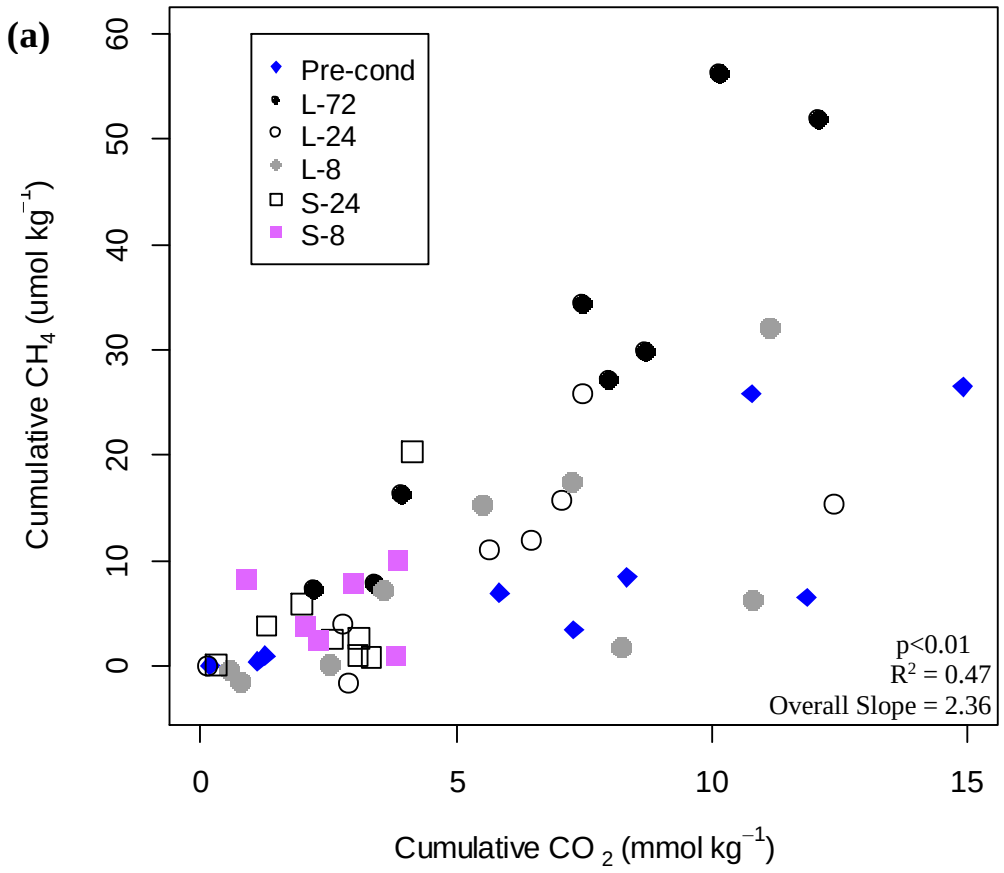
(a)
Pre-cond
L-72
L-24
L-8
S-24
S-8
p<0.01
R2 = 0.47
Overall Slope = 2.36
Cumulative CH4 (umol kg−1)
Cumulative CO 2 (mmol kg−1)
0
10
20
30
40
50
60
0
5
10
15

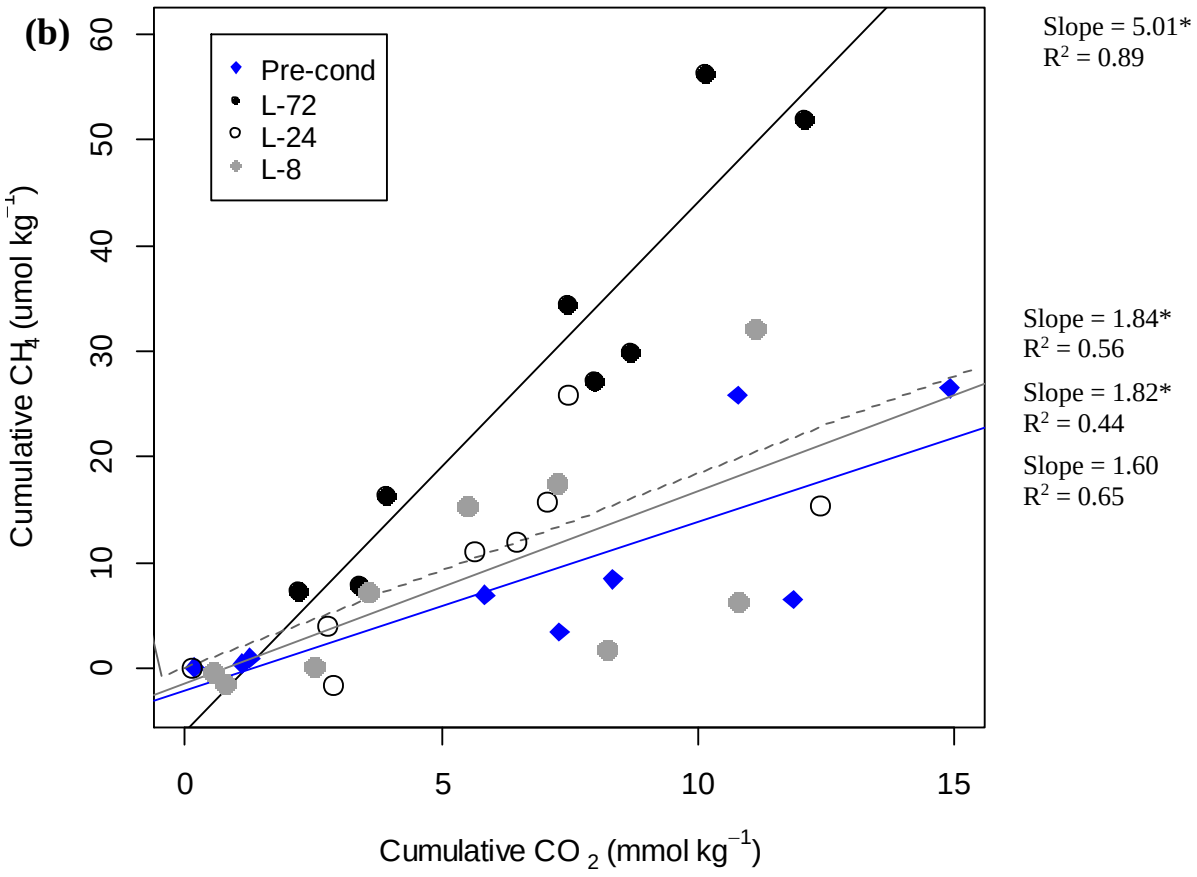
(b)
Pre-cond
L-72
L-24
L-8
Cumulative CH4 (umol kg−1)
Cumulative CO 2 (mmol kg−1)
0
10
20
30
40
50
60
0
5
10
15
Slope = 5.01*
R2 = 0.89
Slope = 1.84*
R2 = 0.56
Slope = 1.82*
R2 = 0.44
Slope = 1.60
R2 = 0.65

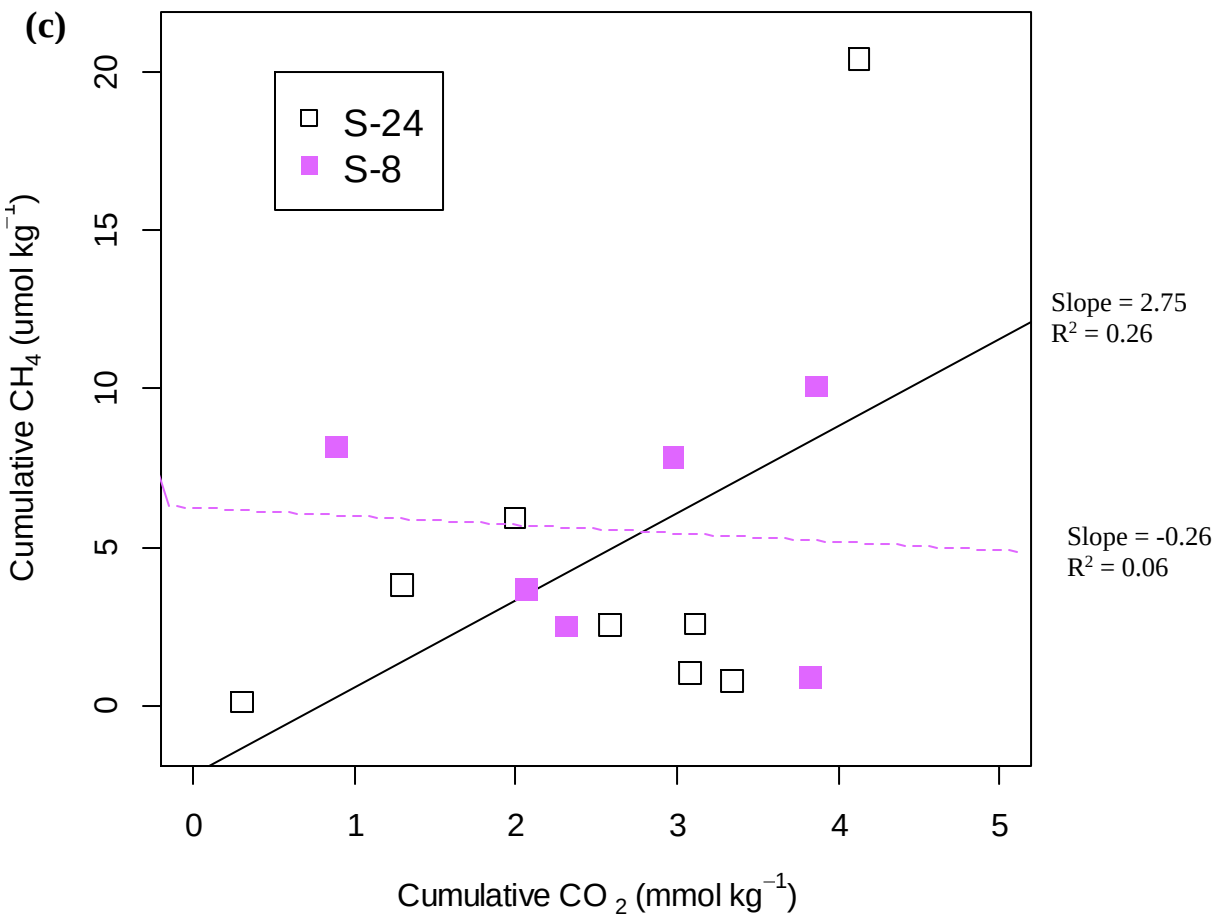

Fig A.5. Linear regressions for Cumulative CO_2 vs Cumulative CH_4 under anoxic conditions only: (a) for all 5 treatments, (b) details for the Long treatments only, (c) and Short treatments only. Asterisks represents slopes that are significant at 5% probably for the linear models. Soils from Bisley watershed, Puerto Rico, sampled in 2015.

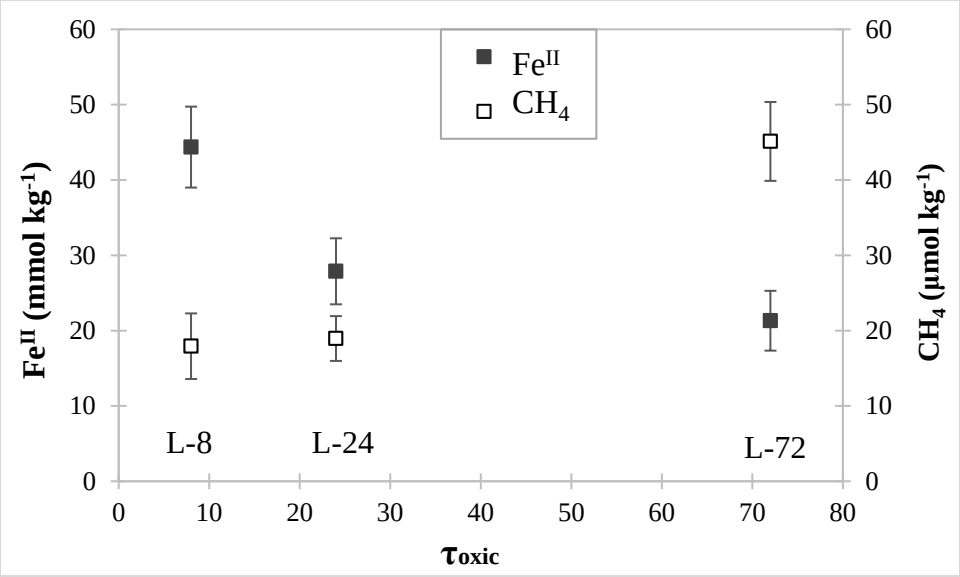

Fig A.6. Soil Fe^{II} concentrations and cumulative CH_4 during anoxic conditions, comparing different previous exposed τ_{oxic} of 8, 24, and 72 h for the treatments with long oscillation period. Soils from Bisley watershed, Puerto Rico, sampled in 2015.

APPENDIX B

SUPPLEMENTAL INFORMATION FOR CHAPTER 4

TABLES AND FIGURES

Table B.1. GPS coordinates of the studied site

Catena	Topographic position	Latitude	Longitude	Altitude (m)
1	Ridge	N 18.32092°	W 65.81729°	414
	Slope	N 18.32077°	W 65.81736°	415
	Valley	N 18.32087°	W 65.81700°	411
2	Ridge	N 18.32143°	W 65.81770°	400
	Slope	N 18.32156°	W 65.81793°	392
	Valley	N 18.32191°	W 65.81818°	379
3	Ridge	N 18.32121°	W 65.81736°	407
	Slope	N 18.32142°	W 65.81754°	401
	Valley	N 18.32141°	W 65.81754°	399

Table B.2. Total elemental analysis (concentrations in %). Soils from Luquillo CZO, Puerto Rico, sampled in 2016

Site	Si	Al	Fe	Ca	Mg	Na	K	Ti	Mn
Valley-1	27.44	12.35	6.43	0.14	0.21	0.06	0.09	0.61	0.06
Valley-2	29.62	10.85	7.55	0.40	0.446	0.23	0.18	0.67	0.170
Valley-3	26.44	12.91	7.87	0.10	0.241	0.05	0.07	0.62	0.085
Slope-1	26.63	13.02	7.83	0.07	0.181	0.05	0.08	0.65	0.062
Slope-2	26.31	12.75	8.39	0.04	0.211	0.04	0.07	0.66	0.031
Slope-3	26.37	12.17	8.01	0.09	0.543	0.05	0.08	0.61	0.271
Ridge-1	24.97	12.95	8.02	0.05	0.20	0.04	0.08	0.63	0.04
Ridge-2	25.16	12.01	7.45	0.04	0.217	0.05	0.08	0.62	0.046
Ridge-3	26.37	12.17	7.48	0.08	0.229	0.06	0.08	0.62	0.101

Table B.3. Turnover Times for Fe^{II} Production and Fe^{II} Consumption: highest frequency, median and mean

Sites	**Fe^{II} Production**			**Fe^{II} Consumption**		
	Highest frequency	Median	Mean	Highest frequency	Median	Mean
	---------- *days* ----------					
All Sites	4	7	23	3 to 4	8	36
Valley-1	3	5	12	4	8	15
Valley-2	5 to 10	25	23	6	8	40
Valley-3	5 to 10	9	10	3 to 11	28	55
Slope-1	8	6	8	5 to 6	12	96
Slope-2	5 to 10	16	16	4	8	15
Slope-3	4	2	10	3 to 4	8	22
Ridge-1	4	5	38	3	10	86
Ridge-2	4 to 18	16	46	4	3	8
Ridge-3	3	2	4	4	4	17

Table B.4. Parameters used for each variable studied before stepwise backward elimination

Catenas	Initial Model (before stepwise backward elimination)
All	Eh = Precipitation, O_2, θ_V
1	O_2 = Precipitation, θ_V
1	θ_V = Precipitation
All	Fe^{II} ~ DOC, Media-Fe^{III}_{RR}, pH, θ_G, Precipitation_2Day
1	Fe^{II} ~ DOC, Media-Fe^{III}_{RR}, pH, Precipitation_2Day, O_2_48, θ_V_12
All	DOC ~ Fe^{II}, Media-Fe^{III}_{RR}, pH, θ_G, Precipitation_2Day, Eh_2
1	DOC ~ Fe^{II}, Media-Fe^{III}_{RR}, pH, Precipitation_2Day, Eh_2, O_2_48, θ_V_36
All	Media-Fe^{III}_{RR} ~ Fe^{II}, DOC, pH, θ_G, Precipitation_2Day, Eh_6
1	Media-Fe^{III}_{RR} ~ Fe^{II}, DOC, pH, Precipitation_2Day, Eh_6, O_2_6, θ_V_24
All	Shewa-Fe^{III}_{RR} ~ Fe^{II}, DOC, pH, θ_G, Precipitation_2Day, Eh_6
1	Shewa-Fe^{III}_{RR} ~ Fe^{II}, DOC, pH, Precipitation_2Day, Eh_6, O_2_3, θ_V_12
1	Flux CO_2 ~ Fe^{II}, Media-Fe^{III}_{RR}, DOC, pH, Precipitation_2Day, Eh_12, O_2_48, θ_V_24, Flux CH_4
1	Flux CH_4 ~ Fe^{II}, Media-Fe^{III}_{RR}, DOC, pH, Precipitation_2Day, Eh_1, O_2_48, θ_V_1, Flux CO_2

Table B.5. Average hours of each environmental factor before soil sampling with the lowest AIC (best model). It represents the best averaged timing to predict each variable in the mixed linear models (from 1 to 48 h of soil sampling).

Variable modeled	Eh_	θ_V_	O_2_
Fe^{II}	-	12	48
DOC	2	36	48
Media-Fe^{III}_{RR}	6	24	6
Shewa-Fe^{III}_{RR}	6	12	3
CO_2	12	24	48
CH_4	1	1	48

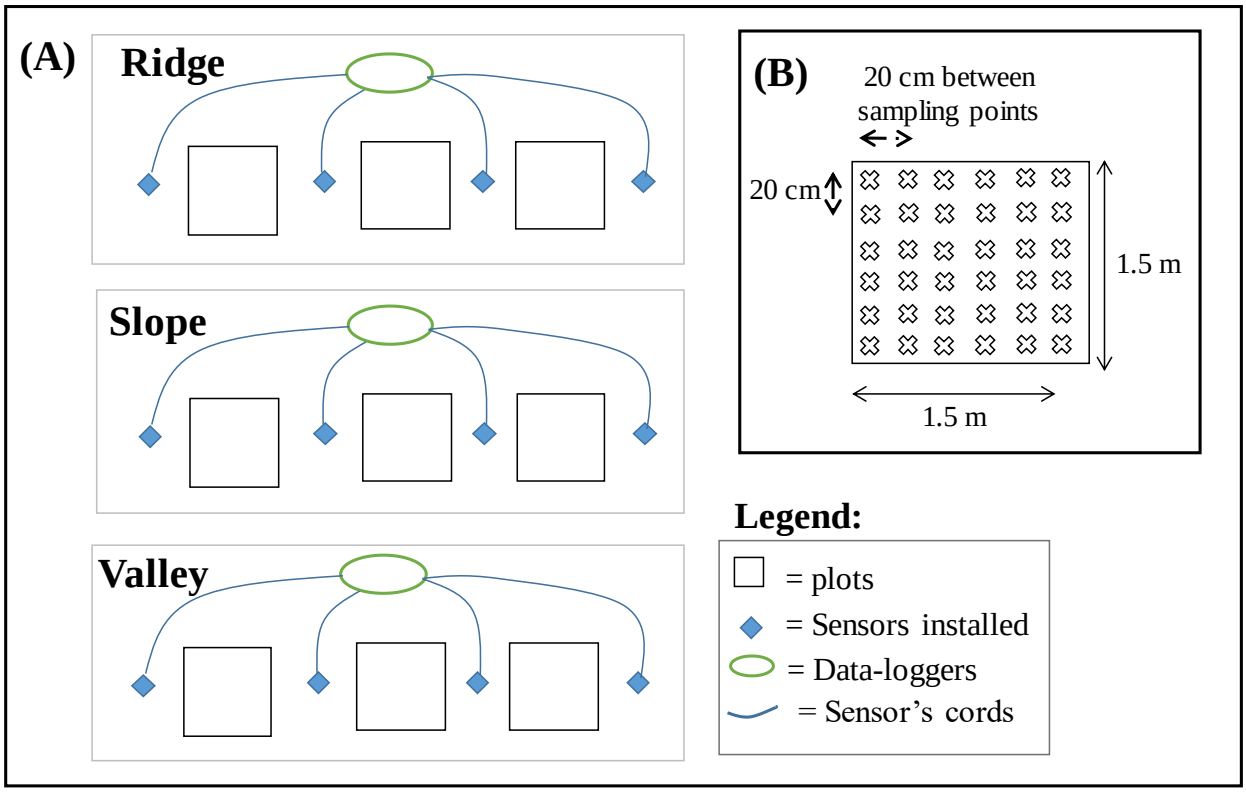

Fig B.1. Illustration for one of the catenas: (A) showing ridge, slope, and valley topographic positions, the 3 plots allocated within each site, the sensors distributed within the plots, and (B) example of 1 subplot of 1.5 m x 1.5 m, sampled at 0-15 cm depth and sampling distanced at least 20 cm apart. Sampling points were randomly selected within the plot. Luquillo CZO, Puerto Rico (2016).

Fig B.2. Examples of plots allocated in the catenas: (a) Slope, Catena-2, (b) Ridge, Catena-2, (c) Valley, Catena-2, and (d) Valley, Catena-3. Luquillo CZO, Puerto Rico (2016).

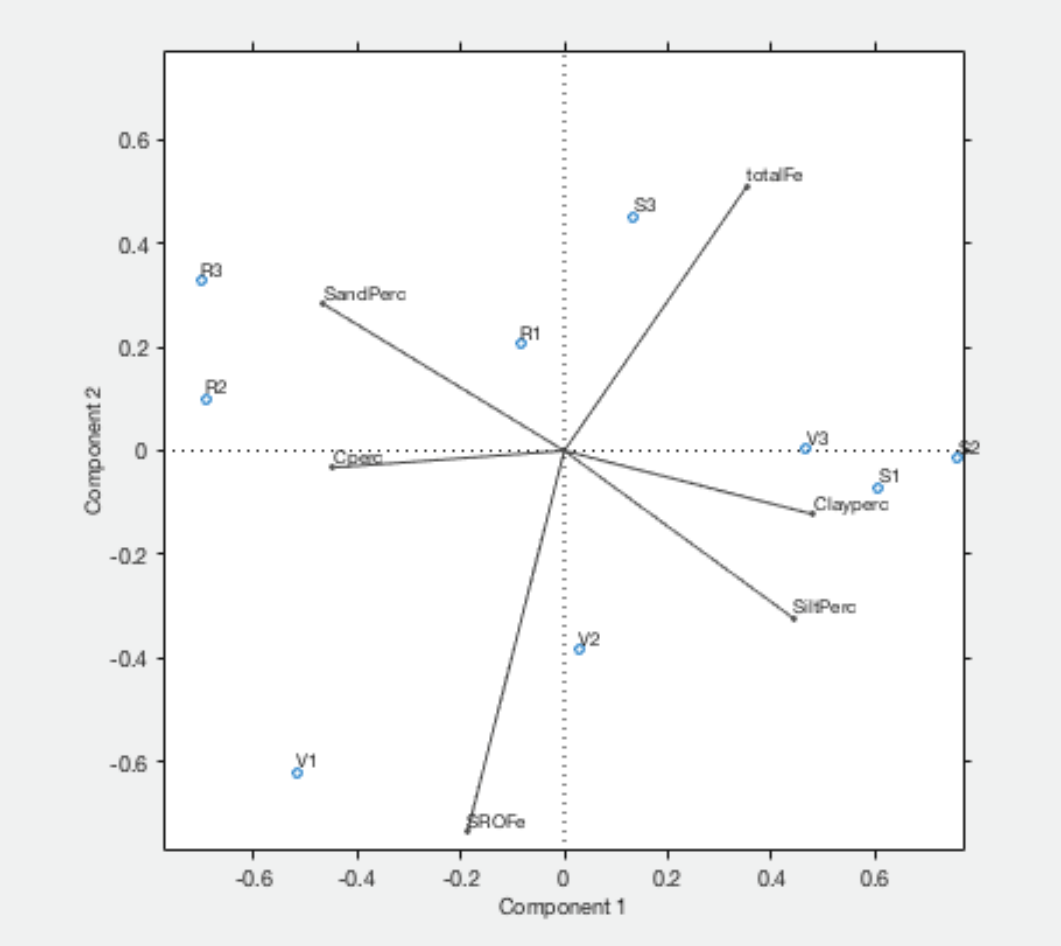

Fig B.3. Principal Component Analysis (PCA) for the 9 sites, valleys (V1, V2, V3), slopes (S1, S2, and S3), and ridges (R1, R2, R3) according to following soil characteristics: Total-Fe, SRO-Fe, Total-C, Sand, Silt, and Clay content. Soils from Luquillo CZO, Puerto Rico, sampled in 2016.

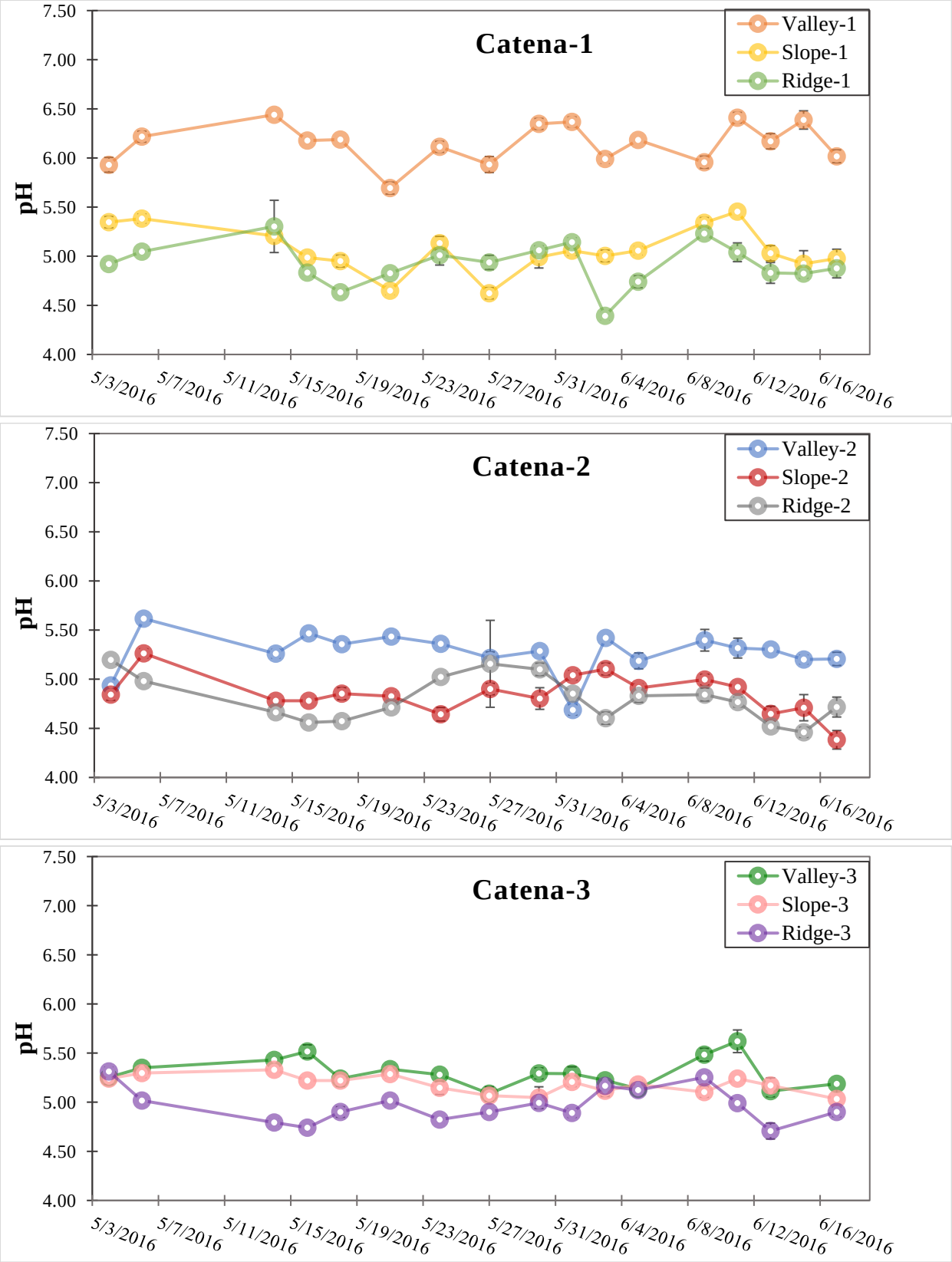

Fig B.4. Soil pH (1:1 soil:water). Soils from Luquillo CZO, Puerto Rico.

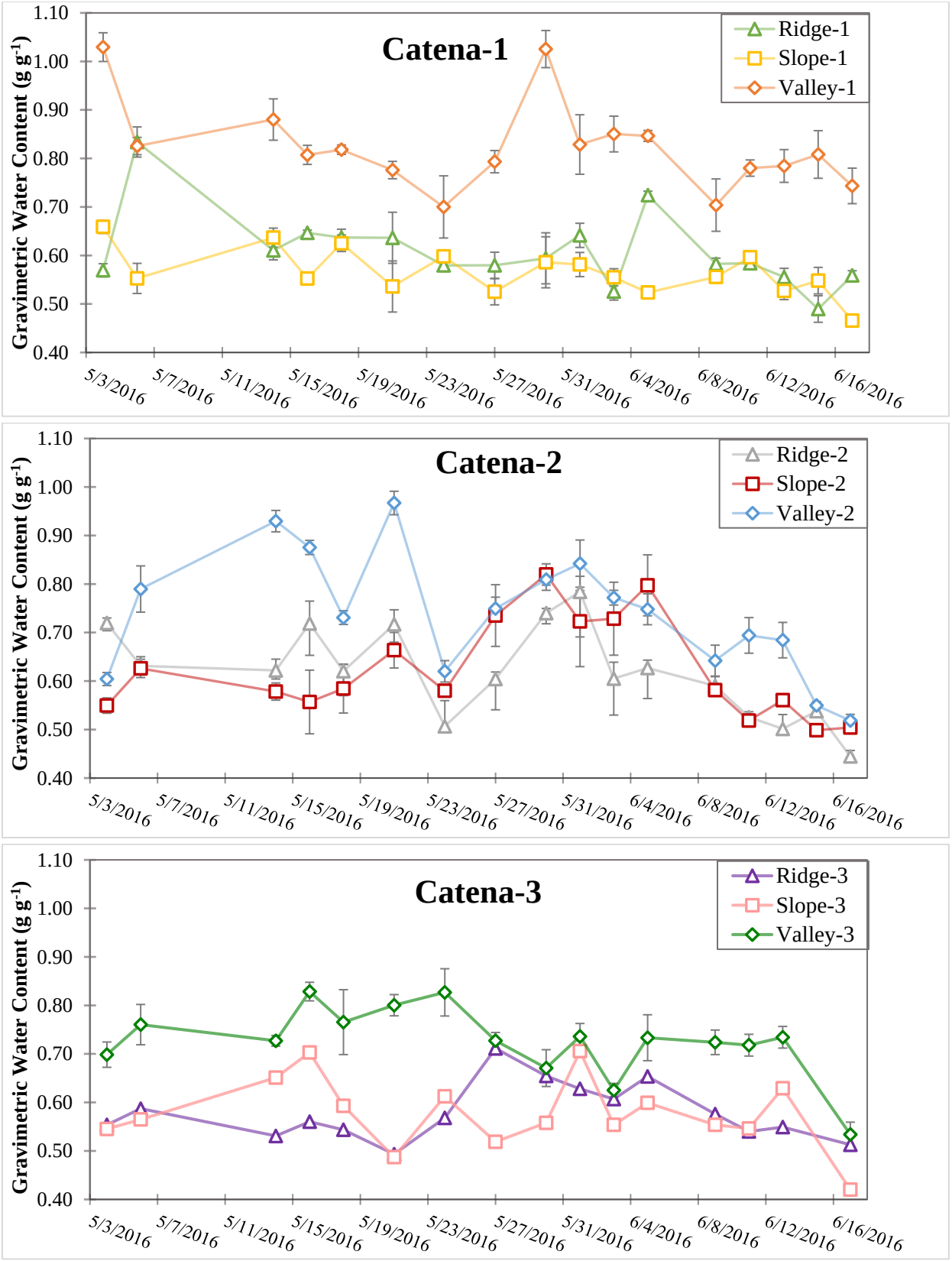

Fig B.5. Gravimetric Water Content. Soils from Luquillo CZO, Puerto Rico.

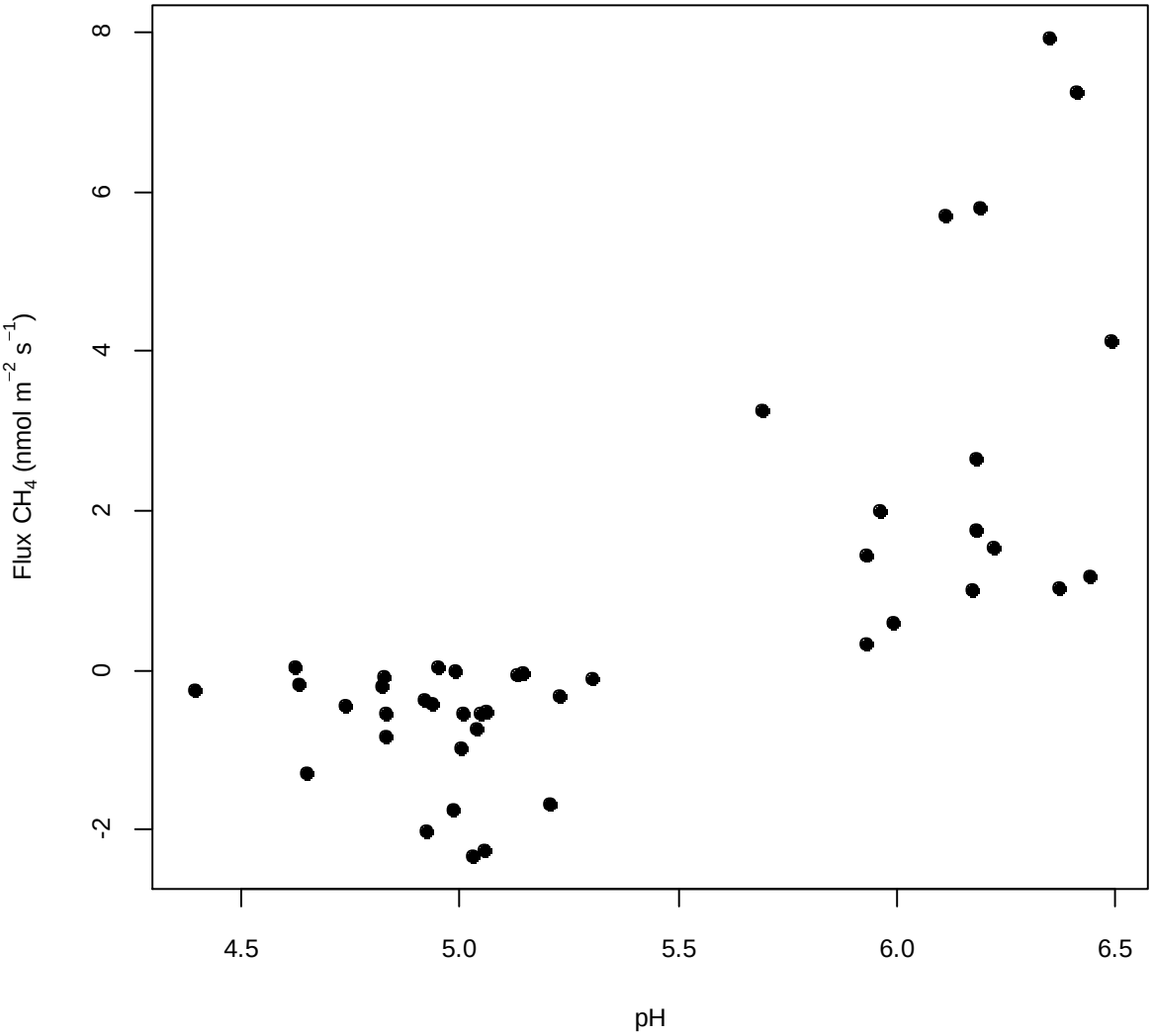

Fig B.6. Correlation between pH and CH_4 flux. Soils from Luquillo CZO, Puerto Rico, sampled in 2016.

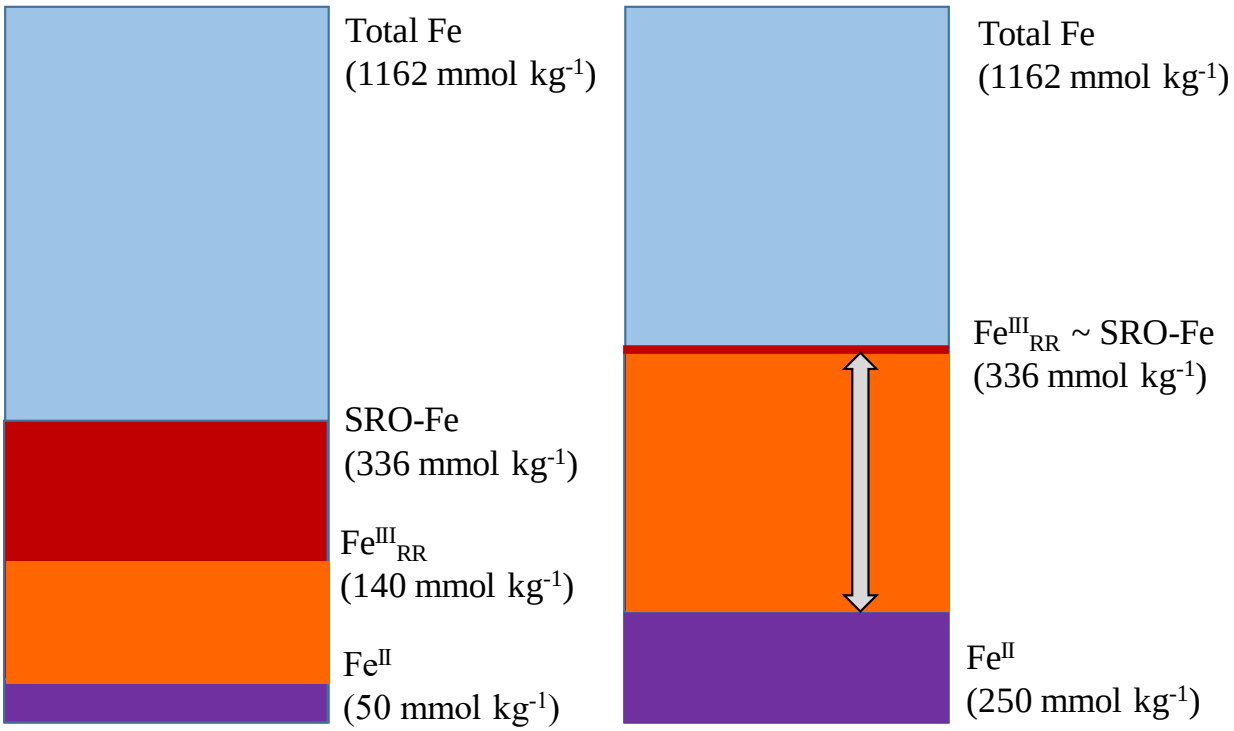

Fig B.7. Pools of Total-Fe, SRO-Fe, Fe^{III}_{RR}, and Fe^{II} for two given sampling days (left and right) for valley-1. The pool of Fe^{III}_{RR} is dynamic and can be as high as the SRO-Fe pool. Soils from Luquillo CZO, Puerto Rico, sampled in 2016.

APPENDIX C

ADDING C SOURCE (AMINO ACIDS) STIMULATED IRON REDUCTION DURING REDOX OSCILLATIONS

Summary

During redox fluctuations in natural systems, iron reduction can be limited by the availability of carbon. New inputs of labile C from litter decomposition may increase Fe reduction rates by stimulating microbial activity (Lovley et al. 1996). Fe reduction rates are typically found to increase when leaf-litter leachate or acetate (Liptzin and Silver 2009) or humid acid analogs (like anthraquinone-2,6-disulfonate, AQDS) (Chacon et al. 2006) are added to the soil. Additionally, soil organic compounds have an electron-transfer capacity that can act as an electron shuttle and catalyst during reductive dissolution of iron minerals (Peretyazhko and Sposito, 2006). Thus, soil carbon content and composition can directly influence Fe reduction in humid tropical forest soils, such as in Luquillo CZO, Puerto Rico.

Complex soil organic compounds can be broken down into soluble amino acids by extracellular enzymes (Pinggera et al., 2015). These enzymes (proteases) can provide important sources of carbon and nitrogen for iron reducers in a system with lower C substrates but iron rich. The objective of this study was to measure how carbon inputs by amino acid additions can influence iron reduction rates during different redox oscillation treatments. We changed the oscillation periodicity and the τ_{oxic} and τ_{anoxic} time lengths among different treatments (Table 3.1) similar to Chapter 3. We used amino acids (Algal Amino Acid Mix, CNLM-452-0) as a labile carbon source and monitored changes in Fe reduction rates across the imposed treatments (Table

3.1). Since microorganisms can metabolize amino acids within a few hours, we added the amino acids just prior to the last redox cycle of each treatment of the experiment. This late addition also ensured that the microbial populations had already adapted to redox fluctuations. Furthermore, since we want to track the iron reducing microbial population, we added the amino acids 24 h before the end of the penultimate τ_{anoxic} allowing the microbes to undergo one more τ_{oxic} and one more τ_{anoxic} with the added carbon source. We analyzed Fe^{II} by Ferrozine (see Methods section 3.2.2 in Chapter 3) to compare Fe reduction rates among the treatments with and without amino acids added. We observed a larger increase in Fe reduction rate, from 1.5 to 10 times higher, when amino acids were added compared to un-amended treatments (Fig. C1).

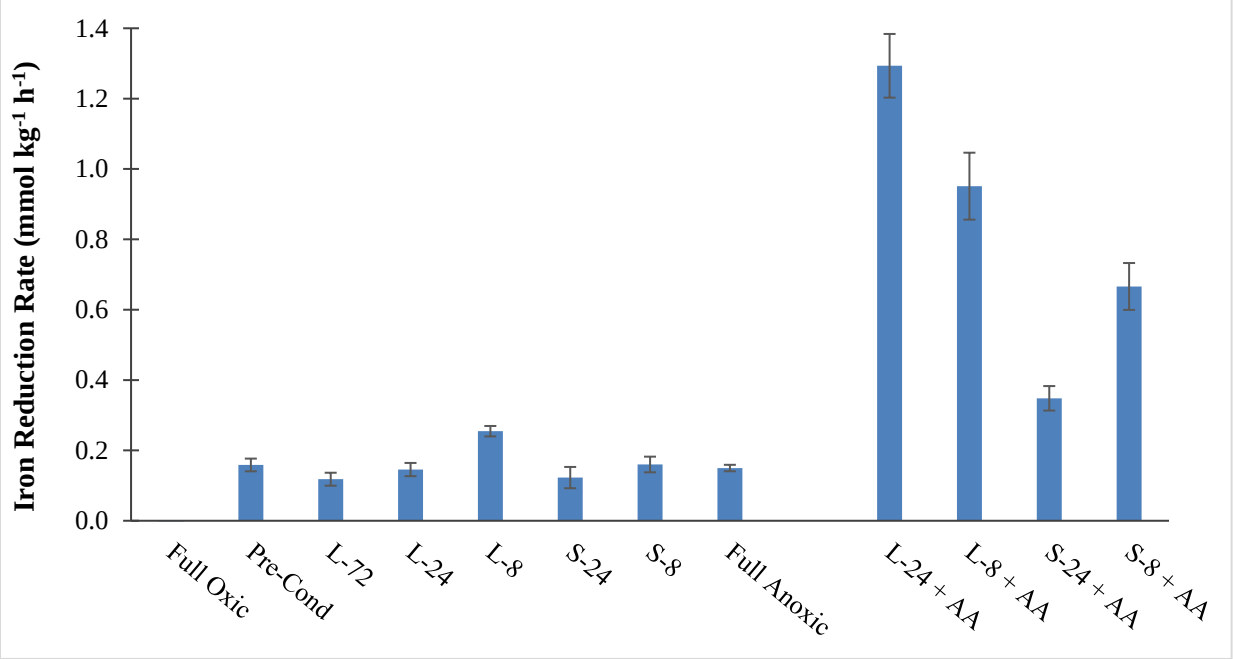

Fig C1. Iron reduction rates comparing treatments without amino acids (Chapter 3), the first eight bars, and treatments with addition of amino acids (+ AA), the last four bars. Soils from Bisley watershed, Puerto Rico, sampled in 2015.

APPENDIX D

SOIL IRON REDUCTION AND CARBON MINERALIZATION IN RECONSTRUCTED AGGREGATES DURING REDOX FLUCTIATIONS

Summary

Oxygen content is extremely heterogeneous within soil microsites, leading to different rates of iron reduction within the bulk soil, and challenging the design of experiments to monitor iron reduction during redox oscillations. Commonly used soil slurry experiments have the advantage of homogenizing the reactants and catalysts. Working with intact/undisturbed soils is complex because of the heterogeneity of soil aggregates and high variability between replicates. But, slurring soils may destroy soil aggregates and disrupt syntrophic association. Thus, I tested a mesoscale approach between a slurry and undisturbed soil by reconstructing soil mini-aggregates. In fluctuating redox environments, we hypothesized that maintaining heterogeneous soil structure conditions would shift the amplitude of the redox fluctuations toward more anoxic conditions. We tested this hypothesis by exposing soil slurries (representing homogeneous conditions) and reconstructed soil mini-aggregates (representing heterogeneous conditions) to redox fluctuations of specific frequency variations. We conducted these two experiments at the same time using the same field-moist soils from Luquillo CZO and under the same redox oscillation treatment conditions (Table 3.1).

For the soil mini-aggregate experiment, we re-constructed 50 ± 10 mg soil aggregates and placed them in 2-mL-microtubes (292 tubes in total) followed by destructively harvest of the

samples throughout the experiment in three replicate batches per analysis. Each mini-aggregate was taken from a soil matrix that was previously passed through a 2-mm-sieve and homogenized within a 95%:5% (N_2:H_2) anaerobic glovebox chamber. For the soil slurry experiment, we used 4.5 g of soil in 45 mL buffered MES solution at pH 5.5 (see Chapter 3), from the same soil matrix as the reconstructed mini-aggregate.

We conducted the redox oscillation experiment with the same treatments as explained in Chapter 3 (Table 3.1). In summary, we pre-conditioned all soils in three cycles of 1 d oxic : 6 d anoxic before imposing five treatments containing three cycles each. Three long-period treatments had τ_{anoxic} fixed at 6 d and τ_{oxic} at either 72, 24, or 8 h (L-72, L-24, and L-8, respectively). Two short-period treatments had τ_{anoxic} fixed at 2 d and τ_{oxic} at 24 or 8 h (S-24 and S-8). We measured 0.5 M HCl-extractable Fe^{II} using the ferrozine method, as described in Chapter 3. In the paired experiments, Fe^{II} increased substantially in the first cycle of the pre-conditioning but dropped in the second and third cycles of the non-slurried soils (Fig. D1). During the subsequent treatments phase, we found that for the non-slurried soils Fe^{II} concentration increased gradually for the L-72 treatment but did not vary for L-24 and L-8. Contrarily, for the slurried soils, we found higher Fe reduction rates in L-8 followed by L-24 and L-72 (Fig. D2). Therefore, the dynamics of redox fluctuations and aggregate structure affects iron reduction processes in these fine textured soils. These changes can be due to different processes of gas diffusion (impediment or facilitation of gas diffusivity) between these two experimental preparations, impacting the soil iron biogeochemical cycling.

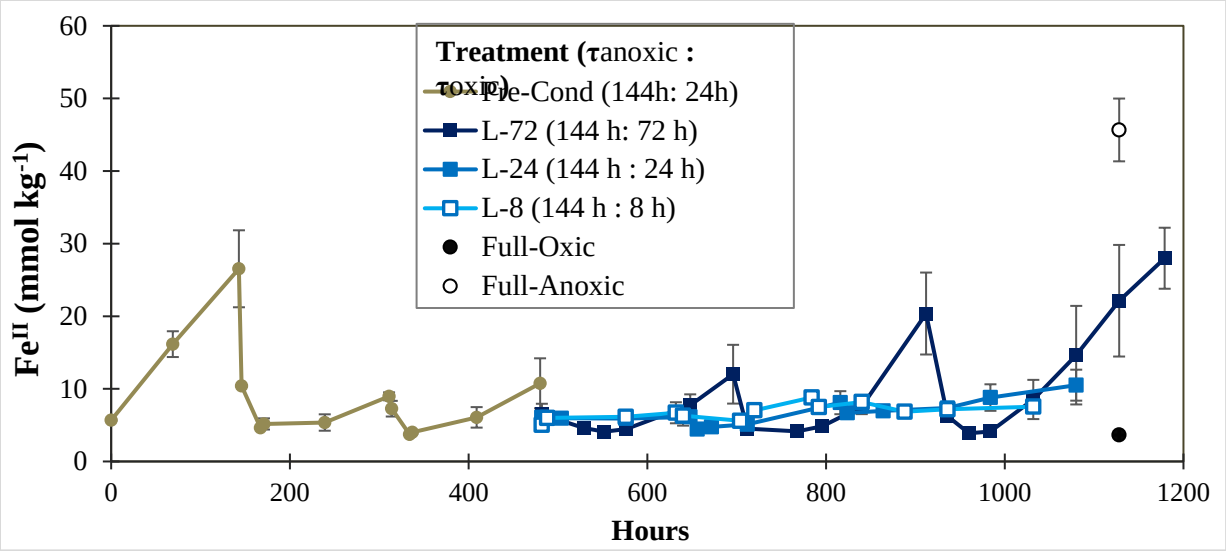

Fig D1. Fe^{II} concentrations for reconstructed mini-aggregate redox experiment. Soils from Bisley watershed, Puerto Rico, sampled in 2015.

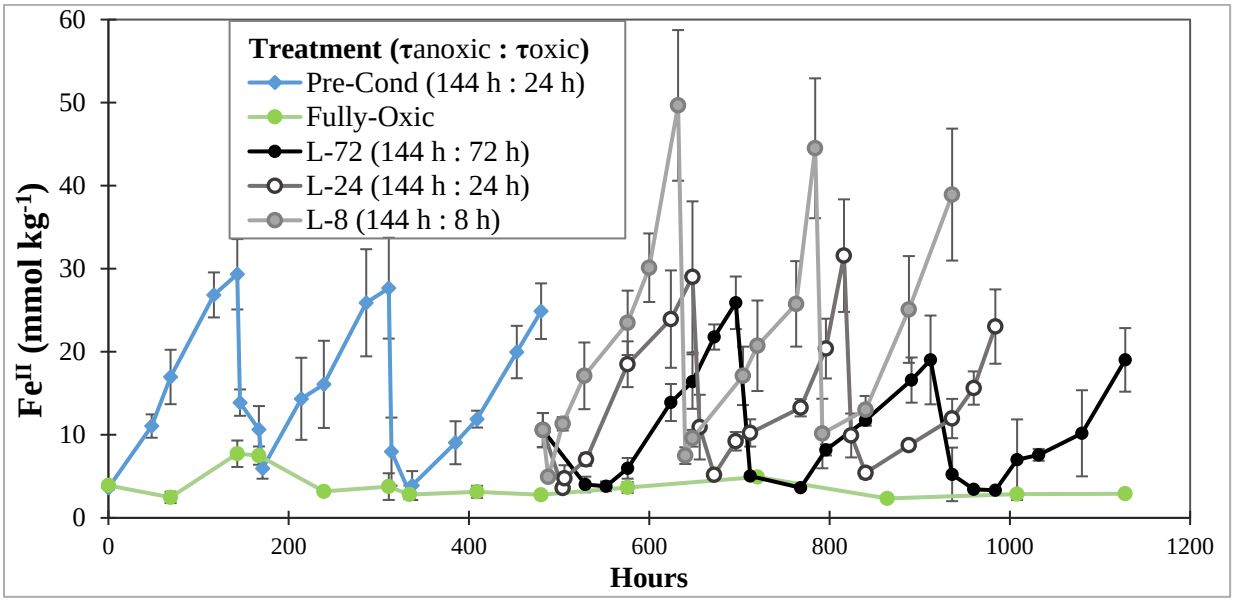

Fig D2. Fe^{II} concentrations for the slurry experiment (Chapter 3). Soils from Bisley watershed, Puerto Rico, sampled in 2015.

APPENDIX E

IRON REDUCTION RATES INCREASED DURING REDOX OSCILLATIONS IN RE-WETTED SOILS THAT WERE PREVIOUSLY DRIED

Summary

We observed striking differences in iron reduction rates during redox oscillation experiments in which soils were either initially air-dried before the experiment (Ginn et al., 2017 and Barcellos et al., 2018/Chapter 2) or the experiment conducted using field-moist and fresh soils (Chapter 3). Comparing the same standard redox oscillation treatment L-24 (6 d anoxic + 1 d oxic, and oscillation period of 7 days, as in Chapter 3), we found that Fe reduction rates remained equal within error (0.15 ± 0.04 mmol kg^{-1} h^{-1}) over the 3 cycles of pre-conditioning and over the next 3 cycles of L-24 (6 complete redox oscillation cycles in total), maintaining Fe^{II} peaks at 27.5 ± 3.1 mmol kg^{-1}. However, in Ginn et al. (2017) there was an increase in Fe reduction rate from 0.11 to 0.62 mmol kg^{-1} h^{-1} over the 6 repetitive redox oscillation cycles for the same oscillation period (6 d anoxic + 1 d oxic) and Fe^{II} peaks increasing from 6 to ~100 mmol kg^{-1} for the unamended-P soil treatment. Correspondingly, in Chapter 2 (Barcellos et al., 2018), using similar air-dried soils as used in Ginn et al. (2017), we found that for the first 2 cycles of the experiment, which had the same oscillation period of 6 d anoxic and 1 d oxic, the Fe reduction rate increased from 0.21 to 0.47 mmol kg^{-1} h^{-1} (Table 2.2). Since soil moisture content is one of the major regulators of soil microbial diversity and function (Bouskill et al. 2013; Evans and Wallenstein 2012; Hueso et al. 2012), these changes in Fe dynamics are likely related to the initial soil moisture state. In Chapter 3, we used fresh field-moist soil that was

collected within 24 h from Luquillo CZO, but in Ginn et al. (2017) and in Barcellos et al. (2018) the soil was air-dried and stored prior to the experiment.

Together with changes in soil moisture, the quality (lability) of the soil organic matter that is used as an electron donor would likely impact Fe-C redox dynamics. We further hypothesized that there will be more soluble organic carbon in rewetted air-dried soils compared to field moist soils during these redox oscillation events (like Ginn et al. 2017 and Chapter 3, respectively), and that this would lead to higher iron reduction rates in the former.

We tested these hypotheses by comparing the same soil either fresh field-moist (24 h from sampling) or air-dried over a week at 30 ^{o}C. The redox oscillation experiment used the same oscillation period of 7 days with τ_{anoxic} = 6 and τ_{oxic} = 1 d, similar to Ginn et al. (2017) and the study in Chapter 3, respectively. We also included fully-anoxic and fully-oxic controls for both soil moisture status treatments. For this experiment, we collected a fresh composite soil sample from the same location (upland valley in Bisley watershed) from Luquillo CZO, on early November 2017, just after the hurricane Maria. The natural soil collected had 97% water content.

We compared the initial soil condition (with no treatment added) between the field moist and air-dried, and we found higher Fe^{II}, SRO-Fe, SRO-Al, and pH, and lower DOC (water extractable dissolved organic carbon) in the field-moist soil compared to the air-dried soil (Table E1). We conducted a redox oscillation experiment using the same methodology as Chapters 2 and 3, as follows: 4.5 g of soil in a 45 mL final solution buffered with MES at pH 5.5. As we hypothesized, we detected a large increase in Fe reduction rates over the course of the experiment for the re-wetted & air-dried soil (similar to Ginn et al., 2017), compared to the field-moist soil (similar to Chapter 3), which maintained similar Fe reduction rates and Fe^{II} peaks throughout the cycles (Fig. E1).

Table E1. Initial Soil Conditions (native soil without any treatment) for both field-moist and air-dried treatments. Soils from Bisley watershed, Puerto Rico, sampled in 2017. Lowercase letters in parentheses (a and b) indicate significant differences at the 5% probability level

	Fe^{II}	SRO-Fe	Total Fe	SRO-Al	Total Al	DOC	Total C	Total N	pH
Soil	---------- *mmol* kg^{-1} ----------					*mg* L^{-1}	------ *g* kg^{-1} -----		
Field-moist (fresh)	4.25 ± 0.39 (a)	525.3 ± 29.1 (a)	1055.7	93.8 ± 4.5 (a)	3089.5	29.2 ± 4.1 (a)	63.1 (a)	3.6 (a)	6.07 ± 0.03 (a)
Air-dried (30ºC)	2.88 ± 0.10 (b)	425.3 ± 34.8 (b)		80.8 ± 4.9 (b)		45.3 ± 0.2 (b)	60.3 (a)	3.5 (a)	5.52 ± 0.12 (b)

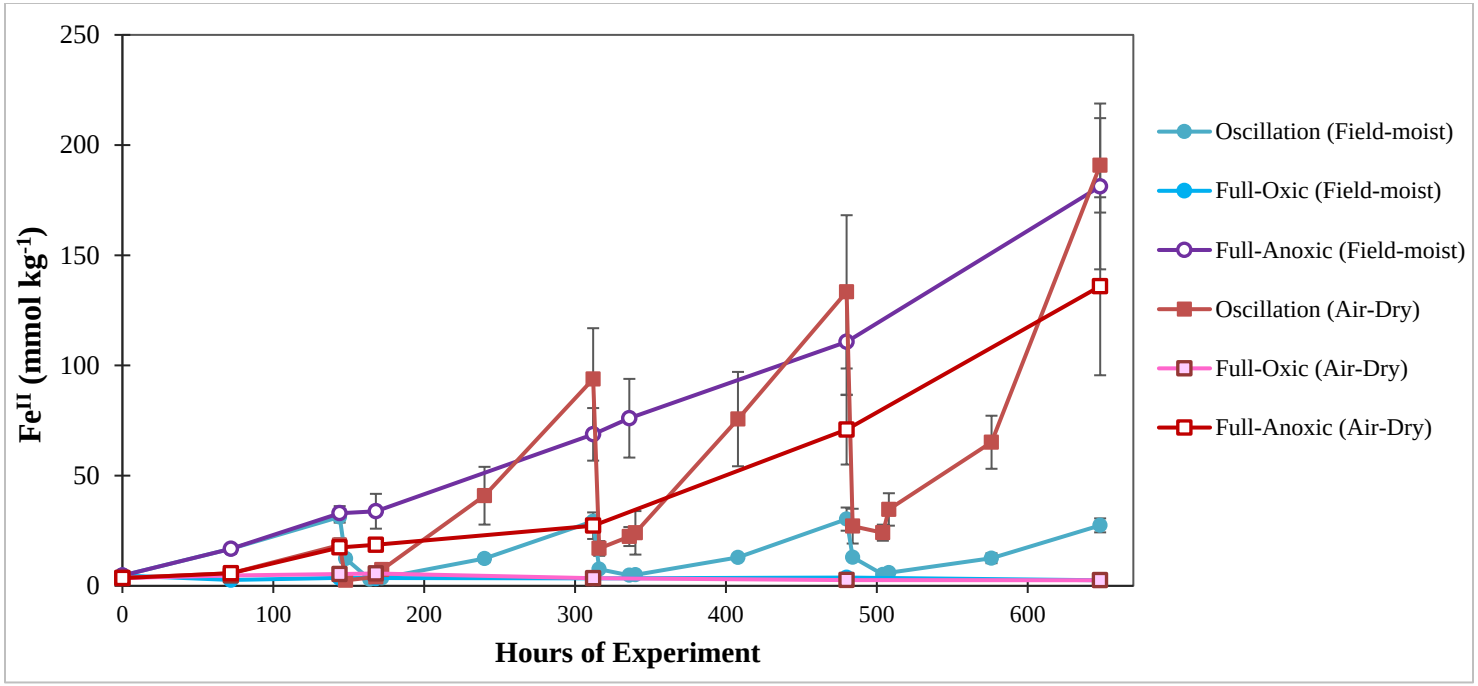

Fig E1. Fe^{II} concentrations for field-moist and air-dried soils during oscillation (6 d anoxic and 1 d oxic) and fully-anoxic and fully-oxic controls. Soils from Bisley watershed, Puerto Rico, sampled in 2017

APPENDIX F

FIELD MEASUREMENTS OF SOIL IRON AND CARBON CYCLING DURING SPRING WARM-UP IN AN AGGRADING PINE FOREST AT THE CALHOUN CZO

Summary

Areas of fluctuating soil moisture are prone to shifts in soil oxygen and redox potential, influencing the propensity for iron reduction, which in turn could affect soil organic carbon accumulation, availability, and mineralization. Previous work from our research group quantified variations in soil wetness across a first-order watershed at the Calhoun Critical Zone Observatory (Calhoun CZO) (Hodges, 2017) in the Piedmont of South Carolina (USA). In this landscape, accelerated erosion from a century of agricultural practices promoted movement of soils from the upland to the bottomland changing the geographical distribution of carbon and nutrients across the landscape and affecting the hydrological and soil moisture patterns. The erosion in the Piedmont has generated soils with contrasting profiles comprising soils with shallow clay-rich layers (e.g., at 10 cm) on the ridges, and deep clay-rich layers (e.g., at 60 to 100 cm from the surface) in the footslopes, as observed in one of the watersheds (W4) of the Calhoun CZO (Ryland 2017).

We aimed to study the impact of soil wetness and soil topographic variation on iron reduction and organic carbon dynamics in the winter and spring seasons. In this aggrading pine and mixed hardwood forest, we hypothesize that during the spring warm-up the soil moisture and oxygen content would decrease leading to increased Fe reduction and potentially the release of DOC forms. We collected soil samples every 10 to 15 days from January to June 2017, in two

ridges and two footslope locations (GPS coordinates in Table F1) (Fig. F1) at 0-10 cm and 10-30 cm soil depths. We also simultaneously measured CO_2 soil flux using a field LiCor LI-8100A Infrared Gas Analyzer (IRGA). For each soil sample, we measured ferrous iron (Fe^{II}), water extractable dissolved organic carbon (DOC), pH, and short-range-order Fe phases (SRO-Fe), using a methodology similar to that used in Chapter 4 (see session 4.2) for the Luquillo CZO field campaign. We installed platinum electrodes and soil moisture sensors and collected hourly data throughout the experiment.

Our results suggest the differences in soil profile texture and landscape position strongly influenced Fe and C cycling. Ridge soils with shallow Bt horizons contained higher carbon content and SRO-Fe than the footslope soils (Table F2). The upper soil horizons (0-10 cm) were also higher in most of the parameters studied compared to the lower soil horizons (10-30 cm). Soil moisture responded to the precipitation patterns, but the redox potential (Eh) remained within oxic conditions (>400 mV) throughout the experiment (Fig. E2 and E3). Within the bi-weekly measurements, ridge-2 had higher values than ridge-1 and the footslopes 1 and 2, for Fe^{II} and WEOC (Fig. F4 and F5). The ridge-2 contained a shallower Bt horizon (at 10 cm) compared to ridge-1 (~30 cm) and footslopes (>100 cm). This shallower clayey horizon in ridge-2 could potentially create a temporal perched water table after rainfall events, which may have facilitated iron reduction processes given the higher soil carbon content at the ridges. During the winter (dormant season), Fe^{II}, DOC, and CO_2 fluxes remained near constant but over the spring Fe^{II} and CO_2 increased, and DOC decreased for most of the sites (Fig. F4, F5, F6, and F7). Apparent changes in iron respiration and carbon mineralization at the study sites are likely due to increases in microbial activity during the spring warm-up. Therefore, in this recovering post-erosion environment, and perhaps many other forested watersheds, depth to clay can be a critical

landscape-level characteristic driving carbon and iron dynamics in soils. We will further conduct mixed linear models to compare these biogeochemical variables, and potentially make comparisons across Luquillo and Calhoun CZOs, since we have measured similar parameters.

Table F1. GPS coordinates for the locations studied at the Watershed 4, Calhoun CZO, South Carolina (sampled in 2017)

Location	Latitude	Longitude
Ridge-1	34.612856	-81.693356
Ridge-2	34.611835	-81.692313
Footslope-1	34.61211	-81.69403
Footslope-2	34.61134	-81.69239

Table F2. Soil characterization for the four locations studied at the Watershed 4, Calhoun CZO, South Carolina (sampled in 2017)

Location	Depth	Fe^{II}	SRO-Fe	Total-Fe	Total-C	Clay	Texture	pH
		---------- mmol kg^{-1} ----------			%	%		
Ridge-1	0-10 cm	2.2	17	482	2.5	6	Loamy Sand	6.2
	10-30 cm	0.2	14	384	0.5	9	Sandy Loam	5.5
Ridge-2	0-10 cm	4.9	47	693	3.5	12	Sandy Loam	5.4
	10-30 cm	0.8	57	804	1.2	39	Sandy Clay	5.2
Footslope-1	0-10 cm	1.5	13	343	1.2	6	Loamy Sand	6.2
	10-30 cm	0.3	12	346	0.3	4	Loamy Sand	5.9
Footslope-2	0-10 cm	2.2	23	423	2.1	4	Loamy Sand	6.1
	10-30 cm	0.3	14	382	0.4	6	Loamy Sand	5.4

Fig F1. Watershed 4 at the Calhoun CZO (2017).

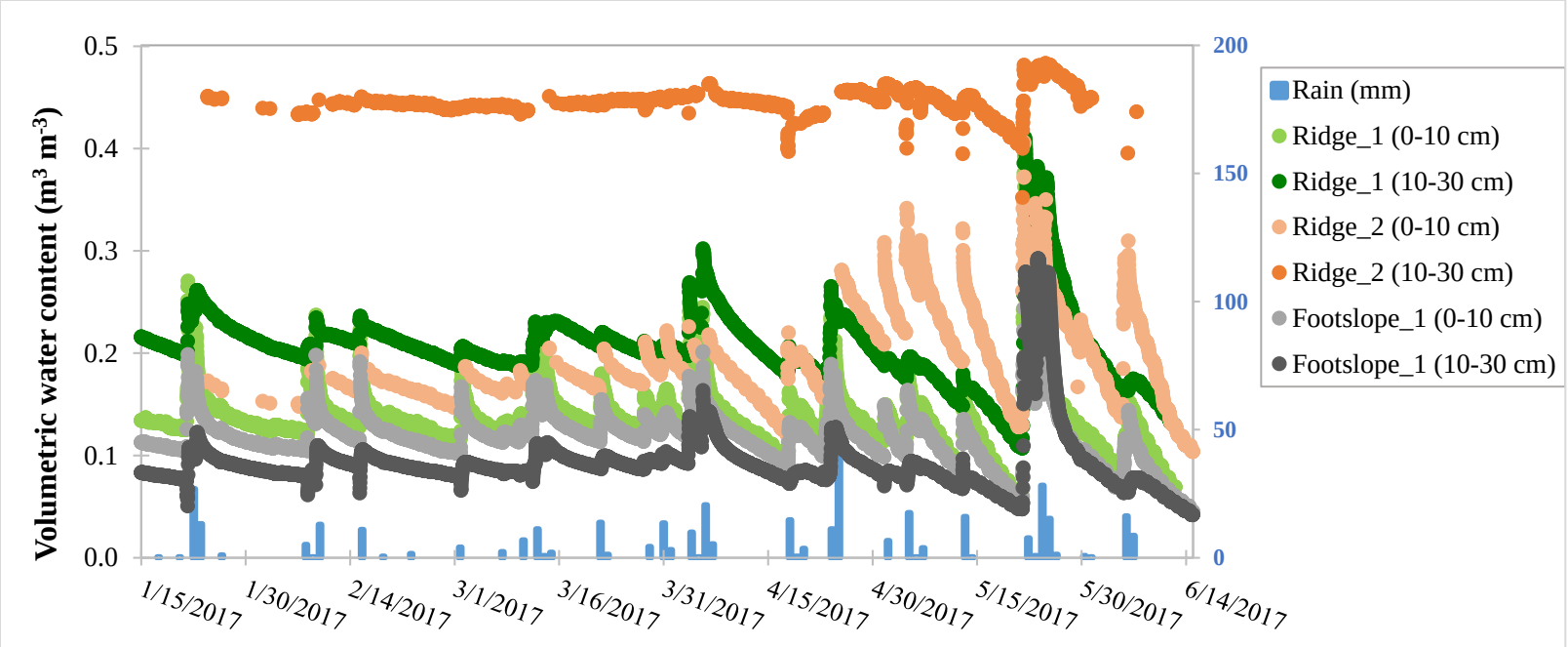

Fig F2. Soil moisture at different locations and depths (Watershed 4, Calhoun CZO, South Carolina).

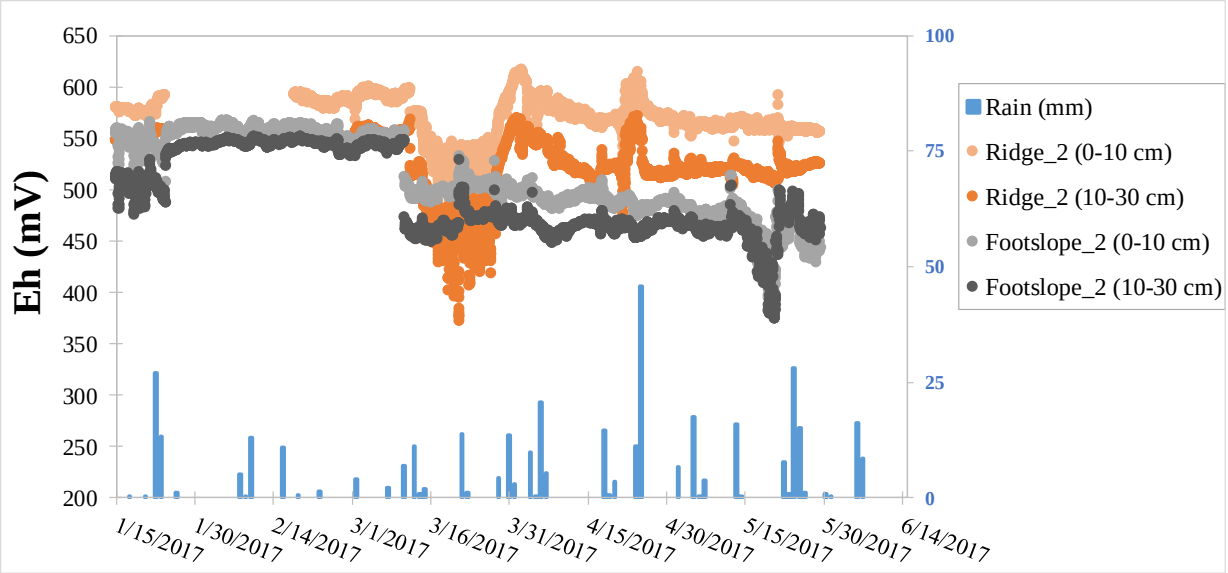

Fig F3. Redox potential (Eh) at two locations and depths (Watershed 4, Calhoun CZO, South Carolina).

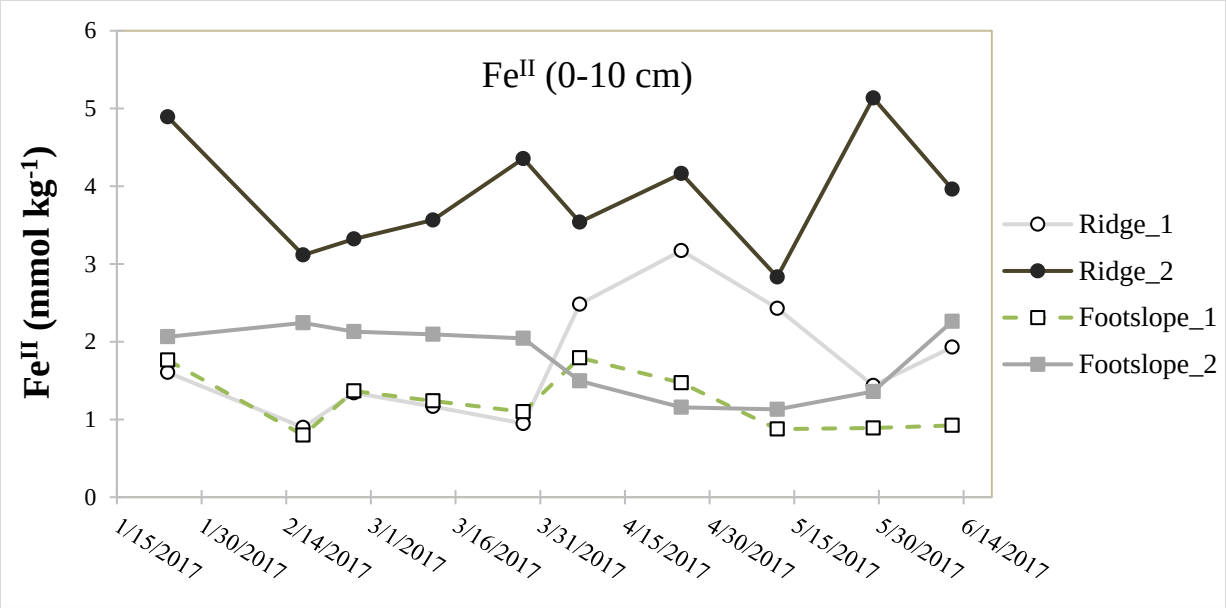

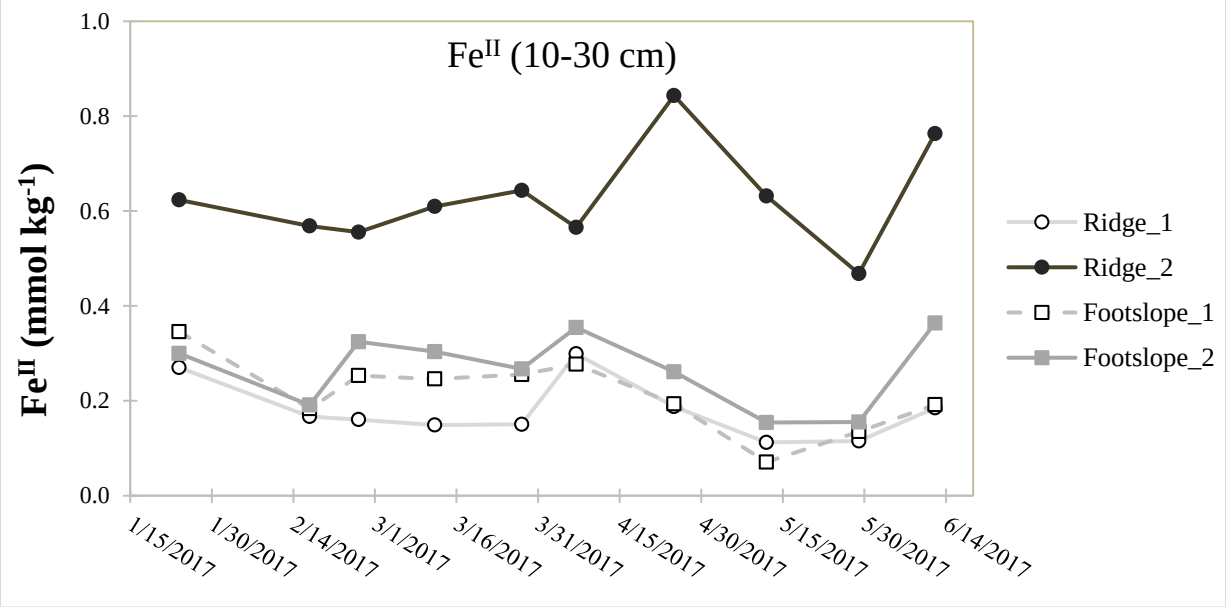

Fig F4. Fe^{II} concentrations at different locations and depths (Watershed 4, Calhoun CZO, South Carolina).

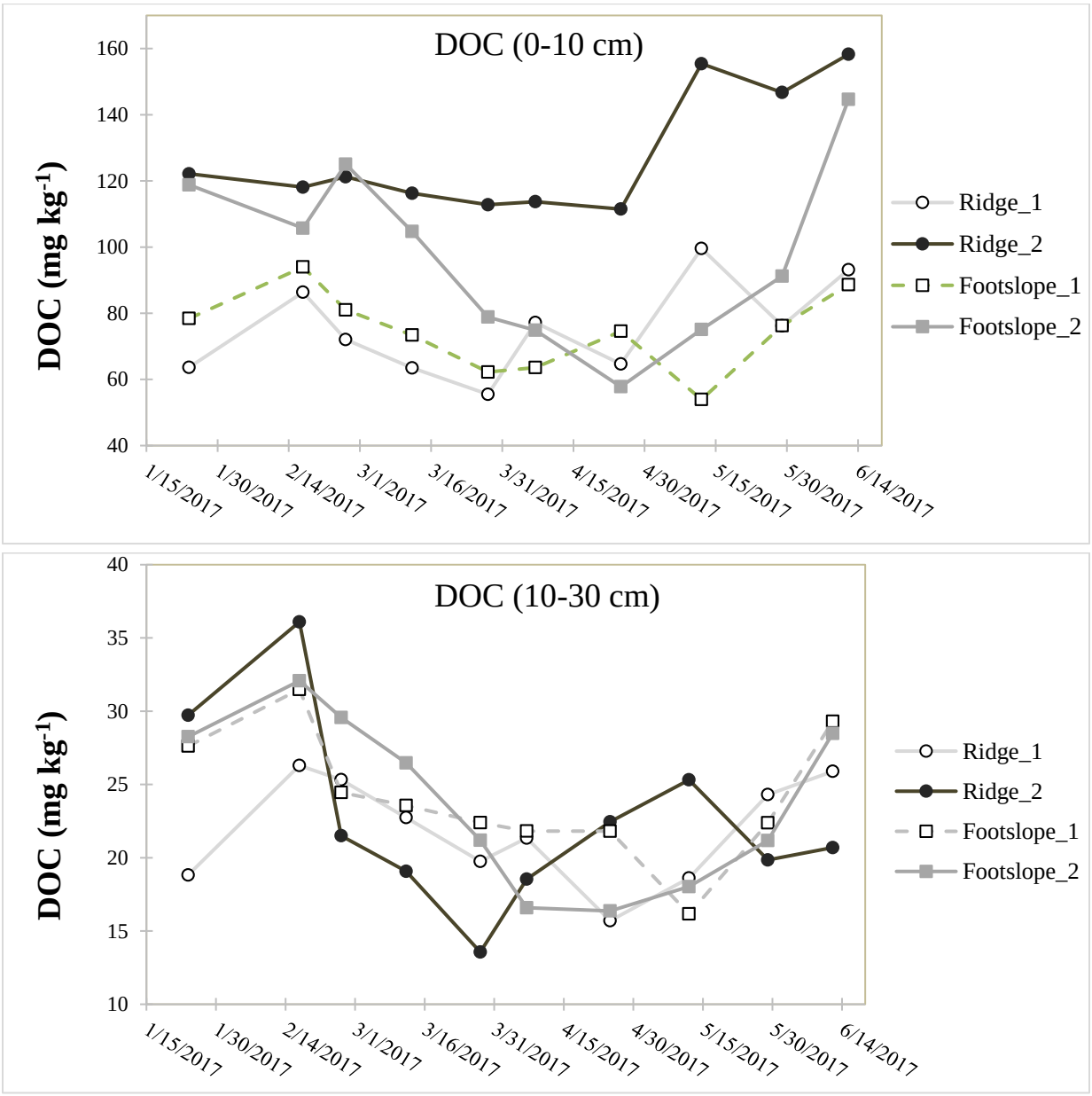

Fig F5. Water Extractable Dissolved Organic Carbon (DOC) at different locations and depths (Watershed 4, Calhoun CZO, South Carolina).

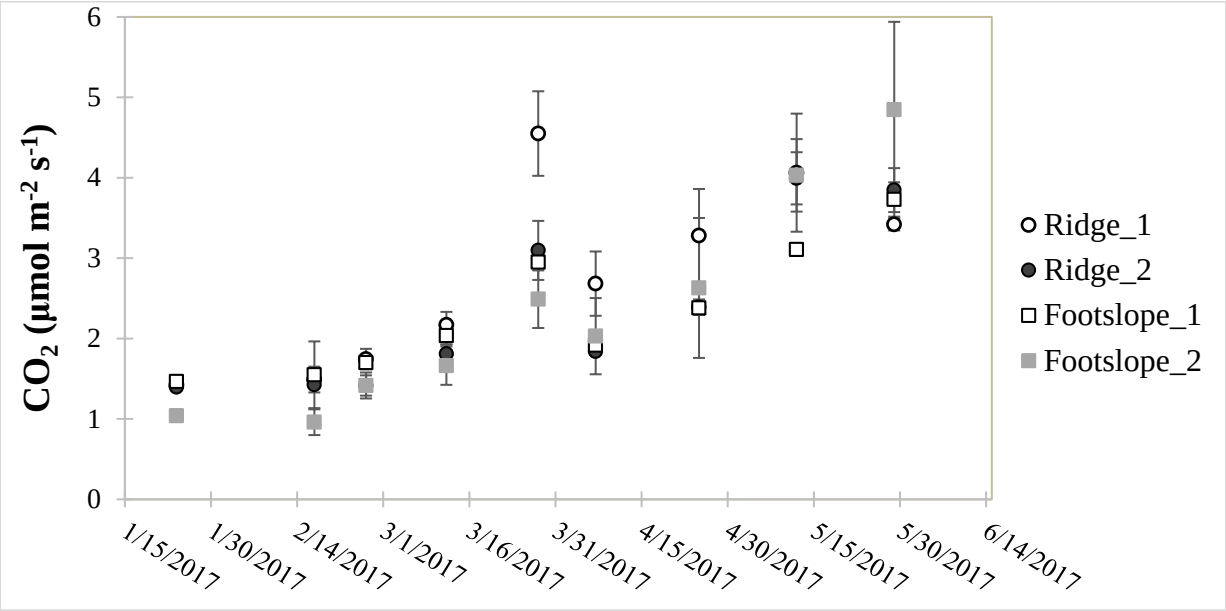

Fig F6. Soil CO_2 fluxes from the different locations (Watershed 4, Calhoun CZO, South Carolina).

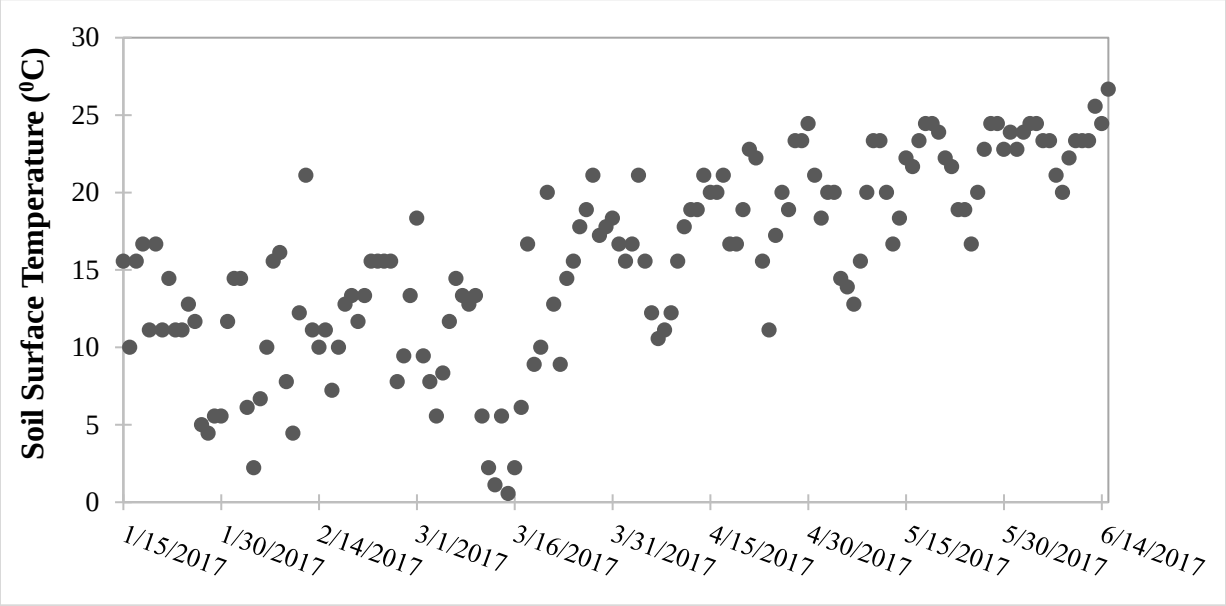

Fig F7. Daily average of soil surface temperature for the locations studied (Watershed 4, Calhoun CZO, South Carolina).